Synthesis, Characterization and Performance Evaluation of Bio-derived Surfactant for Emulsification, Carbon Entrapment and Thermal Energy Storage

Thesis submitted in partial fulfilment

for the Award of Degree

Doctor of Philosophy

By

ALPANA SINGH

RAJIV GANDHI INSTITUTE OF PETROLEUM TECHNOLOGY

JAIS, INDIA – 229304

20PE0002 2025

CERTIFICATE

It is certified that the work contained in the thesis titled "***Synthesis, Characterization and Performance Evaluation of Bio-derived Surfactant for Emulsification, Carbon Entrapment and Thermal Energy Storage"*** *by "**Alpana Singh***" has been carried out under our supervision and that this work has not been submitted elsewhere for a degree.

It is further certified that the student has fulfilled all the requirements of Comprehensive, Candidacy and SOTA/Open seminar.

_____

Supervisor
(Dr. Tushar Sharma)

DECLARATION BY THE CANDIDATE

I, "***Alpana Singh***", certify that the work embodied in this thesis is my own bona fide work and carried out by me under the supervision of "***Dr. Tushar Sharma"*** from "*August 2020" to "July 2025*" at the Rajiv Gandhi Institute of Petroleum Technology, Jais (India). The matter embodied in this thesis has not been submitted for the award of any other degree. I declare that I have faithfully acknowledged and given credits to the research workers wherever their works have been cited in my work in this thesis. I further declare that I have not willfully copied any other's work, paragraphs, text, data, results, etc., reported in journals, books, magazines, reports dissertations, theses, etc., or available at websites and have not included them in this thesis and have not cited as my own work.

_____

Date: **Alpana Singh**
Place: Roll No: 20PE0002

CERTIFICATE BY THE SUPERVISOR

It is certified that the above statement made by the student is correct to the best of our knowledge.

(Dr. Tushar Sharma)	**(Dr. Tushar Sharma)**
(Supervisor)	Head of Department
	(PE & GE)

CERTIFICATE

CERTIFIED that the work contained in the thesis titled "**Synthesis, Characterization and Performance Evaluation of Bio-derived Surfactant for Emulsification, Carbon Entrapment and Thermal Energy Storage**" by Ms. **Alpana Singh** has been carried out under my supervision. It is also certified that he fulfilled the mandatory requirement of TWO quality publications arose out of her thesis work.

It is further certified that the two publications (copies enclosed) of the aforesaid Ms. **Alpana Singh** have been published in the Journals indexed by –

(a) SCI

(b) SCI Extended

(c) SCOPUS

Supervisor	Convener, DPGC
(Dr. Tushar Sharma)	**(Dr. Hemant Kumar Singh)**

COPYRIGHT TRANSFER CERTIFICATE

Title of the Thesis: Synthesis, Characterization and Performance Evaluation of Bio-derived Surfactant for Emulsification, Carbon Entrapment and Thermal Energy Storage

Name of the Student: Alpana Singh

Copyright Transfer

The undersigned hereby assigns to the Rajiv Gandhi Institute of Petroleum Technology Jais all rights under copyright that may exist in and for the above thesis submitted for the award of the "Doctor of Philosophy ".

_____

Date: *Alpana Singh*

Place: Roll No: 20PE0002

Note: However, the author may reproduce or authorize others to reproduce material extracted verbatim from the thesis or derivative of the thesis for author's personal use provided that the source and the Institute's copyright notice are indicated.

Dedicated To

My Beloved Family

For their endless love, support, and encouragement

Acknowledgements

The completion of this doctoral research marks a significant milestone in my academic and personal journey. It is with deep gratitude and humility that I reflect on the collective support, encouragement, and guidance that have brought me to this point. This thesis would not have been possible without the unwavering support of many individuals, each of whom has contributed in their own way to the realization of this work.

First and foremost, I express my deepest gratitude to my Doctoral supervisor, Dr. Tushar Sharma, for their invaluable mentorship, constructive thoughts and unwavering support throughout my PhD journey. Their depth of knowledge, patience and commitment to academic excellence have been a constant source of motivation. I am sincerely thankful for the freedom and trust they extended to me in exploring and shaping my research, as well as for the critical insights that helped refine my ideas and methodologies. I am deeply thankful for the insightful discussions and constructive feedback I received during the course of my thesis work. Each conversation contributed significantly to refining my research and enhancing my skills as a scholar. His mentorship also introduced me to essential professional principles, which I believe will shape me into a more capable and well-rounded individual in both my career and personal life.

I would like to take this opportunity to express my sincere appreciation to the external collaborators who have significantly contributed to both quality and depth of my research. I am especially grateful to Prof. Vikram Vishal (IIT Bombay, India), Prof. Stefan Iglauer and Prof. Alireza Keshavarz (Edith Cowan University, Australia), Prof. Japan Trivedi (University of Alberta, Canada), Prof. Mahmood M.S. Abdullah (King Saud University, Saudi Arabia) and Dr. Muhammad Arif (Khalifa University, United Arab Emirates) for their valuable insights, thoughtful

critiques and unwavering support. Your guidance has played a vital role in shaping my work and helping me present it with clarity and precision. Thank you all for your time, trust and encouragement.

I am sincerely grateful to the faculty members of the Department of Petroleum Engineering and Geo-engineering for their consistent support and guidance throughout my research journey. The academic environment, research infrastructure and administrative support offered by the department have played a crucial role in facilitating my research work. My heartfelt thanks goes to the dedicated research and administrative staff whose efforts ensured a smooth and peaceful academic experience during my time at RGIPT.

Being a part of the Enhanced Oil Recovery (EOR) and Carbon Utilization and Storage (CUS) research group has been a truly rewarding experience. The knowledge, memories and valuable lessons gained here will remain with me throughout my life. I am deeply thankful to all members of EOR and CUS laboratory for fostering a positive and collaborative work environment. A special word of appreciation goes to my labmates, Bidesh Kumar Hembram, Manoj Kumar Yadav, R. Gautam, Prahlad Gurjar, Hari, Anjanay, and Ashim for their camaraderie, which made the lab both engaging and productive. I would also like to extend my sincere thanks to my seniors, Dr. Ramesh, Dr. Ravi Shankar, Dr. Krishna Raghav Chaturvedi, Dr. Abhishek Anand, and many others for their continuous encouragement and guidance. Their unwavering support has played a pivotal role in making my PhD journey truly memorable. I am genuinely grateful for all the help and kindness they have extended to me.

On a personal note, I wish to express my deepest gratitude to my husband Mr Jitendra Kumar, who has been my steadfast companion throughout this journey. His unwavering belief in my aspirations, his understanding during long hours of writing and research and his constant

emotional support made this achievement possible. I am equally grateful to my 8-year-old son Vivaan, whose patience, love and innocent encouragement filled my heart with strength during moments of exhaustion and doubt. Both of them stood by me without hesitation, providing the space and motivation I needed to keep going.

To my parents and in-laws, I owe a special debt of appreciation. Their faith in my goals, moral encouragement and support with family responsibilities allowed me to balance the demands of academic life with those of motherhood and family. Their understanding and kindness gave me the freedom to pursue this dream, even after embracing the responsibilities of parenthood. This thesis is especially meaningful to me as a woman who returned to academia after becoming a mother. The path was not always easy, juggling research with caregiving, deadlines with school runs, but it was deeply fulfilling. Every step forward was a testimony to resilience, and I am proud to share this accomplishment with those who believed in my ability to persevere.

Above all, I thank the Almighty for granting me the health, strength and determination to complete this doctoral work. There were moments of doubt, fatigue and setbacks, but with grace and perseverance, I have reached this goal. This thesis is not just the culmination of academic efforts, it is a tribute to the collective wisdom, patience and encouragement of every person who has walked this journey with me. To all of you, I extend my heartfelt thanks.

……Alpana Singh

Table of Contents

List of Figures

List of Tables

List of Abbreviations

CO_2	Carbon dioxide
CCS	Carbon Capture and Storage
CMC	Critical Micelle Concentration
DI	Deionized water
EDX	Energy Dispersive X-ray
FS	Natural Surfactant from Fenugreek Seeds
FTIR	Fourier Transform Infrared Spectroscopy
FESEM	Field Emission Scanning Electron Microscope
GHG	Greenhouse gas
G′	Elastic modulus
G′′	Viscous modulus
IFT	Interfacial tension
NPs	Nanoparticles
NSP	Nanofluid-surfactant-polymer
O/w	Oil in water
PAM	Polyacrylamide
SDS	Sodium dodecyl sulfate
SP	Surfactant-polymer
XRD	X-ray diffraction

Preface

The pursuit of sustainable solutions to modern engineering challenges has never been more urgent. As the world grapples with accelerating climate change, energy inefficiencies, and environmental degradation, the need for environmentally responsible materials and technologies has become paramount. This thesis is the result of a deep-seated commitment to advancing bio-based alternatives to synthetic chemicals traditionally used in various industrial processes. More specifically, it explores the extraction, characterization, and diverse applications of a natural surfactant derived from *Trigonella foenum-graecum* (commonly known as fenugreek)—a plant with a long history of traditional use, now reimagined as a key component in modern sustainable engineering.

The inspiration for this work originated from the intersection of green chemistry principles and indigenous knowledge systems. In many cultures, fenugreek seeds have been valued for their medicinal and nutritional properties. However, their potential as a source of surface-active biomolecules remains largely underexplored in the scientific literature. Recognizing this opportunity, I embarked on a multidisciplinary research journey to investigate how such a natural, biodegradable, and renewable resource could be harnessed to address pressing energy and environmental problems. From the outset, this research aimed to transcend conventional laboratory experimentation and address real-world challenges. Throughout the course of this work, emphasis was placed on both scientific rigor and practical relevance. The thesis presents not only the fundamental characterization of the natural surfactant but also its integration into complex systems, such as salt-resistant solvents, stable thermal emulsions and carbon entrapment platforms utilizing industrial waste. Each chapter builds upon the previous to form a coherent narrative that highlights both the depth and breadth of the research.

The early phases focused on developing an environmentally friendly method to extract surfactants from fenugreek seeds, ensuring that the process itself adhered to sustainable practices. This green extraction approach avoided toxic solvents and prioritized simplicity, scalability, and cost-effectiveness. The successful isolation of a stable and effective natural surfactant laid the foundation for further exploration into its functional capabilities. The subsequent stages of the research involved rigorous physicochemical characterization. Advanced analytical techniques were employed to evaluate the surfactant's surface activity, thermal behavior and colloidal stability. Special attention was given to understanding how this bio-surfactant behaves in varying saline and alkaline environments, which are typical of many industrial systems. The ability of the surfactant to maintain performance under such challenging conditions highlighted its potential for practical deployment in fluid management and thermal regulation.

This thesis also delves into the integration of the natural surfactant with nanomaterials. Specifically, hybrid nanofluids were developed by combining the surfactant with silica nanoparticles. These formulations were systematically tested for their thermal conductivity, dispersion stability, and rheological properties. Results demonstrated significant improvements in stability and thermal performance, positioning the hybrid systems as strong candidates for use in advanced heat transfer and energy storage technologies. In parallel, the surfactant's role in emulsion stabilization, particularly for phase change materials (PCMs) was investigated. The ability to form stable thermal emulsions has critical implications for the design of energy-efficient systems such as thermal batteries, heat exchangers, and building insulation materials. The findings confirmed that the fenugreek-based surfactant could effectively stabilize PCM emulsions, thereby enhancing their reliability and operational lifespan.

Beyond engineering systems, this research also touches upon environmental remediation. A novel aspect of the work involves combining the natural surfactant with industrial fly ash to explore its utility in carbon dioxide entrapment. This dual-purpose application not only offers a route for carbon capture but also contributes to circular economy models by repurposing industrial waste. The outcomes support the feasibility of using bio-surfactant-assisted materials in mitigating environmental pollution and reducing carbon footprints.

This thesis is dedicated not only to scientific advancement but also to a broader vision of sustainable development. The research presented herein will contribute to ongoing efforts in developing clean technologies, reducing environmental impact, and promoting the use of renewable, bio-based resources in engineering applications. This work inspires further exploration in the field of natural surfactants and encourages continued innovation toward a more sustainable and resilient future.

Thesis Organization

Chapter 1: This chapter outlines the global need for sustainable technological transformation, emphasizing the integration of green chemistry with traditional knowledge to develop bio-inspired, eco-friendly materials. It highlights the thesis's focus on harnessing natural surfactants for multifunctional performance in complex mechanical and energy systems. The chapter also explores hybrid innovations combining surfactants with nanotechnology for enhanced functionality, addresses environmental remediation through CO_2 entrapment and aligns the research with SGD 7 for sustainable and reliable energy solutions.

Chapter 2: In this chapter, natural surfactant was extracted from fenugreek seeds via Soxhlet extraction technique and characterized for mechanical and thermal fluid applications. FTIR, UV-Vis, MBAS, FESEM and surface tension analyses confirmed anionic saponins with strong surface activity, low adsorption, foamability and thermal stability, indicating suitability for fluid transport systems.

Chapter 3: In this chapter, physicochemical performance of a natural surfactant derived from fenugreek seeds was evaluated for its potential in mechanical and industrial systems. Surfactant exhibited strong surface activity, reducing interfacial tension effectively at low concentrations near its CMC (0.2 wt.%). Rheological analysis showed shear-thinning behavior, suitable for flow-based applications. Contact angle measurements indicated enhanced wettability, while stable foam formation under different conditions highlighted its applicability in foam-assisted transport. Its biodegradable, low-toxicity nature supports sustainable use in thermal, fluid and cleaning processes.

Chapter 4: In this chapter, emulsification behavior of paraffinic compounds was examined using a bio-derived surfactant synthesized from fenugreek seeds, targeting mechanical applications involving multiphase flow. Surfactant effectively reduced interfacial tension and stabilized paraffin–water emulsions, even under saline conditions. Optical microscopy revealed uniform droplet distribution, while rheological analysis indicated shear-thinning behavior suitable for dynamic flow environments. Micromodel experiments demonstrated improved phase displacement and reduced trapping in porous structures. These results highlight the surfactant's potential for use in sustainable, salt-tolerant fluid systems relevant to thermal management and flow control technologies.

Chapter 5: In this chapter, use of fenugreek seed-based natural surfactants to enhance fluid flow and displacement in porous microstructures was explored. Evaluations of interfacial tension, emulsion stability, and rheology demonstrated improved phase mobilization and thermal stability. Micromodel tests confirmed better sweep efficiency and reduced fluid trapping, underscoring the potential of bio-based surfactants in multiphase flow systems.

Chapter 6: In this chapter, stability and performance of emulsions were enhanced by combining a natural surfactant with single-step synthesized silica nanofluids. Two formulations: surfactant-polymer (SP) and nanoparticle-surfactant-polymer (NSP) were compared. NSP formulations outperformed SP, showing better interfacial tension reduction, thermal stability and droplet uniformity. Rheology, zeta potential and wettability results confirmed improved structure and stability, making NSP emulsions ideal for heat transfer and multiphase mechanical systems.

Chapter 7: In this chapter, use of natural surfactants in stabilizing n-PCM emulsions was explored for thermal energy storage (TES) applications in mechanical systems. Silica nanofluid-surfactant combination was developed to enhance emulsion stability and thermal efficiency of

PCM. Techniques like DSC, interfacial tension, microscopy, and rheology confirmed improved performance. Lower nanoparticle concentrations offered optimal thermal efficiency and long-term stability, making the system suitable for TES applications in energy management and mechanical heat exchange operations.

Chapter 8: In this chapter, a sustainable approach for CO_2 entrapment was developed using a natural surfactant derived from fenugreek seeds in combination with industrial fly ash. The combination enabled efficient CO_2 capture, as confirmed by pressure decay tests and microscopic analysis showing stabilized gas bubbles. FTIR revealed carbonate formation, indicating chemical interaction. This eco-friendly system offers a dual benefit of effective gas entrapment and industrial waste utilization in mechanical applications.

Chapter 9: In this chapter, thesis concludes by presenting an integrated view of bio-derived surfactants as multifunctional materials for mechanical and energy systems. Extracted from fenugreek seeds, the surfactants showed strong surface activity, thermal stability and compatibility with nanomaterials. Their use in stabilizing emulsions, managing multiphase flow, enhancing thermal energy storage and entrapping CO_2 through fly ash composites was validated. This work underscores the potential of green surfactants in fluid control, heat management and environmental remediation within mechanical applications, aligning with sustainability and circular economy frameworks.

Chapter 1

Introduction

1.1 Background

Surfactants, or surface-active agents, are compounds that possess the unique ability to alter surface and interfacial properties between different phases such as liquid-gas, liquid-liquid or liquid-solid [1] . Structurally, a surfactant molecule consists of two distinct components: a hydrophobic tail, typically composed of a hydrocarbon or fluorocarbon chain, and a hydrophilic head group, which may be ionic or nonionic in nature [2]. This amphiphilic configuration enables surfactants to adsorb at interfaces, resulting in a reduction of surface or interfacial tension and the stabilization of otherwise immiscible phases [3]. The fundamental function of surfactants lies in their ability to mediate interfacial interactions, which has led to their widespread adoption in various scientific and industrial sectors. Their applications span a wide spectrum ranging from detergency, emulsification and dispersion to wetting, foaming and solubilization [4]. In engineering systems, surfactants are crucial for enhancing fluid transport properties, improving heat and mass transfer and stabilizing multiphase systems [5]. Their utility is further evident in areas such as pharmaceuticals (drug delivery) [6], agrochemicals (pesticide formulation) [7], petroleum recovery (chemical flooding) [8], cosmetics [9], and environmental remediation (oil spill treatment, soil washing) [10].

Surfactants are commonly categorized based on the charge of their hydrophilic head group: anionic (negatively charged), cationic (positively charged), nonionic (no net charge), and

zwitterionic (carrying both positive and negative charges) as shown in Figure 1.1 [11]. Each type exhibits distinct physicochemical behavior, solubility profiles, and performance characteristics, allowing for tailored usage in specific applications.

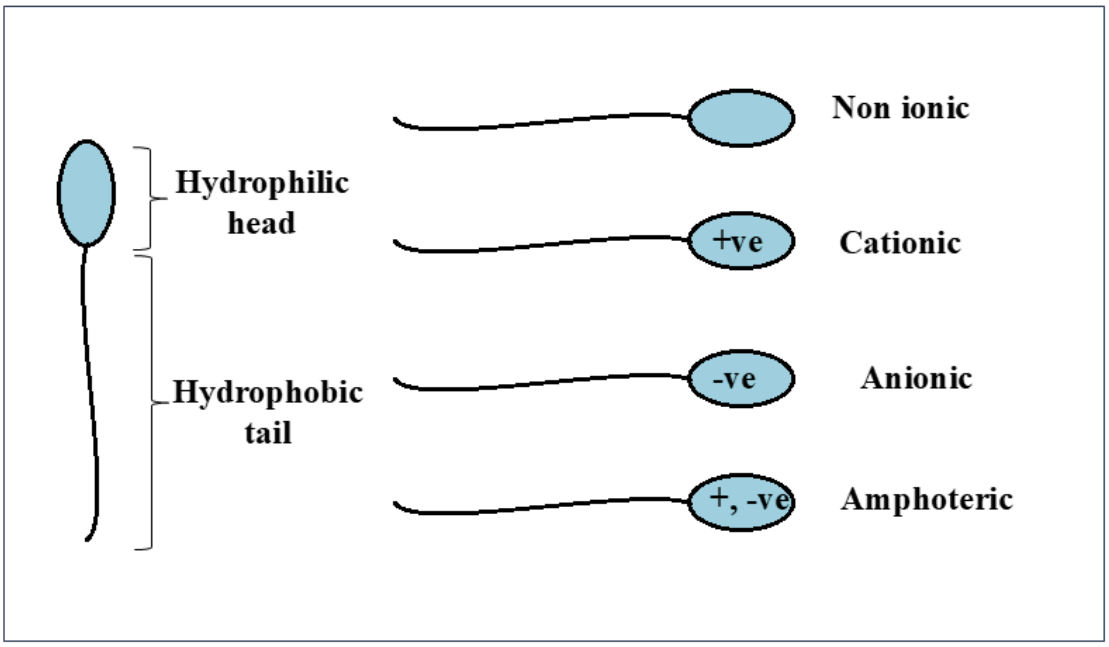

Figure 1.1: Classification of surfactants based on charge present on head group.

The surface activity of these molecules arises from their tendency to align at interfaces, thereby disrupting the cohesive interactions of molecules in one phase and facilitating interactions with another [12]. This results in reduced energy at the interface, promoting processes such as emulsification, micellization, and foam formation [13]. The ability of surfactants to form micelles in solution further extends their relevance in nanotechnology, colloidal science and advanced materials engineering [3,14,15]. Despite their widespread functionality, increasing attention is being directed toward the environmental sustainability and biocompatibility of surfactants issues that have sparked significant interest in alternative surfactant systems derived from natural or renewable sources. As such, understanding the fundamental role and mechanistic behavior of

surfactants is essential in advancing their application in green technologies, sustainable product design and novel functional materials.

1.2 Need of Natural Surfactants

The global transition toward sustainable technologies has intensified the search for materials that are not only functionally effective but also environmentally benign. Surfactants widely used across industries such as energy, pharmaceuticals and environmental management; are essential due to their amphiphilic structure, which enables them to reduce interfacial tension, stabilize emulsions and enhance phase interactions [16,17]. Traditionally, synthetic surfactants derived from petrochemicals have dominated the market due to their strong surface activity and broad utility. However, their environmental persistence, poor biodegradability and potential toxicity have raised significant ecological and health concerns [18]. Many synthetic surfactants tend to accumulate in soil and aquatic environments, posing risks to aquatic life and disrupting microbial ecosystems [19]. Their production often involves hazardous precursors and energy-intensive processes, further contributing to environmental degradation and carbon emissions. Residual traces of these compounds in water, personal care products and packaging materials have also been linked to allergenic and endocrine-disrupting effects [20]. As environmental awareness and regulatory scrutiny increase, the drawbacks of synthetic surfactants have become more apparent.

In response, natural surfactants derived from renewable sources such as plants, microbes, or agricultural residues are emerging as safer and more sustainable alternatives. These surfactants are typically biodegradable, less toxic and capable of performing a wide range of interfacial functions [21]. Their chemical structures, based on lipids, polysaccharides, proteins, or glycosides, offer flexibility and adaptability for diverse applications [22–24]. In addition to environmental

benefits, they enable the value-added utilization of bio-waste and support circular economy models. Given the urgent need to reduce dependence on fossil-based chemicals while meeting modern performance requirements, the development of natural surfactants represents a critical advancement. Their adoption supports global sustainability goals and opens new opportunities for innovation in green engineering, resource-efficient processes and environmentally responsible material design.

1.3 Status of Natural Surfactant

In recent years, natural surfactants have garnered increasing attention as viable and sustainable alternatives to synthetic, petroleum-derived surfactants. Their eco-friendly origin, inherent biodegradability and reduced toxicity make them highly suitable for a broad range of applications where environmental compatibility is essential [19]. Natural surfactants are broadly classified into two categories, that is, plant-based surfactants and bio surfactants. Plant based surfactants are the surfactants which are derived from plants whereas biosurfactants are the natural surfactants that are prepared by fermenting the natural substrate, for instance, alkane, sugar, oil and other waste in presence of microbes like yeast or bacteria [25,26]. With the recent advancement in the field of biotechnology, researchers have developed a new alternative to the chemical based synthetic surfactants by giving rise to biosurfactants that is prepared from microorganisms. Biosurfactants has a wide variety of applications in food processing industry, cosmetics industry, microbial enhanced oil recovery [27]. Apart from this biosurfactants have the applications in medicinal field which is due to its anti-microbial, anti-cancer, anti-viral activity and anti-adhesive agents [28].

In subsurface applications, surfactants play a major role by reducing interfacial tension at oil water interface and recover more oil in order to meet the rising demands. In drilling mud,

application of surfactants are quite popular as the surfactants are quite good at emulsifying and wetting [29]. In order to avoid various concerns of hazardous environmental impact associated with synthetic surfactants, natural surfactants are gaining enormous attention in the field of subsurface system and it is due to its economic feasibility and a viable option [30]. Rigano and Lionetti [31] reported the synthesis of a natural surfactant derived from Quillaja saponaria Molina, extracted from the Chilean soap bark tree. Since then, various natural surfactants have been explored for their potential in modifying interfacial properties. These compounds have demonstrated the ability to lower interfacial tension, reduce contact angles, and alter surface wettability making them valuable in a wide range of interfacial and colloidal systems. Chhetri et al. [32] prepared a natural surfactant derived from Soapnut pericarp which is further used for reducing interfacial tension (IFT) at oil-water interface from 19 mN/m to 2.5 mN/m. Ahmadi et al. [33] developed a novel surfactant derived from the leaves of Glycyrrhiza Glabra and reported that IFT reduction was around 69% in presence of surfactant solution and kerosene oil. Shahri et al. [34] formulated a natural surfactant from the leaves of the tree named Zyziphus Spina Christi and reported the reduction of IFT from 48 dyne/cm to 9 dyne/cm with kerosene oil. Ghahfaroki et al. [35] synthesized the natural surfactants from three new plant that are cationic in nature, derived from leaves of olives, spistan and prosopis. He reported the IFT reduction from 36.5 to 14 mN/m for Olives leaf surfactant, 36.5 to 20.5 mN/m for spistan leaf surfactant and 36.5 to 15.11 mN/m for prosopis leaf surfactant at distilled water and kerosene oil interface. Zhang et al. [36] highlighted the novel zwitterionic surfactant derived from castor oil which helps in reducing interfacial tension to a very low value of 5.4×10^{-3} mN/m at crude oil and water interface. Rahmati et al. [37] introduces two new class of cationic surfactants that are derived from leaves of mulberry and henna. Both the natural surfactant showed great results in reducing IFT, that is, mulberry

leaves surfactant helps to lower from 43.9 - 4.01 mN/m while henna leaves surfactants help to reduce 43.9 – 3.05 mN/m at distilled water and kerosene oil interface. Saxena et al. [38] developed a new anionic surfactant derived from palm oil which results in decreases the IFT to the ultra-low value of 1×10^{-3} mN/m at crude oil and distilled water interface at optimal salinity of 2 wt.% of NaCl. Isari et al [39] extracted a non-ionic surfactant derived from eucalyptus leaves which has shown results by reducing the value of IFT from 35.2 – 10.5 mN/m at oil water interface and contact angle reduction from 140.6º – 60.2º. Saxena et al. [40] synthesized a new anionic surfactant derived from mahua oil and has resulted in lowering the value of IFT to 10^{-2} mN/m at crude oil – water interface with a optimal salinity of 2% of NaCl. Machale et al.[41] explores a plant-derived surfactant extracted from Eichhornia crassipes for its interfacial performance and surfactant achieved a 37-41% reduction in IFT. As the surfactant concentration increased from 0 to 1 wt%, a notable reduction in contact angle was observed, decreasing from 65.74° to 37.5°, indicating effective surface wettability alteration. Magham et al.[42] used Passiflora plant extract as a natural surfactant for subsurface application. At 4 wt% CMC, it reduced IFT to 13 mN/m and contact angle to 55°, enhancing water-wetness.

Despite these encouraging laboratory-scale results, the translation of natural surfactants to industrial-scale processes remains limited. Several factors contribute to this gap, including inconsistent composition due to raw material variability, lack of standardized extraction and purification methods and challenges in maintaining performance uniformity across batches. In addition, cost-effective large-scale production and regulatory standardization are yet to be fully established, hindering their widespread commercial deployment. Moreover, the application of natural surfactants beyond subsurface systems is still underexplored. Their potential roles in fields such as thermal energy storage, colloidal stability engineering, carbon entrapment and industrial

waste treatment have not been fully realized. A comprehensive understanding of their structure-function relationship, performance in different media and synergistic behavior with other functional additives is essential to broaden their scope. This goal of this research focuses on the synthesis and application of a natural surfactant derived from fenugreek seeds. The study encompasses detailed physicochemical and interfacial characterization, followed by the evaluation of its performance across multiple engineering systems. Key areas include its salt tolerance, emulsification behavior, interaction with nanoparticles in colloidal systems, enhancement of phase change materials for thermal energy storage and its role in industrial waste utilization for CO_2 entrapment. The work aims to establish the surfactant's multifunctionality, environmental compatibility and potential for integration into sustainable material and fluid systems. Finally, the objectives of this PhD work are presented.

1.4 Surfactant based Emulsions

Emulsions are thermodynamically unstable systems composed of two immiscible liquids, typically oil and water, where one phase is dispersed in the other in the form of droplets [43]. The stability and formation of emulsions depend largely on the presence of surfactants, which are amphiphilic molecules containing both hydrophobic and hydrophilic groups. These molecules adsorb at the oil-water interface, significantly reducing IFT and facilitating the formation of smaller, more stable droplets as shown in Figure 1.2 [44]. Surfactants play a critical role in droplet size distribution within emulsions. By lowering the interfacial free energy, they reduce the tendency of dispersed droplets to coalesce. Additionally, the formation of a surfactant layer around droplets provides a physical and, in some cases, electrostatic barrier that further resists aggregation and phase separation.

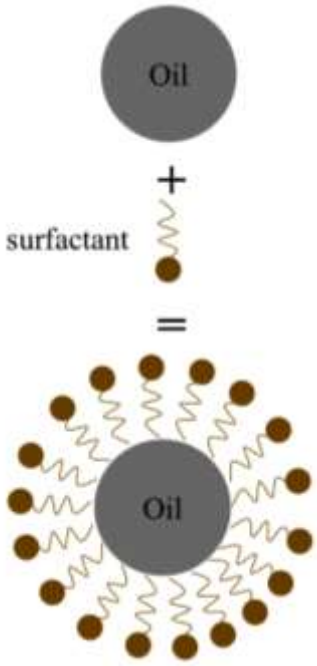

Figure 1.2: Schematic representation of surfactant's role in stabilizing oil droplets by reducing interfacial tension and preventing coalescence.

The type and concentration of surfactant, along with system parameters such as pH, salinity and temperature, strongly influence the emulsion characteristics. Several studies have examined the effectiveness of surfactants in stabilizing emulsions [45–49]. Figure 1.3 shows a schematic overview of primary mechanisms responsible for emulsion destabilization, including coalescence, creaming, flocculation, and Ostwald ripening. These processes collectively influence the stability and lifespan of emulsified systems. For instance, Golemanov et al.[50] investigated the formation of paraffin-in-water emulsions using a mixture containing 15 mL of oil and 35 mL of surfactant solution under mechanical stirring. Their findings highlighted that nonionic surfactants, such as Tween-20 and Tween-60, significantly enhanced the stability of hexadecane emulsions.

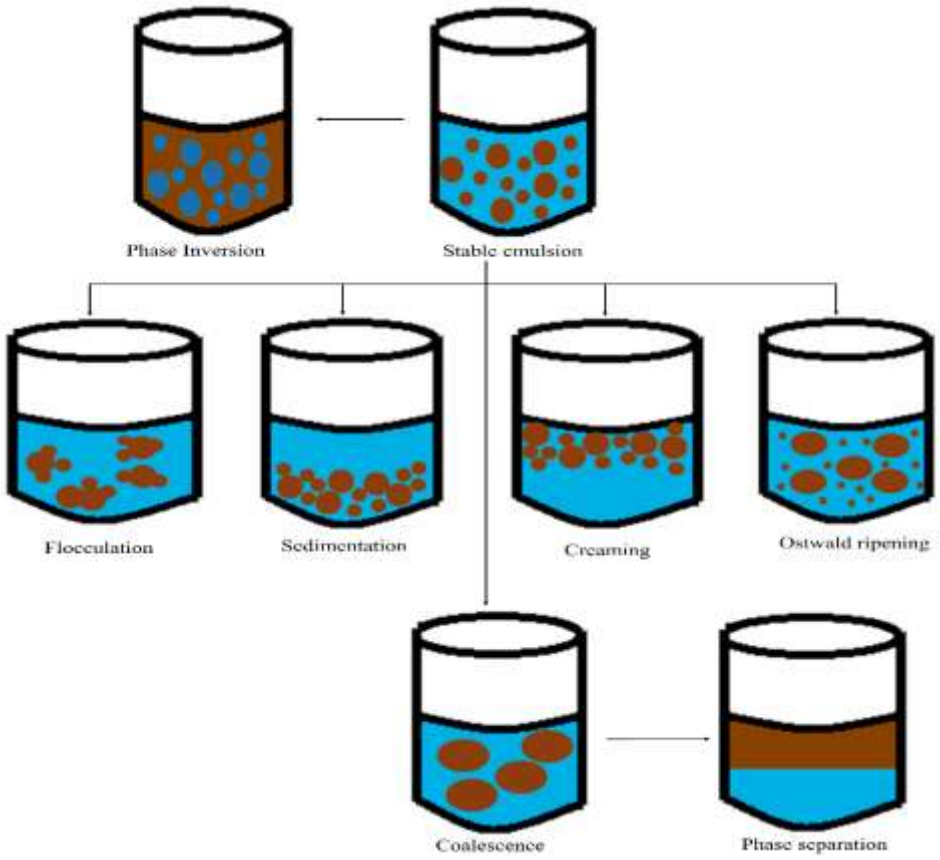

Figure 1.3: Schematic illustration of emulsion destabilization mechanisms.

In engineered systems, emulsions stabilized by surfactants are widely used in areas such as food processing, pharmaceuticals, cosmetics and materials engineering [16,51]. More recently, natural surfactants have gained attention due to their biodegradable and eco-friendly nature, offering a sustainable alternative to conventional synthetic emulsifiers. Kumar and Mahto [52] investigated a natural surfactant derived from sunflower oil for stabilizing heavy crude oil emulsions. A formulation containing 60% heavy crude oil and 2 wt% surfactant remained stable at 25 °C. Nafisifar et al.[53] extracted a natural surfactant from linseeds, referred to as PELS, and evaluated its ability to stabilize crude oil emulsions. The emulsion was prepared at the critical micelle concentration (CMC) of PELS using ultrasonication. Initial stability was maintained for approximately two weeks, after which phase separation began, leading to complete separation of

oil and water within six weeks. A natural surfactant obtained from the bark of the Quillaja saponaria Molina tree was utilized to stabilize medium chain triglyceride (MCT) oil-in-water emulsions. The resulting emulsion demonstrated droplet sizes below 200 nm and maintained excellent physical stability for over a month [54]. Pal et al.[55] studied a Gemini surfactant from sunflower oil (CMC: 0.1496 mM at 303 K) for stabilizing n-heptane-in-water emulsions. Initial droplet sizes ranged from 0.25–3.1 μm, which increased to 0.64–6.2 μm after 15 days, indicating moderate stability. These studies collectively highlight the promising potential of natural surfactants in stabilizing emulsions across various systems. Their ability to form and stabilize emulsions, especially under varying environmental conditions, opens avenues for applications in energy storage systems, waste treatment, and controlled delivery technologies.

1.5 Surfactants in Salt Environment

Surfactants in saline environments face unique challenges due to the presence of high concentrations of dissolved salts, which can significantly influence their interfacial behavior, solubility, and overall effectiveness. Elevated ionic strength can lead to compression of the electrical double layer around surfactant molecules, promoting micelle formation at lower concentrations but also increasing the risk of precipitation or phase separation, particularly for ionic surfactants as shown in Figure 1.4. In such conditions, surfactant performance including interfacial tension reduction, foam stability and emulsification may be compromised. Therefore, the selection of surfactants with high salt tolerance, or the development of formulations using zwitterionic, nonionic, or natural surfactants, is critical for maintaining stability and functionality. Understanding surfactant behavior in saline media is especially important for applications such as subsurface fluid displacement, wastewater treatment, and marine-based processes where salt levels are inherently high.

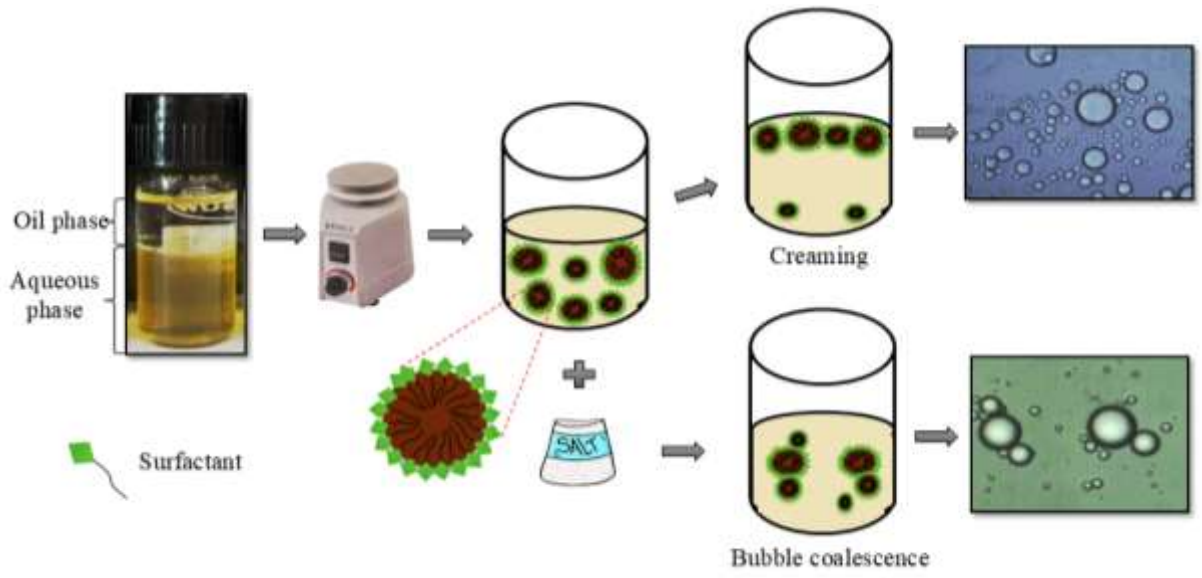

Figure 1.4: Schematic representation of effect of salt concentration on a surfactant-stabilized system.

SDS surfactant improved silica nanofluid stability in saline conditions, extending dispersion from ~4 to ~7 weeks and maintaining rheological performance up to 3 wt% NaCl. Oil recovery increased from 48% to 55% OOIP at 3 wt% salinity, showing strong potential for saline reservoir applications [56]. A study evaluated SDS-based micellar flooding for crude oil emulsification under high salinity (0-4 wt% NaCl/$CaCl_2$) and temperature (40-98 °C). Emulsion stability declined with rising salt concentration more so with $CaCl_2$ and at elevated temperatures due to droplet coalescence [57]. AGES surfactants exhibited ultralow interfacial tension and strong oil solubilization near optimal salinities (ranging from <1% to >20% NaCl) at 85-120 °C. However, phase separation (cloud point) occurred at 120 °C. Blending AGES with IOS surfactants resolved this, producing stable, single-phase solutions even in synthetic seawater, making them suitable for subsurface system in high-temperature, high-salinity reservoirs [58].

In contrast, natural surfactants, derived from plant or microbial sources, have emerged as promising alternatives to synthetic agents due to their biocompatibility, biodegradability and structural adaptability. These surfactants often contain functional groups such as hydroxyl, carboxyl, or glycosidic linkages, which contribute to their surface activity and enable them to form stable emulsions even under high salinity. Their amphiphilic nature allows them to adsorb at oil–water interfaces, reduce interfacial tension, and prevent droplet coalescence. A polymeric surfactant (PMES) synthesized from castor oil showed strong IFT reduction at 5000 ppm concentration, reaching 5.42×10^{-3} mN/m at 4 wt% NaCl. This was due to enhanced interfacial adsorption at higher salinity. Natural surfactants further improved performance, with 4 wt% NaCl identified as optimal for the 1:0.5 surfactant-to-acrylamide ratio [59]. Natural surfactant synthesized from palm oil via transesterification, demonstrated strong salt tolerance. At its critical micelle concentration (8000 ppm), no precipitation was observed between 1% and 7% NaCl. However, surfactant precipitation began at 8% NaCl, indicating stability up to 7% (70,000 mg/L) salinity [38]. Although reported studies demonstrate the potential of natural surfactants in saline environments, further investigation is essential to fully understand their performance, stability and applicability under diverse and extreme salinity conditions relevant to real-world industrial systems. In saline media, natural surfactants offer enhanced stability through steric and electrostatic mechanisms, making them suitable for applications such as enhanced oil recovery, emulsification and CO_2 entrapment where salt concentrations are high and chemical compatibility is essential.

1.6 Nanofluid and their interaction with Surfactant

Nanofluids are engineered colloidal suspensions consisting of nanoparticles dispersed in a base fluid, developed to enhance thermal, rheological or interfacial properties beyond those of

conventional fluids [60]. Due to their high surface area and tunable physicochemical characteristics, nanoparticles in nanofluids significantly improve heat transfer, stability, and transport behavior, making them attractive for industrial applications [61,62]. The interaction between surfactants and nanomaterials presents a synergistic mechanism that enhances the functional performance of both components as shown in Figure 1.5.

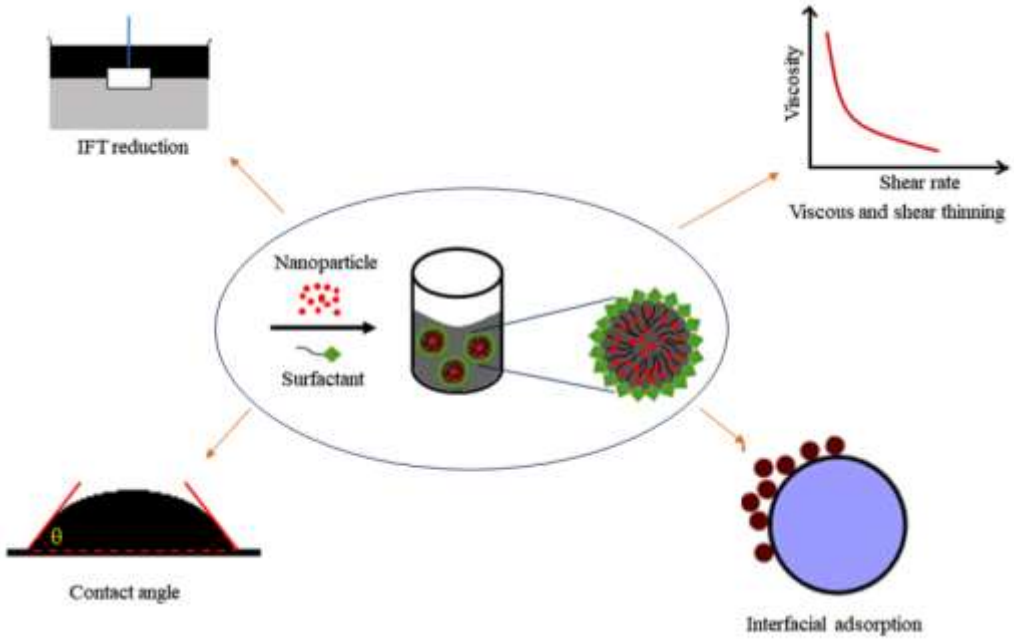

Figure 1.5: Representation of surfactant-nanoparticle interaction enhancing colloidal stability.

Surfactants, when combined with nanoparticles, can significantly improve dispersion stability by reducing interparticle attractions and preventing agglomeration. This stabilization is achieved through electrostatic repulsion, steric hindrance, or a combination of both, depending on the surfactant type and surface chemistry of the nanoparticles [63]. In turn, nanoparticles can influence the interfacial behavior of surfactants by modifying micelle formation, surface adsorption characteristics, and interfacial film strength. Such synergy can result in improved rheological properties, enhanced interfacial activity and more robust emulsion or foam

stabilization. These combined systems are particularly effective in complex environments, including high-salinity or high-temperature conditions, where conventional surfactant or nanoparticle systems may fail independently. Rezvani et al.[64] formulated a surfactant–nanoparticle blend using epoxysilane-modified silica and zwitterionic/nonionic surfactants to enhance oil recovery in calcite-rich reservoirs. The system showed pH-responsive behavior and improved interfacial performance. Oil recovery increased by 36 ± 1% OOIP with surfactant alone and by an additional 14 ± 0.5% OOIP with 0.01 wt% nanoparticles. Farhadi et al.[65] studied CO_2 foam stabilized by silica nanoparticles and a cationic surfactant. Using a novel adsorption index, it was found that foam stability depended on both surfactant and nanoparticle concentrations. The foam showed a peak viscosity of 6.03 cP, about 9 times higher than CO_2/water, linked to maximum adsorption and hydrophobicity. Also, SDS-silica nanoparticle formulation was tested at 20 MPa and 70 °C, showing effective wettability alteration of oil-wet carbonate to water-wet. Contact angle and imbibition tests confirmed its potential for subsurface applications under varying salinity and rock conditions [66]. Recent trends have explored the use of natural surfactants in nanofluid systems to improve sustainability, offering environmentally friendly alternatives without compromising performance. Saponin from natural surfactant (Glycyrrhiza glabra) and hydrophilic silica nanoparticles were used to reduce IFT and enhance oil mobility. Adsorption on carbonate rock showed rapid initial uptake followed by slower adsorption, with results fitting kinetic and equilibrium models [67]. Another study evaluated a natural surfactant (Reetha) combined with xanthan gum and silica nanoparticles to enhance heavy crude oil recovery. Core flooding tests showed 18.5% oil recovery with the surfactant–polymer system, which increased to 27.3% with the addition of nanoparticles, confirming the effectiveness of the nanofluid approach [68]. A separate study used a natural surfactant from Cyclamen persicum (CP) in combination with

ZnO/MMT nanocomposites to enhance interfacial properties. At optimal surfactant concentration, IFT and contact angle were reduced by 57.78% and 61.58%, respectively. The CP-ZnO/MMT hybrid nanofluid improved wettability and IFT performance, especially in the presence of NaCl. Core flooding tests showed oil recovery factor improvements of 8.2% (CP), 6% (ZnO/MMT), and 13% (hybrid), demonstrating strong synergistic potential [69]. The cooperative behavior between natural surfactants and nanomaterials opens new pathways for developing advanced formulations used in applications such as controlled release systems, enhanced fluid mobility and thermal energy storage. Recent attention has turned toward natural surfactant nanoparticle systems, offering not only performance benefits but also improved environmental compatibility and sustainability.

1.7 Surfactant in Thermal Energy Storage

Thermal energy storage (TES) systems play a vital role in enhancing energy efficiency and enabling the integration of renewable energy sources. Among various TES technologies, latent heat storage using phase change materials (PCMs) has gained significant attention due to its high energy storage density and ability to operate at nearly constant temperatures during the phase transition process [70]. PCMs store and release thermal energy through solid-liquid transitions, making them suitable for applications such as solar thermal systems, waste heat recovery, building energy management and thermal regulation in electronic devices. Despite their advantages, many PCMs suffer from challenges such as low thermal conductivity, phase segregation, subcooling and leakage during the liquid phase, which limit their practical applicability [71]. To address these issues, researchers have explored various approaches including the use of encapsulation, composite systems, and functional additives. One promising strategy involves the use of surfactants, which improve the stability and uniformity of PCM-based systems, especially in

emulsified or nano-enhanced formulations. Surfactants, due to their amphiphilic nature, can reduce interfacial tension and promote the dispersion of immiscible components, thus enabling the formation of stable PCM emulsions or micro/nano-encapsulated systems as shown in Figure 1.6. In water-in-oil or oil-in-water PCM emulsions, surfactants help maintain droplet integrity and prevent coalescence during repeated melting and solidification cycles. Additionally, in nano-PCM systems, surfactants aid in dispersing thermally conductive nanoparticles, enhancing heat transfer and maintaining system homogeneity over time.

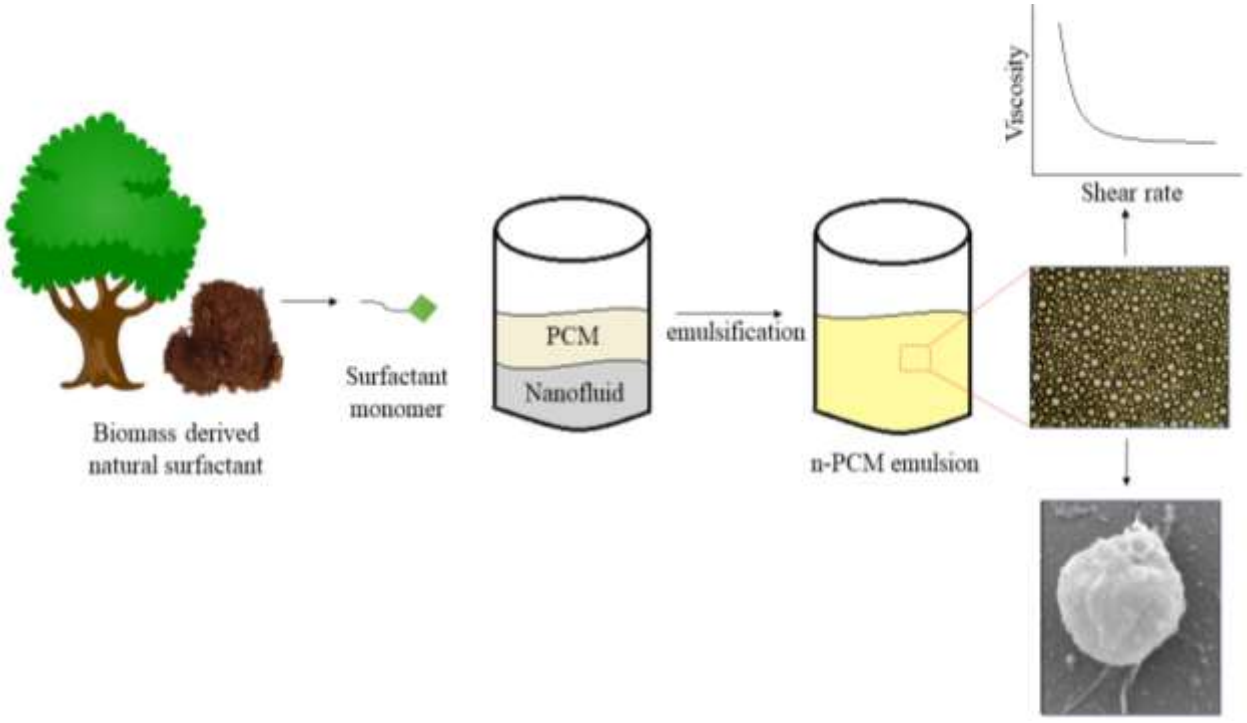

Figure 1.6: Role of surfactant in stabilizing n-PCM (nano-phase change material) emulsions, enhancing thermal performance and dispersion for sustainable energy storage applications.

Chen et al. [72] developed a phase change emulsion using the phase incursion technique, incorporating tetradecane microparticles dispersed in water. The emulsion featured a melting point of 277.7 K and a latent heat of fusion of 73.47 kJ/kg. Zhang et al. [73] formulated a water-based

phase change emulsion for solar thermal applications using n-octacosane as the PCM, which melts at 60 °C. A binary blend of synthetic surfactants (Span and Tween in a 1:1 mass ratio) was employed for emulsification, while SiO_2 nanoparticles (7-40 nm) served as nucleating agents to enhance phase transition performance. Reported studies on PCMs rely on synthetic surfactants for emulsion stabilization and performance enhancement. However, the potential of natural surfactants in PCM systems remains largely unexplored. Exploring bio-based surfactants could offer a sustainable alternative with reduced environmental impact, making it a relevant and timely area for further research. Thus, the incorporation of natural surfactants into PCM-based TES systems not only improves thermal performance but also contributes to long-term material stability and scalability in real-world applications.

1.8 CO_2 utilization with Natural Surfactant

The rising concentration of atmospheric carbon dioxide (CO_2) due to industrial emissions is a major contributor to global climate change. To mitigate its environmental impact, carbon capture, utilization, and storage (CCUS) technologies have emerged as critical strategies. Among various approaches, CO_2 entrapment the process of capturing and immobilizing CO_2 within solid or semi-solid matrices offers a promising route for long-term carbon sequestration, particularly in geologic formations, porous media, and reactive materials [74]. However, the effectiveness of CO_2 entrapment is often limited by poor fluid-solid interaction, insufficient dispersion and low contact area between CO_2 and trapping media. In this context, surfactants play a crucial role by enhancing interfacial interactions, improving CO_2 solubilization and promoting better distribution within the trapping matrix. Their amphiphilic nature enables them to reduce interfacial tension and stabilize emulsions or foams that can improve CO_2 mobility control and retention in porous structures. Furthermore, surfactants can facilitate CO_2 capture when combined with mineral or industrial

waste materials such as fly ash, allowing the formation of stable CO_2-containing phases like carbonates. A wide range of waste products were explored in literature, for instance, steel slag [75], basic oxygen furnace slag [76], blast furnace slag [77], concrete [78], fly ash [79], Sugarcane bagasse fly ash [80]. Reddy et al.[81] were among the first to explore the enhancement of fly ash mineralization through aqueous carbonation methods. Sun et al.[82] utilized brown coal fly ash from Latrobe Valley, Australia, for CO_2 sequestration via indirect mineralization under relatively mild conditions. Their study reported a maximum CO_2 capture capacity of 264 kg per tonne of fly ash. Qian et al.[83] modified municipal solid waste (MSW) fly ash using anionic chelating surfactants specifically ethylenediaminetriacetic acid lauryl and monolauryl phosphate. The results showed that fly ash treated with ethylenediaminetriacetic acid lauryl exhibited a higher activation efficiency, achieving an active ratio greater than 95%, compared to the performance of monolauryl phosphate.

Figure 1.7: Potential of natural surfactant in enhancing CO_2 entrapment through interaction with industrial waste matrix, promoting sustainable carbon storage.

The presence of surfactants can also enhance the wettability of solid surfaces, supporting stronger interactions between CO_2-rich phases and the host matrix. While above mentioned studies have examined the role of synthetic surfactants in enhancing CO_2 entrapment processes, the application of natural surfactants in this area remains largely unexplored. The use of natural surfactants in this process introduces additional benefits, offering biodegradable and non-toxic alternatives to synthetic agents, thus aligning the CO_2 entrapment process with broader goals of sustainability and green chemistry as shown in Figure 1.7. Therefore, this study explores the integration of a plant-derived surfactant with reactive solid waste (fly ash) to evaluate its potential in capturing and stabilizing CO_2, thereby contributing to environmentally responsible carbon management.

1.9 Motivation

The increasing demand for sustainable and eco-friendly alternatives to conventional chemical agents has driven the exploration of natural surfactants. Their potential in enhancing interfacial phenomena, stability under saline conditions and multifunctionality across energy and environmental applications remains underutilized. This research is motivated by the need to synthesize, characterize and use a plant-derived surfactant for advanced applications such as emulsification, nanoparticle stabilization, thermal energy storage and CO_2 entrapment addressing both performance and environmental concerns.

1.10 Objective

The objective of the study includes synthesis, characterization and study the performance evaluation of bio derived surfactants for emulsification, carbon entrapment and thermal energy storage.

1.11 Scope

This study focuses on the synthesis of a natural surfactant from fenugreek seeds and its comprehensive physicochemical characterization. The research explores its application in stabilizing paraffinic emulsions under saline conditions, enhancing multiphase fluid mobility through pore-scale analysis and investigating synergistic interactions with nanoparticles in colloidal systems. Additionally, role of surfactant in improving thermal performance of phase change materials and facilitating CO_2 entrapment via industrial waste utilization is examined. The work aims to establish the surfactant's multifunctionality across energy and environmental domains, offering a sustainable alternative to synthetic agents.

1.12 Novelty of Research

This research presents a novel natural surfactant derived from fenugreek seeds with multifunctional applications. Its effectiveness is demonstrated in stabilizing emulsions under saline conditions, enhancing nanoparticle dispersion and improving thermal properties of phase change materials. Additionally, the integration of the surfactant with industrial fly ash for CO_2 entrapment presents a unique approach to waste valorization. The study offers a sustainable, biodegradable alternative to synthetic surfactants for advanced energy and environmental applications.

Chapter 2

Natural Surfactant for Sustainable Carbon Utilization in Cleaner Production of Fossil Fuels: Extraction, Characterization and Application Studies

Abstract

In this study, the extraction, characterization, and performance evaluation of a green surfactant, derived from bio-resource (Fenugreek seeds), is reported for effective carbon utilization in subsurface applications. Several characterization tools such as Fourier-transform infrared spectroscope, ultraviolet–visible spectroscope, methylene blue active substance test, surface tension tests, and scanning electron microscope were used to confirm saponin (surface activity) in synthesized surfactant and suitably compared with the properties of conventional surfactants in literature. The prepared green surfactant exhibited anionic behavior as validated by elemental analysis and adsorption studies. The critical micellar concentration of surfactant was determined by surface tension and electrical conductivity and its value was found to be around 0.2 wt%. Carbon dioxide absorption potential of green surfactant was envisaged by molality tests which confirmed that carbon dioxide absorption rate of surfactant was 7-18% higher than pure water. As a result, the surfactant showed high foam volume (> 40 ml) and foaming stability (8-10 h). The high temperature performance was also better. At 90 ^{o}C, carbon dioxide bubbles of larger size were present in sufficient quantity which indicated that foaming potential of surfactant was not severely affected by temperature. During adsorption studies, the green surfactant solution showed a mass-loss of 48-60% on a sandstone surface, which is better than the one of a conventional surfactant. It also showed superior property than conventional surfactants in adsorption isotherm

investigations. Thus, the use of these green surfactants in subsurface scenario for carbon utilization and oil recovery from a porous media is recommended.

2.1 Introduction

Every research, involving use of surface active agents, is usually dominated by surfactants and as a result, they have received wide attention in areas such as pharmaceuticals, cosmetics, detergents, bioremediation, emulsions, and enhanced oil recovery (EOR) [84–87] Among other applications, EOR is currently in greater demand to meet surplus requirements of energy. Thus, it is important to improve the efficacy of current chemical-EOR processes and design a surfactant that not only forms greater o/w emulsion through interfacial tension (IFT) reduction of crude oil but also reduces environmental impact of these chemicals in oilfield [88]. These surfactants are good at emulsification, foaming, and thickening functions which are highly preferred in oil recovery mechanism. However, the design of most of these surfactants is based on the utilization of toxic chemicals which not only lead to hazardous environmental issues but also show greater adsorption on surface of reservoir rocks which is a kind of formation damage [89]. In addition, they are hazardous to aquatic life and human health resulting their non-biodegradable nature makes them environmentally a non-viable option. Thus, due to greater demands of energy and necessity to reduce environmental impact of synthetic surfactants, researchers seek alternate solutions for effective utilization of surface-active agents in EOR.

Green extraction of surfactant is gaining enormous attention of researchers, since it is cost effective, abundantly available, eco-friendly, and can be extracted using simple methods than chemically synthesized surfactants [90]. Depending upon the method of preparation, surfactants are broadly categorized as synthetic and natural surfactants [91]. In coming era, natural surfactants can be proven a great alternative to non-biodegradable and toxic chemical-based surfactants in

chemical EOR [92]. Jensen used Soxhlet apparatus to extract natural surfactant from plant material that could be dried in sunlight before obtaining it in powdered form [93]. During extraction process, the temperature was kept same as that of boiling point of solvent. Soxhlet apparatus has been the most commonly used method in surfactant extraction from different plant-based sources.

On the basis of origin, natural surfactants are categorized as plant-based surfactant and bio-surfactant. Plant-based surfactants are naturally driven from plants whereas bio-surfactants are produced by fermentation process in presence of microbes [94]. Saponin is a major content present in natural plant-based surfactants. Saponin originates from the word "sapo" which means soap or natural detergent [95]. As a result, natural surfactants exhibit unique foaming and emulsifying properties as reported by researchers for soap nut shells [32], zyziphus spina Christi [34], prosopis [35], Chamomilla [25], and Eucalyptus [39]. Natural surfactant extracted from natural oil, *i.e.*, castor oil, palm oil, jatropha oil, and other vegetable-based resources have also shown potential in lowering IFT at oil-water interface and in altering wettability of rocks from oil-wet to water-wet [96]. Natural surfactants can also be titled as green surfactants due to their less toxicity and non-hazardous nature to environment resulting these surfactants exhibit various advantages over chemically extracted surfactants. The trends have shown a rise in accelerating the use of natural surfactants in EOR studies. Chhetri et al. extracted a natural surfactant from Soapnut fruit pericarp which shows remarkable performance in reducing IFT between crude oil and water interface from 19 to 2.5 dyne/cm with surfactant concentration from 0 to 12 w/w% [32]. Ahmadi et al. used spray drying technique to develop a natural surfactant, called Glycyrrhiza Glabra, which helped in reducing IFT between kerosene and water from 33 to 9 mN/m (~70% reduction than 52% with alkyl poly glycosides and 41% with alkyl sulfate) [97]. Zhang et al. prepared a natural surfactant from castor oil and it was quite efficient in oil recovery process due to significant lower value of

IFT at crude oil - water interface, *i.e.*, 5.4×10^{-3} mN/m with just the concentration of 0.010 g/L of aqueous solution without any extra alkali [36]. Muntaha and Khan conducted comparative analysis between natural surfactant (Soapnut fruit pericarp) and chemical based surfactants [Sodium Dodecyl Sulphate (SDS)] using surface tension measurements, where natural surfactant was recommended over synthetic surfactant due to its environmentally friendly nature and cost effectiveness [98]. Isari et al. introduced a novel natural surfactant of Eucalyptus and during measurements, its capability to reduce oil-water IFT from 35.2 to 10.5 mN/m and contact angle from 140.6°-60.2° was regarded remarkable for oil recovery applications [39]. Saha et al. focused on studying interaction of natural surfactant (from reetha) with polymer and silica nanoparticles and examined its role on improved oil recovery [68]. It was found that 18.5% additional oil recovery was achievable with surfactant-polymer combination, which further increased to 27.3% in presence of silica nanoparticles. Despite vital importance for natural surfactants in oilfield applications, previous studies focused on plant-based natural surfactants and no literature reported extraction, characterization, and performance evaluation of green surfactant from trigonella foenum-graecum as far as we are aware.

Thus, in this study, we report the extraction of a new surfactant from natural source, *i.e.*, trigonella foenum-graecum followed by its characterization by different techniques such as Fourier Transform Infrared Spectroscopy (FTIR) and X-ray Photoelectron Spectroscopy (XPS) to confirm the presence of functional groups. To confirm the purity of synthesized surfactant, techniques such as Field Emission Scanning Electron Microscope (FESEM) and Energy Dispersive X-ray Analysis (EDX) mapping were used. Critical micelle concentration (CMC) of surfactant was determined by electrical conductivity measurements at ambient conditions. It was expected that synthesized surfactant will work as good surface-active agent and its performance will be comparable with

conventional surfactants in literature. for subsurface applications will be comparable with conventional surfactants in literature. The application of green surfactant was tested through foaming potential on the development of CO_2 foams for carbon capturing in subsurface environment, since CO_2 foam followed by its injection in depleted oil and gas reservoir is the best method to reduce the carbon foot prints from environment [99]. CO_2 foams will not only lead to capturing of carbon in surfactant networks but also minimize greenhouse emissions, and the use of a natural surfactant will further make the process more sustainable and environmentally friendly.

2.2. Materials and Methods

2.2.1. Materials

For this study, fenugreek seeds were collected from local commercial outlet in Amethi, India. The solvent methanol was purchased from SD Fine Chemicals, India. The aqueous solutions of synthesized surfactant were prepared using deionized water (DI), which was obtained from a Millipore® Elix-10 water purification apparatus. Soxhlet apparatus and hot air oven were purchased from Jain Scientific Glassworks, India. The sand was obtained from a commercial vendor and it was washed using a saline solution of 4wt% NaCl followed by drying and sieving (ASTM, Nunes Instruments, India) to attain uniform sand size of 200-380 μm before use [100]. CO_2, of purity 99.95%, was obtained from Sigma Gases, India and used as received.

2.2.2. Extraction of surfactant from fenugreek seeds

The surfactant was extracted by fenugreek seeds using procedure outlined as follows. First, fenugreek seeds were dried in sunlight (for 10 days) to remove excess moisture content followed by drying in hot air oven for 0.5 h at 50°C. This process removed most of the moisture from the seeds and the dried seeds were grinded in an industrial grinder (Oster, India). The obtained powder

was carefully sieved using a standard sieve to remove any coarse grains and only the fine powder of 100-240 μm seeds was used in extraction process. The extraction process was performed using a laboratory grade Soxhlet apparatus [93]. During extraction process, 50 g of sample was wrapped in a muslin cloth (a pouch, made to completely encapsulate powder) and the pouch was placed inside extraction chamber that contained vapor and siphon tubes. Before its use in synthesis, Muslin cloth was hand washed in cold water (with any detergent) and dried under the sun. Then, muslin cloth was dipped in methanol and left undisturbed for 48 h to ensure that any adsorbed surface-active agent had been removed. The entire arrangement was mounted on a heating mantle at 65°C. Methanol is preferred because not only does it has a lower boiling point (64.7°C), as compared to other conventional solvents. Methanol also takes very less time to evaporate at temperature > 65°C. Thus, it is used as solvent for this study. As the temperature of solvent reached to boiling point, the vapor proceeds to condenser where it gets condensed and returned to the extraction chamber. In extraction chamber, the extracted solutes (surfactant) move downward towards round bottom flask. The entire process was repeated for at least 48 h to complete the extraction process of surfactant.

The extracted liquid (a highly concentrated solution of surfactant) was removed from the round bottom flask and heated in an oven at 70°C for 24-48 h to remove any excess solvent that might be present in the system. The dried residue was grinded manually using a mortar and pestle and the grinded extract was referred as green surfactant in powder form, which was dissolved in DI water for the development of surfactant solution in various characterization and experimental studies. The surfactant yield was determined as 12.76 ± 11% gm using raw material of 100 gm of fenugreek seeds. The cost of fenugreek seeds is Rs 88 for 500 gm and extraction was done by using methanol (Rs 920 for 500 ml) as a solvent. Whereas the commercial surfactants like SDS

(sodium dodecyl sulphate) cost for Rs. 620 for 500gm, CTAB (Cetyltrimethylammonium Bromide) cost for Rs 2440 for 500 gm. The prices are approximate and can vary depending on the supplier, quantity purchased, and purity of the product. Natural surfactants derived from agricultural products like fenugreek seeds may be more expensive due to the extraction processes and raw materials used, but they offer advantages such as biodegradability and reduced environmental impact, making them valuable in various applications.

2.2.3. Characterization of green surfactant

After the extraction of green surfactant, its characterization was performed by Fourier Transform Infrared (FTIR) to confirm the presence of functional groups in final product. FTIR was performed by in-built spectrometer (PerkinElmer®, USA). An attenuated total reflectance (ATR) was used to obtain FTIR spectra of surfactant as this enables surfactant analysis to be performed in liquid state. This IR spectra was collected at 4 cm^2 spectral resolution by utilizing data collection time of 1 min [101]. Elemental composition and chemical bonding states of the synthesized natural surfactant was determined by XPS analysis. The dried sample was mounted on a conductive holder using carbon tape and analyzed using a monochromatic Al Kα source. FESEM analysis was performed to visualize the morphology of synthesized surfactant and for that, Nova NanoSEM with range of 0.2-30 kV was used. In addition, gold coating was performed on sample for 30 s using gold sputter coating unit (JEC 3000: JEOL). The elemental composition of synthesized surfactant was also analyzed by Energy Dispersive X-Ray Analysis (EDX) (Model: Carl Zeiss Evo 50, attached to SEM unit).

To determine the charge of surfactant, the commonly used methylene blue analytical method was used [20]. For this, methylene blue reagent was prepared as per the method in literature

and other steps were followed accordingly [20]. A spectrophotometer (UV 3200, Lab India) with an optical cell path length of 10 mm was used for this investigation.

2.2.4. CMC determination of green surfactant

Critical micelle concentration (CMC) of natural surfactant was determined by surface tension (SFT) measurements using the Wilhelmy plate method [102]. For this, synthesized surfactant was added to DI water in small increments of 0.04 wt% and the value of SFT measured until no significant change in SFT was evident. The value of CMC was also confirmed by electrical conductivity method [103]. Conventionally, at low concentration (of surfactant), electrical conductivity of solution is governed by monomers while beyond CMC, it is dominated by micelles and only few monomers contribute in it. This yields a change in the slope of electrical conductivity at CMC value of surfactant.

2.2.5. Molality and foaming potential of natural surfactant

CO_2 absorption studies were performed using a custom designed setup manufactured by D-CAM Engineering, India. The similar setup has been also used in our previous studies [104,105], based on CO_2 absorption in different aqueous solvents. The setup comprised of a stirring pot of capacity 100 ml, a thermocouple, and a pressure gauge (DiGi Gauge TX-430; range 0-350 bar; accuracy $\approx \pm 0.25\%$) mounted on one end of cylinder near the inlet. Temperature inside the pot was maintained by an electrical heating jacket (Swastik Electrical, India) and before use, the entire pot was vacuumed using a vacuum pump. The stirring pot exhibited maximum pressure and temperature rating of 350 bar and 250°C, respectively. The pot was carefully cleaned, vacuumed, and purged by CO_2 repeatedly to remove any traces of gas impurities. Then, surfactant solution of 25 ml was carefully introduced in the pot. The pot was sealed and vacuumed again. Following this, CO_2 was carefully introduced in pot till the pressure reached to desired level.

Agitation in pot was provided through an impeller (at 600 rpm). The drop in pressure was carefully recorded using a pressure transducer while temperature was kept constant throughout the experiment. CO_2 absorption in surfactant solutions was performed by well-established pressure decay method [106,107]. The gas molality was determined through the plot of decrease in pressure (as gas continues to solvate in fluid) *vs*. time.

After molality experiments, CO_2-laden surfactant solution was extracted *via* a sample port into a graduated glass cylinder and analyzed visually to determine foam stability and foaming potential of surfactant solution. The images of glass cylinders, containing foams, were obtained using a camera (Samsung M21). The foaming potential of surfactant solution was determined by changes in total volume of foam over the period of elapsed time. For this, the synthesized foams were carefully analyzed at regular intervals and the residual foam volume (at corresponding interval of time) was simultaneously determined. The foam stability was measured till the entire foam volume had disappeared.

2.2.6. Microscopic analysis of CO_2 foams

After foam preparation, a small volume (2-2.5 ml) of foam was extracted from the glass cylinder using a standard laboratory pipette (Tarsons, United States) and released on a glass slide. The glass slide was observed under an optical microscope (Motic, Hong Kong) and foam images were obtained at regular intervals of time using an inbuilt imaging tool (Moticam-10). Separately, the thermal stability of foam was also investigated using microscopic, equipped with an electric thermal stage (Novel Industries, India) with thermocouple. Once desired temperature reached, the drop of foam was dropped on thermal stage for analysis and image extraction.

2.2.7. Assessment of contact angle between surfactant solution and CO_2

Following foam stability studies, the contact angle between green surfactant solution and CO_2 was measured using a stainless steel pressure cell with glass viewing ports. This assembly was manufactured by D-CAM Engineering, India and its application for the determination of SFT *via* pendent drop method has been reported in our previous study [107]. A small drop of solution was dropped on glass slide and pressure cell was pressurized to desired pressure (12 bar) using a syringe pump (Teledyne ISCO, United States), CO_2 cylinder, and pressure regulator. Images of drop on glass slide in presence of CO_2 were captured using a camera (Phantom VCC, United States) to establish any change in the spreading of droplet on glass slide.

2.2.8. Surface adsorption studies in porous media

Finally, the natural surfactant was tested for its adsorption strength in sandstone media [108]. For this, surfactant solutions of two concentrations (CMC: FS1 and 2CMC: FS2) were chosen and 25 ml of each was put in glass vials containing 10 g sand already. The glass vials were agitated using an orbital shaker (Tarsons®, India) at regular intervals. Equal amount (2 ml) of surfactant solutions was extracted from glass vials at regular interval of 0, 2, 4, 6, and 8 days followed by their analysis in UV-*vis* spectrophotometer (UV-vis 3200, Lab India®). These observations were performed at room temperature with wavelength range of 200-500 nm and scan rate of 1 nm/s. The actual amount of surfactant loss was determined by a calibration curve, prepared by peak absorbance data of surfactant samples of varying concentration (0-0.4 wt%). This method, of determining mass-loss owing to adsorption on solid surface, has been also reported in previous literature [109]. The value of surfactant loss was reported in wt% which was obtained by the difference between initial wt% (from absorbance value on calibration curve) and actual wt% of surfactant sample.

2.2.9. Adsorption isotherms for green surfactants

Finally, the adsorption isotherms were determined for green surfactant. 8 g of sand was uniformly agitated (for 24 h) in 50 ml surfactant solution using a commercial horizontal shaker (IKA HS 501) at room temperature. After adsorption, surfactant solutions were centrifuged at 500 rpm (using a Droplet Medical Laboratory Centrifuge) for 10 min to separate any sand particles from surfactant solution. Amount of surfactant adsorbed, Γ (mg/g), can be calculated using Eq. 1.

$$\Gamma = (C_o - C_e)\frac{V}{m} \quad 1$$

Here, C_o and C_e are surfactant concentration of initial and equilibrium conditions. V represents the volume of surfactant (L) and m represents weight (g) of sand particles, *i.e.*, absorbent used in study. The surfactant concentration at equilibrium was determined *via* chemical oxygen demand of the solution [110].

2.3. Results and discussion

First, the characterization of green surfactant has been reported *via* FTIR, XPS and UV-vis analysis followed by the discussion on SEM and EDX results to establish the morphological and elemental composition of formulated surfactant. The determination of critical micellar concentration (CMC) for surfactant was discussed. For CO_2 foams, molality, foaming potential, and foam stability were reported and discussed. Finally, the results of contact angle measurements (between surfactant solution and CO_2) and rock surface adsorption were presented.

2.3.1. FTIR Analysis of green surfactant

Previous studies have relied on FTIR data to establish the presence of saponin in formulated surfactants [111]. Hence, in this study, FTIR analysis of synthesized green surfactant

has been performed in order to confirm the presence of known saponin functional groups. The result of FTIR spectra has been shown in Figure 2.1. FTIR spectrum was plotted in the band range of 400-4000 cm^{-1}. From FTIR data, the peak at 3284 cm^{-1} indicates the presence of -OH stretching which validates the presence of phenolics compound in synthesized surfactant [22]. The peak observed at 2923 cm^{-1} indicates the presence of -CH stretching to validate the existence of saponin glucosides [112]. The spectra band range from 1600-1200 cm^{-1} confirms the presence of C=O stretching, CH_2, and CH_3 associated with the existence of aromatic rings, carboxyl phenols, saponin glycoside, and amino acids in surfactant, consistent with the research findings on surfactant characterization in literature [112,113]. The existence of glycosidic bonds is the result of C=C stretching at 600 cm^{-1} and C-O-C stretching at 1034 cm^{-1}, which is responsible for the chain of sugar that belongs to saponins [111]. Hence, from the results, it can be established that the extraction method yielded a green surfactant from fenugreek powder.

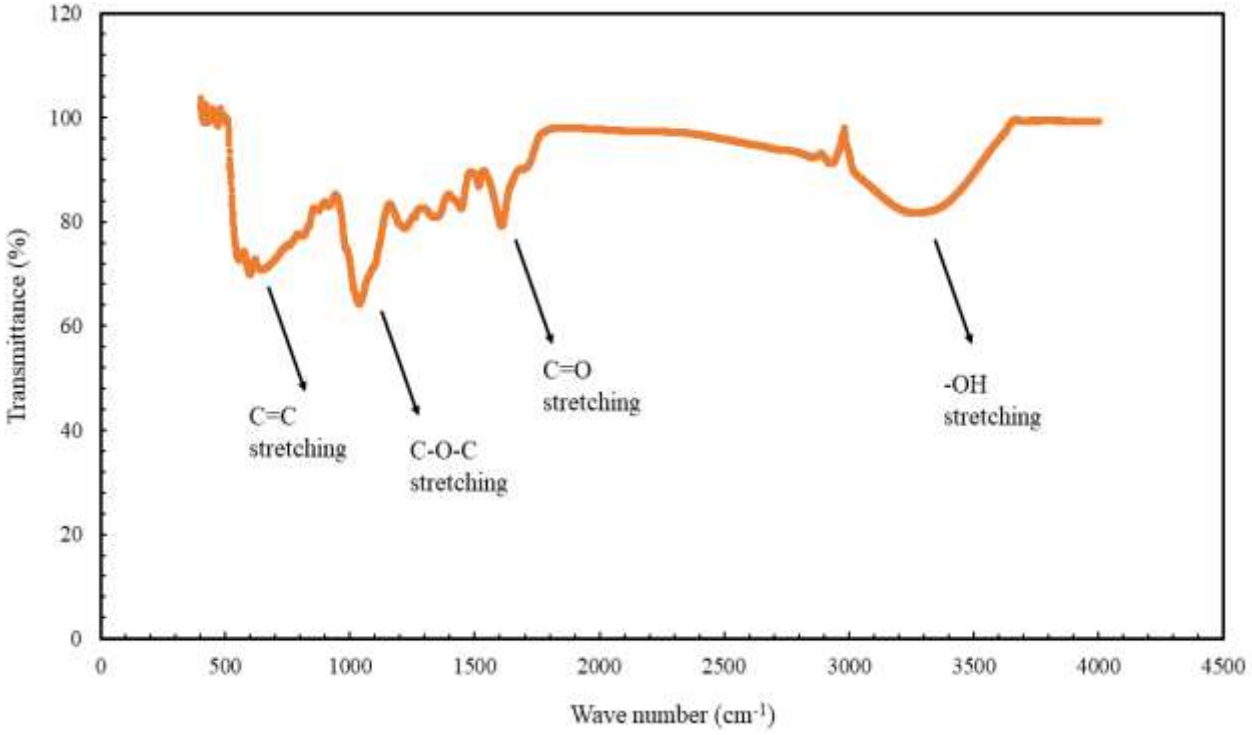

Figure 2.1: FTIR spectra of green surfactant obtained as a function of wave number.

2.3.2. XPS Analysis of green surfactant

XPS was employed to analyze the surface chemical composition and electronic state of the synthesized natural surfactant [114]. A wide survey scan was initially performed to identify the elements present on the surface of the surfactant. This scan typically covered a binding energy range from 0 to 1400 eV. High-resolution spectra were subsequently acquired for the core-levels of elements of interest, such as carbon (C 1s), oxygen (O 1s), phosphorus (P 2p), nitrogen (N 1s) and sodium (Na 1s) in the surfactant (Figure 2.2). The pass energy for high-resolution scans was set at 0.10 eV to ensure adequate resolution. The survey scan revealed the presence of [elements detected, e.g., C, O, P, N, Na], confirming the expected elemental composition of the natural surfactant as shown in Figure 2.2 a. The high-resolution C 1s spectrum exhibited peaks 284.8 eV corresponding to various carbon environments, such as C-C, C-O, and C-H bonds (Figure 2.2 b), indicating the presence of both aliphatic carbon, alcohols and ethers [115,116]. The O 1s spectrum showed peaks 286.5 eV that could be attributed to alcohols and ethers (Figure 2.2 c) [117]. The P 2p spectrum displayed peaks indicative of phosphate species, further corroborating the presence of the phosphate group in the surfactant structure [118]. The N 1s spectrum displayed peaks associated with the protonated amines [119] whereas the Na 1s spectrum displayed peaks at 1071.32 eV attributed to presence of sodium phosphate [120,121]. The XPS analysis provided a detailed insight into the surface chemistry of the natural surfactant, revealing its elemental composition and the chemical states of the constituent elements. These findings are crucial for understanding the surface interactions and the synthesized surfactant was found to be phosphate anionic surfactant.

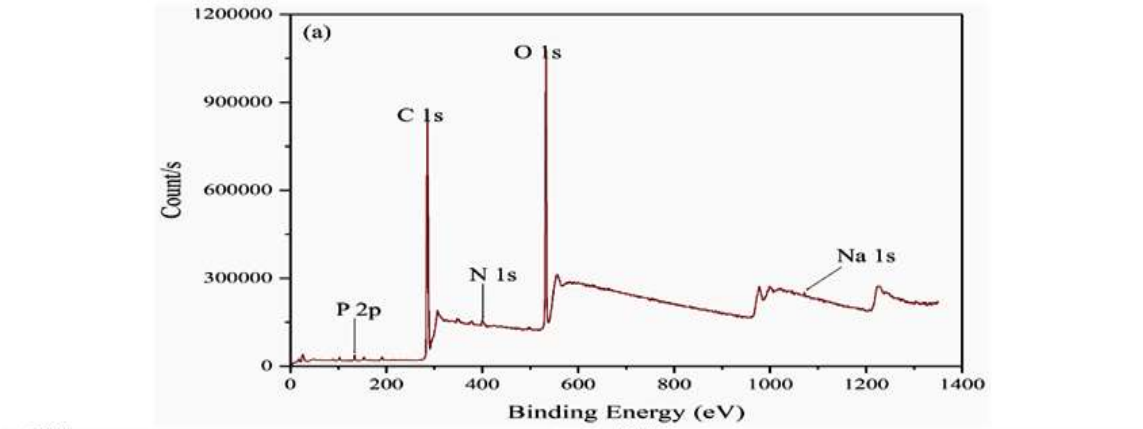

Elements	Atomic %	Binding Energy (eV)	Functional Group
Carbon	68.11	284.8	-C-C-; C-H (aliphatic carbon)
Oxygen	27.15	532.81	C-O (alcohols, ethers)
Nitrogen	1.98	401.09	Protonated amines
Phosphorus	1.21	133.81	Phosphate groups (PO4)
Sodium	0.2	1071.32	Sodium phosphate (Na3PO4)

Figure 2.2: X-ray Photoelectron Spectroscopy (XPS) Analysis of the Natural Surfactant (a) Survey scan showing the overall elemental composition of the surface (b) High-resolution C 1s spectrum, highlighting the various carbon peaks (c) High-resolution O 1s spectrum, illustrating the different oxygen species present and table below shows the elemental composition and atomic percentages along with associated functional groups.

2.3.3 UV-vis analysis of green surfactant

UV-vis analysis was performed to visualize the amount of light that has been absorbed by a chemical substance. Hence, UV-vis analysis of aqueous solution of 0.2 wt% surfactant was

conducted and the result is shown in Figure 2.3. It was observed that an absorbance peak of 3 occurred at wavelength of 230 nm. In previous studies [122,123], the peak of saponin has been obtained in between 210-220 nm. This peak value was determined after the repetition of analysis for 5 times on same surfactant solution and an average value was reported in Figure 2.3. UV-vis analysis was also performed at temperature of 70 ºC and the results are provided in Figure 2.3. The presented values indicate that a small decrease in peak absorbance value took place (2.85 vs. 3) at 70°C, indicating that the material did not lose much functionality even at elevated temperature *i.e.* 70°C.

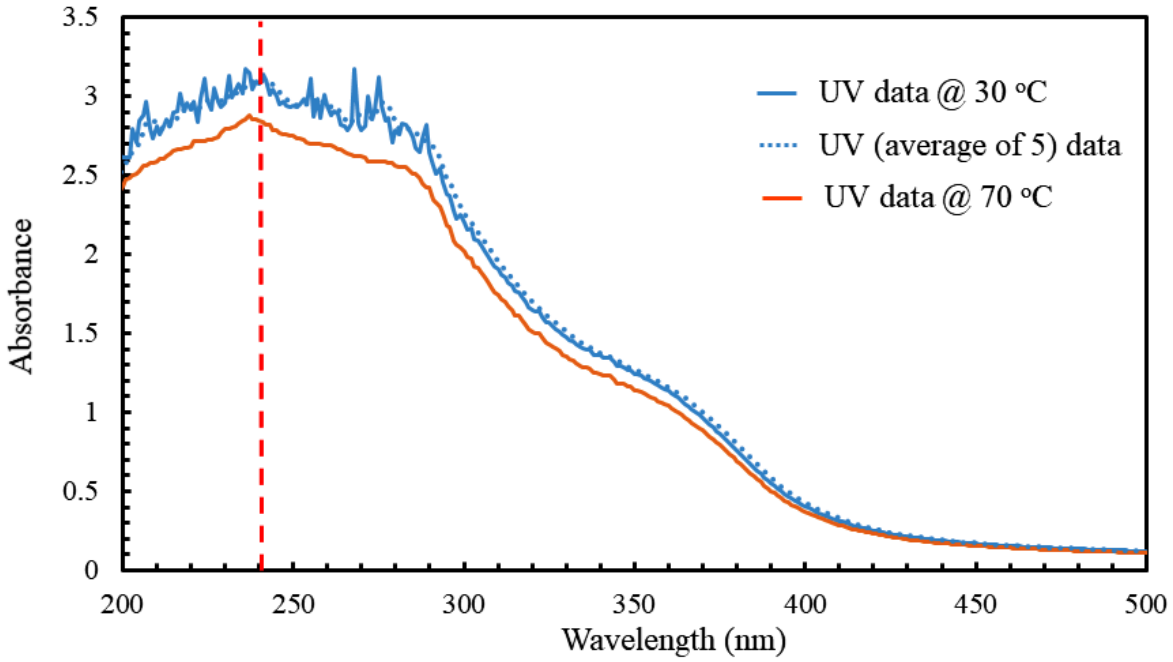

Figure 2.3: UV-*vis* analysis of green surfactant as a function of wavelength at ambient conditions. The green surfactant of 0.2 wt% was used and suspended in DI water.

When UV-vis analysis was repeated after 2 days, no significant change (deviation < 5%) was noticed in absorbance value, indicating that green surfactant retained its stability till the storage period of 2 days. UV-vis and FTIR analysis of each batch was performed immediately

after preparation. Each of these batches were prepared from Fenugreek seed, obtained from different stores within the district to ensure that the surfactant synthesized was not dependent on a single batch or location.

2.3.4. FESEM and EDX analysis of green surfactant

For FESEM, a drop of surfactant solution was dried on aluminum foil and gold coated for 30 s before observation in the instrument. The image obtained from FESEM analysis is shown in Figure 2.4. Conventionally, FESEM is performed to study the surface morphology of a chemical substance. From Figure 2.4a, it can be clearly seen that surfactant accumulations were visible on the surface of aluminum foil. These accumulations were evenly scattered and did not form any cluster. Interestingly, the surfactant accumulations resemble like crushed stones and have no regular shape. The irregularity in surfactant accumulations might occur during extraction process wherein, the fluid extract from Soxhlet was dried and manually grinded to obtain surfactant powder. The effect of extraction process on shape of green surfactant is random as shapes such as rod-like and irregularity has also been observed in previous studies [124].

With FESEM, EDX analysis (a method for elemental composition of substance) of surfactant is also provided in Figure 2.4. During this analysis, five different elements were observed; carbon (C), oxygen (O), phosphorous (P), sodium (Na), and nitrogen (N). All these five elements were the inherent components of synthesized surfactant, consistent with research findings in literature [124]. The dominating element in surfactant was carbon (83.4%), which was probably due to the biological origin of surfactant from a carbon based flora. Other elements, i.e., oxygen (O), phosphorous (P), sodium (Na), and nitrogen (N) were present in lower amounts (15.3, 1, 0.3, and 0.01%, respectively). The presence of Na indicates the anionic nature of the surfactant which

may be attributed to sodium salts [124]. Apart from these elements, no other element was observed during analysis, which further validates that synthesized surfactant was pure and exhibited no contamination by other impurities.

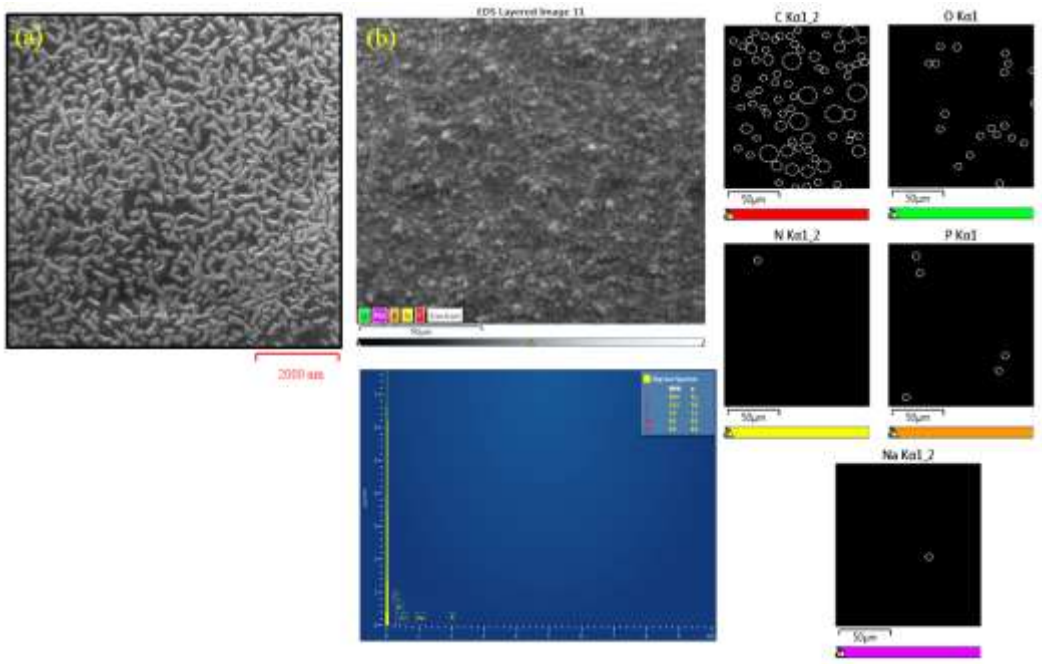

Figure 2.4: SEM and elemental composition mapping of green surfactant, obtained after drop-casting method. The dotted white circles indicate the presence of elements in elemental mapping results.

2.3.5. Charge validation of green surfactant

To establish charge on green surfactant, a methylene blue active substances assay (MBAS) test was performed. MBAS assay test is a simple method and most commonly used to validate the presence of anionic surfactant in a liquid media [125]. Initially, pH of the sample reduced by acidizing it (in this case by 0.1M diluted HCl) followed by the inclusion of chloroform and methylene blue in system. Since methylene blue is a cationic dye and with agitation, it formed pair

with anionic surfactant which is then extracted in an organic solvent [126]. When MBAS test was performed with green surfactant, ion exchange took place between cationic methylene blue dye and anionic green surfactant which was also validated by visual and spectrophotometric analysis. This validates the anionic nature of green surfactant.

2.3.6. CMC determination by SFT measurements

At liquid–air interface, SFT results from greater attraction of liquid molecules (called cohesion) to each other than to the molecules in air (called adhesion). Due to high attraction of water molecules (result of strong hydrogen bonds), water exhibited high SFT value of 72.8 mN/m at 20°C, consistent with SFT value of water in literature [127]. SFT value of water reduced with the inclusion of surfactant in the system as shown in Figure 2.5, plotted to show SFT variation of water/air interface as a function of increasing surfactant concentration (wt%). When surfactant is dissolved in water, it gets adsorbed at the interface of air-water with hydrophobic part in air and hydrophilic part in water (Figure 2.5). Consequently, the population of water molecules, at air-water interface, will reduce and this has caused decrease in attraction between water molecules and thereby, SFT. From Figure 2.5, it is clear that SFT value decreased with increasing surfactant concentration in system as more surfactant molecules were available to get adsorbed at air-water interface. At 0.05 wt%, the value of SFT was measured as 44 mN/m which further reduced to 26 mN/m at 0.15 wt%. These values are significantly lower than SFT value of pure water. Thus, this information can be used to determine CMC value of surfactant. Conventionally, CMC is the point where decrement in SFT value almost ceased and a plateau will exist with further increase in surfactant concentration. With the increase in surfactant concentration from 0-0.4 wt%, SFT trend followed almost a constant horizontal line after 0.2 wt%. This represents the existence of CMC in surfactant. At CMC, surfactant molecules will participate in the formation of micelles, which is of

key importance in the design of surfactant solution for CO_2 foaming and IFT reduction of crude oil in practical applications. Thus, the obtained CMC value of 0.2 wt% at SFT of 22 mN/m was used in all experimental tests of this study.

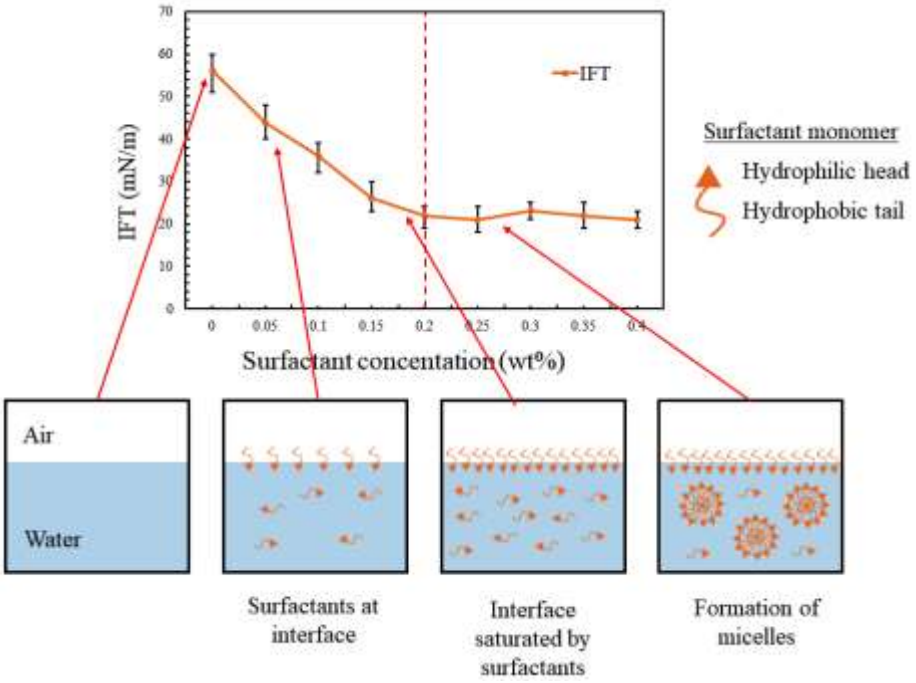

Figure 2.5: Surface tension measurements of surfactant solutions of varying concentration (wt%). The dotted red line denotes the presence of critical micellar concentration (CMC) in system.

2.3.7. CMC confirmation by electrical conductivity measurements

To verify CMC value of SFT method, electrical conductivity measurements were conducted and a curve was obtained between electrical conductivity and surfactant concentration as shown in Figure 2.6. The concentration of aqueous surfactant solution varied from 0-1.6 wt% and the electrical conductivity measurements showed increase up to the concentration of 0.2 wt%. It was observed that the increase in surfactant concentration was directly proportional to increase in electrical conductivity of surfactant solution. Beyond 0.2 wt%, the slope of the curve changed as evident from Figure 2.6. This sudden change in slope at 0.2 wt% confirms the existence of CMC

in aqueous surfactant solutions of varying composition. At low concentration (< 0.2 wt%), the surfactant monomers were responsible for the adequate conduction of electricity in solution. However, at CMC and beyond, the electrical conductivity was the function of surfactant micelles which showed different nature than monomers in electricity conduction hence, a change in slope occurred. Thus, from these results, the value of CMC as 0.2 wt% was confirmed which is consistent with the value obtained during SFT measurements. From these two methods, it is clear that CMC value of synthesized surfactant should be chosen as 0.2 wt%. Previous studies have also relied on a combination of methods to confirm CMC of surfactants, both green and commercial. Pal et al. reported the use of IFT and conductivity methods to obtain CMC value of several quaternary Gemini surfactants with different spacer lengths [128]. Saxena et al. utilized SFT and electrical conductivity methods to establish CMC value of anionic green surfactant, derived from Sapindus laurifolius [124]. Thus, SFT and electrical conductivity methods are well-practiced approaches to establish and validate CMC value of surfactants.

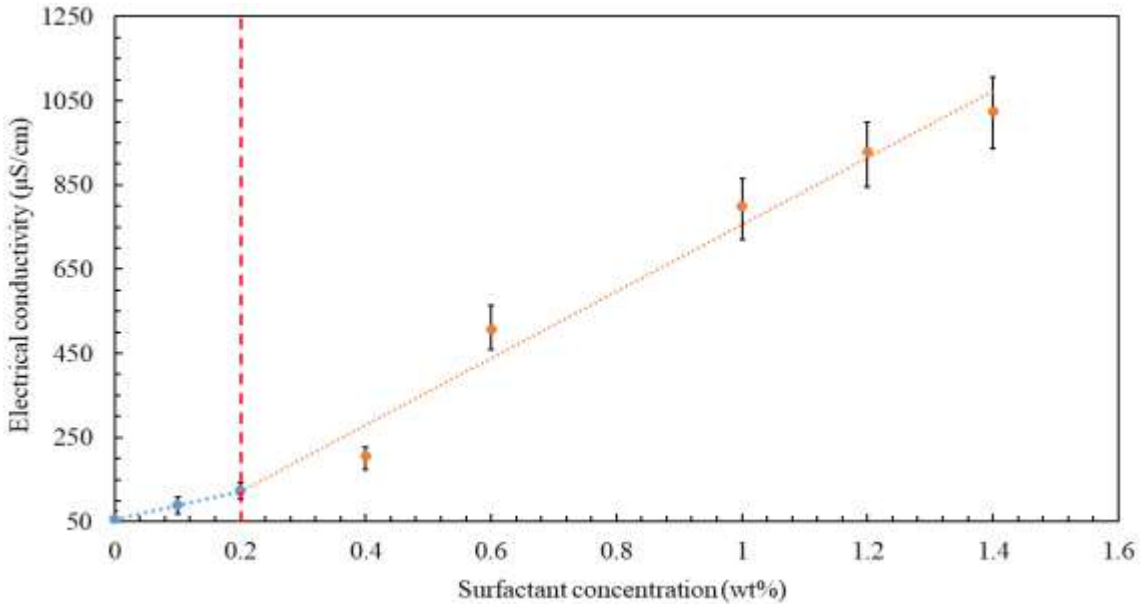

Figure 2.6: The determination of critical micellar concentration (CMC) of green surfactant by electrical conductivity method at ambient conditions.

2.3.8. CO_2 molality results for surfactant

CO_2 molality results were conducted to compare CO_2 absorption potential of water and surfactant solution. For molality study, a widely practiced pressure decay approach was utilized [129]. In this method, CO_2 at high pressure comes in contact with solvent and gets entrapped in the interstitial voids of solvent. As a result, the pressure continuously decreased with gas entrapment and reached to a level at which no further drop in pressure was witnessed. This value of pressure is called equilibrium pressure of system. Using pressure values of initial and equilibrium condition, CO_2 molality (number of gas moles trapped in 1 kg of solvent) was obtained by ideal gas equation. Each investigation was performed five times and the average value of CO_2 molality as a function of confining pressure (4-12 bar) and temperature (303-353 K) has been provided in Figure 2.7.

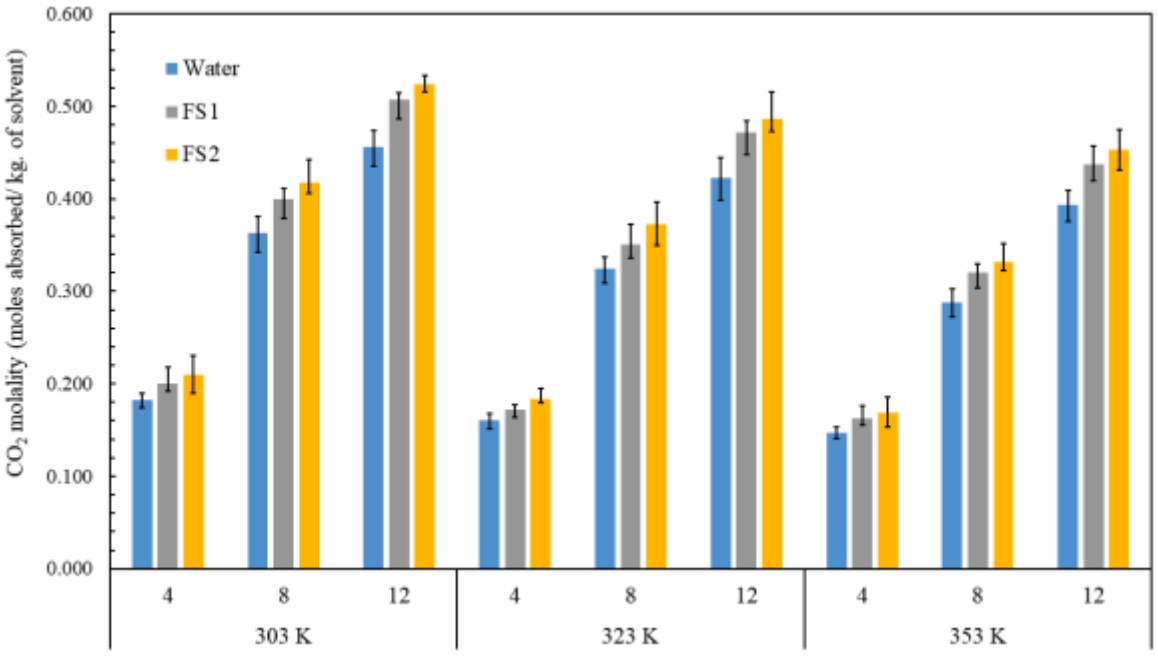

Figure 2.7: CO_2 molality (moles absorbed in kg. of solvent) data for green surfactant as a function of varying pressure (4-12 bar) and temperature (303-353 K). FS1 indicates surfactant concentration of 0.2 wt% while FS2 involves 0.4 wt% of surfactant.

For water, the value of CO_2 molality was determined as 0.184 mol/kg of solvent at 4 bar, which increased to 0.363 and 0.456 mol/kg of solvent at 8 and 12 bar, respectively. Hence, increasing confining pressure offered positive increment on the molality of solvent as more gas gets absorbed into the solution [130]. With surfactant, CO_2 molality increased due to the rapid formation and deformation of small CO_2 bubbles. It can be expected that CO_2 entrapment in cages of foam resulted into greater CO_2 retention inside the body of fluid. In addition, it is likely that surfactant monomers acted as carrier and transferred the gas phase from liquid-gas interface to bulk body of surfactant. Consequently, CO_2 loading was reported higher for FS1 (0.507 mol/kg of solvent) and FS2 (0.524 mol/kg of solvent) at 303 K and 12 bar. However, CO_2 molality for surfactant solutions decreased with increasing temperature. CO_2 molality for FS1 and FS2 decreased to 0.172 and 0.183 mol/kg of solvent, respectively, at 353 K and 4 bar. With surfactant, CO_2 molality increased significantly. This can be attributed to the rapid formation and deformation of small CO_2 bubbles in solvent. The effect of temperature on can be correlated with increase in kinetic movement of gas molecules and micelles, making the entire system more chaotic and reducing the stability of entrapped CO_2 bubbles [101,131]. From the results, it can be established that increase in pressure is beneficial, while increase in temperature bears inverse relation.

A comparative assessment of quantum of increase in CO_2 molality by surfactant over water was also conducted. For FS1 and FS2, % change in CO_2 molality was determined at various experimental conditions and these results are provided in Figure 2.8. To obtain % change, CO_2 molality in water has been chosen as base case for comparison with CO_2 molality in FS1 and FS2 solutions. From Figure 2.8, it can be observed that FS1 yielded an increase of 7.5-11% in CO_2 molality, while FS2 showed 14-18% increase in CO_2 molality (for pressure increase from 4 to 8 and then to 12 bar). Thus, a higher value of CO_2 molality was observed for FS2 than FS1, which

might be due to higher surfactant concentration in the system. Increasing temperature reduced the absorption efficacy of both FS1 and FS2 solutions which is attributed to the degradation of micelles at high temperature, a behavior which has also been reported for other surfactant laden solution [102]. Hence, from the results, the application of synthesized surfactant is recommended for CO_2 absorption applications. It can be used for post-combustion capture of CO_2 from flue gas streams.

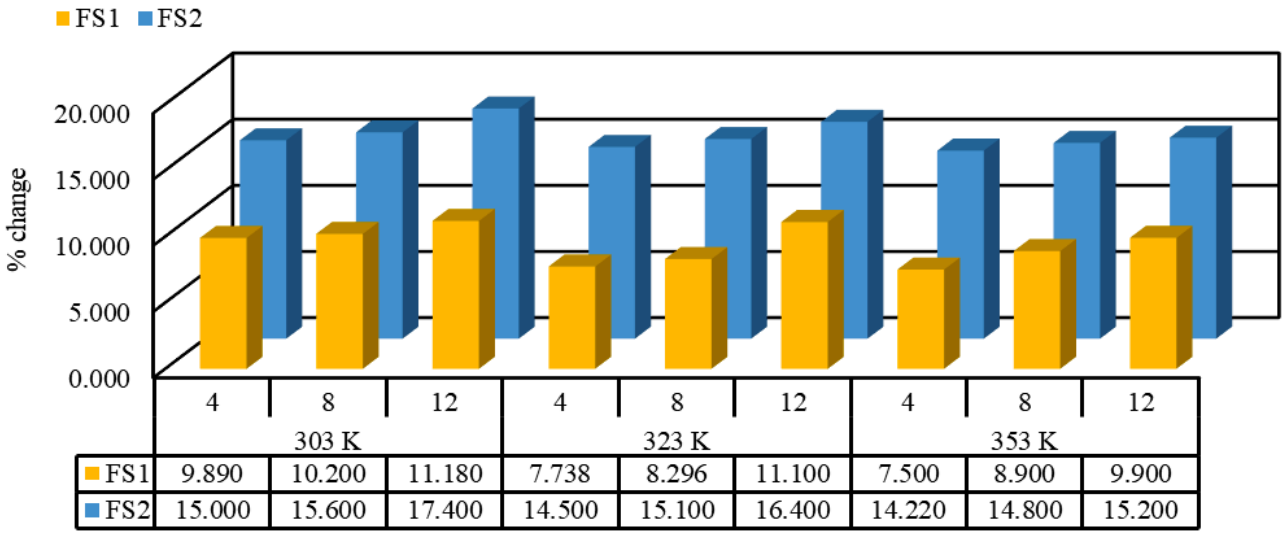

	303 K			323 K			353 K		
	4	8	12	4	8	12	4	8	12
FS1	9.890	10.200	11.180	7.738	8.296	11.100	7.500	8.900	9.900
FS2	15.000	15.600	17.400	14.500	15.100	16.400	14.220	14.800	15.200

Figure 2.8: The effect of varying pressure (4-12 bar) and temperature (303-353 K) on CO_2 absorption value (% change) of FS1 and FS2 surfactant solutions.

2.3.9. Foaming and foam stability results

CO_2 foaming potential of surfactant was assessed from the volume of foam generated by its different concentration. A varying concentration (0-0.5 wt%) of surfactant was added to DI water and the entire solution agitated in a stirring pot at 350 rpm under a pressure of 4 bar for 15 min. The process resulted into the development of aqueous foam in which CO_2 bubbles were enclosed by the film of continuous surfactant solution. For each composition, the amount of foam volume is plotted as a function of surfactant concentration and the results are shown in Figure 2.9.

From Figure 2.9, it can be established that foaming behavior of surfactant depends on its concentration and as the number of monomers increase in solution, so does the volume of foam generated. For example, with 0.1 wt% surfactant, the volume of foam generated was 18 ml which increased to 46 ml at 0.2 wt%. However, with further increase in surfactant concentration, the quantum of increase in foaming was negligible (Figure 2.9). This indicates, that beyond CMC, an increase in foaming was hardly possible. The similar has been reported for conventional surfactant such as SDS and therefore, surfactant concentration, *i.e.*, CMC was regarded as the most desirable concentration for various industrial applications [92].

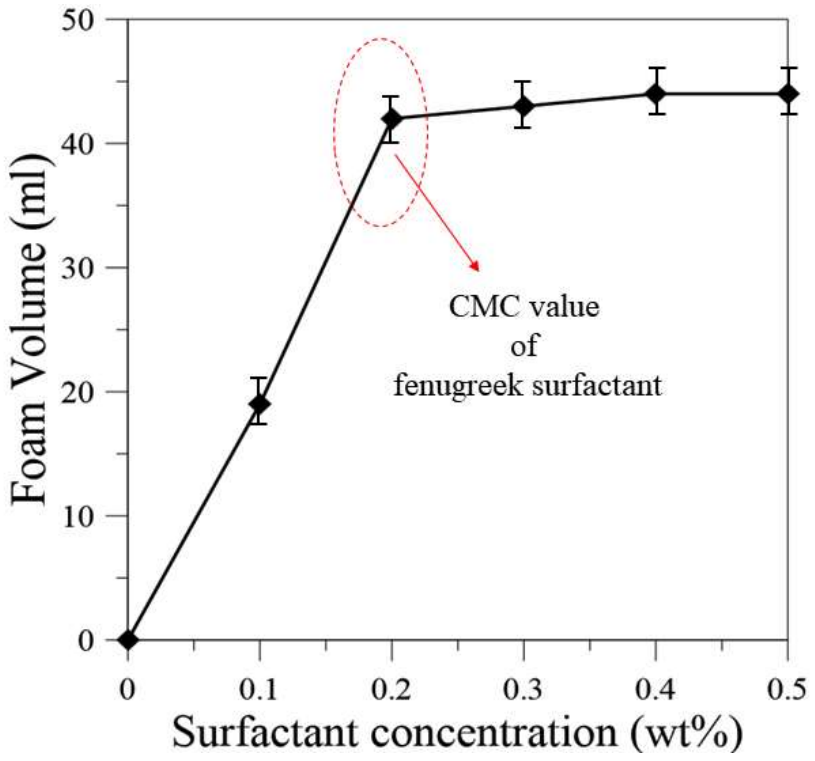

Figure 2.9: Verification of surfactant CMC by foaming method (volume of foam generated) as a function of surfactant concentration (wt%). Above CMC, little increase (> 10%) was observed in generated foam volume.

Next, the results of foam stability of FS1 (CMC) and FS2 (2CMC) were reported as a function of time. For this, the changes in the height of foam in glass cylinder was monitored and normalized foam height (*i.e.*, foam height at time t/initial foam height) was plotted in Figure 2.10. Initially, in both FS1 and FS2, the volume of generated foam was ~ 45-49 ml with some amount of surfactant solution beneath foam. With time, liquid from the foam lamella drained under gravity (phenomena referred to as liquid drainage) and volume of underlying surfactant solution increased over time which correspondingly decreased the foam volume (Figure 2.10). Within 6 h, more than half of foam volume disappeared and the normalized foam height reached to ~0.5 for both the surfactant solutions (Figure 2.10). After 12 h, almost entire volume of foam disappeared for both the surfactant solutions resulting foams exhibited stability of ~10 h. In previous study performed with conventional chemical surfactant (SDS), CO_2 foams yielded a foam volume of 60 ml but a half-life of less than 30 min at ambient condition [132]. However, compared to FS1, FS2 displayed slightly higher foam stability which can be attributed to the presence of more surfactant in solution. Since that increase was not significant, the quantity of surfactant inclusion must be carefully optimized to obtain the most effective technical and economic performance. In FS2, the availability of more surfactant monomers probably resulted into greater absorption on the surface of CO_2 bubbles and provided higher resistance to bubble coalescence [92].

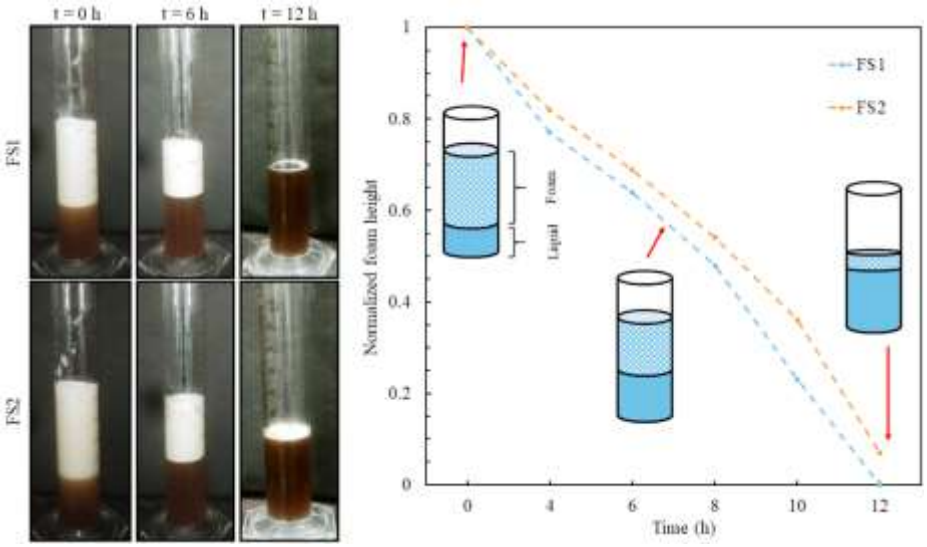

Figure 2.10: Visual appearance images and foam height of surfactant solutions (FS1 and FS2) as a function of time. The observations were performed at ambient conditions.

2.3.10. Microscopic analysis of CO_2 foams

For microscopic analysis, CO_2 foam was taken on a glass slide and visualized under microscope. Foam images as a function of time and temperature are shown in Figure 2.11 and 2.12, respectively. From Figure 2.11, it can be seen that foam bubbles were initially small with average bubble size ~150-180 µm. However, these CO_2 bubbles coalesced to minimize their surface energy with time and converted into large size bubbles. The increase in bubble coalescence was confirmed from the increase in average bubble size and as a result, bubble size for FS1 increased to ~240 µm after 4 h and 470 µm after 8 h. Similarly, FS2 exhibited increase in bubble size from 160 µm (at 0 h) to 270 µm (at 4 h) followed by 400 µm after 8 h. It is to be noted here that the rate of coalescence (size increase) in FS2 was lower than FS1 and therefore, the foam size in FS2 (after 8 h) was found lower (400 µm) than the one (470 µm) of FS1. Thus, it can be stated that the presence of high surfactant concentration (in FS2) is believed to provide slight

improvement in the stability of CO_2 foams. In FS2, the availability of more surfactant monomers probably resulted into greater absorption on the surface of CO_2 bubbles [102].

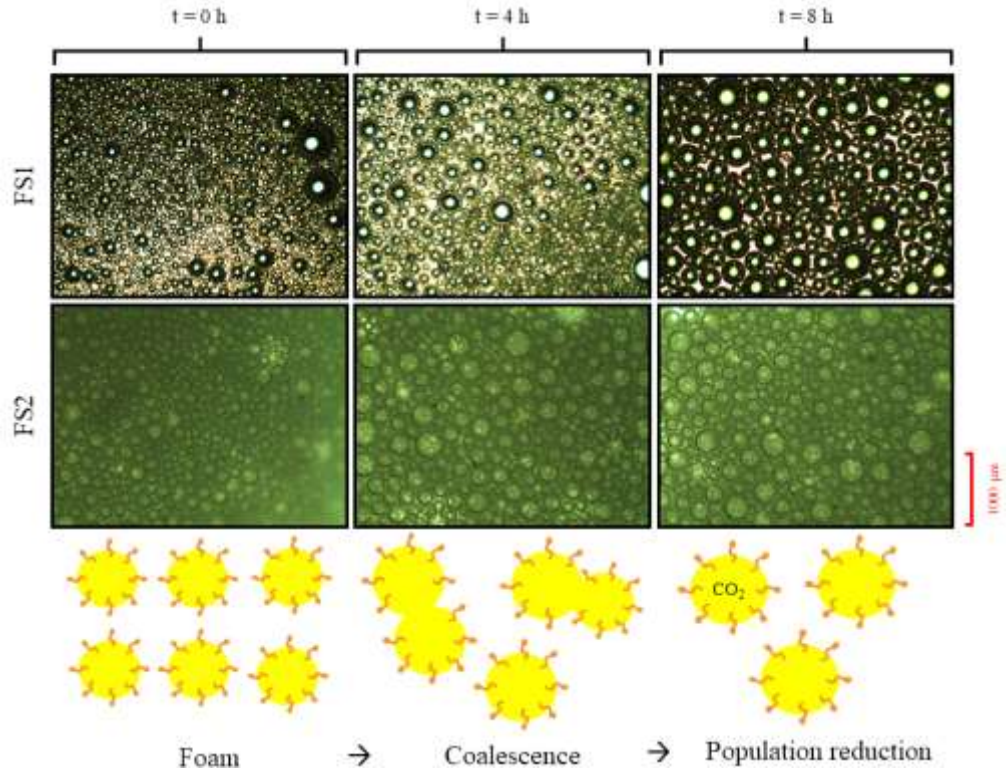

Figure 2.11: Microscopic images of CO_2 foams of surfactant solutions (FS1 and FS2) on different time (0, 4, and 8 h). With time, foams were found to coalesce (increase in size) and undergo phase separation, reducing their population.

Figure 2.12 shows the effect of increasing temperature on average bubble size. It was observed that increasing temperature showed significant increase in bubble coalescence and thereby, average foam bubble size increases. The average bubble size in FS1 was 120 µm at 313 K which increased to 380 µm at 333 K and 500 µm at 363 K. Similarly, in FS2, the average bubble size of 160 µm increased to 340 µm, and 450 µm at 313, 333, and 363 K, respectively. This effect of increasing temperature on coalescence and bubble size can be attributed to rise in kinetic energy

of trapped gas molecules which causes them to interact and coalesce with other bubbles. The thermal stability of CO_2 foams was tested for 4 h, and the presence of enough number of CO_2 bubbles at 90 ^oC suggested that surfactant provided reasonable stability to foam systems.

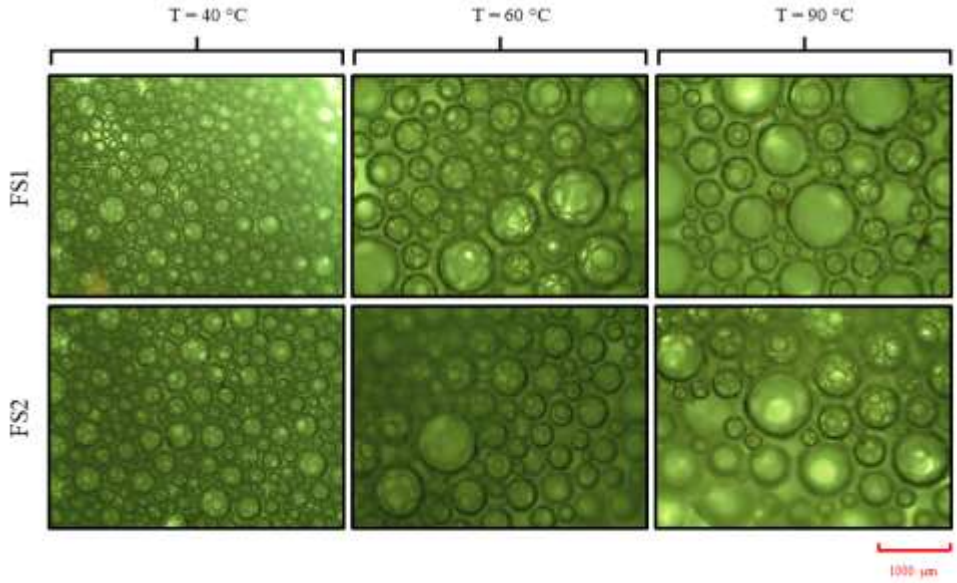

Figure 2.12: Effect of increasing temperature (40, 60, and 90°C) on microscopic characterization of CO_2 foams. Compared to FS1, FS2 exhibited slightly better stability at high temperature due to the presence of higher surfactant concentration in solution.

Furthermore, the interfacial interaction between CO_2 and surfactant solution that leads to CO_2 entrapment is also proposed through a schematic in Figure 2.13. Initially, both surfactant solution and CO_2 exist as separate phases inside the stirring pot and no intermingling between them takes place resulting a contact angle higher than 90°C develops. The initiation of mechanical agitation (provided by impeller) induces rapid intermingling between both the phases (CO_2 and surfactant solution) which enables entrapment of CO_2 bubbles by the surrounding layer of surfactant solution. Higher the entrapment, higher the drop in contact angle. At contact angle < 90^o, the surfactant monomers start to adsorb on the surface of CO_2 as a result, the interface shifts

to other direction and offers progressive coverage of CO_2 to form a bubble. Contact angle 90° indicates neutral condition. At this point, CO_2 and surfactant solution are in equilibrium and have no intention to interact. The results indicate that the application of green surfactant in CO_2 foaming and retention is recommended even at high temperature such as 363 K.

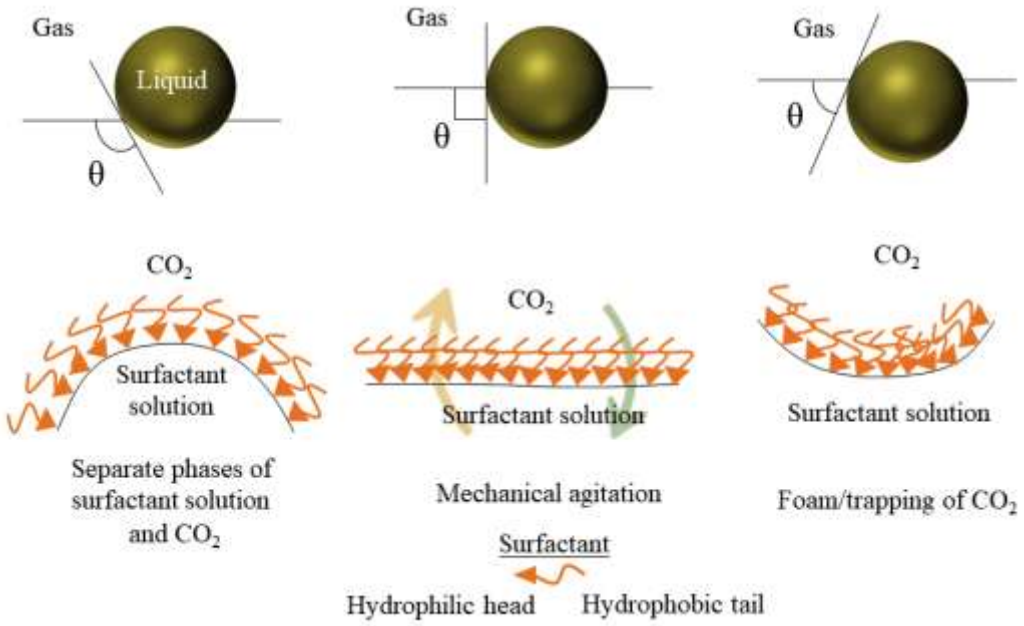

Figure 2.13: Proposed mechanism of surfactant role into the development of curvature around CO_2 bubble. The contact angle between liquid and CO_2 determines the surfactant role in foam formulation.

2.3.11. Contact angle study b/w CO_2 and green surfactant

It has been well established that water potential to make foam with a gas is negligible unless a surface-active agent or mechanical agitation is introduced in the system. In water, this lack of foaming can be credited to the presence of high surface tension (Figure 2.5, Section 2.3.5). While SFT determination is one way to identify this property, contact angle measurements can be further used to visualize alteration in CO_2-liquid interface for the promotion of better foaming attributes.

The proposed changes on the interface between liquid (surfactant solution) and gas (CO_2) can be understood with the help of schematic provided in Figure 2.13. Correspondingly, the values of contact angle as a function of time for the same system has been reported in Figure 2.14. Initially, given strong adherence between water-water molecules at the interface, the droplet would try to minimize spreading and show least amount of surface area, available to interact with gas molecules [133]. This results in a high contact angle as evident from Figure 2.14; a value of 74-78^o was observed over the entire test interval of 20 min due to no change in surface activity of water droplet. The inclusion of surface active agent (green surfactant) increased the surface activity as surfactant monomers substitute the water molecules at CO_2-liquid interface. Consequently, the droplet exhibited spreading and offered more surface area to interact with CO_2 molecules. This caused a significant drop in the contact angle of CO_2-FS1 solution as evident from Figure 2.14. For FS1 and FS2, the contact angle of system reduced from 62-65^o (at 0 min) to 44-47^o (at 20 min), indicating significant change in interfacial behavior of CO_2 and surfactant solution. This change can be attributed to the presence of absorbed surfactant monomers on gas-liquid interface, which altered the contact angle and made liquid film to exhibit more contact/interaction with CO_2. Thus, change in contact angle between CO_2 and FS1 indicates that CO_2 pushed the surfactant droplet and tried to entrap inside it, as observed in previous study for oil foams [134]. This surfactant role on the entrapment of CO_2 seems favorable for the development of CO_2 bubble (foaming) surrounded by continuous layer of surfactant solution, also stated in past study [135].

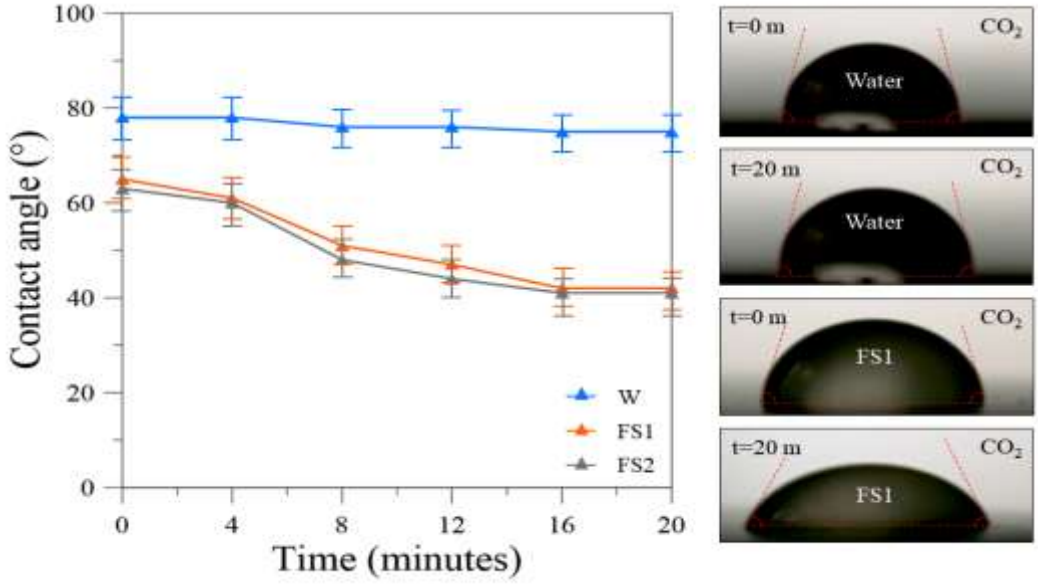

Figure 2.14: Time dependent contact angle measurements between CO_2 and water/surfactant solution (FS1). These experiments were performed at ambient temperature and under 12 bar pressure.

2.3.12. Rock surface adsorption of surfactant

The adsorption behavior of synthesized surfactant was investigated for a sandstone media, a typical reservoir rock of subsurface environment. One of the primary challenges with surfactant application in subsurface is associated with its tendency to get adsorbed on the surface of rock, which typically affects the rate of surfactant adsorption on interface of crude oil for IFT reduction. For all surfactant-based EOR methods, one of the most important requirements is the development of a surfactant system that has minimal chemical adsorption and low mechanical entrapment onto the reservoir rock [110,128,136]. Generally, adsorption of a surfactant on solid surface is due to the complex interaction between surfactant species and the species on or near the solid surface [128]. Factors that affect surfactant adsorption include solution pH, temperature, type of surfactant and its concentration, morphological and mineralogical characteristics of rock, type of electrolytes

present in solution, and concentration of co-surfactants present. Since injected surfactant solution moves forward in the reservoir (see Figure 2.15), its adsorption will reduce concentration required to create sufficient IFT reduction of oil (for recovery) or CO_2 (for viscous foaming). This may render them ineffective in practical applications of EOR and CO_2 sequestration. Thus, an understanding of the adsorption behavior of surfactant will be helpful for the development of surfactant methods in such applications.

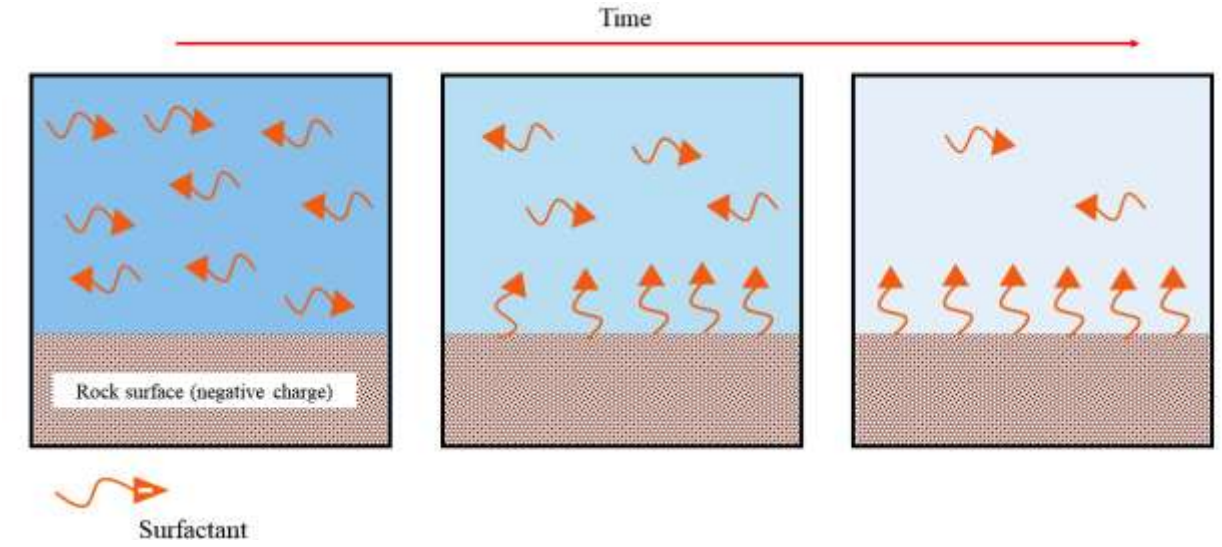

Figure 2.15: Schematic showing the mechanism of surfactant adsorption on rock surface with time. The lighter solution of lower surfactant monomers correspondingly gives low peak during UV-*vis* absorbance study.

For this, a constant volume of surfactant solution (FS1 and FS2) was taken in a glass vial with sand followed by the intense mixing to allow surfactant contact with sand grains. The effluent extracted, at regular intervals of time (day 0-8), was analyzed by UV-*vis* method to establish any change in absorbance. These results are provided in Figure 2.16.

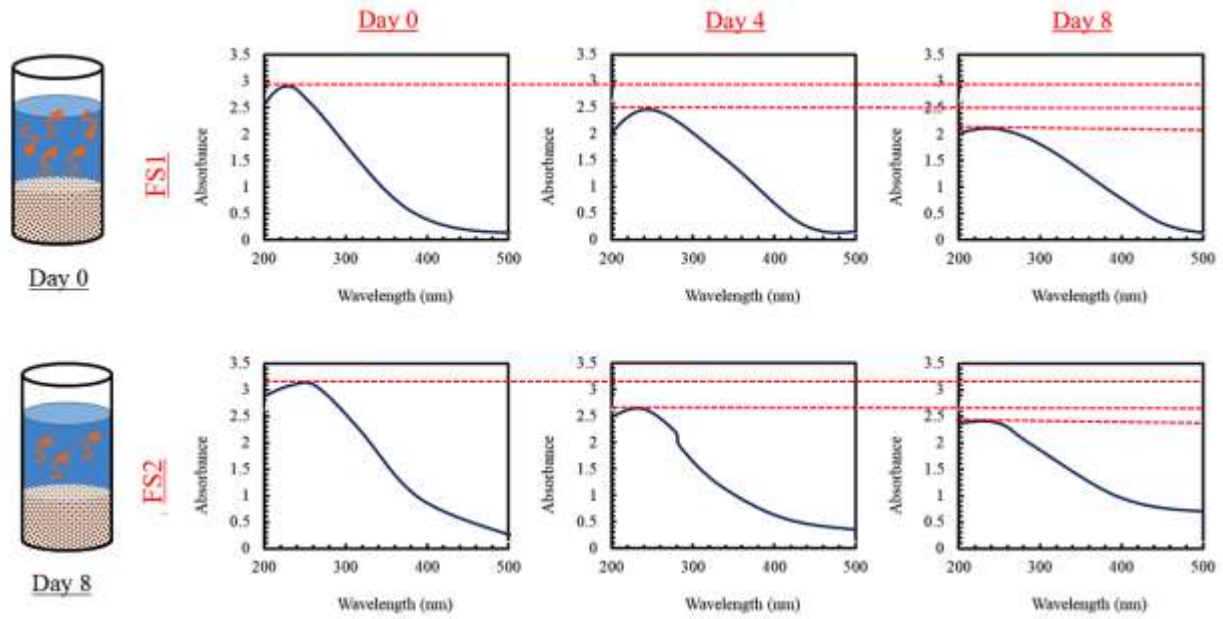

Figure 2.16: UV-*vis* analysis of effluent of surfactant solutions (FS1 and FS2) on different days (0, 4, and 8). The green surfactant solution was put in a glass vial containing sand and the effluent was extracted at regular intervals to establish surfactant loss due to rock surface adsorption.

The peak absorbance value in FS1 solution dropped from 3 (on day 0) to 2.45 on measurement day 4 and 2.08 on measurement day 8. Similarly, in FS2, the peak absorbance value dropped from 3.12 (on day 0) to 2.58 (on day 4) and 2.28 (on day 8). To compute actual mass loss of surfactant on sand-surface, calibration curves were prepared by UV-*vis* analysis on surfactant solutions of varying composition (0 to 0.4 wt%) (see Figure 2.17). It was observed that increasing surfactant wt% increased the opacity in solution as a result, a higher value of peak absorbance obtained for samples of higher wt% (Figure 2.17). Comparing previous absorbance value (for FS1 and FS2 in presence of sand) with calibration curve, the surfactant loss in FS1 was 0.07 wt% on day 4 followed by total loss of 0.12 wt% in porous media on measurement day 8. On the other hand, surfactant loss for FS2 was found 0.13 wt% and 0.19 wt% by measurement day of 4 and 8, respectively. This represents a total mass-loss of 60% (FS1) and 47.5 wt% (FS2) for green

surfactant. However, from the results, it can be established that the quantum of surfactant adsorption on rock surface was not severe (see Table 2.1), as reported in the case of conventional surfactant in previous studies [137] Hence, the synthesized surfactant has potential to utilize in subsurface applications such as EOR, CO_2 sequestration, and CO_2 foaming.

Table 2.1: UV-peak absorbance values and surfactant loss as a function of time on rock surface.

S.No.	Study	Sample	Peak absorbance values			Surfactant lost (wt%)		Total loss (%)
			Day 0	Day 4	Day 8	Day 4	Day 8	
1	This study	FS-1	3	2.45	2.08	0.07	0.12	60%
2		FS-2	3.12	2.58	2.28	0.13	0.19	47.5%

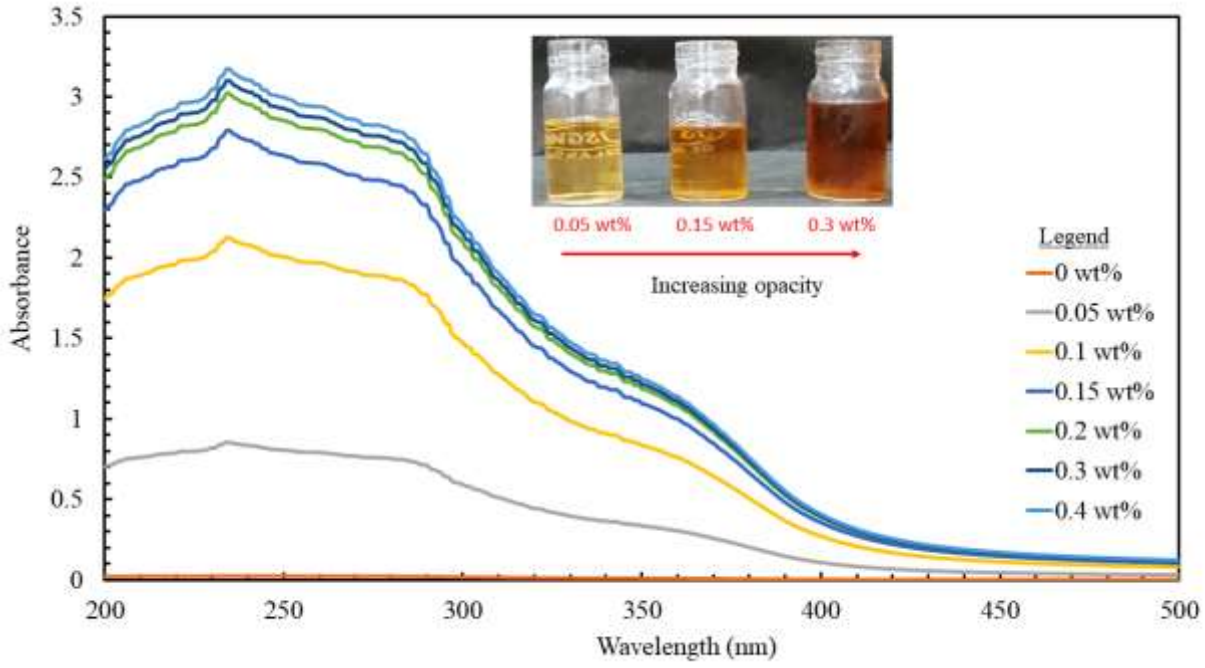

Figure 2.17: Calibration curve prepared by UV-*vis* analysis of surfactant solutions of varying concentration (0-0.4 wt%). Increasing surfactant concentration increased the opacity and peak absorbance value in solution.

2.3.13. Adsorption isotherms of green surfactant

The most commonly used adsorption isotherms are Langmuir and Freundlich isotherms. These isotherms are used to quantify sand adsorption on a rock surface, which is essentially important during surfactant use in EOR and foam injection operations. Adsorption isotherm indicates relationship between adsorbate (i.e. surfactant) suspended in liquid phase and adsorbate already adsorbed on surface of absorbent [138]. First, Langmuir isotherms were obtained using a reported methodology in literature [110]. Next, the value of surfactant adsorption determined as a function of equilibrium concentration and Langmuir parameters were established by a close fit of the curve in Figure 2.18. R^2 value of 0.987 indicates good curve fitting. Langmuir adsorption isotherm is usually applicable to conditions, involving monolayer adsorption on a homogenous surface (in this case, sand). The adsorption data for green surfactant as a function of adsorbent dose (concentration) has been shown in Figure 2.18. The initial value of adsorption was 0.42 mg/g for 100 mg/L equilibrium concentration. It increased to 0.61 mg/g for 400 mg/L solution, indicating increasing surfactant concentration suggested increase in surfactant loss. However, beyond (400 mg/L), it can be understood that increasing concentration did not further cause an increase in surfactant adsorption. From the data, it can be established that Γ_{max} (maximum adsorption) value was 0.6223 mg/g (Figure 2.18). This value is comparatively lower than adsorption value of anionic surfactant (SDS: 0.771 mg/g), cationic surfactant (CTAB: 0.867 mg/g), and non-ionic surfactant (Tergitol: 0.816 mg/g) reported in literature [110]. Since the formulated surfactant is anionic, it will show lower adsorption on sand surface than cationic and non-ionic surfactants. Also, given negative charge of sand, only weak interactions took place between anionic surfactant (like SDS and proposed green surfactant) and sand since the adsorption for them was lower. This indicates that formulated green surfactant can show better performance than

conventional oilfield synthetic surfactants. Also, along with Γ, R_L (a non-dimensional separation factor) is an important parameter [139]. To estimate R_L, the following Eq. 2 was used.

$$R_L = \frac{1}{1 + K_L C_0} \quad (2)$$

Here, C_o indicates initial concentration of adsorbate (green surfactant) in mg/L while K_L indicates Langmuir's constant. For R_L value between 0 and 1, a favorable nature of adsorption is achieved while value greater than 1 indicates unfavorable adsorption. For $R_L = 0$, it indicates that adsorption is irreversible and surfactant has now been lost forever on the surface. In this study, the values of R_L varied in between 0.0324 to 0.31, consistent with research findings of surfactant adsorption on sand surface [89,140].

Alternatively, Freundlich's isotherms were also determined for green surfactant. Freundlich's isotherms are used to indicate surfactant adsorption on a heterogeneous surface, involving multi-layer sorption obtained by curve fitting in Figure 2.18 [141]. The value of R_2 was 0.983 for Freundlich's fit, indicating a close fit for the variables of this study. K_F (mg/g) indicates Freundlich sorption capacity. In this study, K_F value of green surfactant was ~ 0.221 mg/g which is comparable with the value of anionic surfactant (SDS, 0.225 mg/g) (Figure 2.18). Also, Freundlich constant (1/n) denotes adsorption intensity of sand surface. For 1/n, a value between 0.1 and 0.5 indicates favorable adsorption while values 0.5-1 and greater than 1 indicate easy adsorption and difficult adsorption, respectively [142]. For green surfactant, Freundlich constant value of 0.182 was obtained which indicates favorable adsorption and moreover, its value was consistent with the value reported for SDS (0.177) in literature (Figure 2.18). Hence, from the data, it can be established that the performance of formulated green surfactant was similar to the performance of commercial alternatives in terms of adsorption nature (indicated by Langmuir and

Freundlich's isotherms). The primary objective of this study was to explore the role of natural surfactant for enhanced carbon storage in oil and gas reservoirs, and compare its performance with a surfactant typically used for these applications. SDS is a commonly used oilfield surfactant and it covers several applications in enhanced oil recovery, foam flooding, and mobility control of injected gas [9,35,50]. Hence, the natural surfactant was only compared with SDS to establish its application in areas where availability and use of synthetic surfactants is limited.

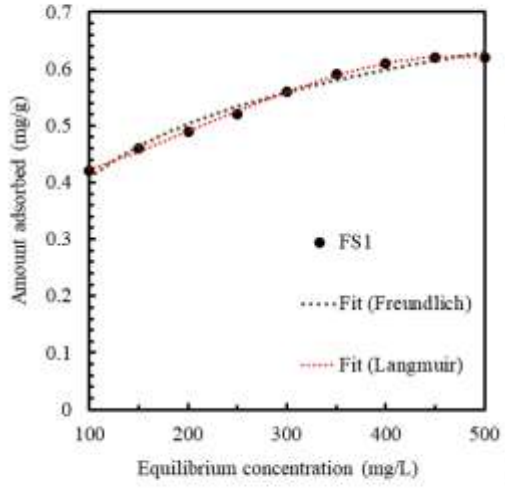

Modelling of adsorption isotherms and comparative performance with conventional surfactants

Isotherm Models	Parameter	Surfactant: FS (This study)	SDS [35]	CTAB [35]	Tergitol [35]
Langmuir	Γ_{max} (mg.g^{-1})	0.6223	0.771	0.867	0.816
	K_L *10^2 (L.mg^{-1})	1.889	2.212	1.851	2.152
	R^2	0.987	0.975	0.968	0.958
Freundlich	K_F (mg.g^{-1})	0.221	0.225	0.302	0.256
	1/n	0.182	0.177	0.149	0.177
	R^2	0.983	0.957	0.812	0.908

Figure 2.18: Langmuir and Freundlich isotherms to establish adsorption data of green surfactant for varying equilibrium concentration (100-400 mg/L).

2.4. Conclusion

In this study, a green surfactant of bio-resource (fenugreek seeds) was synthesized by Soxhlet method and its performance was evaluated for industrial applications such as CO_2 foaming and surfactant adsorption on sandstone surface. The surfactant nature was confirmed by the characterization results of different techniques such as FT-IR, XPS, UV-*vis*, and surface tension,

and compared with the properties of conventional surfactants in literature. The presence of irregularly shaped surfactant monomers was established by SEM/EDX methods, which also helped to identify carbon (≈ 84%), oxygen (≈ 15%), and traces of sodium, nitrogen, and phosphorus in surfactant. Surface tension measurements were conducted to determine CMC value (0.2 wt%) of surfactant, consistent with CMC values of commercial surfactants. CMC value of 0.2 wt% was also validated by electrical conductivity measurements. For foaming, CO_2 absorption in surfactant solution was understood through molality results, which demonstrated increased CO_2 absorption by 7-18% over water. The maximum CO_2 absorption (0.524 mol/kg of solvent) was obtained with surfactant solution FS2 at 12 bar and 30 ^oC. The green surfactant showed significant foaming potential as evident from foam volume (> 40 ml) and foam stability (10 h) results. In addition, CO_2 foams showed significant thermal stability with increasing temperature and CO_2 bubbles showed progressive increase in bubble coalescence. At 90 ^oC, significant CO_2 bubbles were present and foam maintained bubble coherence for a time period of ~ 8 h. Thus, the green surfactant can be used in CO_2 foaming for CO_2 based EOR and sequestration applications at elevated temperature. The green surfactant also showed superior foaming nature by altering the fluid-gas interfacial behavior as established by contact angle measurements. For water, contact angle value remained ~ 78^o over the entire test duration however, its value for green surfactant was significantly lower (44-48^o). Thus, surfactant inclusion made gas-liquid interface more suitable for the development of CO_2 bubble/foam. The surfactant adsorption tests on sandstone surface were performed where green surfactant solution yielded a mass-loss of 60%, which was better than the reported mass-loss of conventional surfactants. Green surfactant also showed favorable adsorption characteristics as it exhibited comparatively lower Γ_{max} than commercial surfactants in literature. The synthesized surfactant showed comparable adsorption behavior of an anionic surfactant as demonstrated by

both Langmuir and Freundlich isotherms. Hence, the use of green surfactant is proposed for CO_2 foaming and transport applications for effective CO_2 utilization in porous media.

Chapter 3

Physiochemical Characterization of Natural Surfactant

Abstract

Surfactants play a crucial role in diverse interfacial and multiphase systems due to their unique amphiphilic structure, enabling them to alter surface and interfacial phenomena effectively. Natural surfactants, derived from renewable sources, have garnered significant attention due to their environmental compatibility, biodegradability, and functional versatility in interfacial systems. Thus, this study insight a physiochemical characterization of saponin derived from Fenugreek seed as a natural surfactant. Natural surfactant was found to be effective at low concentrations based on its IFT value (10 mN/m at CMC 0.2 wt.%). The natural surfactant solution profile exhibited shear-thinning behavior at ambient and high temperature conditions. This study also reports the synthesis of alkali-surfactant-polymer (ASP) slug with the use a natural surfactant and natural polymer as an alternate for foaming in saline environment in practical applications. The natural surfactant (used at CMC level) derived from fenugreek seeds and guar gum (4000 ppm) was used as natural polymer, while the concentration of $NaHCO_3$ (alkali) was tuned to curtail the impact of salt-ions on foam-ability of ASP slug for practical applications. The desired ASP slug (nomenclature: 0.5ASP1) of 0.5 wt% alkali, 0.2 wt% surfactant (CMC), and 4000 ppm guar gum was developed after significant tuning in alkali concentration as per the variation in NaCl concentration (1-8 wt%). The desired slug 0.5ASP1 showed significant foaming potential till NaCl concentration of 2 wt% as demonstrated by superior foam height of 139.8 mm at span of 60 seconds which was only 113.4 mm for ASP slug (at salinity 2wt%). Microscopic investigations

were also conducted to visualize packing and coverage of foam bubbles stabilized by 0.5ASP1 and ASP slugs. 0.5ASP1 slug sustained bubbles for longer duration than ASP slug. The results concluded that inclusion of natural derivative in form of surfactant and polymer along with inexpensive alkali makes ASP slug a green alternative for practical applications such as oil recovery, crude emulsification, CO_2 foams, and IFT reduction.

3.1 Introduction

Globally, a significant portion of energy processes depends on efficient extraction and transport of fluids from porous and permeable geological formations [143]. While alternative energy technologies are emerging, conventional fluid-based systems still contribute substantially to the global energy portfolio [144]. With increasing population and improved living standards, the demand for efficient resource utilization from subsurface environments continues to rise [145]. Notably, a large fraction of the accessible subsurface fluids remains unrecovered, highlighting the need for advanced methods to enhance fluid displacement efficiency [146,147]. To improve the recovery rate, various enhanced fluid transport techniques have been developed. Among these, chemically-assisted displacement methods are receiving growing interest due to their improved performance and adaptability across a wide range of subsurface conditions [59,148]. These methods typically involve the injection of specially formulated slugs designed to alter the physicochemical environment and improve the mobility of trapped fluids [149,150]. Chemical approaches generally include the use of alkalis, surfactants, polymers, or combinations thereof. Among them, surfactant-based methods are particularly noteworthy, as they significantly reduce interfacial tension (IFT) between immiscible phases [151]. This reduction in IFT increases the capillary number and facilitates wettability alteration, enabling more effective fluid mobilization within porous networks and contributing to enhanced displacement efficiency [152]. Addition of

surfactants seems highly effective in reducing IFT in oil-water system and the charge on the surfactant has to play a major role in reduction of IFT as the molecules of ionic surfactant possess some charge and these charge form a monolayer at the interface of the system [3]. Additionally, surfactants have favorable impacts on emulsion formation and rock wettability [153,154]. Bigger droplets of oil are transformed into fine droplets which may easily travel through the porous and permeable reservoir rock matrix [155]. However, chemical based surfactants are toxic and non-biodegradable, causing environmental concerns before their application [32]. In addition, the high cost of synthetic surfactants is making a huge impact on the economy [68].

Surfactant extraction from green origin is gaining enormous attention from the relevant scientific community, due to various value addition as compared to synthetic surfactants, economical, widely available, environmentally friendly, non-toxic, and the simplest extraction process [90]. Soxhlet apparatus has been used to extract natural surfactant from various biomass derived sources [23,30]. Table 3.1 presents a summary of previous studies on synthesized natural surfactants, highlighting their potential in reducing interfacial tension and contact angle for improved interfacial behavior in fluid transport systems. Chhetri et al. [32] developed a natural surfactant from Soapnut pericarp and used it in reducing IFT between oil-water. Moreover, it was established that natural surfactant was environmentally friendly as well as economical compared to synthetic surfactant [98]. Rehmati et al. [26] introduced natural surfactants from two leaves of mulberry and henna. Surfactant derived from mulberry exhibited IFT reduction from 43.9 to 4.01 mN/m. Natural zwitterionic extracted from castor oil was developed by Zhang et al. [36] and it showed potential in IFT reduction of oil-water to the value of 5.4×10^{-3} mN/m. Saxena et al. [38] also synthesized a biodegradable surfactant from palm oil. A natural non-ionic surfactant was

derived from eucalyptus leaves, which showed potential in IFT reduction from 35.2 to 10.5 mN/m at a CMC of 3.5 wt.% [39].

Table 3.1: Natural surfactants and their potential in reducing interfacial tension and contact angle as reported in the literature.

References	Surfactant	IFT range (mN/m)	Contact angle Reduction
[32]	Soapnut pericarp	19 - 2.5	-----
[33]	Glycyrrhiza Glabra	33 – 9	-----
[34]	Zyziphus Spina Christi	48 -9	-----
[35]	Leaves of Olives	36.5 – 14	-----
	Leaves of Prosopis	36.5 – 15.11	-----
	Leaves of Spistan	36.5 – 20.15	-----
[36]	Castor Oil	5.4×10^{-3}	-----
[26]	Mulberry leaves	43.9 - 4.01	62.5^{o}- 48.5^{o}
	Henna leaves	43.9 - 3.05	66^{o} – 37^{o}
[38]	Palm oil	1×10^{-3}	-----
[39]	Leaves of Eucalyptus	35.2 – 10.5	140.6^{o} – 60.2^{o}

Moreover, the inclusion of surfactants is not only limited to IFT reduction but also exhibits effective wettability shifts, that is, from oil-wet to water- wet and typically assessed via contact angles of the rock/fluids systems [156,157]. For instance, the contact angle before natural surfactant on a carbonate surface was 140.6º which reduced to 60.2º [39]. Pal et al. [158] extracted a novel Gemini surfactant from sunflower seeds and it exhibited a significant shift in wettability. Pure saponin surfactant can lower the IFT values of kerosene/water system by 66.98–77.31% [159]. Alsabagh et al. [160] developed a non-ionic surfactant and used it to achieve ultra-low IFT of 0.06 mN/m.

In all studies, natural surfactants have shown to be a better alternative (economical and eco-friendly) to synthetic surfactants of chemical origin. Also, some study has also reported that foaming potential as well as foam stability is higher in case of ionic surfactants as compared to nonionic surfactants [161]. Despite their relevance in various fluid transport and interfacial engineering applications, the potential of green anionic surfactants derived from fenugreek remains largely unexplored in the context of advanced subsurface displacement or flow enhancement processes; which is noteworthy. Therefore, the novelty of this work lies in the development of a newly synthesized surfactant derived from an agricultural source (fenugreek seeds) offering a sustainable and biodegradable alternative for interfacial engineering. Additionally, the integration of this biosurfactant with natural polymers and alkali presents a novel formulation aimed at enhancing fluid displacement, wettability control and interfacial modification in thermofluid and porous media systems.

Thus, this study presents the synthesis and development of green surfactant extracted from fenugreek seeds using the Soxhlet extraction technique. Interfacial tension of green surfactant was determined and surfactant solutions of different concentrations ranging from 0 to 0.5 wt% was

explored. Rheological and contact angle measurements were performed to evaluate the flow behavior and surface wettability characteristics of the natural surfactant. The foamability of the natural surfactant was assessed in combination with a natural polymer and alkali to investigate its potential for stable foam generation under varying conditions. This was followed by analysis showing impact of salinity (1-8 wt% NaCl) on suppression/promotion of foam prepared by ASP slug. Thereafter, the concentration of alkali was tuned to envisage any improvement in foam-ability of ASP slug and a slug of optimum foaming was conceived for saline conditions where initial ASP slugs failed to exhibit foaming. The help of several experiments such as surface tension, IFT, microscopic analysis, and contact angle measurements was taken for foaming studies of ASP slugs. The findings suggest that ASP formulations based on natural derivatives hold potential as alternative chemical strategies for improving fluid displacement in subsurface systems that (1) contain a significant fraction of immobile fluid and (2) experience dynamic changes in salinity.

3.2 Materials and Methods

3.2.1 Materials

For this study, the agro-product fenugreek seeds were procured from a retail outlet in Amethi (Uttar Pradesh), India. The solvent methanol was used as purchased from the supplier (SD Fine Chemicals, India). The aqueous solution of natural surfactant was prepared using deionized (DI) water, which was procured from Millipore® Elix-10 water purification apparatus. The Soxhlet apparatus and hot air oven were used and were provided by Jain Scientific Glassworks, India for surfactant extraction and drying of samples, respectively. The sand properties have been provided in detail in our previous work.[57] The crude oil properties are provided in our previous works.[57,162] The alkali Sodium bicarbonate ($NaHCO_3$; purity > 99%), polymer (guar gum; purity 99%), and salt (NaCl; purity 99.5%) were purchased from SD Fine Chemicals, India. All

the aqueous solutions were properly mixed using magnetic stirrer (Model: IKA-C-MAG-HS7). The electrical conductivity of DI water was 0.0054 $mS.cm^{-1}$ and it has no total dissolved solids (TDS) content. Foaming potential of ASP slugs was checked by a dynamic foam analyzer (DFA, Model: KRUSS DFA100).

3.2.2 *Interfacial tension measurements*

To understand the surfactant potential, the determination of CMC is an essential governing parameter that optimally reduces IFT between aqueous solution and organic compound (crude oil). Moreover, IFT reduction is a major trait for surfactant performance in various industrial applications. Thus, CMC was determined using Wilhelmy plate method (model: K12 Kruss® Germany). These investigations were performed at least 5 times and averaged a value with deviation have been reported.

3.2.3. Rheological behavior of green surfactant

Rheological studies of biomass derived green surfactant was performed to investigate the flow behavior using a modular compact rheometer (MCR-52, Anton Paar, Austria). Surfactant solution was poured into cup and double gap system of rheometer followed by measurement of viscosity over a wide range of shear rate (1-1600 s^{-1}) [163].

3.2.4. Contact angle measurements

Contact angle measurements were conducted in a stainless-steel pressure cell, equipped with glass viewing ports to visually observe the droplet of surfactant solution. The entire set up was manufactured by D-C

AM Engineering, India. This setup was used for surface tension measurements by the help of pendant drop method [164], under the environment of high pressure (12 bar) maintained by the help of a syringe pump (Teledyne ISCO, USA). A high-resolution camera (Phantom VCC, USA) was used to record the images of droplet of surfactant solution on a glass slide in the presence of pressurized air [165].

3.2.5. Method of foam preparation and its analysis

First, the natural polymer solution of 4000 parts per million (PPM) was prepared by mixing natural polymer guar gum (4 gm) in 1000 ml of DI water. Next, 60 ml of polymer solution was taken into a beaker and 1 wt% of alkali ($NaHCO_3$) added while mixing was kept on, followed by surfactant addition at critical micelle concentration (CMC, 0.2 wt%) using magnetic stirrer in order to obtain ASP formulation. The concentration of the chemicals were chosen from literature, considering an optimal performance and economics [166,167]. Surfactant was used at CMC as beyond CMC, surfactant monomers are highly dominated by micelles and reverse impact on IFT and wettability alteration can be observed [30,42]. To prepare and analyze foaming potential of prepared slugs, dynamic foam analyzer (DFA) was used. DFA is quite easy to use and analyze liquid foams *via* precise measurements of volume and its degradation (e.g., foam stability/height) over a period of time. To prepare foam, 50 ml of each slug was taken in test column of DFA and software-controlled air purged at flow rate of 0.3 L/min. In general, there are various methods of generating foams, which includes stirring, shaking, and sparging. A comparative study of various methods of foam generation was conducted in previous literature [168]. According to this, foam generation by sparing method was comparatively better than three methods (*i.e.*, stirring, shaking, and sparging). DFA also helps in the determination of total height along with foam and liquid heights. Moreover, it is helpful in quick and precise measurement of foam stability as it accurately

measures the content of liquid in foam, which thereby saves the time of manual calculations. Furthermore, to examine foaming potential of ASP slug in saline environment, NaCl concentration was varied from 1-8 wt% similar to the ones prepared during forming tests of AP slug in saline conditions. To study the role of alkali, $NaHCO_3$ concentration was varied from 1-5 wt% while the concentration of polymer (60 ml), surfactant (CMC, 0.2 wt%), and NaCl (8 wt%) was kept constant. These tests help to tune the composition of ASP slug so that its foaming potential can be revived at severe condition (8 wt%) of saline environment. Therefore, concentration of $NaHCO_3$ was checked both ways (increased/decreased) to optimize the amount of alkali in ASP slug. ASP slug of reduced $NaHCO_3$ concentration was prepared with 60 ml of polymer solution, 0.2 wt% surfactant, 0.5 wt% $NaHCO_3$, and examine its foaming potential in NaCl concentration ranges from 1-8 wt%. The compositional details and nomenclature of prepared slugs have been provided in Table 3.2. Lastly, the concentrations of alkali and salt were tuned to achieve an optimum ASP slug in saline environment.

3.2.6 Microscopic analysis

After the preparation of foam, small quantity (1.5-2.5 ml) was extracted by standard laboratory pipette (Tarsons, United States) and carefully released on clean glass slide. The glass slide was taken under an optical microscope (Motic, Hong Kong) and the images of foam recorded at regular time interval using an inbuilt imaging tool (Moticam-10).

3.3 Results and Discussion

In this section, initially discussion on IFT results between crude oil and surfactant solution, rheological behavior of extracted surfactant solution and contact angle measurements was done. Next, a discussion on foaming potential of synthesized different slugs (see Table 3.2) was

examined by the help of DFA followed by discussion on role of alkali and surfactant in ASP slugs. Next, the role of salt in suppressing/improving foams was investigated. Among tested slugs, the desired formulation has been identified on the grounds of foaming and better stability in saline environment. Last, the results of microscopic analysis were presented and discussed accordingly.

Table 3.2: Summary of nomenclature, compositional details, and description of different samples prepared.

Serial number	Slug	Sample Nomenclature	Sample description (for 60 ml solution)
1	Alkali-surfactant-polymer (ASP) slug	ASP	1 wt% alkali + 4000 ppm guar gum + surfactant at CMC (0.2 wt%)
2		ASP1	1 wt% alkali + 4000 ppm guar gum + surfactant at CMC (0.2 wt%) + 1 wt% NaCl
3		ASP2	1 wt% alkali + 4000 ppm guar gum + surfactant at CMC (0.2 wt%) + 2 wt% NaCl
4		ASP3	1 wt% alkali + 4000 ppm guar gum + surfactant at CMC (0.2 wt%) + 4 wt% NaCl
5		ASP4	1 wt% alkali + 4000 ppm guar gum + surfactant at CMC (0.2 wt%) + 6 wt% NaCl
6		ASP5	1 wt% alkali + 4000 ppm guar gum + surfactant at CMC (0.2 wt%) + 8 wt% NaCl
7	ASP slug with higher alkali concentrations	2ASP	2 wt% alkali + 4000 ppm guar gum + surfactant at CMC (0.2 wt%) + 8 wt% NaCl
8		3ASP	3 wt% alkali + 4000ppm guar gum + surfactant at CMC (0.2 wt%) + 8wt% NaCl
9		4ASP	4 wt% alkali + 4000 ppm guar gum + surfactant at CMC (0.2 wt%) + 8 wt% NaCl
10	ASP slug with lower alkali concentrations	0.5ASP	0.5 wt% alkali + 4000 ppm guar gum + surfactant at CMC (0.2 wt%) + 8 wt% NaCl
11		0.5ASP1	0.5 wt% alkali + 4000 ppm guar gum + surfactant at CMC (0.2 wt%) +2 wt% NaCl
12		0.5ASP2	0.5 wt% alkali + 4000 ppm guar gum + surfactant at CMC (0.2 wt%) + 4 wt% NaCl
13		0.5ASP3	0.5 wt% alkali + 4000 ppm guar gum + surfactant at CMC (0.2 wt%) +6 wt% NaCl

3.3.1. Interfacial tension measurements

The injection of surfactant slug within porous media tends to enhance the mobility of residual oil by decreasing IFT at oil and water interface resulting in a corresponding improvement in capillary number thus lower residual oil. When surfactant comes into contact with immiscible fluids (e.g., water and crude oil), the hydrophobic portion of surfactant micelles position itself towards crude oil whereas hydrophilic portion align itself towards water. This orientation of surfactant micelles leads to reduction in surface free energy [12]. Figure 3.1 shows a graph plotted between IFT (mN/m) and surfactant concentration (wt.%) at ambient conditions.

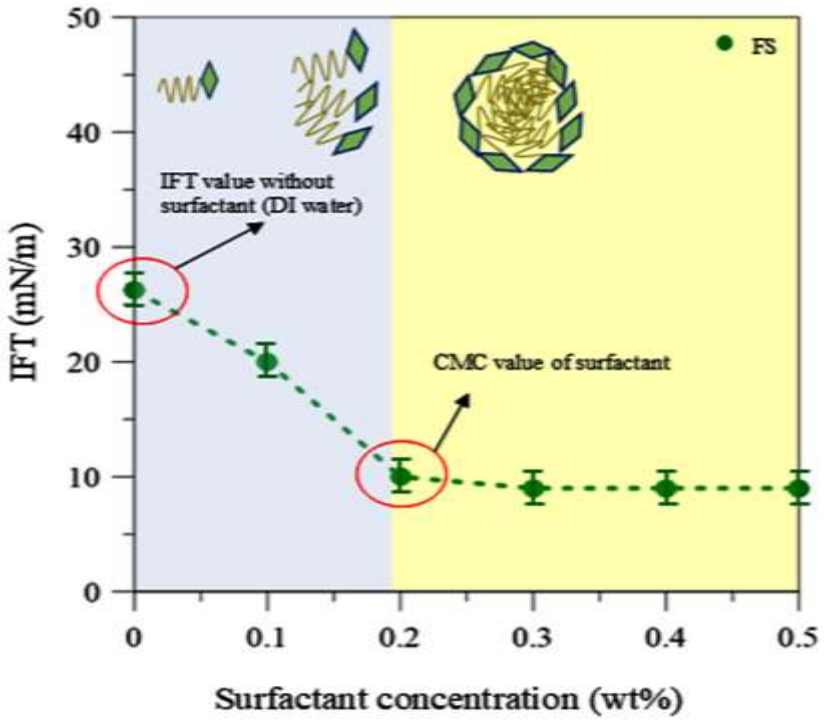

Figure 3.1: IFT measurements between crude oil and natural surfactant in varying concentration for determination of CMC (0.2 wt%) and surfactant interaction profile with crude oil.

It was observed that the value of IFT at crude oil and DI water interface was around 27 mN/m, which is in line with the reported study [165,169]. Similarly, in other observation

[32,39,170,171], the value of IFT between crude oil and DI water was found to vary in the range of 19-36 mN/m. This confirms that IFT value of 27 mN/m, observed in the study, is fairly aligned in the range of reported literature. With increasing surfactant concentration, IFT initially decreased which might be due to the fact that surfactant molecules at lower concentration tends to adsorb at oil-water interface [102,165,172]. At 0.1 wt.% surfactant, IFT was measured to be around 20 mN/m and with 0.2 wt.%, this value was further reduced to ~10 mN/m. IFT value of 10 mN/m at 0.2 wt.% was found to be the minimum as thereafter, IFT exhibited a constant trend and barely showed any variation till the concentration of surfactant was explored (0.5 wt.%). The trend of reducing IFT with increase in surfactant concentration has been also reported in the literature and in Table 3.1 [68,173]. The point, where IFT curve showed a constant trend despite of increasing surfactant concentration, is said to be CMC value of surfactant, consistent with research findings in the literature [39]. It is expected that oil-water interface is saturated by surfactant micelles at CMC and above CMC, these micelles prefer to stay in bulk liquid phase [98]. This indicates the impact of largest change in IFT value of crude oil is possible at CMC and concentration more than that will hardly produce any effect on crude oil mobilization. Thus, surfactant use at CMC level is recommended for field applications.

3.3.2 Rheological measurements of surfactant solution

Rheological measurements were performed to elaborate the effect of shear deformation and temperature on flow characteristics of natural surfactant (SS: fenugreek surfactant) during injection operations [174]. Whenever stress is applied, it leads to some changes in the flow behavior of matter which is very important for effectiveness of formulation, as its performance remains stable as long as it maintains sufficient viscosity to ensure proper interaction with the target medium and reduce interfacial tension. To quantify the impact of shear deformation,

viscosity measurements were performed over a wide range of shear rate (1-4000 s^{-1}) and the result is provided in Figure 3.2a. It is clear from Figure 3.2a that viscosity of FS was around 0.6 Pa.s at shear rate of 6 s^{-1}. Next, with increasing shear rate, viscosity tends to decrease and reached to the minimum level of 0.006 Pa.s at 100 s^{-1}. With further increase in shear rate to 4000 s^{-1}, viscosity did not decrease much and was sustained at the level of 0.0016 Pa.s.

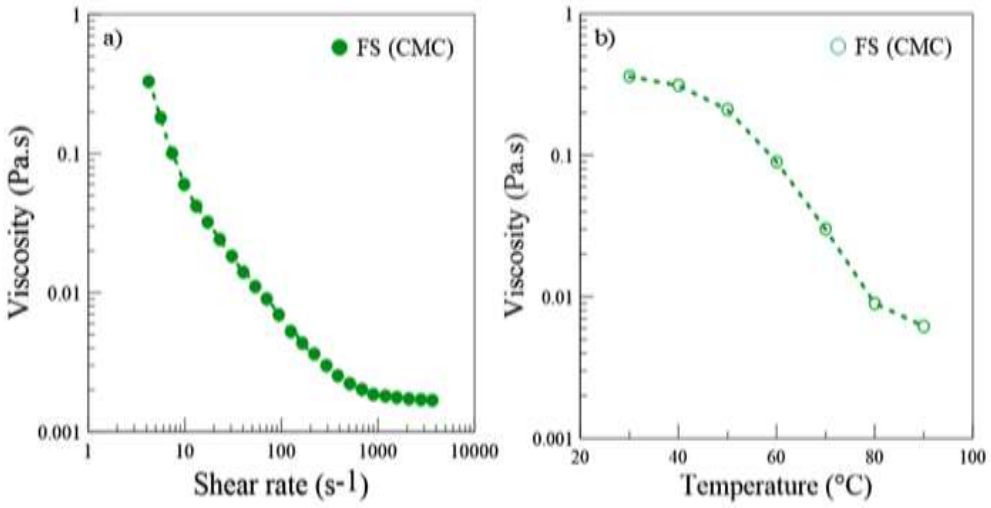

Figure 3.2: Plots showing viscosity of natural surfactant solution at 0.2 wt% (CMC) as a function of varying shear rate at (a) constant temperature ~30ºC (b) at varying temperature ranges from 30-90ºC.

Similar rheological behavior of a natural surfactant has been also explained in previous literature [41,175]. In addition, it can be stated that surfactant exhibited non-Newtonian shear thinning behavior because viscosity decreased with an increase in shear rate. It is a classical shear thinning profile, as observed in various other oilfield suspensions like polymers, surfactants, and nanofluids [102]. Later, the rheological analysis was performed for viscosity (zero-shear) *vs.* temperature where viscosity was initially recorded to be 0.6 Pa.s at 30 ºC (see Figure 3.2b). With an increase in temperature, viscosity followed decreasing trend till it reached to the level of 0.009

Pa.s at 80 ºC. This can be attributed to the effect of temperature as natural surfactants tend to degrade at higher temperatures [98]. However, the viscosity results of FS are in line with research findings in the literature [41,102], where other surfactant solutions also showed similar behavior as a function of shear rate and temperature.

3.3.3. Contact angle measurements

Contact angle study helps to analyze the wetting property of a liquid through alteration in air-liquid interface [176]. Wettability term here refers to the increase in wetting tendency of fluid, which was understood through contact angle measurements in the presence of air [165,177,178]. The wetting tendency of a fluid on solid surface can be measured by contact angle [179]. Contact angle is always measured from denser to lighter phase and increase in contact angle indicates increase in wetting property of fluid however, decrease in contact angle is related to more wetting by non-wetting (air) phase on surface or decrease in wetting tendency of fluid. These measurements were conducted for FS in presence of air at ambient conditions and compared with the ones of DI water in Figure 3.3. It was observed that contact angle results of FS were better than the results of DI water as lower the contact angle, higher the wetting on surface. It is evident from Figure 3.3 that FS exhibited lower contact angle values than DI water over the entire range of period (min) explored. For FS, the initial (0 min) contact angle was measured as 74º as shown in Figure 3.3. It is also clear that the maximum change in contact angle occurred during initial 8-10 min and after that, contact angle almost exhibited a plateau. Contact angle value of 48º was recorded after 8 min, which indicates a good wetting characteristic of FS over DI water. DI water showed contact value of 70º after 8 min. A similar study was reported in the literature where reduction in contact angle from 62.5º to 48.5º was observed for mulberry leaf extract and 66º to 37º for Heena leaf extract [26].

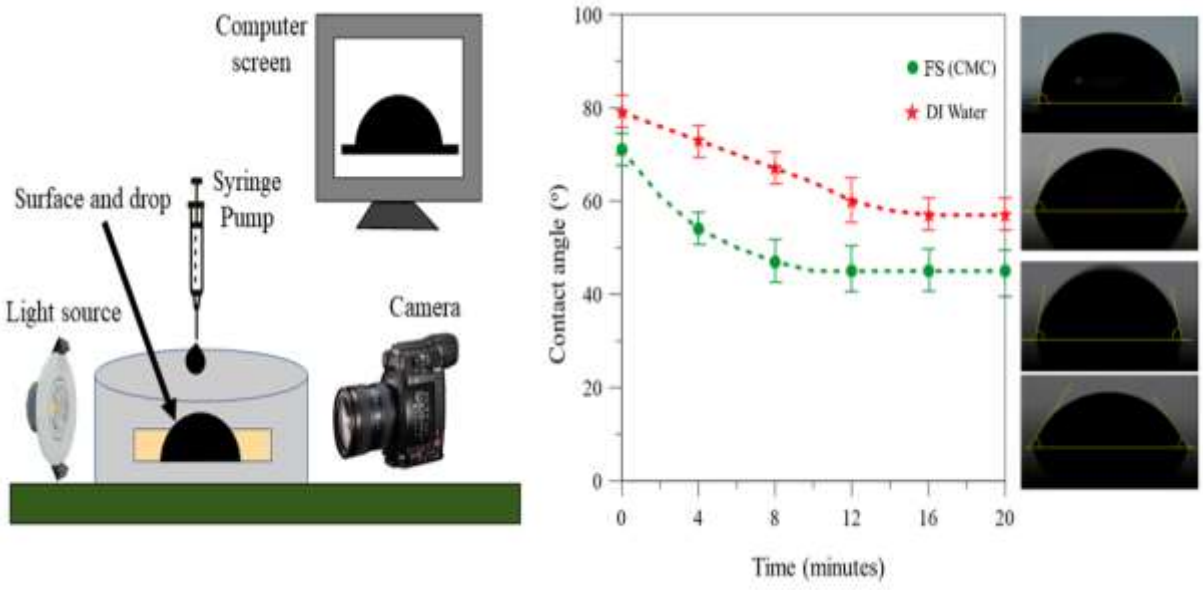

Figure 3.3: Schematic showing instrumental details of contact angle measurement. The real image the measured contact angle and their variation with time for DI water and 0.2 wt% (CMC) natural surfactant solution at ambient conditions.

A lower contact angle value (in presence of FS) indicates that the surface is highly wetted by that liquid. It indicates that the liquid droplet spreads more extensively across the surface, suggesting improved displacement of the existing fluid from that surface. Therefore, the use of natural FS is encouraged for enhancing the displacement efficiency of trapped fluids within narrow channels.

3.3.4. Foaming of surfactant with alkali and polymer

It is well-known that the presence of alkali tends to reduce the adsorption of surfactant on rock surface [180]. As a result, the combined use of alkali, surfactant, and polymer has received significant attention as a highly effective formulation strategy, owing to the synergistic benefits offered by each component [181]. Figure 3.4 presents a schematic to show the role of surfactant

in IFT reduction and emulsification of ASP slug. Surfactant plays a significant role in IFT reduction.

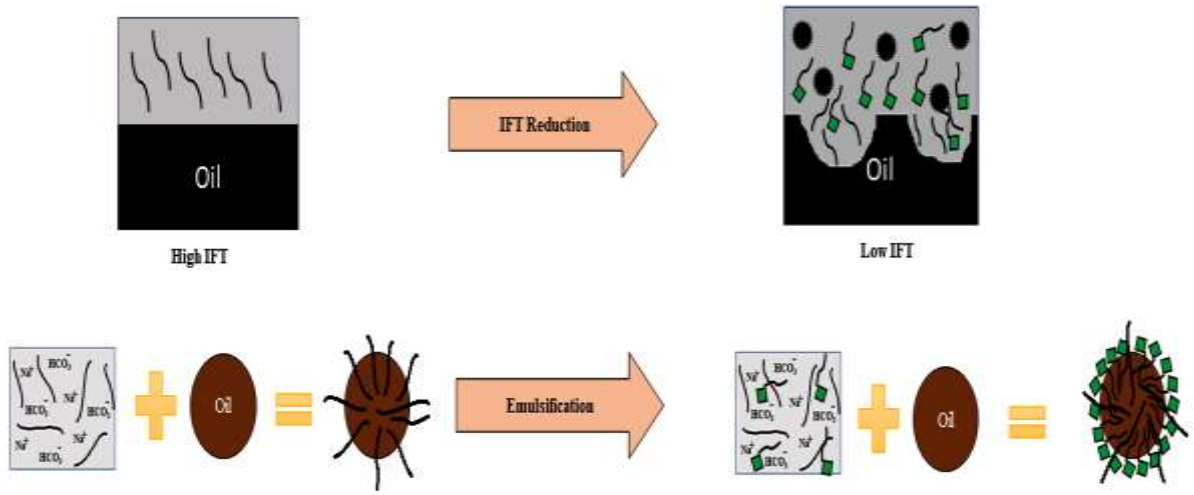

Figure 3.4: Role of surfactant on IFT reduction and emulsification.

The presence of alkali facilitates the formation of surface-active agents in situ through chemical interactions with native organic compounds. When combined with externally introduced surfactants, this synergy significantly reduces interfacial tension [182]. Surfactant micelles assist in dispersing trapped hydrophobic substances into finer droplets, enabling their mobilization within the medium as stable emulsions (oil-in-water)[183,184]. Thus, surfactants play a crucial role in such chemical systems, as supported in literature[185–188]. In a foam mixture, water film between bubbles is thinning constantly while liquid is flowing. Surfactants are added to form and stabilize the foam and prevent it from coalescing [189,190]. The water drainage between bubbles is reduced due to added surfactants at the bubble surface due to Marangoni effect, thereby controlling the foam behavior [43,191,192].

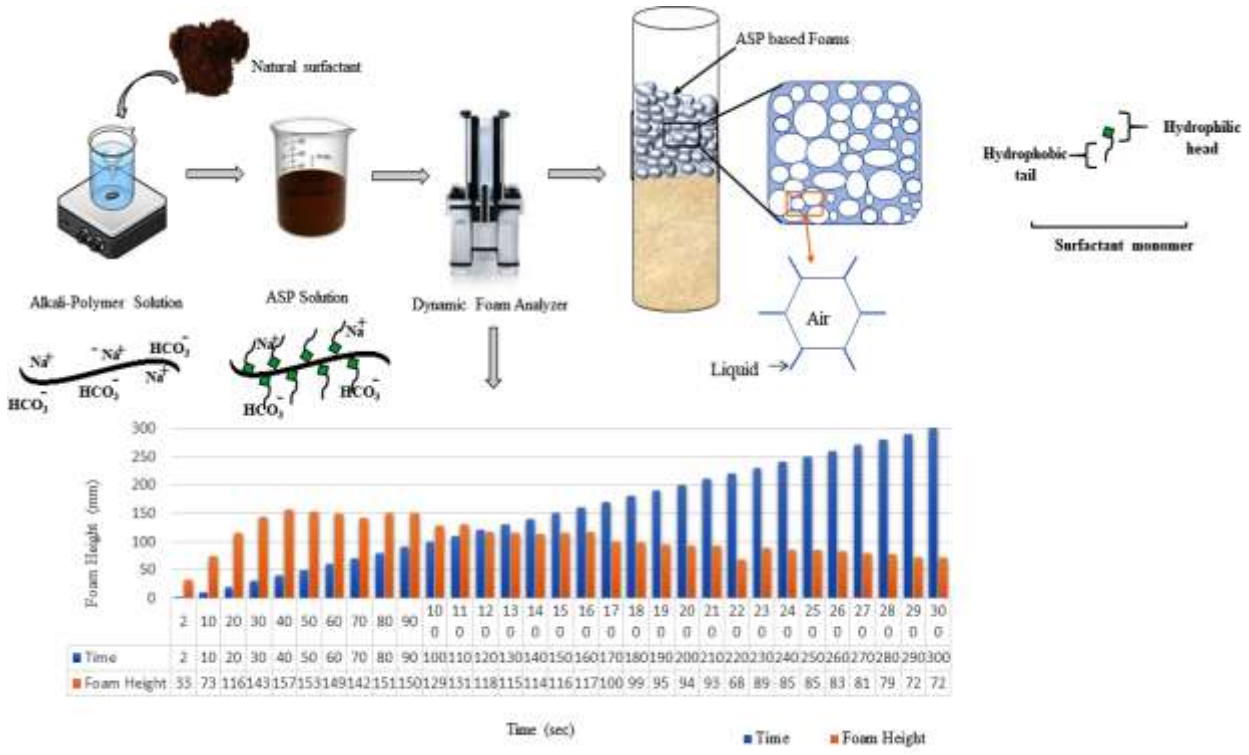

Figure 3.5: Schematic showing formulation details of ASP solution using alkali- polymer solution and natural surfactant along with its foam height as a function of time at ambient conditions.

Figure 3.5 shows the results of time dependent foam height for ASP slug prepared by 60 ml of gaur gum solution (4000 ppm), 1 wt% alkali, and 0.2 wt% surfactant. With ASP slug, foam height of 157 mm was achieved at 40 s. In ASP slug, foam was found to be much more stable as foam height reduced only to the level of 99 mm after 180 sec and ~ 72 mm after 300 sec (Figure 3.5). This clearly indicates the role of surfactant in producing stable foams and thus, the use of fenugreek-based surfactant can be promising, eco-friendly and great green alternative over synthetic and toxic harmful surfactants in industrial and environmental applications.

3.3.5. ASP slug performance in saline environment

Foaming potential of ASP slug in saline environment has been analyzed and reported in form of foam height in Figure 3.6 where, salinity was varied from 1-8 wt%. From the Figure

3.6, it can be seen that foam tends to degrade with increasing NaCl concentration except in the case of 1 wt% NaCl (ASP1 slug).

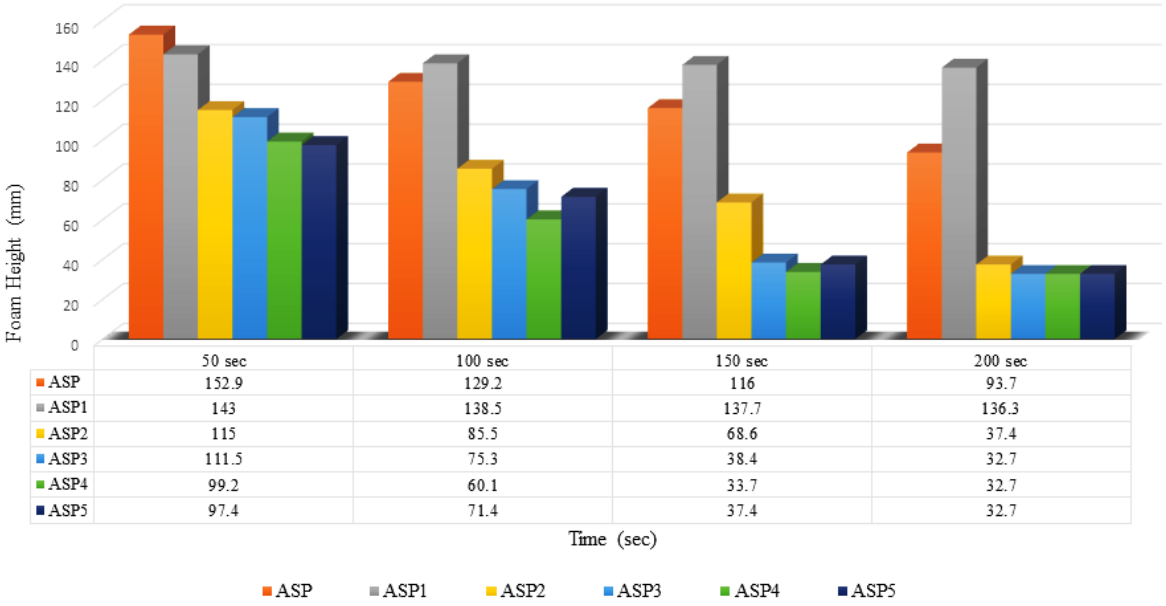

	50 sec	100 sec	150 sec	200 sec
ASP	152.9	129.2	116	93.7
ASP1	143	138.5	137.7	136.3
ASP2	115	85.5	68.6	37.4
ASP3	111.5	75.3	38.4	32.7
ASP4	99.2	60.1	33.7	32.7
ASP5	97.4	71.4	37.4	32.7

Figure 3.6: Salt tolerance potential of ASP slug on different periods of measurement. ASP1 exhibited minimal degradation in foam height.

For example, with 1 wt% NaCl, the initial foam height of ASP1 slug was lower than the foam height of ASP slug without NaCl. But, its performance was better as it exhibited only 4.68% loss in foam height after 200 sec, which was higher (38.72%) in ASP slug after 200 sec (Figure 3.6). It has been studied that salt increases the foam stability owing to enhanced adsorption however, this is valid below or near to CMC value of surfactant in solution [193]. With concentration above CMC, structural forces tend to appear which are likely to rupture film [194]. With further increase in NaCl concentration, the foaming potential of ASP slug gets significantly affected as resulting foam height reached to minimum level of 32 mm approximately in ASP2, ASP3, ASP4, and ASP5 for 2, 4, 6, and 8 wt% NaCl, respectively. Thus, maximum reduction (70.67%) in foam height was measured for ASP3 slug of 4 wt%

NaCl. It might be credited to the fact that salt tends to improve durability in foam systems stabilized by ionic surfactants [195,196]. However, dubious effect may also work after a certain concentration of salt [197], which mechanistically signifies salt as foam destructor or stabilizer in foam systems. Thus, salt behavior on foaming should be related to concentration added and presence of other ingredients in system [198,199]. From results, it may be concluded that ASP based air foams can only be stable around salinity of 1 wt% NaCl, whereas foams of other ASP slugs (ASP2, ASP3, ASP4 and ASP5) showed unstable foaming behavior.

The role of salt in micellization of an anionic surfactant in bulk phase is shown by schematic in Figure 3.7. At higher salinity, surfactant molecules precipitate or tend to form crystals which ultimately results in lowering foam-ability [200,201]. It is to be noted here that surfactant micelles develop only when surfactant amount in bulk phase is near to CMC level.

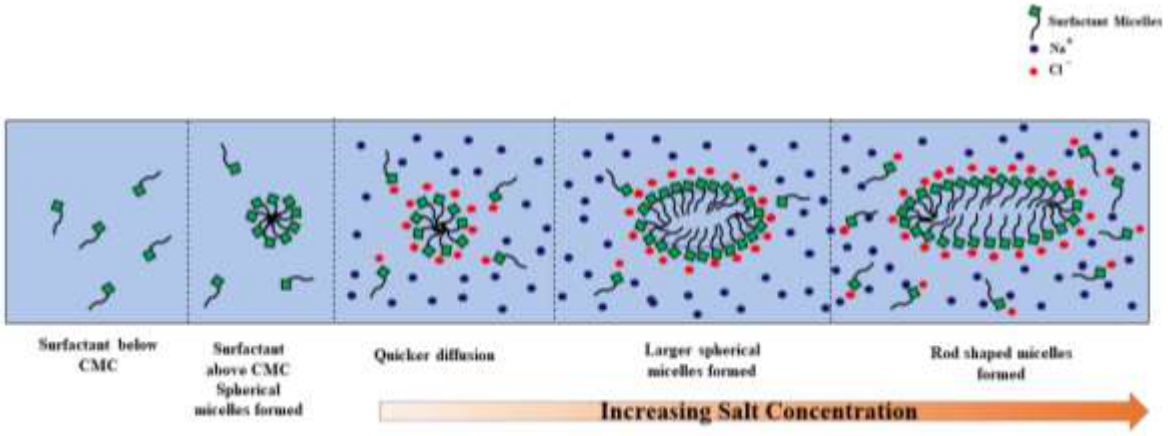

Figure 3.7: Schematic to show impact of increasing salt concentration on surfactant micelles involved in the formation air foam.

With the increase in salt concentration, rod-shaped micelles are expected to form as shown in Figure 3.7. It might be credited to the fact that salt usually alters CMC value due to electrostatic repulsion that occurs among head groups of surfactant [202]. In addition, it is to be noted here that the concentration of other chemicals (polymer and alkali) was constant

throughout the variation of NaCl in ASP slug. Moreover, surfactant was added only at CMC level (0.2 wt%). Thus, it is interesting to vary the concentration of other ingredients and check the possibility of reviving foaming in surfactant-based air foams at high levels of NaCl concentration.

3.3.6. Tuned alkali concentration on foaming potential of ASP slug

Foam height results of ASP slug concluded that it was performing better at 1 wt% NaCl and afterwards (NaCl concentration > 1 wt%), foams progressively failed to show enough foaming. Though ASP5 exhibited foaming even at 5 wt% NaCl but this foam was not enough stable due to excessive coalescence between large sized bubbles. To revive foaming in ASP5 slug, alkali concentration was tuned to 0.5 wt% (decrement) as well as 2-4 wt% (increment). The effect of tuned $NaHCO_3$ concentration on foam height of ASP slug in saline environment of 8 wt% is shown in Figure 3.8.

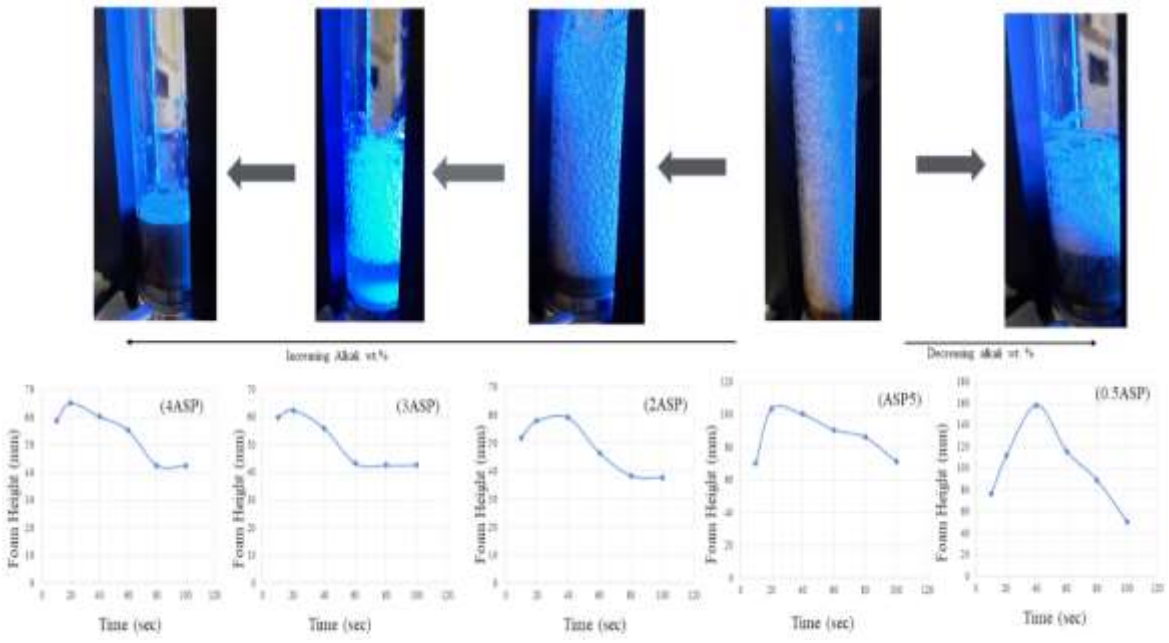

Figure 3.8: Effect of different alkali concentration on foaming and foam height results of ASP slug in high saline environment (8 wt% NaCl).

Here, concentration of surfactant and polymer was kept constant e.g., 0.2 wt% (CMC) and 4000 ppm, respectively. It was observed that the quality of foam slightly deteriorated with increasing $NaHCO_3$ concertation from 1 to 2 wt%. As a result, foam height decreased from 52 mm to 37.6 mm. With further increase in $NaHCO_3$ concentration (3 wt%), foaming significantly reduced (foam height 42.7 mm only) as large size bubbles formed followed by eventual disappearing from the test column of DFA. Moreover, at $NaHCO_3$ concentration of 4 wt%, a very thin layer of foam developed on the surface of aqueous solution which can be evident from actual images in Figure 3.8 as well as foam height (peak value = 65.1 mm at 20 sec). Thus, it can be concluded that increasing alkali concentration could not curtail the adverse effect of salinity and produce foaming in ASP slug. An accepted hypothesis concludes that the presence of alkali leads to the reduction of surfactant adsorption [180]. On the other hand, 4 wt% alkali promoted more unstable behavior and hardly produced any foaming in ASP slug under saline conditions of 8 wt% NaCl with an average foam height of ~54 mm. When the concentration of alkali is quite high, the oppositely charged ions tend to enter from diffusion layer to adsorption layer [186]. As a result, the electrostatic repulsion between surfactant and rock surface becomes weaker. This facilitates the adsorption of surfactant on rock surface [203]. Further, polymer hydrolysis is increased with increasing alkaline concentration in ASP system.

In most of the practical applications, salinity is much higher than alkaline concentration which is likely to be around 1-2% [204]. In this study, lower concentration of $NaHCO_3$ (0.5 wt%) was also chosen to analyze its effect on foaming in adverse condition of 8 wt% NaCl. Interestingly, it was found that the inclusion of lower alkali concentration (0.5 wt% $NaHCO_3$) significantly improved foaming in 0.5ASP slug as compared to ASP slug with $NaHCO_3$ concentration > 1 wt%. Though foaming revived at lower $NaHCO_3$ concentration but foam was not stable as desired for

practical applications. Initially, the foam height was observed to be 75.9 mm at 10 sec thereafter, it increased to 110.2 mm at 60 sec followed by peak value of 158.3 mm at 40 sec. Further, the high salinity witnessed deterioration in foam resulting foam height reduced to minimum level of 50.5 mm in 100 sec. For this purpose, the concentration of salt reduced this time so that NaCl concentration, that resulted into superior foaming in 0.5ASP slug, is identified. Figure 3.9 shows results of foam height in 0.5ASP slug as a function of decreasing NaCl concentration such as 8 wt% (Figure 3.9a), 6 wt% (Figure 3.9b), 4 wt% (Figure 3.9c), and 2 wt% (Figure 3.9d). With higher salinity (8 wt% NaCl), foaming was observed at its peak only in initial 30 sec with a value ~128 mm after which foam height decreased and reached to the value of ~37 mm in span of 150 sec (Figure 3.9a). Similarly, at 6 wt% NaCl, foam height was at its peak (129.2 mm) at 60 sec and thereafter, a sudden drop recorded with a value of 58.4 mm at 90 sec followed by 40 mm at 120 sec. Finally, it reached to lowest level of 36.1 mm at 150 sec (Figure 3.9b). At 4 wt% NaCl, the foam height was found to be 135.7 mm at 30 sec before it reaches to the level of 105.8 mm at 90 sec (Figure 3.9c). After 120 sec, the foam significantly deformed and reached to the level of 52.9 mm which further continued to decline to 38.4 mm at 150 sec. Moreover, it was observed that 2 wt% NaCl yielded stable foam with peak value of 139.8 mm at 60 sec (Figure 3.9d). Foam height gradually decreased but foam exhibited its significant value (110.1 mm) after a span of 150 sec. Thus, among all formulations, 0.5ASP1 has shown greater potential in foam-ability which witnessed only 20.8% reduction (Figure 3.9d) in foam height as compared to 71% reduction in foam height of 0.5ASP (Figure 3.9a).

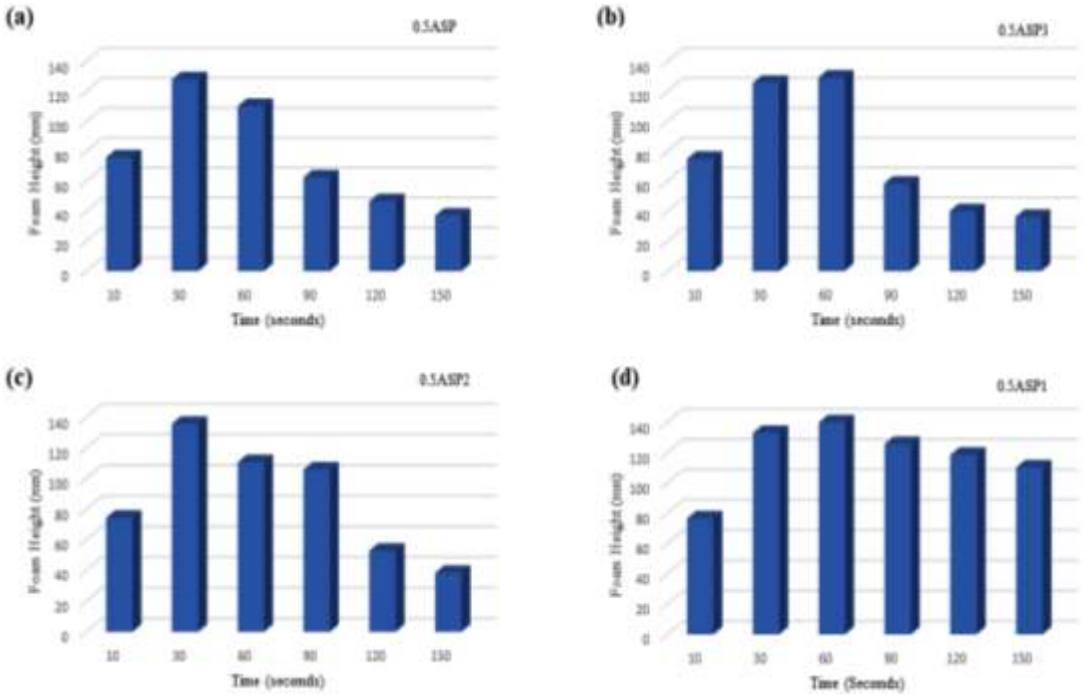

Figure 3.9: ASP slug of tuned alkali concentration (0.5 wt% $NaHCO_3$) for optimum foaming in saline environment (a - 8 wt%: b - 6 wt%: c - 4 wt%, and d - 2 wt% NaCl).

Figure 3.10 shows the rate of liquid drainage from foam stabilized by 0.5ASP1 slug. The actual images of foam, generated by column of DFA, are also shown. Initially, the liquid drainage was found to decrease from 32.7 (0 sec) to 4.75 mm (30 sec). Its value reached to minimum level of 2.5 mm at 60 sec, which directly confirmed the attainment of maximum foam height at this period (139.8 mm, Figure 3.10).

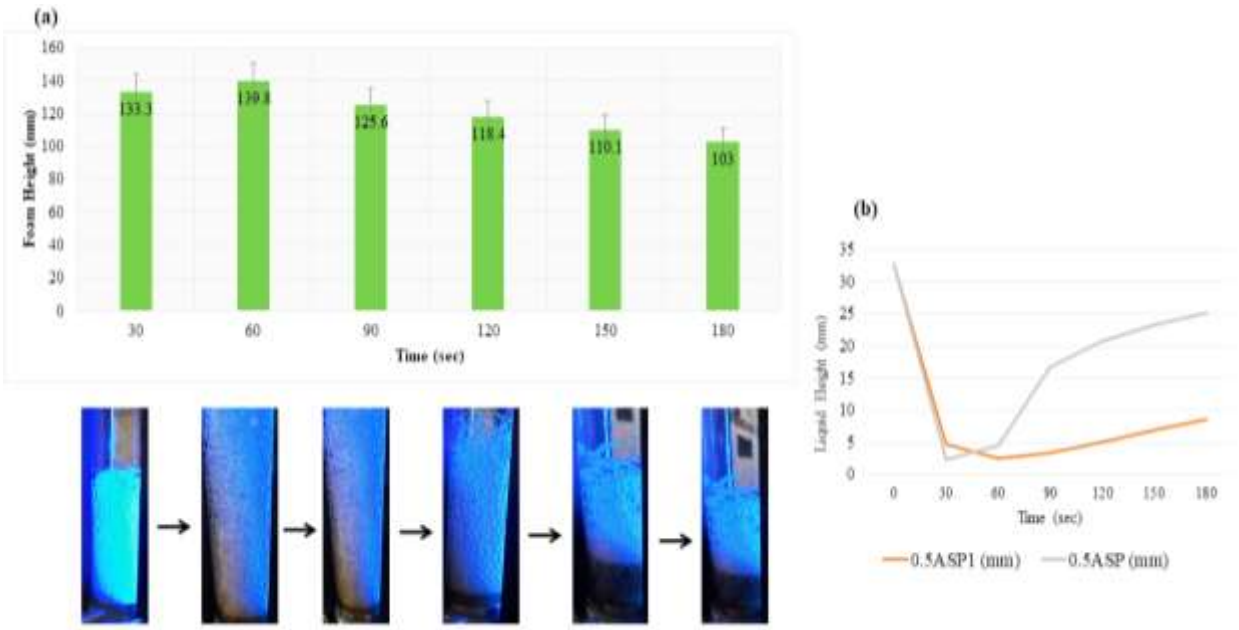

Figure 3.10: Results of (a) foam height of desired ASP slug (0.5ASP1) as a function of time and (b) time dependent liquid drainage rate of desired ASP slug (0.5ASP1) and 0.5ASP of 8 wt% NaCl.

With the decrease in foam height, the increase in liquid drainage is evident from Figure 3.10b: the liquid drainage value of 3.32 mm (at 90 sec) increased to 5 mm (at 120 sec) followed by 6.94 mm (at 150 sec) and 8.58 mm (at 180 sec). This ensures that the foam height of 0.5ASP1 was more stable than the one of 0.5ASP as shown in Figure 3.9d and Figure 3.9a, respectively. For 0.5ASP, the liquid drainage was minimum (2.4 mm) at 30 sec (Figure 3.10b). Its value significantly increased over the time span and as a result, 0.5ASP exhibited 4.54 mm at 60 sec, 16.7 mm at 90 sec, 20.76 mm at 120 sec, 23.24 mm at 150 sec followed by final value of 25.14 mm at 180 sec. These values are significantly higher than the values measured for 0.5ASP1. Thus, the rate of liquid drainage was greater in 0.5ASP than 0.5ASP1 as evident from Figure 3.10b. A slight tuning (0.5 wt% $NaHCO_3$) of alkali led to improved performance of 0.5ASP slug in saline conditions (2-4 wt% NaCl), whereas ASP slug of 1 wt% $NaHCO_3$ showed limitations. The alkali ($NaHCO_3$), used in this study, is quite inexpensive as compared to sodium hydroxide (NaOH),

which is being widely used [180,182,205,206]. Also, $NaHCO_3$ has lower pH than NaOH which is a trait for chemical-EOR to deal with the emulsion and scale related issues. The additional advantage of using $NaHCO_3$ is associated with its favorable impact on precipitation that can occur in carbonate reservoir [207] and therefore, 0.5ASP1 is proposed to be tested for carbonate reservoir enriched with saline environment.

3.3.7. Microscopic investigations

Microscopic analysis was conducted for 0.5ASP1 (slug of superior foaming, 2 wt% NaCl) and 0.5ASP2 (4 wt% NaCl), and compared their performance to visualize the impact of salinity on size distribution and bubble coverage. Figure 3.11 shows microscopic images of 0.5ASP1 and 0.5 ASP2 as a function of elapsed time. For 0.5ASP1, it can be seen that initially bubbles were smaller in size and they were uniformly packed with varying size distribution (Figure 3.11a). With the increase in time, the coalescence occurred which led to the formation of large-sized bubbles. After 8 h, 0.5ASP1 hardly exhibited bubbles as evident from Figure 3.11a. Thus, bubble coverage of 80% reduced to almost 0 after total elapsed time of 8 h. On the other hand, foam stabilized by 0.5ASP2 was more unstable and it exhibited lower bubble packing and coverage (only 60%), which reduced to 0 only after 6 h (Figure 3.11b). The bubbles were also relatively large in with non-uniform packing. Also, with increase in time, this foam exhibited greater coalescence resulting bubbles disappeared and no bubble was present after 6 h. From results, it can be concluded that 0.5ASP1 exhibited better stability and foam durability than 0.5ASP2 of higher salinity, consistent with foam height results of these foams (Figure 3.9d and Figure 3.9c).

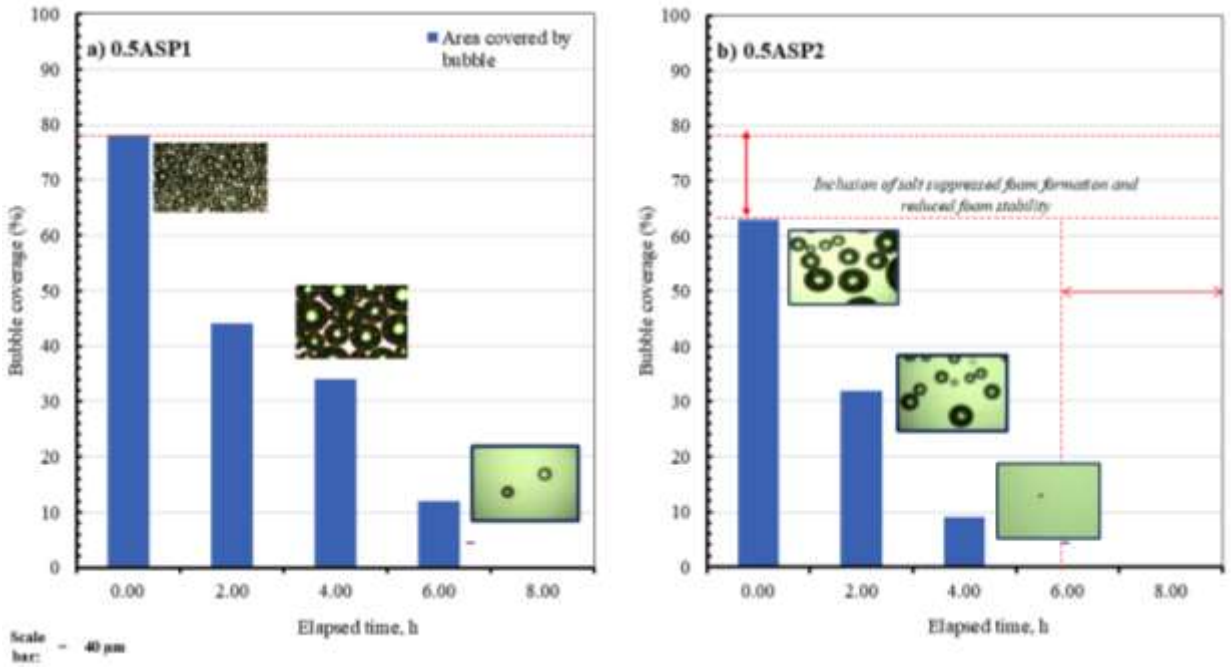

Figure 3.11: Microscopic analysis to visualize impact of salinity on bubble density (coverage) as a function of time in 0.5ASP1 and 0.5ASP2 slugs.

Thus, ASP formulation, of 0.5 wt% $NaHCO_3$, CMC of natural surfactant, and 4000 ppm of natural polymer, suggested a cost-effective green approach in chemical-EOR of moderate salinity (2-4 wt% NaCl), where conventional synthetic polymer/surfactant may show significant challenges due to toxicity and health issues.

3.4. Conclusion

This research presents a provides valuable insights into the development and performance of environmentally friendly and cost-effective natural surfactant. The findings highlight significance of combining natural materials to achieve desirable physicochemical properties, making the formulation suitable for a range of industrial and mechanical processes. Outcomes not only validate effectiveness of the approach but also contribute to the growing body of research

focused on sustainable material solutions. The key conclusions possessing notable findings are as follows: -

- The natural surfactant significantly contributed to IFT reduction using fenugreek-derived bio-surfactant showed great ability in IFT reduction and a lower IFT value of 10 mN/m was obtained at CMC (0.2 wt%).
- Based on the IFT value, the natural surfactant was found effective at low concentrations of 0.2 wt%
- The developed biosurfactant showed a shear thinning profile and was comparatively less effective at the higher temperature explored in this study (90 ^{o}C).
- The developed biosurfactant effectively reduces the contact angle from 74º to 48º, enhancing surface wettability and thereby improving fluid displacement efficiency within the medium.
- In this study, an effective formulation of alkali-surfactant-polymer was prepared and tested its performance for foam-ability. Surfactant played a crucial role in formulation of ASP system. Incorporation of a natural polymer enhanced the overall compatibility of system, making it environmentally friendly and non-toxic. Furthermore, use of a cost-effective alkali component contributes to reducing the overall material and processing expenses, which is advantageous for large-scale mechanical or industrial operations.
- Increasing alkali concentration led to decay in foams whereas lower concentration of alkali preferentially generated stable foams.
- Salt may promote both foam formation or foam decay in ASP systems depending upon the nature of salt, surfactant, alkali, and their concentrations used.

- The performance of desired formulation (0.5ASP1) has been evaluated by measuring its foam-ability and stability as a function of foam height. Moreover, the microscopic behavior of 0.5ASP1 also confirmed superior stability in foam as compared to other foam systems.

This study successfully demonstrated the effectiveness of a natural surfactant derived from fenugreek in reducing interfacial tension and contact angle, thereby enhancing interfacial interactions and surface wettability in fluid transport systems. The biosurfactant exhibited shear-thinning behavior and maintained functional stability at moderate temperatures, highlighting its suitability for thermomechanical applications. Future work may focus on improving its thermal tolerance for high-temperature operations and assessing compatibility with a wider range of natural and synthetic polymers. Moreover, scaling the optimized formulation (0.5ASP1) for pilot-scale implementation and evaluating its long-term performance under dynamic flow conditions will further support its applicability in various industrial systems. The use of biomass-derived surfactant and natural polymer components makes the formulation environmentally benign and non-toxic, while the incorporation of an economical alkali enhances its cost-efficiency. Overall, this green and sustainable formulation shows promise for advanced emulsion stabilization and foam generation in engineered porous media, as well as in systems requiring pH buffering.

Chapter 4

Investigation on Rheological Characterization and Salt Tolerance Potential of Paraffinic O/W Emulsions of Natural Surfactant for Crude Emulsification and Mobilization

Abstract

While the presence of long chain paraffinic compound in crude oil seriously impacts oil production, they tend to form emulsions during flow through restricted pores. In turn, these emulsions help mobilize additional oil due to pore throat plugging, reducing interfacial tension, altering the wettability, and flow redistribution. The inclusion of a surfactant, especially of a natural biodegradable origin, can not only help promote emulsion formation to boost oil recovery but also lower the chemical footprint of the oil recovery process, making the entire process more sustainable. Therefore, in this study, a natural surfactant obtained from Fenugreek seeds has been explored to produce oil-in-water emulsions in conjunction with oil phases: n-pentane (EP-1), n-hexane (EP-2), n-heptane (EP-3) and n-dodecane (EP-4). Using visual observation and interfacial tension measurements over a range of 0.05-0.3 wt%, the optimum emulsifying surfactant concentration was identified to be 0.2wt%. The emulsions were observed to be creamed by separating aqueous phase over span of 10 days which was observed under a microscope. All emulsions tend to exhibit a shear thinning profile at ambient conditions and the best fit was observed with Power law with R^2 values of 0.93, 0.91, 0.94 and 0.97 for solutions EP1, EP2, EP3 and EP4 respectively. Furthermore, the effect of monovalent (NaCl) and divalent ($CaCl_2$) salts was explored with EP4 found to be comparatively more stable than other emulsions. To understand the

effect of heterogeneity of reservoir, contact angle measurements were performed on sand-base prepared with different sizes and pore size was found to be a critical factor influencing wettability alteration. Finally, the potential of natural surfactant in displacing the oil was visualized using a microfluidic setup wherein the injected surfactant solution was able to mobilize oil, paving a potential pathway for future field implementation for enhanced oil recovery operations.

4.1 Introduction

Crude oil is a mixture of various heavy to lighter hydrocarbons and elements such as sulfur, nitrogen, and oxygen *etc.* in liquid state. Mechanistically, three types of crude oil e.g., paraffin, naphthenes, and aromatics play predominate role in meeting global energy demands [208,209]. In paraffinic crude oil, hydrocarbons are characterized by single bond between carbon atoms whereas other bond between hydrogen atoms are saturated with carbon atoms (C_nH_{2n+2}) for instance n pentane, n hexane, and n heptane, *etc.* Globally, majority of trapped crude oil is in the form of paraffin base (around 80%) [210] and the rate of conventional oil recovery methods has sustained at 50-60% of original oil in place (OOIP) [33,211,212]. Moreover, the rate of paraffin recovery in crude oil not only impacts the transportation of crude oil but also affects the global demands of hydrocarbon energy. A considerable amount of oil still remains trapped within reservoir [213–217] and the recovery of this oil depends on the type of applied recovery method and its synergy with paraffin of crude oil. Over the past few decades, chemical-EOR has shown tremendous results in oil recovery projects which includes the application of surfactant [218], alkali [219] and polymer [220]. Surfactants are often used as they have the ability to reduce interfacial tension (IFT)of paraffinic oil and affect the rock properties [221]. Several research works have established that the application of different surfactants offer varying oil recovery rates and it may be due to the fact that each paraffin has different synergy with injected surfactant [89,145,222–224]. For example,

each paraffin has its own role in defining the physical properties of crude oil and previous study entails that the stable emulsion leads to improved oil recovery [225,226]. Thus, it is imperative to understand and analyze the synergetic effect of surfactants with different paraffins of crude oil. This is important to investigate as surfactant, exhibiting superior emulsification with one paraffin, may mislay emulsifying capacity in the presence of other paraffin, and this might be the possible reason of unsuccessful recovery rate of surfactant flooding from a reservoir. Thus, the investigation may help to choose right surfactant for a right paraffinic crude oil, which will not only save dollars of industry but also may improve the recovery of particular paraffin.

Therefore, various researchers investigated the role of surfactant in stabilizing paraffin-based emulsions. For example, Golemanov et al. [50] studied the stabilization of paraffin in water emulsion using 15 ml oil and 35 ml surfactant solution by means of stirring and concluded that a nonionic surfactant *i.e*., Tween-20/Tween-60 showed positive impact in stabilizing hexadecane. Baloch and Hameed [47] studied emulsification of various paraffins (n hexane, n heptane, n decane and kerosene) in water by ultra-sonification where quantity and size of droplets was observed to be in order, that is, n hexane < n heptane < n decane< kerosene and are found dependent on parameters such as ultra-sonication time and composition of oil. The use of surfactant *i.e*., sodium dodecyl sulfate (SDS) in stabilizing emulsion of dodecane-water was investigated by Llamas et al. [45] who concluded that bubble coalesced when surfactant amount exceeded 10^{-7} M in the system. Kichatov et al. [46] also used SDS (16 g/L) and prepared heptane in water emulsion, which exhibited droplet size of 37 μm and IFT value of 3.3 mN/m between heptane and surfactant solution. Anano-emulsion of water in hexane was developed with the help of mixed surfactants (Brij-30/Span-80) and low energy emulsification method [49]. For this emulsion, average particle size ranges between 39 to 204 nm and IFT was found to be 11 mN/m between hexane and

surfactant solution of 10^{-5} M. A series of surfactants of different combinations (Tween-80/Span-80, Tween-80/Span-85, OP-10/Span-80 and OP-10/Span-80) were used to envisage emulsification between octane and water [48]. It was found that the emulsion, stabilized by combination Tween-80/Span-80, was highly stable as compared to the ones of other combinations, and no phase separation was seen till storage period of 26 d. Though surfactants have global importance in sstabilizing paraffin-based emulsions, previous research works only focused on the use of synthetic surfactants and no research highlighted the application of natural derivatives in stabilizing paraffin emulsions for oilfield applications. The surfactants of natural derivatives have no harmful issues on health and land and moreover, their use will directly benefit the agricultural sector that can also be cost effective for surfactant manufacturing industries.

In addition, for sustainable hydrocarbon energy, there is an urgent need of utilizing natural derivatives in oilfield applications. Natural surfactants are now a days gaining tremendous attention of researchers as they offer various advantages such as biodegradability, non-toxicity, natural availability, and environmental friendly, etc [98,227]. Various natural surfactants, derived from plants *viz*., soapnut, mulberry leaves, heena leaves, eucalyptus leaves, quinoa, fenugreek seeds, have found significant industrial application [23,26,30,32,39]. All these surfactants have shown remarkable and comparable results in oilfield applications which include IFT reduction, wettability alteration, and enhanced oil recovery (EOR). Nafisifar et al. [53] extracted natural surfactant from linseeds (PELS) and analyzed its performance for crude emulsification. Here, emulsion was stabilized by surfactant PELS at CMC *via* ultra-sonication method and the separation in emulsion was seen after two weeks followed by clear separation between oil and water in six weeks. A natural surfactant was extracted from bark of tree, named Quillaja Saponaria Molina tree [54]. Extracted surfactant was used to stabilize MCT (medium chain triglyceride) oil in water, and

the resultant emulsion exhibited droplet size < 200 nm with superior physical stability over one month. Ogino and Onishi [228] also investigated the emulsification of dodecane and water in presence of few natural surfactants (lecithin, oleic acid cholesterol) however, the results did not confirm the development of any emulsification between paraffin and oil and hence, no emulsion was reported. Separately, Pal et al. [55] investigated the performance of natural Gemini surfactant, extracted from sunflower oil, in stabilizing (CMC: 0.1496 mM at 303 K) oil (n-heptane) in water emulsion, where emulsion showed droplet size in between 0.25-3.1 μm at day 1 which further increased to 0.64-6.2μm after15 days of storage. The performance evaluation of natural green surfactant, extracted from quinoa, in emulsifying crude oil was tested by Norouzpour et al., [23] who reported that stable and dense emulsion was observed with HLB (hydrophilic-lipophilic balance) value of 12.8. Although few researchers have explored the application of natural surfactants in emulsification of crude oil and n-paraffins but still the work showing use of other natural surfactants and their test for emulsification with lighter components of crude oil (n-alkanes) is limited in literature as far as we are aware. Thus, the novelty of this work lies in exploring the role of natural surfactant, extracted from fenugreek seeds, in emulsification of paraffins (n-pentane, n-hexane, n-heptane and n-dodecane) for its possible implementation in improved recovery of crude oil.

Thus, in this study, oil (paraffin)-in-water emulsions were prepared using 1000 ppm polymer PAM (polyacrylamide) and natural surfactant extracted from *Fenugreek* seeds. Four different paraffins was used in the study: n-pentane, n-hexane, n-heptane and n-dodecane. The emulsions were prepared at varying surfactant concentrations (0.05-0.3 wt%) and visual observations were made to predict the range of CMC. This was followed by the IFT measurements to validate the CMC value for each paraffin. All further investigations were performed using the

CMC value. To further validate the role of surfactant in emulsification, microscopic investigations were performed. Next, the rheological behavior of the prepared emulsions was analyzed by viscosity and G′ measurements. Following this, the stability of all emulsions was observed in presence of both monovalent and divalent salt. To understand the impact of grain size in wettability alteration, contact angle studies were conducted on normal, small, and high sand size. Finally, pore scale analysis was done to visualize the flow pattern of surfactant and its potential in displacing oil from pore channels by means of microscopic results.

4.2 Materials and Methods

4.2.1 Materials

In this study, the application of agricultural based natural surfactant from *Fenugreek* seeds was explored [30]. This surfactant was extracted by means of a Soxhlet Apparatus, provided by Jain Scientific Glassworks, India. Polymer (PAM) exhibiting molecular weight of 10^7 g/mol (98 % purity) was procured from SNF Floerger. Salts, sodium chloride (NaCl) and calcium chloride ($CaCl_2$) in granular form with 99.5% purity were used after procurement from Sisco Research Laboratory (SRL) India. Fine measurements of PAM, surfactants and salts was done by digital weighing balance (Mettler Toledo, ME204/A04; repeatability approximately 0.1 mg). For preparation of PAM solution, deionized (DI) water was used. Aqueous PAM solution was prepared on the magnetic stirrer (IKA-C-MAG-HS7) with stirring speed of 600 rpm for about 7 hrs. The paraffins used in study are n-pentane (>99 mol%), n-hexane (99 mol%), n-heptane (>99 mol%) are obtained from Sisco Research Laboratory (SRL) India and n-dodecane (>95% purity) procured from S D Fine Chemicals, India. The sand used for contact angle measurements was obtained from commercial vendor and impurities within sand was removed by washing using toluene and oven drying.

4.2.2 Emulsion Preparation by using natural surfactant

In this study, emulsion was stabilized in presence of natural surfactant and polymer PAM. Four different paraffins are used for the study, that is n-pentane, n-hexane, n-heptane and n-dodecane. The emulsions were prepared by mixing paraffin and surfactant-polymer (SP) solution on a Vortex shaker. Ratio of 60:40 was taken for preparing the emulsion system, where 60% of SP solution and 40% of paraffin was used. Initially, n-pentane emulsion was prepared at increasing surfactant concentration, that is, 0.05, 0.1, 0.15, 0.2, 0.25, and 0.3wt% to analyze the emulsification. Similarly, emulsions with increasing surfactant concentration were used to prepare n-hexane emulsion, n-heptane emulsion and n-dodecane emulsions. All the prepared emulsions were kept under observation for about 10 days to visualize the phase separation.

4.2.3 Interfacial studies for CMC determination

To determine the CMC, the IFT studies were conducted for the promising range of surfactant concentration between SP solution and paraffin. Range of CMC was identified using visual observation. A schematic representation of interfacial activity between paraffin and surfactant solution is shown in Figure 4.1. As the surfactant concentration increases IFT tends to become lower due to micelles formation above CMC value. Below the CMC, the monomers are aligned within the dispersed phase, as no micelles formation takes place. When aqueous surfactant solution comes in contact with the oleic phase, the hydrophilic head position towards the aqueous phase whereas hydrophobic tail towards the oleic phase. These measurements were performed by means of Wilhelmy plate method using dynamic tensiometer (Model: K12 Kruss® Germany) as done in our previous study [229]. During the measurement, SP solution was filled in the measuring cup and later filled with the paraffin in order to form a layer at the interface of paraffin and aqueous phase. The Wilhelmy plate fixed at one end was allowed to pass through the measuring cup till it

reaches the interface by means of command given in the measuring unit. As the Wilhelmy plate reaches the interface of oil-fluid, IFT value are automatically recorded in the measuring system. The whole procedure is repeated for each paraffin separately for the explored range of surfactant concentration. The detailed composition for emulsion preparation at CMC and its nomenclature is shown in Table 4.1.

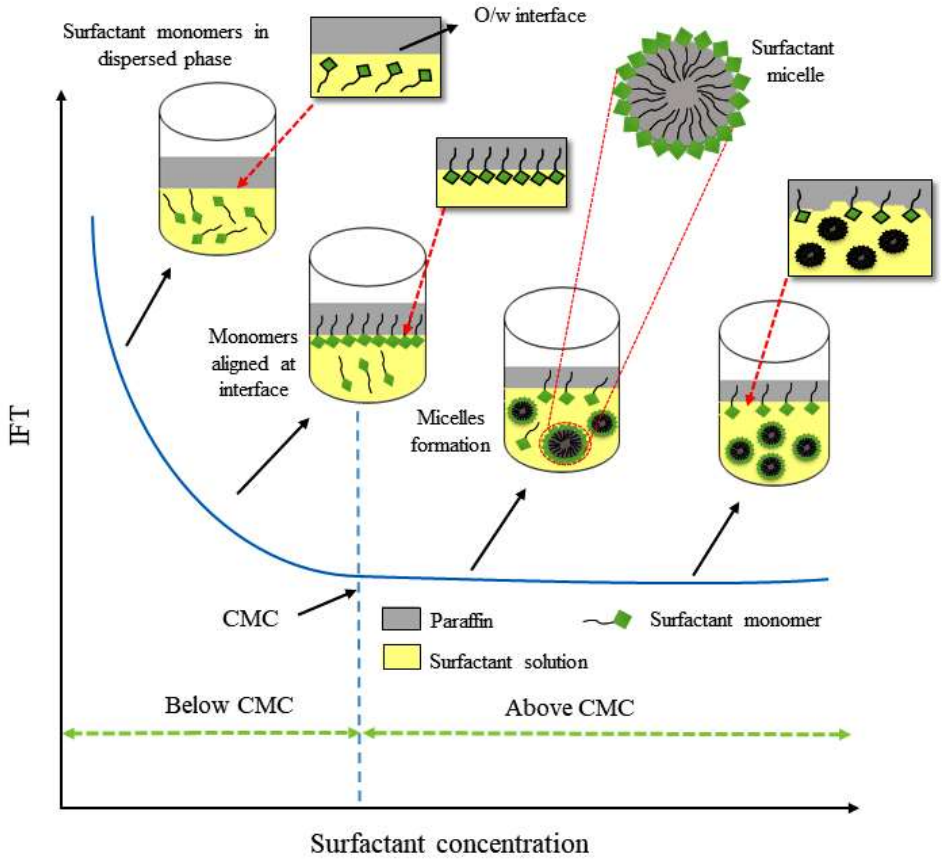

Figure 4.1: Schematic representation of the interfacial activity between oil phase (paraffin) and aqueous phase (surfactant solution) against varying surfactant concentration.

Table 4.1: Nomenclature and details of Emulsion formulation.

S. No.	Emulsion Nomenclature	Paraffin Used	SP formulation	Emulsion Composition
1	EP1	n-pentane	1000 ppm PAM + 0.2 wt% natural surfactant	(o/w: 40/60)
2	EP2	n-hexane		
3	EP3	n-heptane		
4	EP4	n-dodecane		

4.2.4 Microscopic Studies of emulsion system

For the microscopic characterization, an optical microscope (Motic, Hong Kong) was used. After emulsion preparation, they were kept under observation till the phase separation occurs. Microscopic investigations were done to visualize the difference in creaming layer and separated aqueous phase. For this, drop of creamed layer from emulsion (EP1) was placed on clean glass slide with the help of laboratory pipette (Tarsons, United States) and placed under microscope where images were captured automatically using an inbuilt Moticam-10 tool. Later, a drop was taken from separated aqueous phase from emulsion (EP1) and placed on glass slide to observe the presence of oil droplet if any. Similar observation was done for all paraffin emulsions, that is, EP2, EP3 and EP4.Glass slide was cleaned thoroughly after every observation.

4.2.5 Rheological investigations

To ascertain the flow dynamics of the prepared emulsions, rheological measurements were done using Modular compact rheometer (MCR-52, Anton Paar, Austria). In rheometer, bob and cup assembly was used as reported in previous studies [163,229]. For the measurements, freshly prepared emulsion (EP1) approximately 20 ml was poured in the cup fixed at the base of rheometer

and measurements were carried out. Rheological analysis was conducted in both shear and dynamic modes. Shear rate was varied from 1-1000s^{-1} for viscosity measurements whereas for dynamic mode (G′) strain-sweep analysis was done where frequency was kept constant, that is, 10 rad s^{-1} and strain amplitude was varied from 0.1-100%. Similar rheological findings were done for all the emulsions, that is, EP2, EP3 and EP4. All sets of experiment were conducted thrice to get reproducibility in results and uncertainty of ±0.6-7% of the recorded value was observed. After every rheological examination, bob and cup was thoroughly cleaned with the help of toluene to remove any leftover impurity followed by air drying with the help of air drier.

4.2.6 Effect of wettability on grain size via Contact angle measurement

To ascertain the wetting property of natural surfactant, contact angle studies were performed between rock surface (sandstone saturated with n-dodecane on glass slide) and a drop of SP solution at ambient conditions. Wettability is one of the property of the rock surface and traditional method to characterize the spread ability of fluid over the rock surface can be understood by means of contact angle studies [30,165]. For this, normal sand was sieved using 60 mesh size to get low sand size grains and high size sand grains. For measuring contact angle, normal sand was saturated with n-dodecane and placed on clean glass slide to form uniform and even smooth finished rock surface that can replicate reservoir conditions. Thereafter, the slide was placed in a stainless-steel pressure vessel having a glass viewing port (assembled by D-CAM Engineering, India) and a drop of SP solution was released by using syringe pump (provided by Teledyne ISCO, United States) on the slide and image was captured at different time interval using a high-resolution camera (Phantom VCC, United States). Same procedure was repeated for low sand size and high sand size separately to analyze the effect of grain size on wetting property of natural surfactant.

4.2.7 Effect of salt on emulsion system

To analyze the stability of prepared emulsion systems in saline environment, microscopic investigation was done to establish the role of salt. Both monovalent (NaCl) and divalent ($CaCl_2$) salts were explored on all four-emulsion systems (EP1, EP2, EP3 and EP4). For this study, both the salts (NaCl and $CaCl_2$) with concentration 1, 2, 3, and 4wt% were added simultaneously to the emulsions and a drop of emulsion was placed on clean glass slide for microscopic observation. All the tests were performed at ambient condition and glass slide was properly cleaned after each observation.

4.2.8 Microfluidic investigation

A microfluidic flow investigation was conducted to observe the flow of fluid within a microfluidic chip. Figure 4.2 shows detailed schematic for the setup of microfluidic investigations. Microfluidic experimental setup was comprised of a syringe pump, an optical microscope, accumulators for pumping oil and surfactant solution, valves and a microfluidic chip. The complete set up was utilized for interpreting and visualizing the flow behavior and fluid mobilization studies. All these tests were conducted at ambient conditions and natural surfactant has shown its potential in mobilizing the oil from the pore channels of microfluidic chip. The microfluidic chip was completely transparent, and the pattern of fluid flow was observed by using an optical microscope. A syringe pump (100 DX, Teledyne ISCO, USA) was used for maintaining the uniform flow rate of fluids to be injected. Initially brine solution was injected and the salinity was kept equivalent to ~17297 ppm (as that of Cambay basin). The brine injection was kept constant with a uniform flow rate of 1 ml/min for about 15-20 min till the microfluidic chip was completely saturated restricting presence of air bubbles as evident from microscopic studies. Further n-dodecane was injected with a uniform flow rate of 0.5 ml/min for about 15-20 min. The other end of microfluidic chip was

kept closed for sometimes (2-3 min) in order to ensure the flow of n-dodecane across the different sections of microfluidic chip. The flow pattern of n-dodecane was captured and the complete image of chip entails about the distribution, storage, and movement of n-dodecane. The microfluidic chip was allowed to get saturated with n-dodecane for 24 h. Finally, the natural surfactant was injected (flow rate ~ 0.5 ml/min) for 15-20 min, which lead to the displacement of n-dodecane from some sections of the microfluidic chip. The image of complete chip was recorded carefully and compared with the n-dodecane saturated chip to understand the role of natural surfactant in displacing oil (n-dodecane) and its movement across the microfluidic chip.

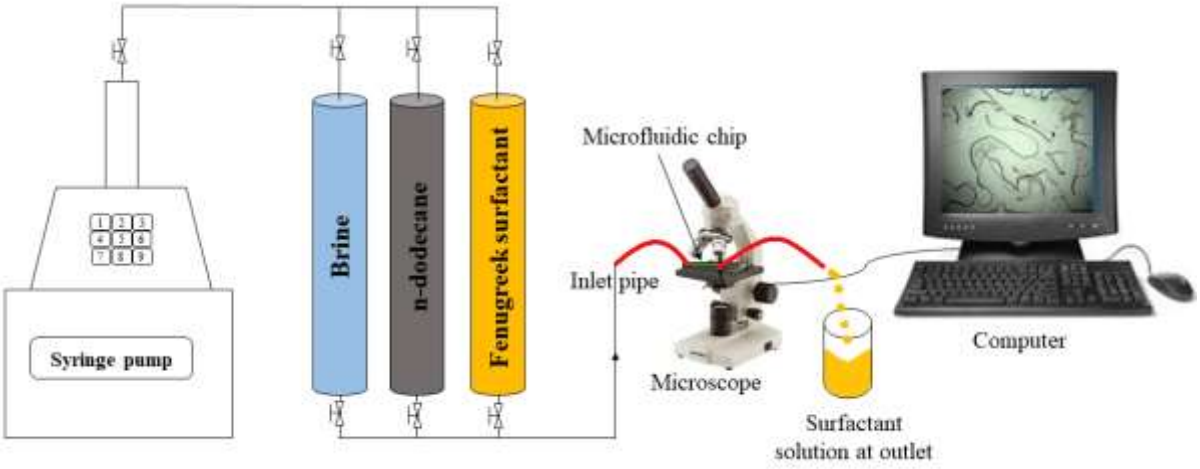

Figure 4.2: Schematic of the microfluidic experimental setup utilized for analysis of flow behavior and fluid mobilization studies.

4.3 Results and Discussion

In this section, initially, the observations related to the expected range of CMC for all emulsions has been reported by visual observation. This was followed by the IFT measurements to obtain the CMC value for each paraffin explored in the study. As the emulsion tends to be creamed over the course of time, its microscopic investigation was performed next and the results

along its discussion have been provided. Later, the rheological studies were performed for all the paraffin emulsions at CMC value. Then, the stability of emulsions was investigated in presence of monovalent and divalent salt. Finally, the results and discussion related to the effect of sand size on wettability alteration followed by the pore scale analysis to visualize the surfactant's potential in displacing oil has been provided.

4.3.1 CMC determination of emulsion system

The concentration of surfactant is of key importance in formation of emulsion as well as the stability of emulsion [230]. Initially the prepared emulsions (n-pentane, n-hexane, n-heptane and n-dodecane) of varying surfactant concentration (0.05, 0.1, 0.15, 0.2, 0.25, and 0.3 wt%) (see Figure 4.3a) were kept under observation to investigate the emulsion stability. After a span of 10 days, phase separation was observed in all emulsion system as shown in Figure 3b. The experiment of determining emulsion stability, as a function of days, was regularly monitored till a clear and distinct layer was evident on the surface of continuous phase. After 7 days (1 week), each emulsion almost had no noticeable change in its appearance except few. Therefore, the emulsion stability was determined after a time period when no noticeable change was seen in all emulsions. It was observed that 10 days was the adequate time to achieve stabilization in emulsion phases and thus, 10 days was chosen for determining stability in emulsions.

The visual appearance of the oil in water emulsion systems freshly prepared using varying concentration of (0.05-0.3 wt%) surfactant solution seems to be homogenous (Figure 4.3a) but after a span of 10 d, phase separation was observed in all the prepared emulsions (Figure 4.3b). The ratio of oil to SP solution was kept as 40:60. The expected range of CMC was found to be in the range of 0.15-0.25 wt%. The emulsion stability is also demonstrated through additional graphical element, that is, volume of emulsion/ water release (%) against varying surfactant

concentration in Figure 4.3c. From Figure 4.3c, it can be observed that emulsion prepared with lower concentration of surfactant (0.05 wt% and 0.1 wt%) possessed poor stability due to more water release. As surfactant concentration increased to 0.15 wt%, the stability of emulsion improved with ~ 20% reduction in water release from emulsion samples. With further increase in surfactant concentration (0.2-0.3 wt%), prepared emulsions were found to be much more stable (due to lower water release and better emulsion volume) than emulsions with lower surfactant concentration (0.05-0.15 wt%). This may be credited to the formation of micelles and their role on stabilization of oil droplets.

The amount of water release varied with the concentration of surfactant involved. At lower surfactant concentrations (e.g., 0.05 and 0.1 wt%), the amount of water release was higher as no emulsion formed and all the continuous water phase remains separated (Figure 4.3c). This might be attributed to lower concentration of surfactant, where micelle formation could not take place resulting oil droplets did not develop due to insignificant emulsification of paraffin. A better emulsion stability was observed with surfactant concentration $\geq$ 0.15 wt%, which indicates that micelle formation took place beyond a certain concentration of surfactant. The emulsion system comprises of a creamed layer (top, see white layer in Figure 4.3b) and separated aqueous phase (bottom). At lower surfactant concentrations, more waster release was observed as evident from Figure 4.3b. This may be attributed to the presence of surfactant monomers which restricts the micelles formation till it reaches the CMC value [231]. To determine the CMC of emulsion system, a range of surfactant concentration, *i.e.*, 0.15, 0.2, and 0.25wt% were taken into consideration (as observed from Figure 4.3b) to be stable. At higher surfactant concentrations (0.3wt%), the emulsion was unstable and water release can be clearly observed in case of n-hexane and n-heptane emulsions.

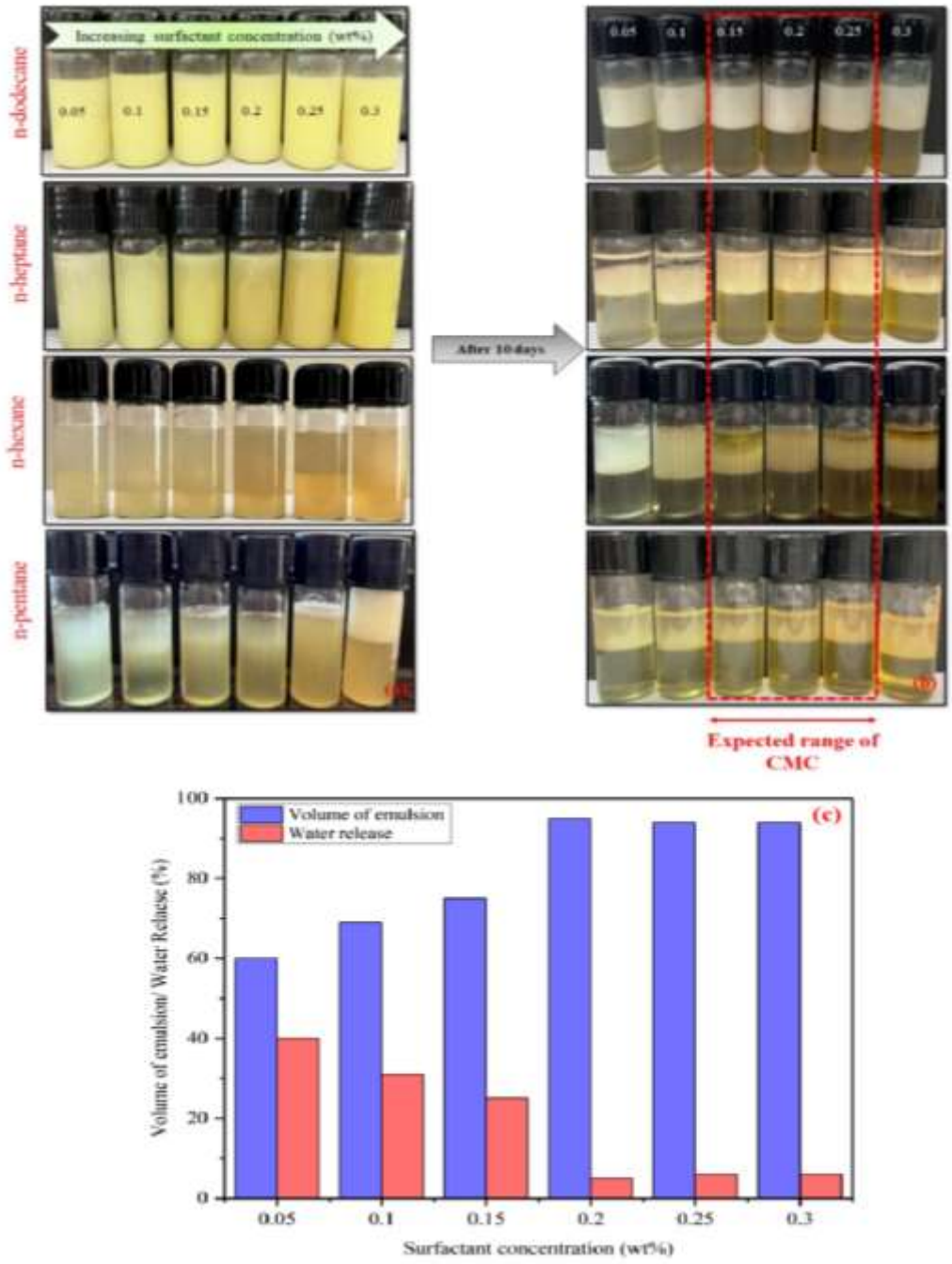

Figure 4.3: Visual appearance of the oil in water emulsion systems (a) freshly prepared using 0.05-0.3 wt% surfactant solution, (b) emulsion after the span of 10 d and (c) represents the volume of emulsion/ water release (%) against varying surfactant concentration. The oil to SP solution ratio was kept as 40:60. The expected range of CMC was found to be in the range of 0.15-0.25 wt%.

This may be due to the fact that use of surfactants above CMC contributes in formation of micelles but failed to decrease the surface free energy of the system and therefore the use of surfactant above CMC is not recommended for oilfield applications [232]. As the addition of right amount of surfactant offers several advantages while reducing wastage [222,227,233], there is need to determine the right value of CMC that enhances the potential of emulsions for EOR applications.

Figure 4.4 shows the IFT measurements between paraffins and surfactant solution at varying surfactant concentration (0.15, 0.2, and 0.25wt%), where the emulsions were found to be stable as evident from visual observation. When surfactants are introduced into an oil-water system, they migrate to the oil-water interface, where they orient themselves to minimize the energy associated with the interface [23]. This reorientation of surfactant molecules effectively reduces the IFT between the oil and water phases. CMC is the concentration of the surfactant at which micelle formation takes places which further helps in reducing the IFT to the minimum value [212]. From Figure 4.4a, it can be observed that IFT value between paraffin and surfactant solution (0.15wt%) was observed to be 9.3, 16.23, 9.45, and 9.67 mN/m for n-pentane, n-hexane, n-heptane and n-dodecane respectively. Larger IFT values may be attributed to the presence lesser concentration of surfactant that are not sufficient for micelles formation. A significant reduction in IFT was observed at surfactant concentration 0.2wt% as evident from Figure 4.4b. The reduction in IFT values was observed to be from 9.3 to 6.25 mN/m for n-pentane, 16.23 to 12.39 mN/m for n-hexane, 9.45 to 6.62 mN/m for n-heptane and 9.67 to 6.87mN/m for n-dodecane. Total IFT reduction was found to be ~ 23-33% when surfactant concentration was increased from 0.15 to 0.2wt%. Furthermore, the increased surfactant concentration of 0.25wt% (Figure 4.4c) was used, the IFT values (6.5, 12.45, 6.6, and 6.99 mN/m for n-pentane, n-hexane, n-heptane and n-

dodecane, respectively) were found to be almost same as that was recorded for IFT at surfactant concentration 0.2 wt% in Figure 4b. As IFT value (at surfactant concentration = 0.15 wt%) are comparatively higher than the IFT values at surfactant concentration of 0.2wt% and 0.25 wt%, entails that CMC value is 0.2wt%. It is due to the fact that the lowest value of IFT are observed when surfactant is added at CMC [55,163,234]. Thus, CMC determination plays a vital role as the surfactant monomers tends to align themselves spherically and micelles formation takes places [38]. Also, the use of surfactant beyond CMC value is not recommended as it reduces the economic viability of the project [198,235]. All the further studies were conducted only for emulsions at the CMC value determined, that is, EP1, EP2, EP3 and EP4 as shown in Table 4.1.

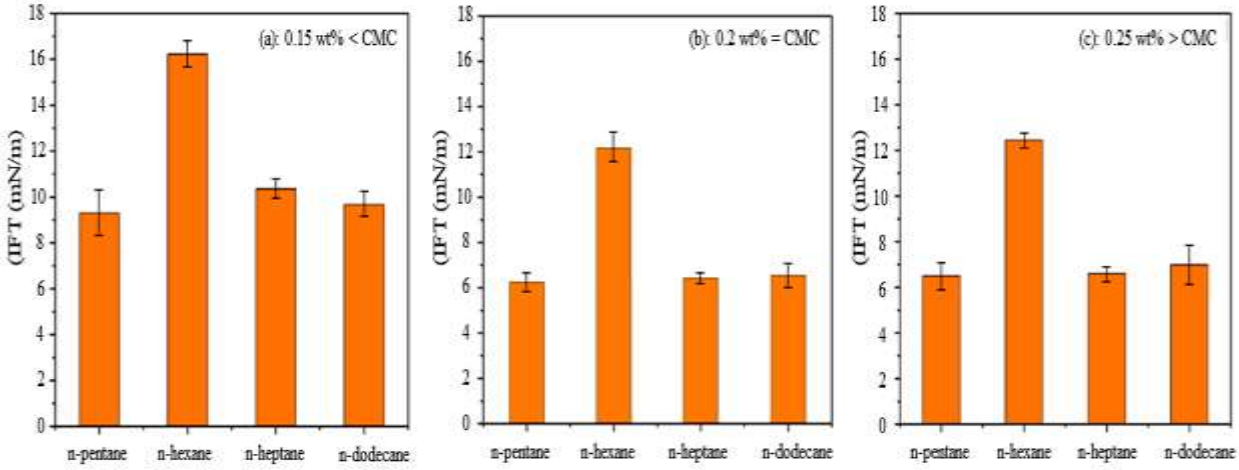

Figure 4.4: Plot of Interfacial tension (IFT) values obtained for the various oil systems at (a) 0.15, (b) 0.2, and (c) 0.25 wt% surfactant concentration (as determined from Figure 4.3).

4.3.2 Microscopic investigations

Next, the microscopic studies were conducted for EP1, EP2, EP3 and EP4 to investigate the distribution of oil droplets after span of 10 d. Initially, the prepared emulsions were of cream color (refer Figure 4.3a) but in span of 10 d phase separation occurs (refer Figure 4.3b), separating

the creamed layer and aqueous phase. Figure 4.5 shows the appearance of emulsion systems under a microscope after 10 d. A denser and uniform packing in the creamed layer and a loose packing in the aqueous phase was observed. The distribution of oil droplets plays a crucial role in the stability and properties of the emulsion. Emulsions can be classified based on the size of the dispersed phase: macroemulsions contain droplets visible to the naked eye, while microemulsions consist of much smaller droplets that require magnification to be observed. Within prepared emulsions, the oil droplets tend to move towards the interface with passage of time and the height of emulsion reduces. The creamed emulsion was taken into consideration for microscopic investigations as shown in Figure 4.5. From this Figure 4.5, it can be observed that a dense and tight packaging of oil droplets was observed in creamed layer for all emulsions EP1, EP2, EP3 and EP4. The microscopic observations are aligned with the literature [45–47]. Oil droplets seem to be smaller, uniformly distributed and varying in size, thereby densely packed. This may be due to the surfactant's adsorption on the oil droplet, that help in stabilizing the oil droplet by surfactant micelles [41]. Stability of creaming can be defined as the rate of movement of oil droplet towards the emulsion surface [236]. The reason for dense packaging of oil droplets can be attributed to the presence of natural surfactants used at CMC [237] which further helps in micelle formation and emulsify the paraffin oils. This may also be attributed to the chemical composition of surfactants, which leads in emulsification of paraffins [4]. Furthermore, the microscopic investigations were also done for the separated aqueous phase to visualize presence of oil droplet if any. On observing these images (bottom panels of Figure 4.5), the loose packaging of oil droplet can be observed. Comparatively the oil droplets were large in size, and this may be due to coalescence and the nature of surfactant, which participate in stabilizing emulsion and tend to move toward the surface.

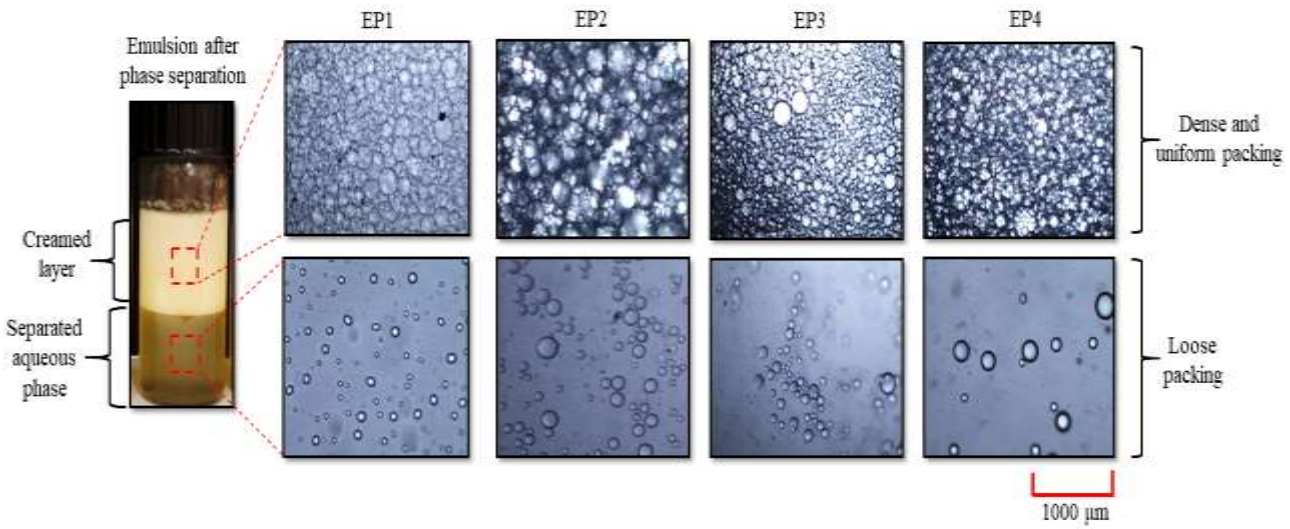

Figure 4.5: The appearance of emulsion systems under a microscope after 10 d. A denser and uniform packing in the creamed layer and a loose packing in the aqueous phase was observed.

4.3.3 Rheological Investigations

4.3.3.1 Shear Mode

Before proposing any emulsion system, its stability and flow pattern should be known for its successful and potential application within porous media. While injecting emulsions within porous media, various mechanism like surfactant adsorption, mechanical trapping, flow diversion etc. take place that reduce the efficacy of the emulsions due to degradation of its fluid properties. In general, the adsorption of surfactant occurs in monomer form, thus there is need to analyze the rheological behavior of emulsions. Figure 4.6 shows the viscosity results for emulsions EP1 (Figure 4.6a), EP2 (Figure 4.6b), EP3 (Figure 4.6c) and EP4 (Figure 4.6d) against the varying shear rate (1-1000 s^{-1}). All the emulsions showed non-Newtonian shear thinning profile as evident from figure and align with literature [57,238] exhibiting pseudoplastic behavior. All the emulsion system possesses higher viscosity at lower shear rate. For EP1, the viscosity was 1179.8 mPa.s at

shear rate of $1s^{-1}$ followed by a tremendous reduction in viscosity with a value of 26.961 mPa.s at 1000 s^{-1}. Similarly, significant reduction in viscosity was observed for EP2 and EP3, that is, from 2872.1 mPa.s and 1489 mPa.s at $1s^{-1}$ to 29.168 mPa.s and 24.204 mPa.s at 1000 s^{-1} leading to 98.9% and 98.3% reduction respectively. Higher viscosity was recorded for EP4 of 2349.7 mPa.s at 1 s^{-1} followed by consistent reduction in viscosity with 431.75 mPa.s at 10.8 s^{-1}, 77.821 mPa.s at 100 s^{-1} and finally with lowest value of 14.903 mPa.s at 1000 s^{-1}.

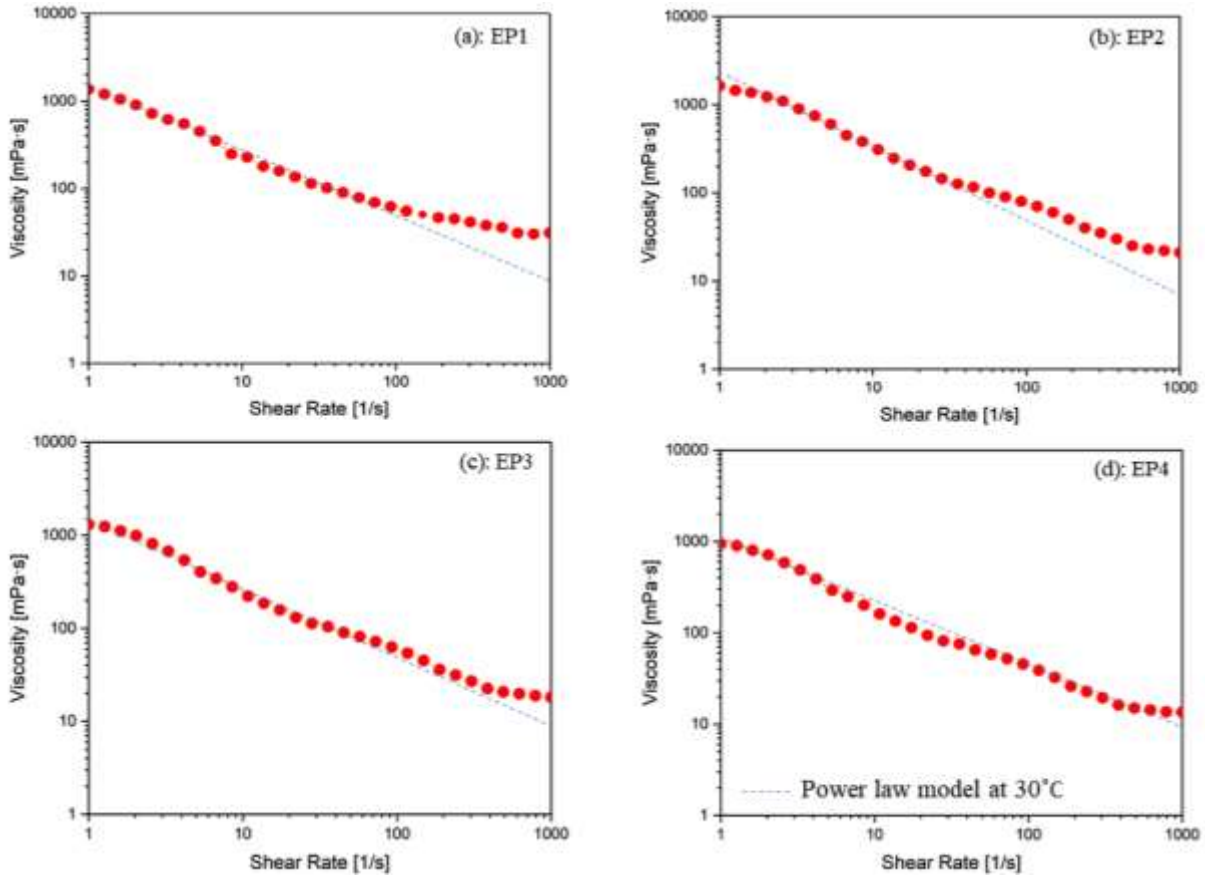

Figure 4.6: Plots of viscosity results obtained for the emulsion systems using the bob and cup setup. All sets of experiment were conducted thrice to get reproducibility in results and uncertainty of ±0.6-7% of the recorded value was observed.

Natural surfactant solution reduces IFT between the oil and water phases, facilitating the detachment of oil droplets from the microfluidic chip's surface and enhancing oil mobilization. It further promotes emulsification by stabilizing oil droplets in the aqueous phase. Surfactant solution has shown its potential in mobilizing the oil from the pore channel of the chip, as evident from microscopic images of different sections.

Next, the Power Law model fitting was performed for the viscosity profiles of EP1, EP2, EP3 and EP4 with the value of R^2 as 0.91, 0.91, 0.94 and 0.97, respectively as shown in Table 2. Power law model [239] can be defined as the mathematical expression shown in equation 1.

$$\eta = K.\gamma^n \quad (1)$$

where K = consistency index,

n = flow behavior index and

γ = shear rate.

Table 4.2: Details of the parameters of model fitting for the prepared emulsions. Power Law model was the best fit for the viscosity curve and all the measurements were conducted at 30˚C.

S No.	Emulsion	R^2	K	n
1	EP1	0.93	4.45	0.74
2	EP2	0.91	4.58	0.77
3	EP3	0.94	5.00	0.82
4	EP4	0.97	5.58	0.86

Power law model found to be best fit with highest R^2 value for EP4, along with better shear thinning profile when compared to other emulsion system. Thus, it can be concluded that flow behavior of EP4 is much stable and recommended for its potential application.

4.3.3.2 Dynamic mode

To investigate the dynamic rheological characterization of prepared emulsions, strain-sweep analysis was conducted. This was done to analyze the viscoelastic properties of emulsion system which entails the exact emulsion flow properties and their causes for any change in flow pattern. Emulsions exhibit complex rheological behavior due to the presence of dispersed droplets within a continuous phase. The strain-sweep investigations of EP1, EP2, EP3 and EP4 was conducted at 30˚C and frequency was kept constant at 10 rad s^{-1} as per literature findings [163,240] as shown in Figure 4.7. Dynamic rheology's are analyzed in terms of storage modulus (G') and loss modulus (G"). The storage modulus represents the elastic component of the emulsion, reflecting its ability to store energy, while the loss modulus represents the viscous component, indicating energy dissipation. For EP1, the recorded value of G´ was 960.245 Pa and reduced to 3.301 Pa over the explored range (0.01-100%). An increase of 26%, 15 % and 7.6 % was observed in the value of G´ (at 0.01%) for EP2, EP3 and EP4 respectively. Lowest value of G´ was observed for EP3 as evident from Figure 4.7. Also, the strain deformation seems to follow similar trend for EP1, EP2 and EP3 whereas EP4 is observed to be least affected by strain deformation. EP4 has more potential as compared to other prepared emulsions as evident from viscosity and strain deformation results. Thus, the application of EP4 is recommended for the reservoir dominated by n-dodecane paraffin oil.

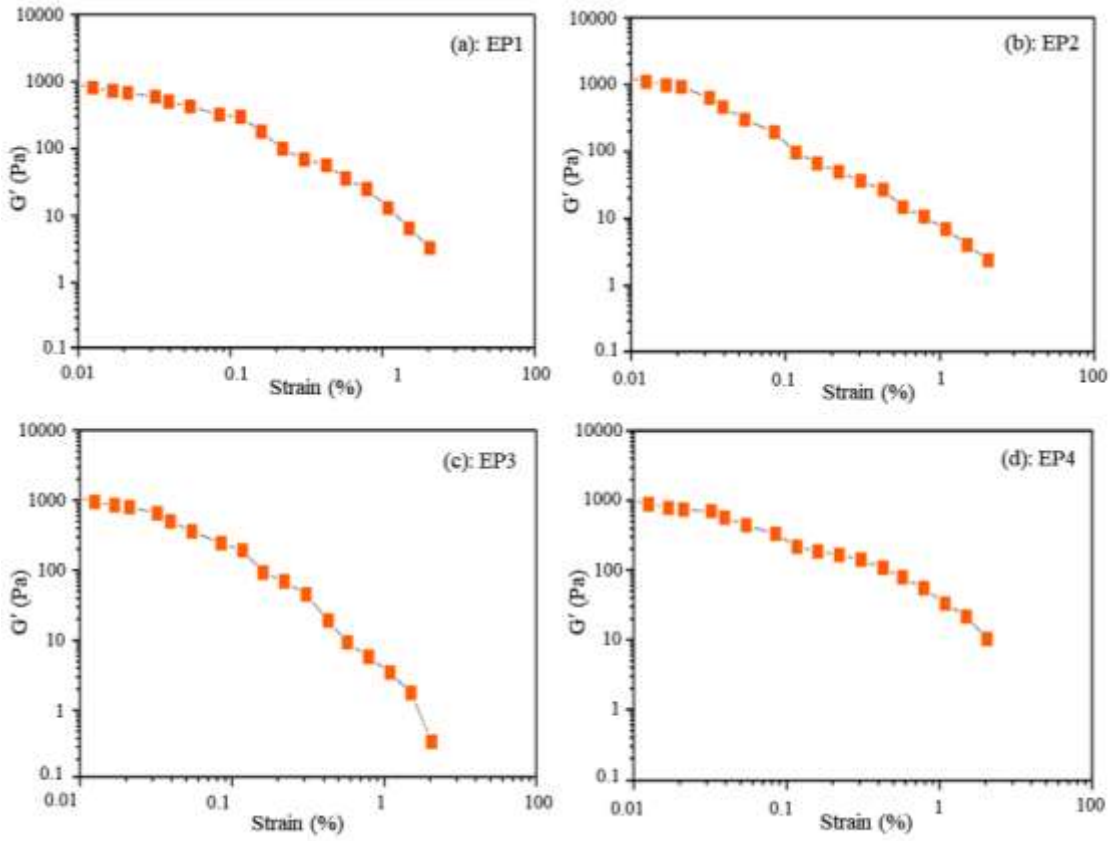

Figure 4.7: Dynamic rheological investigation of the emulsion systems. All sets of experiment were conducted thrice to get reproducibility in results and uncertainty of ±2.8-6.5% of the recorded value was observed.

4.3.4 Effect of salt on Emulsion system

Salinity is one of the major parameters impacting emulsion stability. Salts can influence emulsion stability by affecting the interfacial properties of the emulsion [53]. Specifically, salts can alter the charges on emulsion droplets, impacting electrostatic repulsion or attraction between them. This electrostatic modification can lead to changes in droplet size distribution and overall stability. Additionally, salts may influence the viscosity of the continuous phase, affecting the emulsion's rheological properties. For this purpose, the effect of both monovalent and divalent salt

was studies by means of microscopic investigation. Figure 4.8 shows the effect of increasing concentration of monovalent salt (NaCl: 1- 4wt%) on stability of emulsions EP1, EP2, EP3 and EP4. The inclusion of NaCl to emulsions can have significant impacts on their stability and properties. This can also alter the ionic strength of the aqueous phase, leading to changes in the electrostatic interactions at the oil-water interface. From this figure, it can be observed that EP1 was less stable at 1-2 wt% of NaCl as larger size of oil droplet was observed (2wt%) through microscopic results and this may be due to the presence of salt promoting coalescence of oil droplet. At 3wt% of NaCl, the distribution of oil droplets seems to be less, and more coalescence was observed and very limited oil droplets was observed at higher concentration of NaCl (4wt%) due to increasing coalescence. Furthermore, the stability of EP1 was drastically impacted by the presence of divalent salt ($CaCl_2$) as shown in Figure 4.9. The impact of a divalent salt ($CaCl_2$) in varying concentration (1-4 wt%) on the emulsion systems (EP1, EP2, EP3 and EP4) was observed via microscopic studies. Divalent salt drastically impacts the stability of emulsion due to presence of calcium ions that interact with the emulsifiers and results in altering the properties of emulsion, for instance, induce droplet coalescence, rheological parameters etc. It can be observed that very limited oil droplets are present at concentration of 1wt% whereas at higher salt concentration (2-4wt%), no oil droplets were observed (Figure 4.9). Thus, it can be concluded that the reservoir dominated by n-pentane paraffin at higher salinity, mobilization of oil will be difficult as no emulsification was observed at higher salinity as evident from Figures 4.8 & 4.9. The emulsion EP2 seems to be stable till 2wt% of NaCl as a fine packet of oil droplets was observed from microscopic results. At 3wt% of NaCl, lesser coalescence of oil droplet was observed due to presence of loose packets of oil droplets whereas at 4wt% of NaCl, no oil droplets were observed as evident from Figure 4.8. Whereas the stability of EP2 was adversely affected in presence of

divalent salt ($CaCl_2$) as shown in Figure 4.9. A loose packaging of oil droplets smaller in size can be seen from microscopic investigations at salt concentration of 1-2wt% of $CaCl_2$ and emulsion EP2 becomes completely unstable at higher concentration (3-4wt%). EP2 seems to possess better stability than EP1in presence of divalent salt. This may be attributed to the reduced efficacy of natural surfactant micelles in presence of high saline environment in order to form emulsions, thereby may reduce its potential in recovering oil from high saline reservoirs. From Figure 4.8, the emulsion EP3 seems to be highly stable in presence of 1wt% NaCl as a dense and tight packet of oil droplets was observed. Increasing salt concentration from 2-3wt% of NaCl tend to break the emulsion as more coalescence of oil droplets was observed as evident from microscopic results and EP3 becomes completely unstable at 4wt% of NaCl due to presence of limited and large-sized oil droplets. Stability of EP3 has detrimental effect in presence of divalent salt as evident from microscopic result (Figure 4.9). As the salt concentration was increasing from 1-4wt%, the large sized oil droplets with loose packaging were observed. This may be due to one of the literature finding stating that presence of salt beyond 1wt%tends to decrease the electrostatic repulsion and further promotes the flocculation among the micelles of surfactant [241]. Due to flocculation, the micelles of natural surfactant tend to disperse within the solution, as a result adsorption at oil-water interface is reduced restricting emulsion formation. This may be the reason for the presence of few and large sized oil droplets at increasing salt concentration. Finally, the stability of emulsion EP4 was studied in presence of salt and it was observed that EP4 was stable from 1-3wt% of NaCl as a dense and very light packet of oil droplets was observed as evident from microscopic results shown in Figure 4.8. At higher concentration of NaCl (4wt%), large-sized oil droplets were observed, and this may be due to increased coalescence of oil droplet at higher salinity. Moreover, EP4was observed to be stable in presence of 1-2wt% of $CaCl_2$ and by increasing concentration of

divalent salt, that is, at 3and 4wt%, large-sized oil droplets were observed due to coalescence. Therefore, it can be concluded that EP4 possess higher stability when compared to EP1, EP2 and EP3 in saline environment. In addition, the stability in presence of monovalent salt (NaCl) was higher as compared to divalent salt ($CaCl_2$) and this may be attributed to nature of divalent salt as it may segregate with increased number of ions that that of NaCl [57]. Thus, application of EP4 is recommended for application in high saline reservoir dominated by n-dodecane.

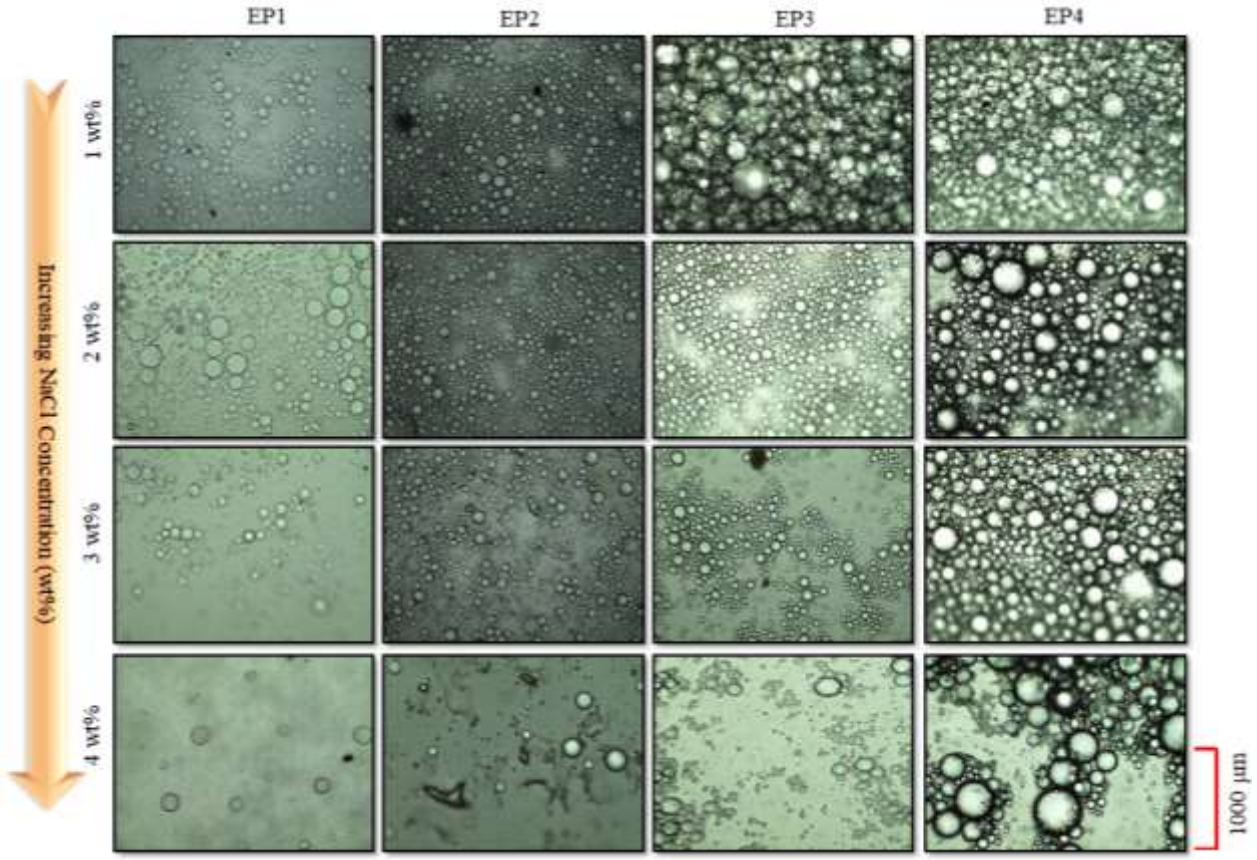

Figure 4.8: Microscopic investigation of the impact of monovalent salt (NaCl) in varying concentration (1-4 wt%) on the emulsion systems (EP1, EP2, EP3 and EP4).

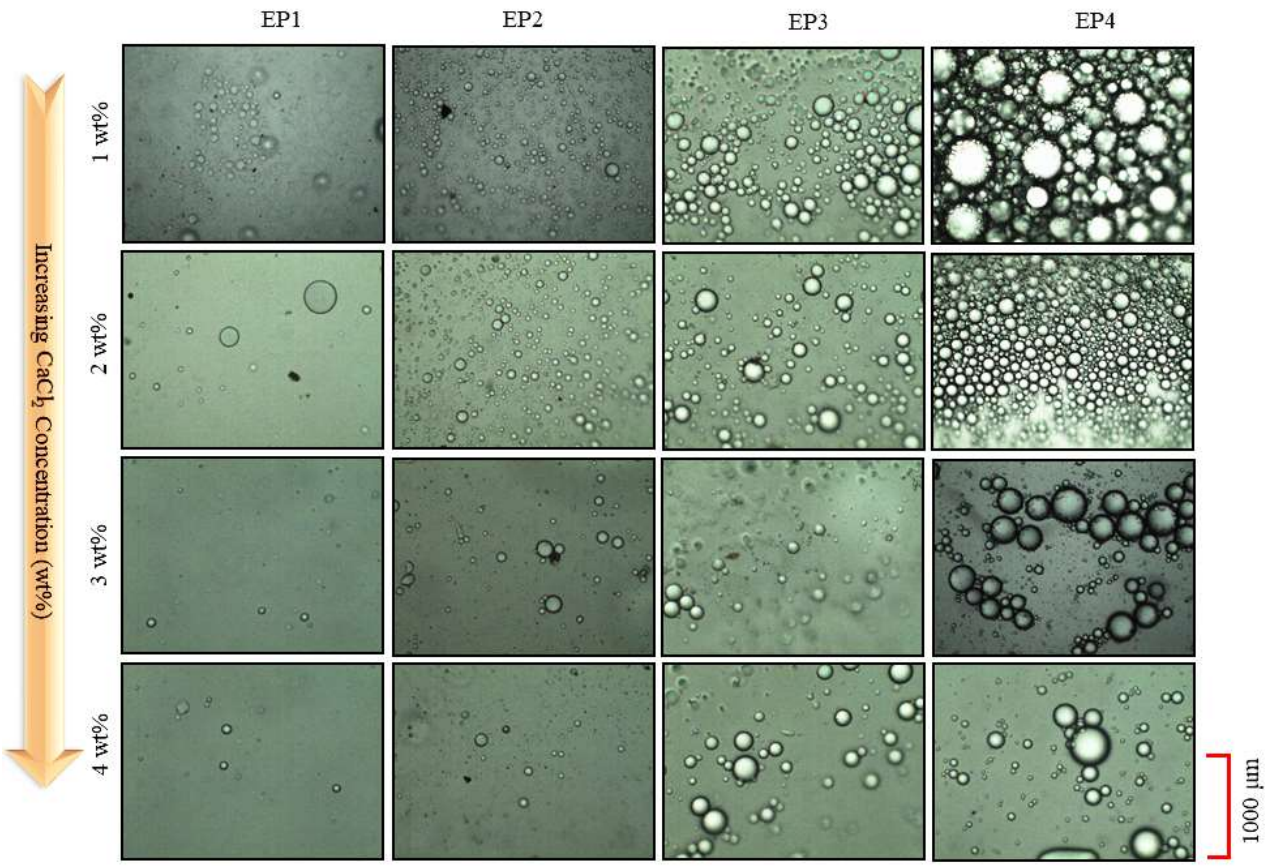

Figures 4.9: Microscopic observations of the impact of a divalent salt ($CaCl_2$) in varying concentration (1-4 wt%) on the emulsion systems (EP1, EP2, EP3 and EP4).

4.3.5 Effect of Grain size on wettability alteration

Wettability alteration is one of the important parameter affecting the reservoir condition favorable for producing more oil [235]. In general, majority of reservoirs are oil wet in nature and to recover oil from the reservoirs, rock surface needs to be water wet and this is where the surfactant plays a crucial role. Surfactants has the huge potential in IFT reduction, altering the wettability of rock surface and describes the wetting or non-wetting characteristic of fluid [26,182,242]. The effect of surfactant on wettability alteration can be analyzed by contact angle which is defined as the angle between liquid-solid/gas interface [178]. For analyzing the nature of

rock surface if contact angle varies from 0˚-75˚ is considered to be water-wet, from 76˚-115˚ intermediate-wet above 115˚ is considered to be oil-wet [243]. Contact angle studies were conducted on the sandstone surface saturated with n-dodecane in presence of SP solution at ambient conditions as shown on Figure 4.10. The sand grains used for study were untreated and of varying sand size. All measurements were conducted thrice, and average value obtained was plotted with uncertainty ~ 3%. SP solutions are designed to alter the interfacial properties between different phases, such as oil and water [41]. The contact angle measurement provides valuable insights into the wettability of the oil surface by the SP solution. By reducing the contact angle, the SP solution can increase the spreading and penetration of the solution into the oil phase, enhancing its effectiveness in various applications. Initially the contact angle was observed to be 76˚ at 0 min and significant reduction in contact angle was observed between 4-12 min where ~34% reduction was observed. After 12 min the contact angle was recorded as 43˚, making it water wet. This may be attributed to the potential of surfactant in displacing oil from rock surface at the interface between n-dodecane and aqueous SP solution. The surfactant used at CMC offers favorable results in making the surface more water-wet [38]. A consistent decrease in contact angle was observed over a span of 20 min with a net reduction of ~ 69.7% with the minimum vale of 23˚ (at 20 min). The decrease in contact angle may associated with the attraction of ion-pair between the polar head of surfactant micelle, that is, anionic in nature and the oil component adsorbed on sandstone having cationic charge [244].

Later to investigate the effect of grain size on wettability alteration, contact angle studies were conducted on different grain size, that is, low sand size (less than 250 μm) and high grain size (more than 250 μm). Different sized sand grains have drastic effect on its properties, for instance, compressibility, strength, void ratio, etc [245]. The size and roughness of the sand

particles can influence the contact angle. Smaller particles may have a larger surface area per unit volume, potentially leading to different wetting behaviors compared to larger particles.

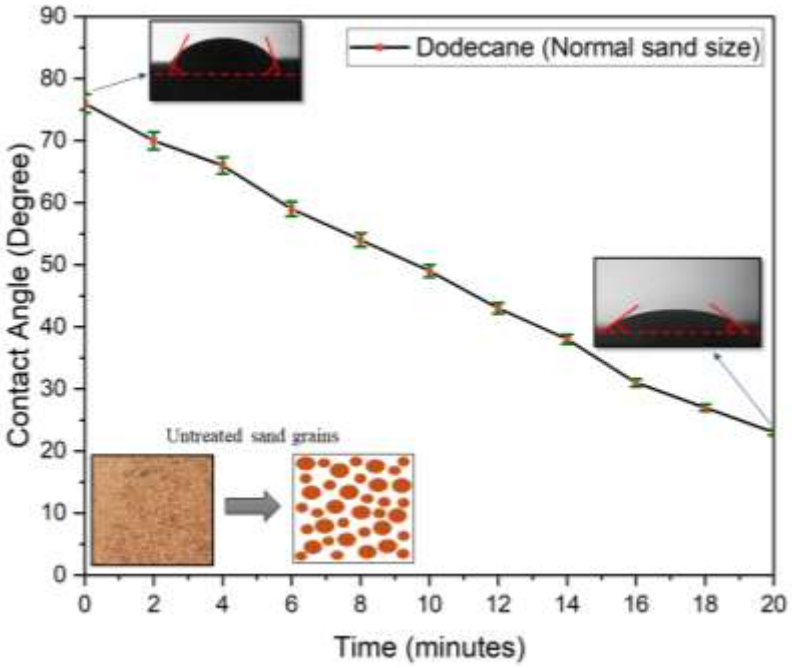

Figure 4.10: Plot of the contact angle values against time. Contact angle was conducted between sand saturated with n-dodecane and SP solution.

Additionally, surface roughness can affect the contact angle by providing more sites for interaction between the liquid and solid phases. Larger sand particles have less overall surface area, their surfaces can still exhibit significant roughness. This roughness can affect the contact angle by providing more irregularities for the SP solution to interact with, potentially altering wetting behavior. Figure 4.11 show the contact angle measurements for low sand size and high sand size over a span of 20 min. Initially the contact angle was recorded to 74˚ (at 0 min) and start decreasing to 54˚ at 4 min, 41˚ at 8 min, 32˚ at 12 min with a minimum value of 20˚ after 20 min with a considerable reduction of ~ 73% which is lower than that of contact angle result obtained for normal sand size (~ 69.7%). This may be due to reduced sand size causing increase in surface

area of the sand grains and thus enhances the flow of SP fluid making the surface more water-wet [246]. This results in achieving lower value of contact angle. Due to low grain size, compact and smooth surface can be obtained with lesser porosity [247]. For high grain size, the contact angle was recorded as 84˚ at 0 min higher than that of low grain size (74˚ at 0 min) as evident from Figure 4.11. This may be due to increased porosity, due to uneven grain size. In addition, a sharp reduction in contact angle was observed with a minimum value of 10˚ (at 20 min) with a total reduction of ~ 88% over the range of time explored. This may be attributed to Gibbs-Marangoni effect. Sand grains initially saturated with oil tends to become thinner with time due to synergetic interaction surfactant micelles, which ultimately detaches the sand grains from oil [63]. Lower value of contact angle (10˚) may be due to the smaller area exposed to oil as well as the large distance between oil and surface [190].

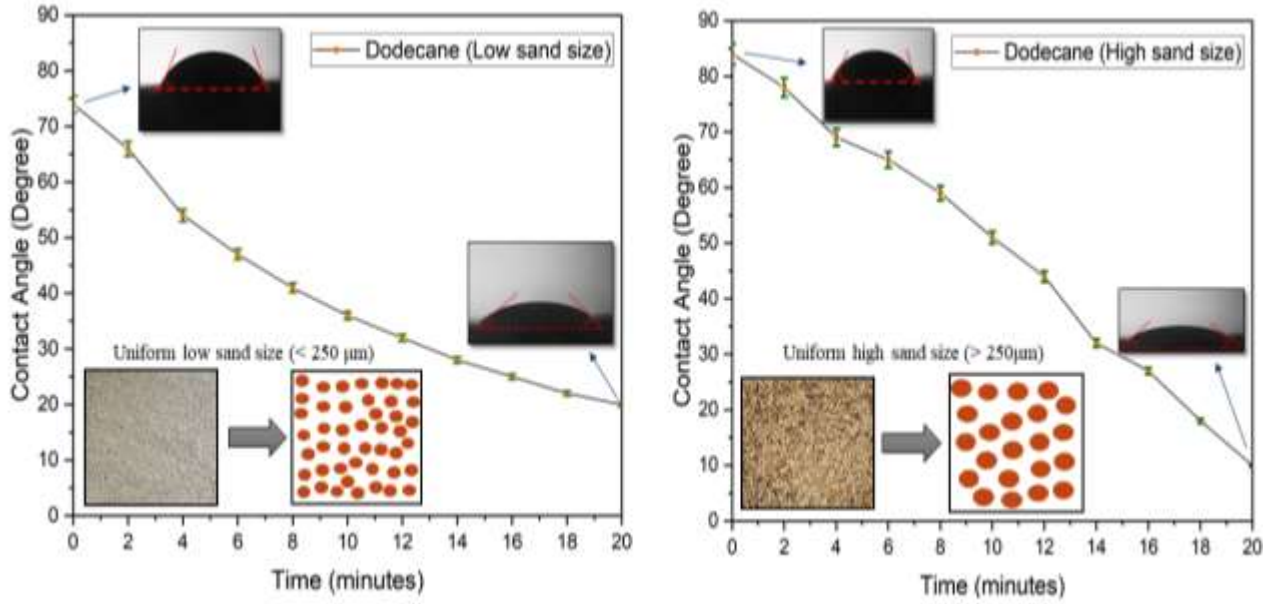

Figure 4.11. Variation of contact angle with respect to time obtained for varying sand sizes. Normal sand was sieved to obtain the low sand grain (size < 250 µm) and high grain size (size >250 µm).

4.3.6 Pore Scale Analysis of Surfactant flooding

Microfluidics are gaining huge attention as it helps in visualizing the potential of surfactant in displacing oil by means of pore scale analysis. Conventionally, surfactant flooding are performed in core samples as well as sand pack for analyzing the potential of surfactant [159,234,248,249]. The core samples and laboratory sand pack resemble quite similar with the rock formation [250], but the visual observations in real time are challenging to perform. Thus, there is a need for microfluidic chip that allows clear visualization and helps in understanding flow of fluid. Various microfluidic studies have been reported in the literature which confirms the better understanding of the mechanism possessed during surfactant flooding [251–253]. This study delves into the microscopic analysis of displacement of oil (n-dodecane) by means of surfactant flooding. Initially, the microfluidic chip was flooded with brine, which resembles the tradition oilfield formation with salinity as that of Cambay basin. The chip was saturated with brine so that the brine reaches at most of the pore channels. This was followed by capturing the microscopic image of microfluidic chip from inlet to outlet as shown in Figure 4.12. Brine injection helps clean and prepare the microfluidic chip, removing any residual fluids or contaminants. Brine injection establishes the initial conditions for the experiment, replicating typical reservoir condition that provides a realistic starting point for studying fluid displacement processes. From Figure 4.12, it can be inferred that no air bubble was encapsulated within the pores. As the oil (n-dodecane) was flooded, initially brine flush out and oil was observed to be encapsulated at various pore channels, shown in Figure 4.13.

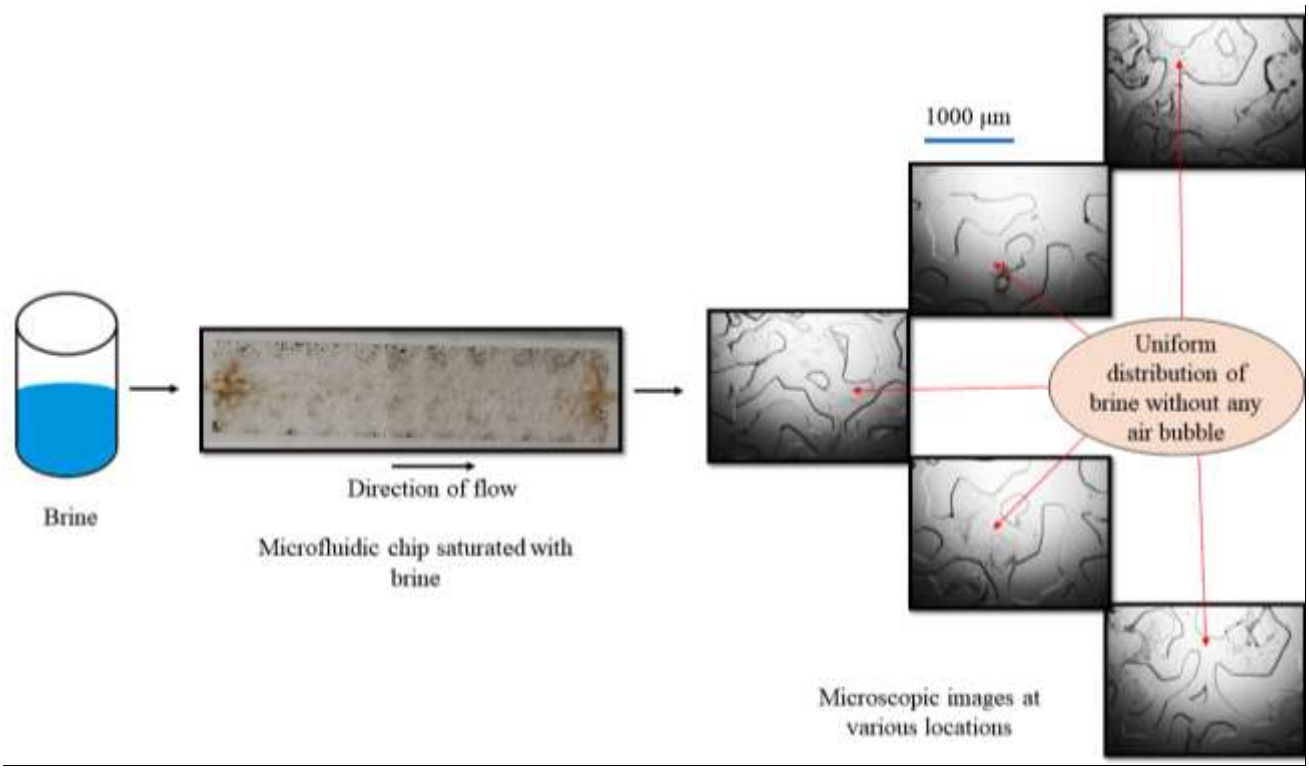

Figure 4.12: Visual appearance of the microfluidic chip during brine pre-flush and injection. As observed from the presented images, a uniform distribution of the injected fluid was observed and no air bubble was encapsulated during brine injection.

Oil was encapsulated within the pore channels of microfluidic chip. Enlarged view of encapsulated oil at some pore channels has been provided (and highlighted in yellow) for clear visualization which shows the uneven distribution of the oil. The uneven distribution of oil may be due to oil being unable to access some of the constricted pores in the microfluidic setup. Finally, natural surfactant was flooded in the microfluidic chip (saturated with oil) and this was quite imperative to analyze the surfactant's potential in displacement of oil. Figure 4.14 shows the microscopic images of the microfluidic chip after injection of surfactant from inlet to outlet. The pore scale analysis was performed to envisage the potential of natural surfactant in mobilizing oil from the micro channels.

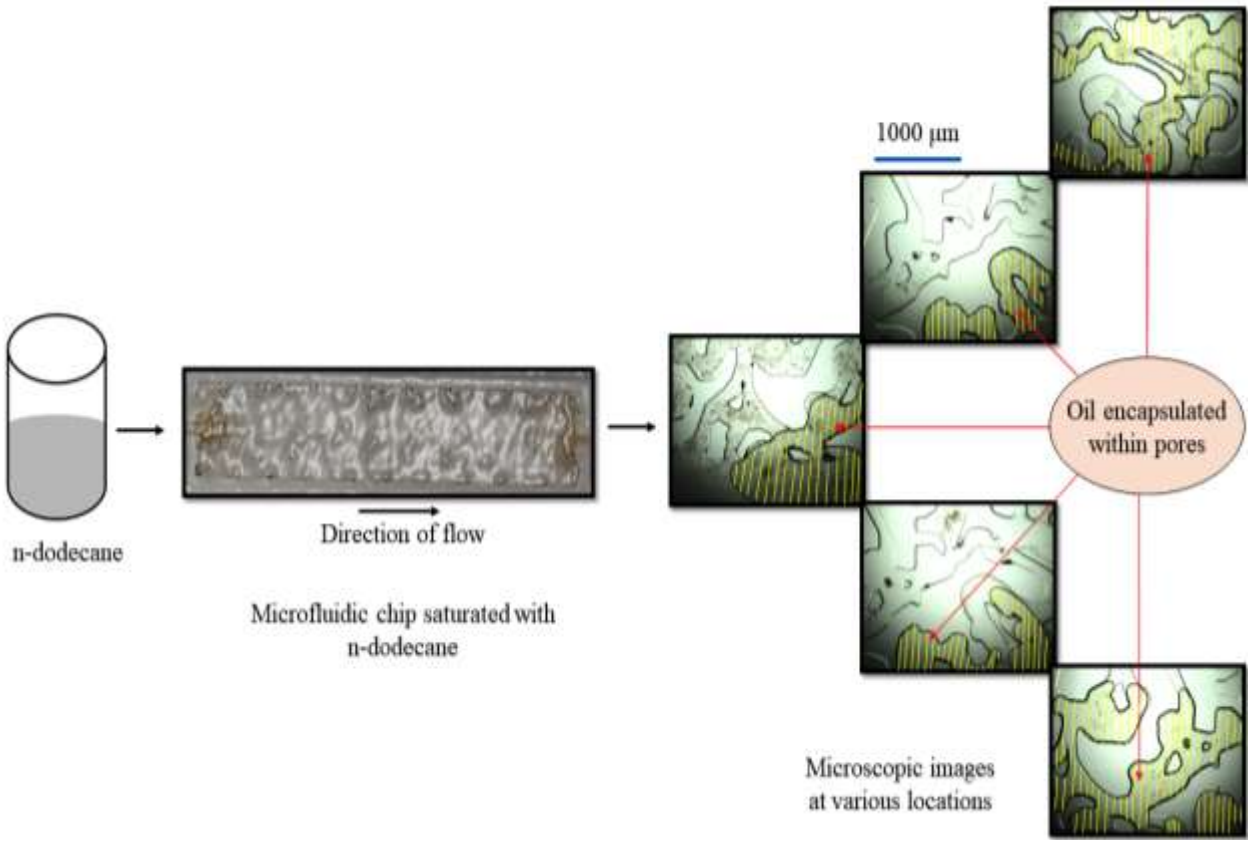

Figure 4.13: Visual appearance of microfluidic chip saturated with n-dodecane. With closer observation, the presence of injected paraffin (highlighted in yellow) can be observed from an un-even distribution in micro channels.

After the injection of oil at rate of 0.5 ml/min, the natural surfactant solution was flooded with same flow rate of 0.5 ml/min. The flow rate was kept constant and oil started to mobilize from the pore channels. Oil was collected in small beaker at the outlet of micromodel. The injection of surfactant solution was kept on with 0.5 ml/min till no oil droplet was seen at the outlet of micromodel. Natural surfactant has shown its great potential in displacing all the encapsulated oil as evident from Figure 4.14. Natural surfactant solution reduces IFT between the oil and water phases, facilitating the detachment of oil droplets from the microfluidic chip's surface and enhancing oil mobilization. It further promotes emulsification by stabilizing oil droplets in the

aqueous phase. Surfactant solution has shown its potential in mobilizing the oil from the pore channel of the chip, as evident from microscopic images of different sections.

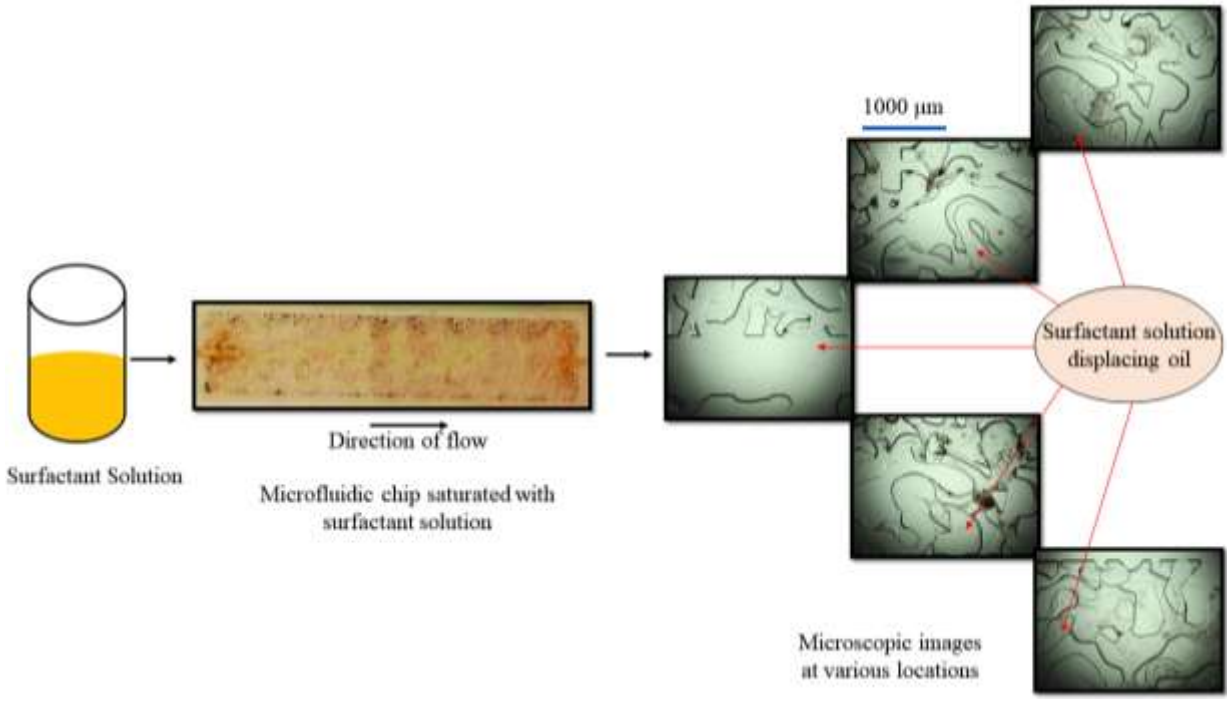

Figure 4.14: Visual appearance of the microfluidic chip during surfactant flooding and oil recovery. Surfactant solution was able to easily displace the oil in the chip, evident from microscopic studies at different sections.

After displacement of oil (n-dodecane), surfactant solution has been distributed within the microfluidic chip which can be clearly seen from the enlarged view of some pore channels provided in Figure 4.14. This may be attributed to the various mechanism possessed by natural surfactant within the pores, for instance, IFT reduction, altering wettability, emulsification, the detailed explanation of which can be found in our previous studies [30,229,254].

4.4 Conclusion

The present study delves in the application of natural surfactant for stabilizing the paraffin emulsions. In addition, microscopic, wettability alteration and rheological findings are taken into consideration for its successful subsurface application. This was followed by the pore scale analysis of surfactant potential in displacing oil. Mobilizing additional encapsulated oil from existing pores through enhanced oil recovery (EOR) process can be more economically viable than drilling new wells as drilling new wells involves significant upfront costs including exploration, drilling, and infrastructure development. EOR, on the other hand, utilizes existing wells and infrastructure, reducing capital expenditures. EOR techniques can increase the percentage of oil recovered from existing reservoirs, often extracting oil that was previously deemed economically unviable to produce. This higher recovery rate means more revenue from existing assets. The key points of the study are summarized below:

- Initially emulsion preparation was done with n-pentane, n-hexane, n-heptane and n-dodecane at varying surfactant concentration to visualize the stable emulsion, which further helps in determining the expected range of CMC. It was found that emulsion was stable in the range of 0.15 - 0.25wt% of surfactant concentration.
- To determine the CMC value, IFT measurements were conducted for all paraffin explored and found the surfactant concentration of 0.2wt% as CMC. Minimum IFT values were obtained at 0.2wt%, that is, 6.25 mN/m, 12.39 mN/m, 6.62 mN/m and 6.87 mN/m for n-pentane, n-hexane, n-heptane and n-dodecane, respectively.
- All emulsions were kept under observation for 10 days, and emulsion was observed to be creamed. Microscopic investigation of creamed layer of emulsion was done which entails

the dense and tight packets of oil droplet present whereas very loose packaging of oil droplets was observed in separated aqueous phase.

- All the prepared emulsions exhibited shear thinning profile and viscoelastic behavior as evident from rheological measurements.
- Among all prepared emulsions, n-dodecane emulsion was found to be stable in presence of both monovalent (3wt%) and divalent (2wt%) salt.
- Minimum value of contact angle was obtained with the high sand size as compared to low sand size due to surface irregularity.
- During pore scale analysis, natural surfactant was found potential in displacing encapsulated oil in the pore channels.

The observations reported in this study provide a strong case for the application of natural green formulations for emulsion formulation and application in oil reservoirs with high paraffin content. EOR is crucial because it helps to extract more oil from existing reservoirs than traditional methods can. As conventional extraction techniques become less effective, EOR becomes essential for maintaining production levels and maximizing resource utilization. It also extends the life of existing oil fields, which is vital for energy security and economic stability. Additionally, drilling new wells can have environmental consequences, including habitat disruption, water contamination, and greenhouse gas emissions. EOR can extend the productive life of an oil field, providing a more prolonged revenue stream and allowing companies to defer high costs associated with decommissioning and site restoration.

Chapter 5

Effect of Natural Surfactant (fenugreek seeds) on Emulsification and Mobilization of Paraffins *via* Pore-scale Micromodel Experiments

Abstract

The surface characteristics of minerals have been crucial in predicting the interactions between chemicals, particularly in chemical flooding. Thus, this technical paper evaluates the viability of natural surfactants derived from agricultural products for oil recovery studies from a micromodel filled with paraffinic oil. The study investigates the interfacial tension, viscosity, microscopic, dilution studies and oil mobilization characteristics of the natural surfactants. The experimental setup involves conducting interfacial tension measurements between the surfactant solution and paraffinic oil using the Wilhelmy plate method and was found to be 14.2mN/m, 10.92mN/m and 9.8mN/m. Additionally, viscosity measurements and frequency sweep analysis were performed to assess the rheological properties of the prepared emulsion which was stabilized using a natural surfactant. Microscopic evaluation depicts that amongst the prepared emulsions, n-heptane emulsion seems more stable at both 30˚C and 90˚C. Moreover, dilution studies were conducted for each emulsion system and dilution ratio was varied from 1:5 to 1:1 (emulsion: saline solution). It was found that n-heptane emulsion possesses better stability at higher dilution (till 3:5 ratio). Oil mobilization studies are conducted using a glass micromodel to simulate reservoir conditions and observe the displacement efficiency of the surfactant solutions. The results indicate that natural surfactants exhibit competitive interfacial tension reduction and viscosity modification properties compared to commercial surfactants. Furthermore, oil mobilization studies demonstrate

the effectiveness of natural surfactants in enhancing oil recovery from paraffinic oil reservoirs. These findings suggest the potential of natural surfactants derived from agricultural products as sustainable alternatives for improving oil recovery efficiency in petroleum reservoirs.

5.1 Introduction

Paraffin is a type of hydrocarbon molecule found in crude oil. They are alkanes, and consist solely of hydrogen and carbon atoms arranged in straight or branched chains [228]. Paraffins are typically lighter hydrocarbons with low viscosity, which makes them flow more easily compared to heavier compounds like asphaltene and resins. Conventionally, the presence of paraffin can promote oil recovery, as compared to those reservoirs containing other heavier components as their low viscosity enables them to flow more easily through porous rock formations, facilitating oil extraction [212]. Paraffin can also be targeted in subsurface applications such as injection of water. Injection of chemicals can help boost oil recovery by targeting paraffin to alter their properties, making them more amenable to extraction. Surfactants and polymers can be used to modify the interfacial tension (IFT) between oil and water, aiding in mobilizing paraffin and increasing oil recovery [148,223,255,256]. Paraffin also tend to form stable emulsions with water, making it difficult to separate oil from water during extraction processes [50]. However, during oil recovery, it is essential to carefully optimize the chemicals used for emulsion formation as the paraffin may deposit and accumulate in pore spaces within the reservoir, reducing permeability and hindering oil flow. Thus, while paraffin can facilitate oil recovery through their low viscosity and response to various extraction techniques, they also present challenges such as unstable emulsification and deposition that must be addressed to maximize oil production from reservoirs.

Surfactants play a crucial role in enhancing oil recovery from reservoirs dominated by paraffin by altering the IFT between oil, water, and rock surfaces [198,257]. The application of

surfactants tends to lower the IFT between oil and water, making it easier for water to displace oil from the rock pores [242]. In reservoirs dominated by paraffin, where oil-water IFT can be high, surfactants help in breaking down this barrier, facilitating oil displacement and recovery. Using ultra-sonication, Baloch and Hameed [47] investigated the emulsification of different paraffins, for say, n-hexane, n-heptane, n-decane, and kerosene in water. It was concluded that the quantity and size of droplets were dependent on factors like the composition of the oil and the span of the ultra-sonication process, with n-hexane < n-heptane < n-decane< kerosene. Golemanov et al. [50] examined various commercial surfactants, including anionic, nonionic, and polymeric ones. hexadecane or tetradecane was used as a dispersed phase. It was reported that except for the nonionic Tween 40 and Tween 60, most of the investigated individual surfactants are found to be ineffective stabilizers. On the other hand, the addition of suitable cosurfactants, like hexadecanol, Brij 52, or cocoamidopropyl betaine, considerably improves the dispersion stability. A study involved in preparation of water in hexane nano emulsion stabilized by Brij 30 or Span 80 by means of low energy method reports Ostwald ripening as a primary destabilization mechanism of the systems [49]. Another study reports that lower value IFT (14.46 mN/m) and primarily water-wettable rock surface, with a diluted salinity of 25 percent of the initial quantity (that is, TDS ~8500 ppm). It was also concluded that TDS of about 8500 ppm may be the ideal salinity for low salinity water flooding in light oil reservoirs [243]. Surfactants can help in the formation of stable emulsions from paraffin by reducing the IFT between the oil and water phases. This allows for better mixing of the two immiscible phases, leading to the formation of stable emulsions. In the context of oil recovery, stable emulsions can help by improving the mobility of oil in the reservoir, reducing its viscosity, and enhancing its displacement from porous rocks. Additionally, surfactants can alter the wettability of the rock surface, promoting better contact between the oil and the

injected fluids, thus increasing oil recovery efficiency [160]. This enhances the mobility of oil within the reservoir, allowing for better sweep efficiency and increased oil recovery. In water flooding operations, surfactants can improve the efficiency of water displacement by reducing the capillary forces that trap oil in the pore spaces of the reservoir rock. This promotes better sweep efficiency and more effective oil recovery. Thus, as evident from several past experimental studies, the application of surfactants has been found to aid in enhancing oil recovery from paraffin-dominated reservoirs by reducing IFT, forming stable emulsions, mobilizing paraffin, and improving the efficiency of water flooding operations.

In most prior applications, the studies have reported the utilization of commercial surfactants like SDS (sodium dodecyl sulphate), Tween 60, Tween 40, Brij 30 and Span 80, offer significant benefits in enhancing oil recovery, but also come with several challenges. Commercial surfactants can be expensive, especially if large quantities are required for oil recovery operations. Cost-effectiveness is a crucial consideration, particularly for large-scale applications. Additionally, some commercial surfactants may have environmental implications, such as toxicity or persistence in the environment [12,258]. Ensuring that surfactants used in oil recovery operations are environmentally friendly is essential to minimize adverse effects on ecosystems. Furthermore, the commercial surfactants may not be compatible with all reservoir conditions or other chemicals used in oil recovery processes. Compatibility issues can affect the effectiveness of surfactants and may require additional testing and optimization. Here, there is a potential to investigate the application of natural surfactants, derived from renewable sources such as plants or microorganisms, which can offer potential alternatives to commercial surfactants. Several natural surfactants have been extracted from various green sources, for instance, palm oil, heena leaves, mulberry leaves, eucalyptus leaves, soapnut, quinoa, fenugreek seeds etc. and found suitable for

various industrial applications [23,26,30,38,39,259]. These surfactants have all demonstrated impressive and similar outcomes in oilfield applications, such as enhanced oil recovery, wettability modification, and IFT reduction. Compared to commercial surfactants, natural surfactants tend to have minimal environmental impact, and are usually biodegradable and possess low toxicity [256,260]. From an environmental standpoint, natural surfactant's have a better environmental footprint, and this remains crucial to ensure sustainability and compliance with regulatory requirements. Pal et al.[8] extracted natural surfactant from coconut oil and used it at critical micelle concentration (CMC) (23.5294 mmol/l) for stabilizing crude oil-water emulsion at 343 K. Prepared emulsions was found to be stable for 21 d and thereafter phase separation was observed. Another study employed in emulsification of crude oil by using natural surfactant extracted from Eichhornia crassipes. The ratio of oil and water was 5:1 and the viscosity of emulsion was recorded at $1s^{-1}$ was 10.1 mPa s. Norouzpour et al. [23] conducted emulsification of crude oil by employing natural surfactant extracted from quinoa at CMC (1500 ppm), synthetic surfactant NX-610 and TR-880 at CMC 2000 ppm. Emulsion was stored for 90 d and phase separation was observed. It was reported that more emulsification was observed for emulsion stabilized by natural surfactant than that of synthetic surfactants. However, several key criterions must be considered before their substitution. The stability and performance of natural surfactants under varying reservoir conditions, such as temperature, pressure, and salinity, can be a challenge. Ensuring consistent performance over time is critical for successful oil recovery operations. Additionally, natural surfactants must demonstrate comparable or superior performance to commercial surfactants in enhancing oil recovery. This includes factors such as reducing IFT, breaking emulsions, and mobilizing hydrocarbons. Natural surfactants must be compatible with reservoir conditions and other chemicals used in oil recovery processes. Ensuring stability and performance under varying

environmental conditions is essential for successful substitution. Overall, while natural surfactants hold promise as substitutes for commercial surfactants in oil recovery, thorough evaluation of their effectiveness, availability, environmental impact, compatibility, stability, and cost-effectiveness is necessary before their widespread adoption. Even though the use of natural surfactants in the emulsification of crude oil and n-paraffin has not received much attention from researchers, and there is a dearth of literature describing the use of other natural surfactants and their testing for emulsification with lighter components of crude oil (n-alkanes). Thus, investigation of a natural surfactant, derived from fenugreek seeds, in the emulsification of paraffin (n-pentane, n-hexane and n-heptane), with the potential application in enhanced crude oil recovery, is what makes this work novel. The cost of fenugreek seeds is Rs 88 for 500 gm. The surfactant yield was determined as 12.76 ± 11% gm using raw material of 100 gm of fenugreek seeds by using methanol (Rs 920 for 500 ml) as a solvent. Whereas the commercial surfactants like SDS (sodium dodecyl sulphate) cost for Rs. 620 for 500gm, CTAB (Cetyltrimethylammonium Bromide) cost for Rs 2440 for 500 gm. The prices are approximate and can vary depending on the supplier, quantity purchased, and purity of the product. Natural surfactants derived from agricultural products like fenugreek seeds may be more expensive due to the extraction processes and raw materials used, but they offer advantages such as biodegradability and reduced environmental impact, making them valuable in various applications.

Thus, in this study, the performance evaluation of a natural surfactant was employed for preparing oil in water emulsion at CMC (0.2wt%), and n-pentane, n-hexane and n-heptane was used as oleic phase. This was followed by IFT measurements as a function of time for each paraffin explored in the study with and without surfactant. Thereafter, microscopic analysis was done for freshly prepared emulsion, emulsion after 48h and emulsion at elevated temperature. To establish

the flow behavior of emulsion, rheological studies were performed at 30˚C, 60˚C and 90˚C. By using microscopic results, fluid displacement studies were carried out to visualize the surfactant's flow pattern and its potential to displace oil from paraffin flooded glass micromodel. Lastly, dilution studies were conducted to analyze emulsion formation and stability within reservoir in saline medium.

5.2 Materials and Methods

5.2.1 Materials

This study deals with the extraction of natural surfactant from a biomass source, that is, fenugreek seeds. Seeds are procured from local commercial outlet at Amethi (U.P). For extraction of natural surfactant, Soxhlet apparatus (Jain Scientific Glassworks), hot air oven and solvent methanol (SD Fine Chemicals, India) was used. Polymer polyacrylamide (PAM) was used as base fluid (molecular weight: 10^7 g/mol; purity 90%) and obtained from SNF Floerger. Digital weighing balance (Mettler Toledo, ME204/A04; repeatability approximately 0.1 mg) was used for measuring the samples. For preparing the aqueous solution, deionized (DI) water was used and obtained from Millipore® Elix-10 water purification apparatus. PAM solution was prepared (stirring speed: 600 rpm) by using magnetic stirrer (IKA-C-MAG-HS7) for about 7 hrs. Paraffin used in present study are n-pentane (>99 mol%), n-hexane (99 mol%) and n-heptane (>99 mol%), obtained from Sisco Research Laboratory (SRL) India.

5.2.2 Extraction of natural surfactant

Natural surfactant extracted from biomass source, that is, fenugreek seeds is reported in detail in our previous work [30]. A brief outline on extraction process is listed below:

- Primarily, fenugreeks seeds are allowed to dry in sunlight for about 7-10 days followed by drying it in hot air oven at 50˚C for 0.5 h. This was done to ensure the removal of excess moisture content.
- Later, seeds were grinded by using industrial grinder (Oster, India) and sieved in order to obtain fine particles of uniform size 100-240 μm.
- For extraction of surfactant, Soxhlet apparatus [93] was used, wherein the sieved powder (50 g) of fenugreek seeds were encapsulated in muslin cloth and placed in extraction chamber. Initially, muslin cloth was properly cleaned and sun dried. Thereafter, muslin cloth saturated in solvent methanol (for about 48 h) to ensure complete removal of adsorbed detergent if any.
- The whole setup was placed on heating mantle and heated at temperature ~ 65˚C (boiling point of methanol). As methanol starts boiling, the vapor moves towards the condenser, where condensation takes place and gets collected in extraction chamber. When extracted solutes reaches the level of siphon tubes (attached to extraction chamber), it moves in downward direction and gets collected in round bottom flask.
- The whole procedure was left undisturbed for about 48 h till the concentrated surfactant solution was obtained.
- Finally, obtained surfactant solution was oven dried at 70˚C to remove any solvent present. The dried residue was then grinded manually into a fine powder (natural surfactant) by using mortar and pestle arrangement. Schematic representation of the preparation of natural surfactant is shown in Figure 5.1.

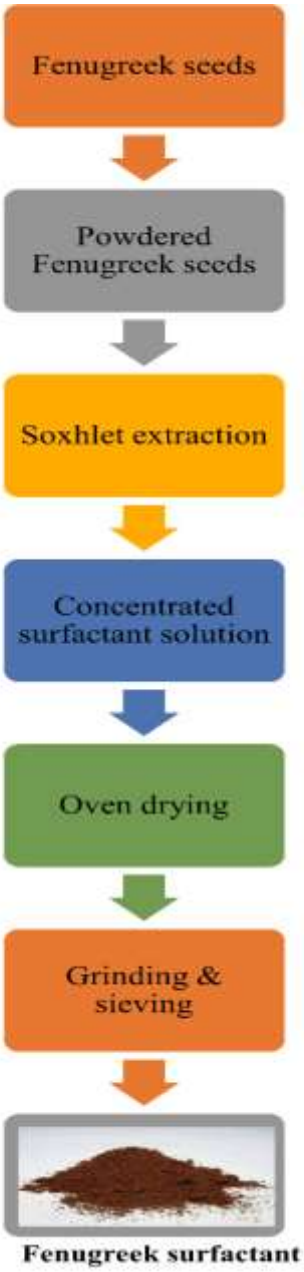

Figure 5.1: Workflow denoting the processes performed to extract the surfactant powder from the agricultural product (fenugreek seeds).

5.2.3 Preparation of emulsion

Present study deals with the preparation of paraffin oil in water emulsion stabilized in presence of natural surfactant. n-pentane, n-hexane and n-heptane were used as oil phase whereas

SP solution as aqueous phase in 40:60 ratios as shown in Table 5.1. Surfactant was used at CMC value, that is, 0.2 wt%. CMC of natural surfactant was obtained by means of electrical conductivity as well as surface tension (SFT) measurements [30]. Initially, DI water was used for preparation of polymer (PAM) solution at concentration 1000 ppm [261] by using magnetic stirrer (at 600 rpm) for about 7 h. After preparation of PAM solution, surfactant was added and allowed to mixed uniformly till 1 h. Prepared SP solution and paraffin oil was taken into a glass vial and mixed using a vortex shaker for about 0.5 h till single phase is obtained.

Table 5.1: Details of paraffin, surfactant, and phase ratio in preparing emulsion.

Paraffin Type	**Formula**	**Mol. Weight**	**Surfactant Concentration**	**Ratio (Oleic phase : aqueous phase)**
n-Pentane	C_5H_{12}	72.15 g/mol	Fenugreek Surfactant (CMS: 0.2 wt%)	40:60
n-Hexane	C_6H_{14}	86.18 g/mol		
n-Heptane	C_7H_{16}	100.21 g/mol		

5.2.4 IFT Measurements

The Wilhelmy plate method was used to investigate the interfacial activity between aqueous and oleic phase. This was done by using the dynamic tensiometer (Model: K12 Kruss® Germany) as reported in our previous studies [229,254,262]. Paraffin oil being light in nature overlays on the aqueous solution (water as well as SP solution) within the sample cup used in IFT investigation. Sample cup filled with aqueous and oleic phase was placed in transparent chamber wherein the Wilhelmy plate was fixed at one end. The Wilhelmy plate was allowed to submerged and locked at the interface of aqueous and oleic phase and simultaneously measurements were

recorded automatically. IFT investigation was done with respect to time, that is, 0-150 minutes and values were recorded every 30 minutes at 30°C. After each observation, sample cup was thoroughly cleaned and dried to avoid any errors during measurement.

5.2.5 Microscopic characterization of emulsions

Microscopic studies of prepared emulsion were done by using optical microscope (Motic, Hong Kong). Images at different locations were captured with the help of inbuilt imaging software (Motic Images Plus 2). With the help of laboratory pipette (Tarsons, United States), a drop of freshly prepared emulsion was placed clean glass slide and kept under microscope for observation. A heating plate mounted on the microscope was used (Thermocon® Instruments Pvt. Ltd., India) having temperature ranging from 25–200 °C) mounted on microscope stage, the emulsion's temperature (40–98 °C) was adjusted. A digital camera (Moticam-10) connected to an optical microscope was used to track and record the heat changes in the emulsion's tiny texture.

5.2.6 Rheological Studies

Rheological findings of prepared emulsion system were done by using compact rheometer (MCR-52, Anton Paar®, Physica, Austria). The rheometer was set up with a bob and cup arrangement for the rheological studies. The bob was mounted on a moving arm, whereas the cup was fixed on the rheometer's base. In order to take the measurements, the bob was gradually lowered until it was completely submerged in the 20 ml of emulsion that had been carefully poured into the cup. Following each measurement, the bob and cup were taken out of the rheometer and cleaned with water and toluene, a laboratory solvent. Ten minutes were needed for the entire experimental run, and each measurement was recorded at a time interval of ~10 s.

Rheological studies were conducted in both shear and dynamic modes as reported in our previous studies [165,263–265]. Shear measurements on the emulsion sample were conducted on varying shear rates, ranging from 1 to 1000 s^{-1}. Measurements of dynamic frequency-sweep were carried out in the angular frequency range of 1 to 100 rad/s. To homogenize the distributed oil droplets, the emulsion sample was gently shaken prior to each measurement. To ensure reproducibility, all rheological measurements were performed at 25 °C and tripled. Nonetheless, it was discovered that the rheological results uncertainty fell between ± 0.7 and 11% of the stated value.

5.2.7 Dilution studies

Dilution studies were conducted to visualize the emulsion stability. For this, saline solution was prepared as that of Cambay basin salinity. Within n-pentane emulsion system (10 ml), saline solution was diluted in five different ratios, that is, 1:5, 2:5, 3:5, 4:5 and 1:1. Each mixture was allowed to shake properly for about 20 min till homogeneous phase achieved. Later with the help of laboratory pipette, a drop of mix was placed on clean and dry glass slide and microscopic observation was recorded. Similar observation was done for n-hexane and n-heptane. After every microscopic observation glass slide was properly cleaned and dried.

5.2.8 Pore scale Analysis of various paraffin in presence of natural surfactant

The fluid flow within a microfluidic chip was observed through pore-scale analysis. A comprehensive schematic for the microfluidic investigation setup is shown in the Figure 5.2. An optical microscope was used to analyze the fluid flow pattern on the microfluidic chip, which was totally transparent.

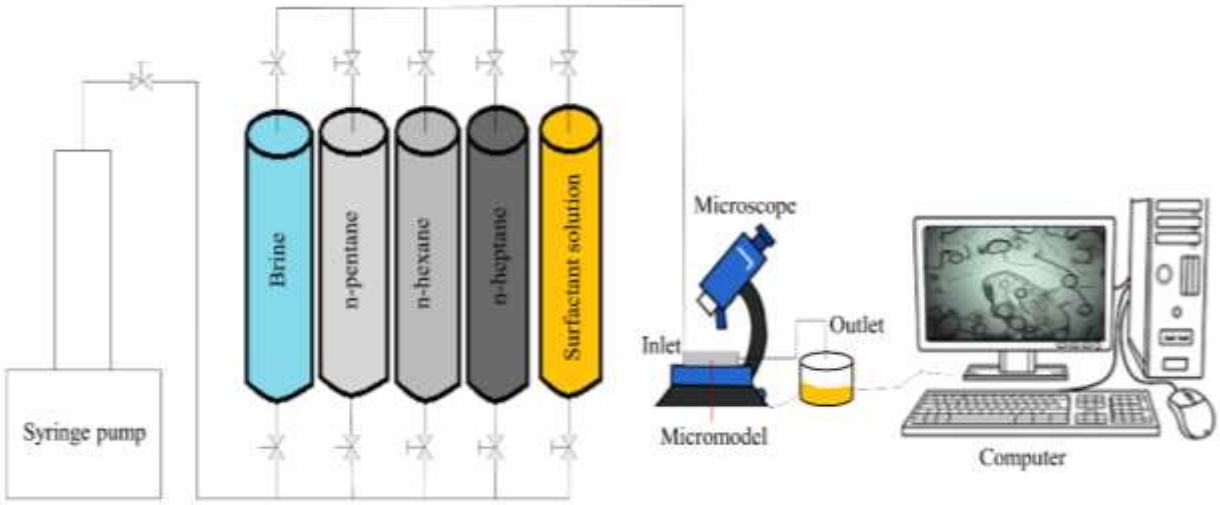

Figure 5.2: Schematic representation of the fluid displacement studies by using glass micromodel. Images were captured by using optical microscope.

A syringe pump (100 DX, Teledyne ISCO, USA) was employed to ensure that the fluids to be injected flowed at a consistent rate. Primarily, brine solution was injected, and the salinity was maintained at ~17297 parts per million (as in the Cambay basin). The brine injection was maintained at a steady flow rate of 1 ml/min for approximately 15-20 minutes, or until the microfluidic chip was totally saturated and thereby preventing the formation of air bubbles as evident from microscopic results. For approximately 15-20 minutes, n-pentane was injected at a constant flow rate of 0.5 ml/min. The other end of microfluidic chip was closed for a period of 2-3 min to ensure that n-pentane flowed through its various sections. The distribution, storage, and movement of n-pentane are all depicted in the full chip image, which also includes the flow pattern of n-pentane. For about 24 h, n-pentane was allowed to saturate the microfluidic chip. Ultimately, n-pentane was displaced from certain areas of the microfluidic chip by injecting the natural surfactant (flow rate ~ 0.5 ml/min) for 15-20 minutes. To comprehend the function of the natural

surfactant in displacing oil (n-pentane) and its movement across the microfluidic chip, the image of the entire chip was meticulously captured and compared with the n-pentane saturated chip. Analogous studies were conducted on n-hexane and n-heptane, and a recording of the entire chip was made to comprehend the function of natural surfactant in mobilizing the oil and its movement within the microfluidic chip.

5.3 Results and Discussion

5.3.1 Emulsion formation and stability analysis

Initially, paraffin oil in water emulsion was prepared by using natural surfactant extracted from fenugreek seeds at micelle concentration, that is, 0.2wt%. Stabilized emulsion with natural surfactant at CMC were moved into clean glass vials and visual appearance of the same is shown in Figure 5.3. The CMC of surfactants is the concentration at which surfactant solutions start to aggregate and form micelles in significant quantities. The physicochemical characteristics of surfactants differ significantly below and above the CMC, therefore CMC is a crucial parameter that affects surfactant adsorption behaviors [193,237]. Higher emulsion formation is associated with the better surfactant performance [266]. The amount of surfactant molecules adsorbed at the oil/water interface increases as the surfactant concentration rises. Because the adsorbed surfactant molecules are anionic, they act as both a steric and an electrostatic barrier to the dispersed oil droplets' coalescence [50,165]. Also, no "vacant sites" are available for surface adsorption at the CMC value and the bulk aqueous phase of surfactant molecules forms micelles. Because of the maximum saturation of the surface with surfactant molecules, the minimum value of surface tension is thus observed at CMC as reported in our previous work [30].

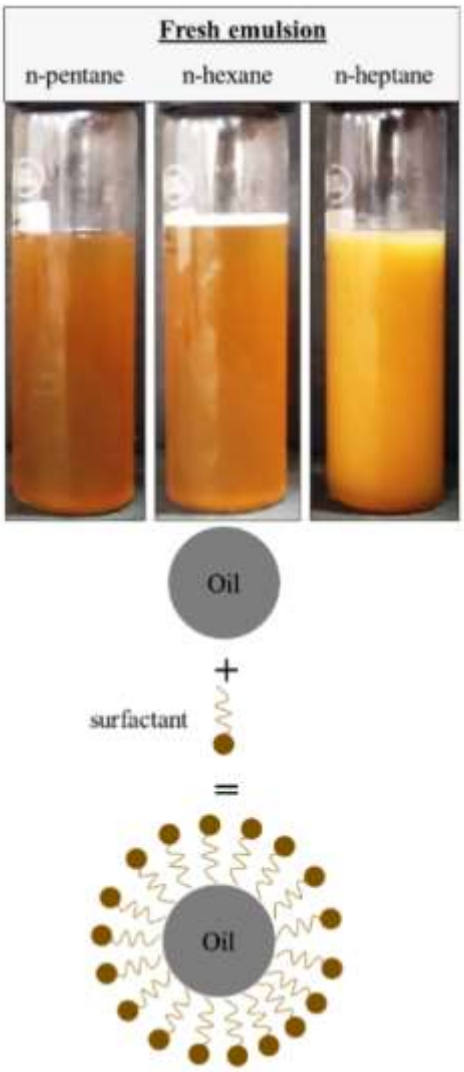

Figure 5.3: Visual images of the freshly prepared emulsions (n-pentane, n-hexane and n-heptane as oleic phase) and schematic visualization of alignment of surfactant micelles over the oil droplet.

The relative spontaneities of the adsorption and micellization processes can be predicted using the CMC measurement, which also provides insight into the aggregation behavior of surfactant molecules in different reservoir conditions. In the prepared system (oil-in-water emulsion), the emulsion was initially found to destabilize through mechanisms like creaming, where droplets move upwards due to lower density, and then coalescence, where droplets merge to form larger ones. Separately, the occurrence of flocculation causes droplets to aggregate without

merging, increasing coalescence risk. In the final stage, Phase separation was found to occur when extensive coalescence breaks the emulsion entirely. Additionally, some instances of Ostwald ripening where larger droplets grow at the expense of smaller ones, were also observed, which contributed to the destabilization of the emulsion system.

5.3.2 Interfacial tension studies

At the interface between two fluids, there is a force of attraction known as interfacial tension. Oil production decreases with a higher IFT value, therefore lower values of IFT is quite favorable for displacement of trapped oil within reservoir [172,267]. When surfactant is added at CMC value, the IFT drops to the lowest level and more oil can be recovered [218,268]. IFT measurements were performed for different oleic phase (n-pentane, n-hexane and n-heptane) against DI water and surfactant solution separately with respect to time. All the measurements were performed at ambient condition as shown in Figure 5.4 and surfactant was used at CMC value. The surfactant concentration at which micelle formation occurs is known as the CMC, and it further aids in lowering the IFT to the lowest possible value [212]. Higher IFT values could be the result of using lower surfactant concentration, which is insufficient to form micelles. It is evident from the Figure that IFT value between n-pentane and DI water was initially 58mN/m and seems to decrease gradually to 46 mN/m over the time explored. A significant reduction in IFT was observed in presence of surfactant solution that is, from 28 mN/m to 14.02 mN/m, leading to total reduction of 51.7% initially. When surfactant micelles come into contact with oleic phase, they contribute to a decrease in surface free energy, which leads to reduction in IFT [12].

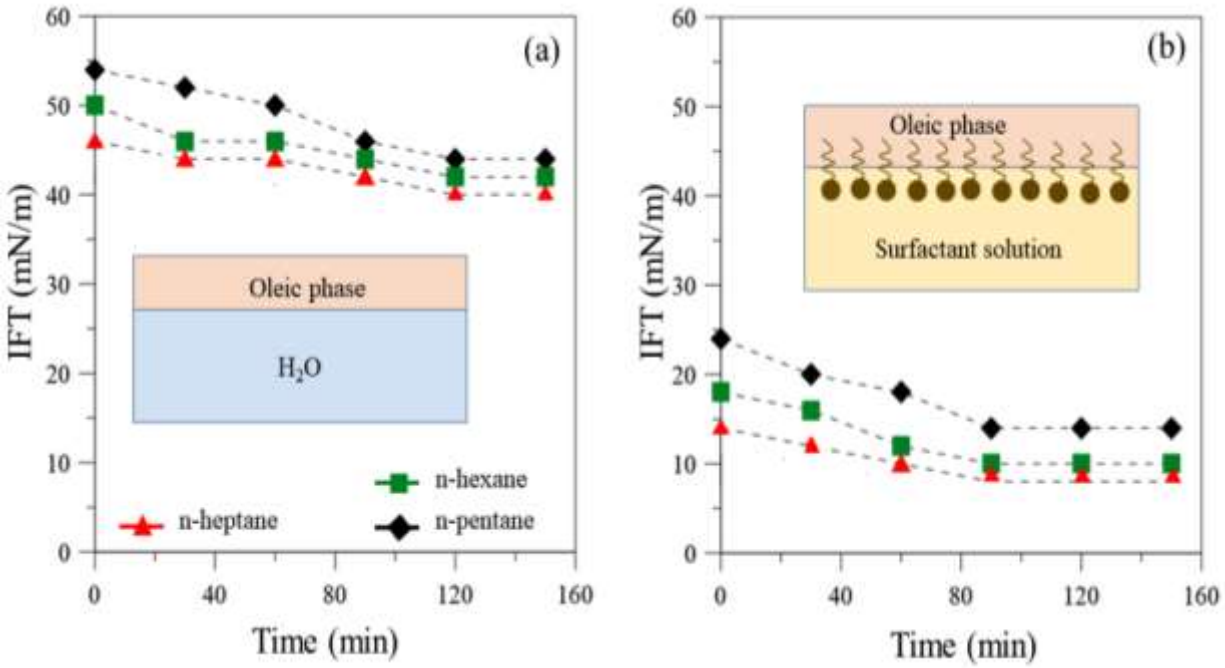

Figure 5.4: Results of IFT obtained between oleic phase and water (a) and with surfactant solution (b) at CMC (0.2 wt%).

For n-hexane, IFT value with DI water was observed to be 50 mN/m and is perfectly aligned with the literature finding [269] whereas in presence of surfactant solution IFT value reduces to 10.92 mN/m as a function of time. The capillary force, which is crucial for hydrocarbon trapping in porous media, increases as a result of the interfacial tension that exists between hydrocarbons and water molecules [270]. Consequently, injecting surfactant is one way to lower the interfacial tension. Thus, the new interaction across the oil–water interface is noticeably stronger due to the presence of surfactant and results in less interfacial tension [242]. Lowest value of IFT 46 mN/m was recorded for n-heptane and DI water [241] and inclusion of surfactant leads to achieve ultra-low IFT value of 9.8 mN/m among explored oleic phase in this study. The decrease in interfacial tension is also determined by the compositional characteristics of oleic phase. Different molecular weights of oleic phase used in this study are 100.21 g/mol for n-heptane, 86.18

g/mol for n-hexane, and 72.15 g/mol for n-pentane as mentioned in Table 5.1. From literature finding, it is quite known that increase in IFT value is observed with a reduction on molecular weight of oleic phase [271]. Therefore, IFT value of n-pentane was greater than n-hexane and n-heptane IFT values and is evident from Figure 5.4.

5.3.3 Microscopic observations of emulsions

Microscopic investigation was performed for freshly prepared emulsions (n-pentane, n-hexane and n-heptane) as shown in Figure 5.5(a-c). From Figure 5.5(a-c), the oil droplet packing is comparatively denser for n-heptane emulsion than that of n-hexane and n-pentane emulsion. The average size was in the range of 3 μm to 50 μm for n-pentane emulsion, 2.5 μm to 60 μm for n-hexane emulsion and 1.2 μm to 30 μm for n-heptane emulsion. Oil droplets appear to be more compact, evenly spaced, and come in a range of sizes. This might be the result of the surfactant adhering to the oil droplet, as a result stabilizing the oil droplet [41]. The presence of natural surfactants used at CMC, which further aid in micelle formation and emulsify the paraffin oils, is responsible for the dense packing of oil droplets [237]. This could also be understood by the presence of surfactants (due to chemical structure), causes paraffins to emulsify [4]. Primarily, small size oil droplets are evenly distributed throughout the analyzed area (Figure 5.5a, 5.5b, 5.5c) and gradually tends to get bigger over time as shown in Figure 5.5(d-f). The small sized oil droplets eventually combine to form large sized droplets as a result of coalescence. Figure 5.5(d-f) illustrates that as the time passes, oil droplets of n-heptane emulsion are still smaller in size as compared to n-pentane and n-hexane emulsion. Consequently, it is clear that as time passes, there is a great chance of a droplet coalescence. When the interface is broken, two or more emulsion drops fuse together to form a single, larger drop and the process is irreversible. As previously mentioned, the interfaces interact and start to deform when large drops get closer to one another

without any background electric field. The formation of a plane parallel thin film may be primarily dependent on the rate of thinning, which in turn affects the emulsion's overall stability [158].

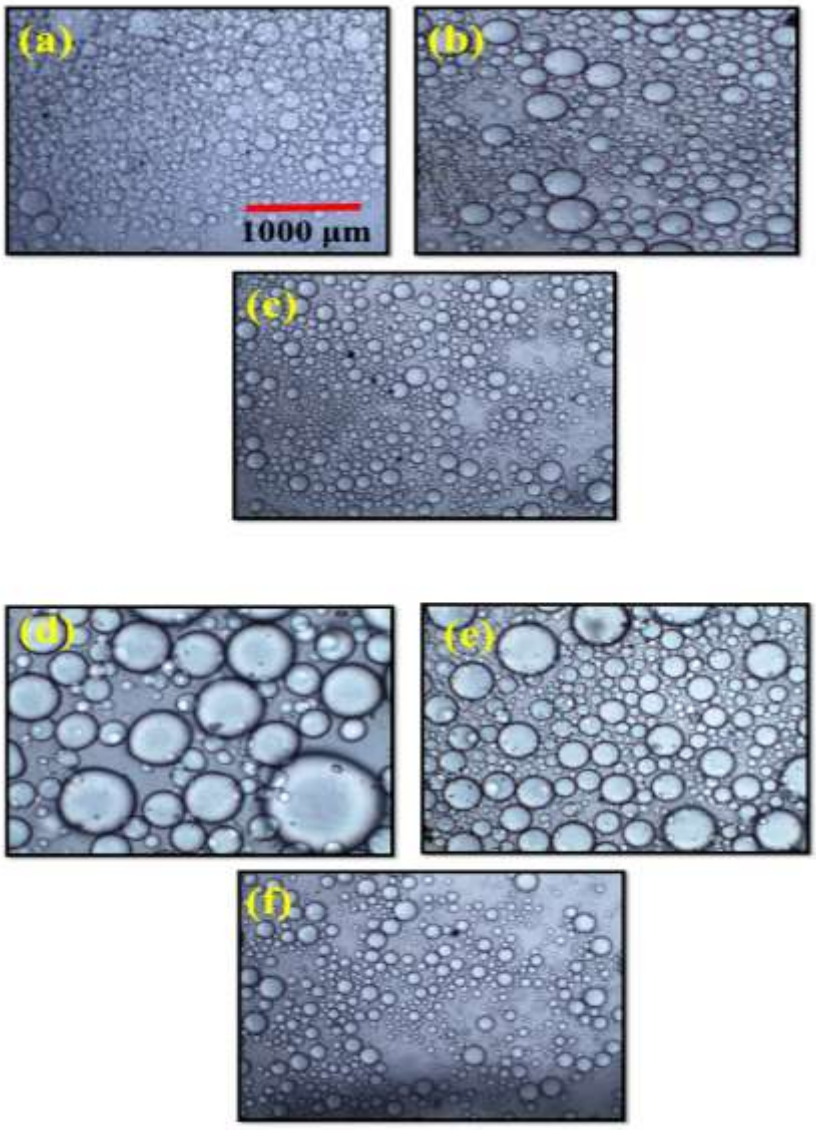

Figure 5.5: Microscopic images of freshly prepared emulsion (a) n-pentane emulsion (b) n-hexane emulsion (c) n-heptane emulsion and time-based microscopic images of prepared emulsion after 48 h (d) n-pentane emulsion (e) n-hexane emulsion and (f) n-heptane emulsion. All the tests were conducted at 30˚C and surfactant used at CMC (0.2 wt%).

Microscopic studies were also performed for emulsions at elevated temperature to analyze their thermal stability as show in Figure 5.6.

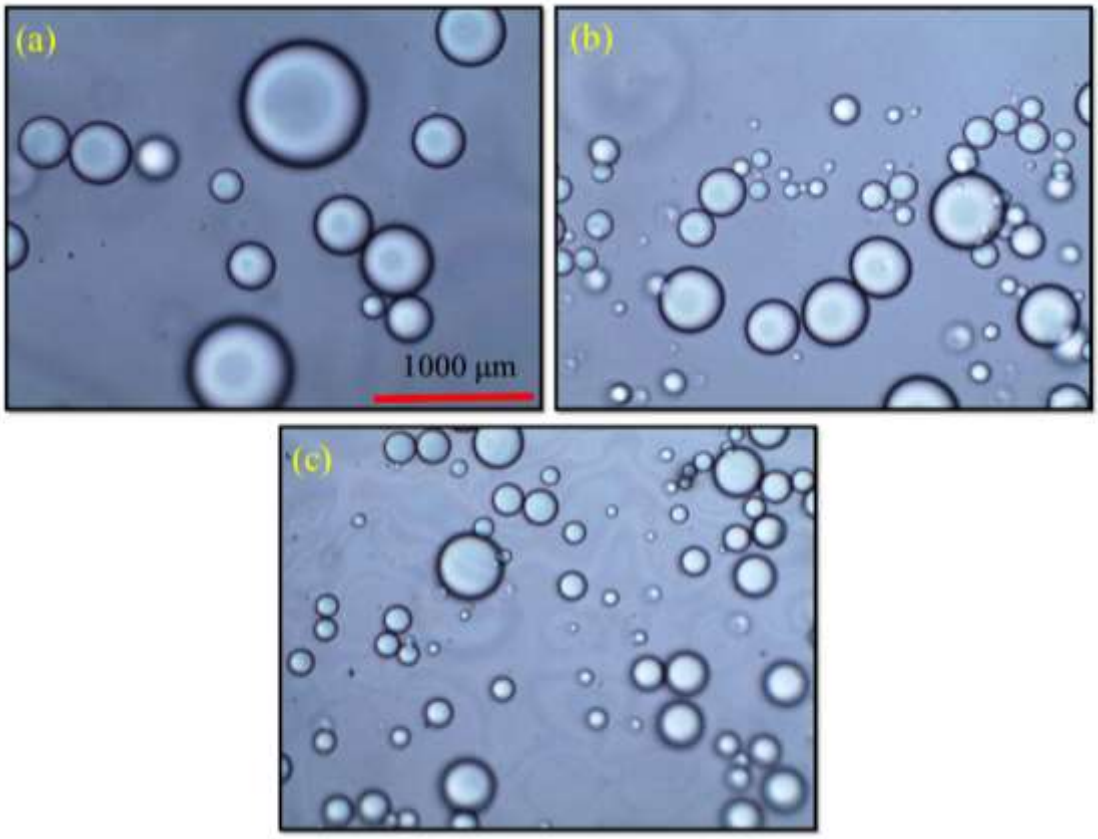

Figure 5.6: Optical micrograph of prepared emulsion at elevated temperature (a) n-pentane emulsion (b) n-hexane emulsion and (c) n-heptane emulsion. All tests were recorded at 90˚C and coalescence of oil droplet was observed.

From Figure 5.6, it is evident that more coalescence was observed in n-pentane emulsion at higher temperature whereas in n-hexane emulsion, less oil droplet coalescence can be observed as compared to former. Also, the size and number of oil droplet is higher in n-hexane emulsion that that of n-pentane emulsion. Furthermore, n-heptane emulsion possesses better thermal stability than n-pentane and n-hexane emulsion as the number of oil droplets are more, as well as are smaller

in size. These findings are aligned with the IFT measurements where lowest value of IFT was observed for n-heptane and is favorable for mobilizing oil.

5.3.4 Rheological studies

While using an emulsion in subsurface areas, its flow behavior is crucial. Any emulsion system's stability and flow pattern should be considered when preparing it for effective and potential applications in porous media. Numerous mechanisms, such as surfactant adsorption and mechanical trapping, occur when injecting emulsions into porous media. These mechanisms further limit the potential application of the emulsion because they alter its fluid properties. Since surfactant adsorption typically takes place in monomer form, the rheological behavior of emulsions must be examined. All the prepared emulsion system tends to exhibit a non-Newtonian shear thinning profile, which is in accordance with previous research finding [158,272] showing pseudo plastic behavior. High value of viscosity was observed in all emulsion systems at lower shear rates. The viscosity of the n-pentane emulsion was 1179.8 mPa.s at a shear rate of 1 s^{-1}, and then it drastically decreased to 26.961 mPa.s at a shear rate of 1000 s^{-1}. Similar to this, n-hexane and n-heptane emulsions showed a significant reduction in viscosity from 2872.1 mPa.s and 1489 mPa.s at 1 s^{-1} to 29.168 mPa.s and 24.204 mPa.s at 1000 $s^{-1}$and leads to 98.9% and 98.3% reduction, respectively as reported in our previous study [272]. The viscosity of the emulsion was found to decrease as the shear rate increased because the emulsion molecules tend to break down and provide less resistance to the spindle's rotation [238]. Based on the data presented above, n-heptane emulsion has a better shear thinning profile than n-pentane and n-hexane. The lowest value of viscosity attained by n-heptane emulsion (24.204 mPa.s) suggests that this is least impacted by shear deformation and may be the result of the synergistic interaction between n-heptane and SP

solution. As reported in our previous study, the natural surfactant used in this investigation was anionic in nature [30]. This may contribute in emulsion stability, as shown by microscopic studies, where the surfactant micelles covering the oil droplet possess a repulsive energy barrier.

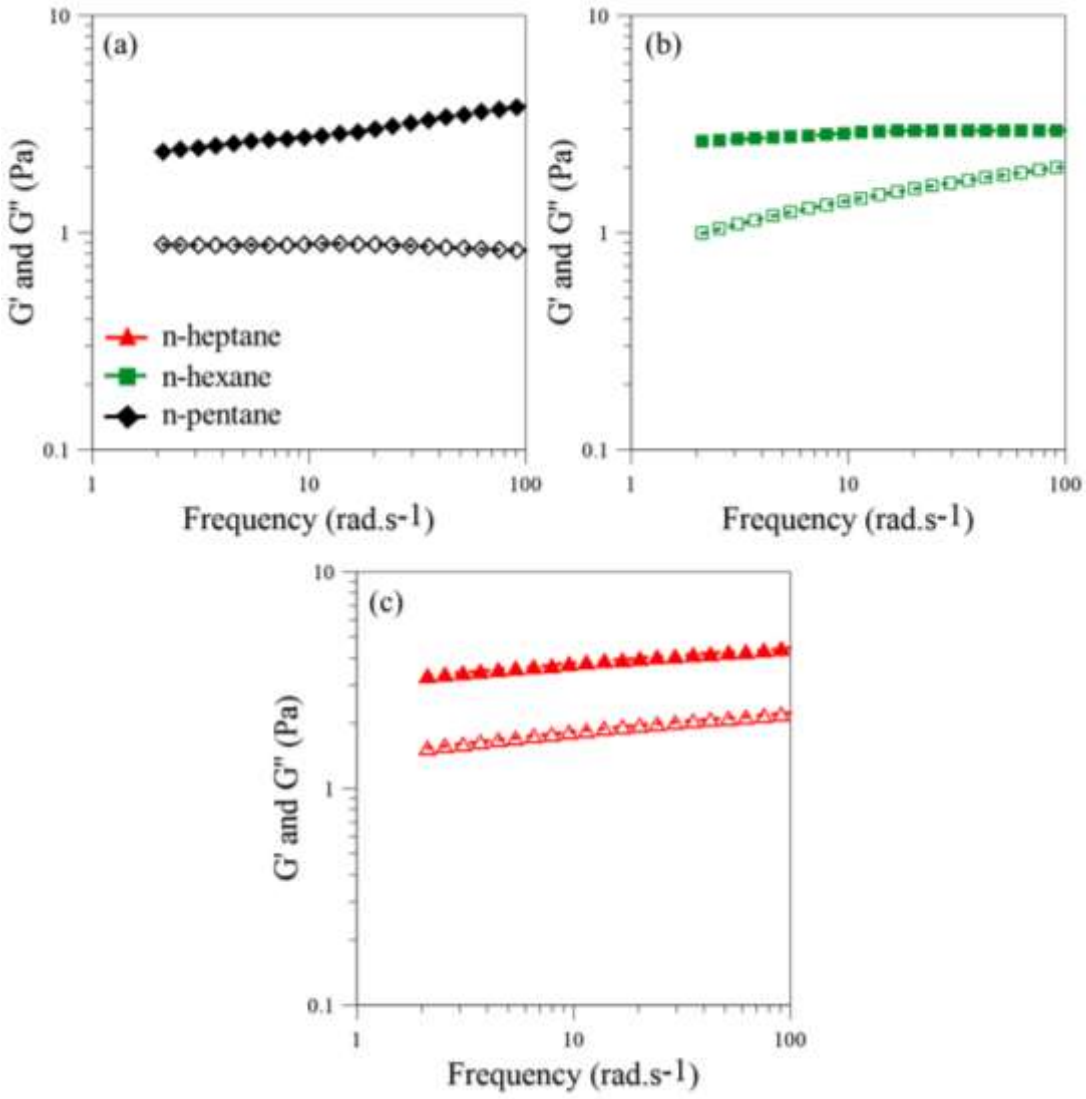

Figure 5.7: Frequency sweep analysis of prepared emulsions (a) n-pentane (b) n-hexane and (c) n-heptane emulsions. Solid symbols represent G′ (elastic modulii) and hollow symbols represent G″ (viscous moduli). These tests were performed at 30˚C.

Furthermore, it was anticipated that the dynamic rheological characteristics of the emulsion samples would yield outcomes like those of the shear rheological analysis. Frequency-sweep analysis was used to examine the dynamic rheological response of emulsions stabilized by natural surfactant at 30˚C (Figure 5.7), 60˚C (Figure 5.8) and 90˚C (Figure 5.9).

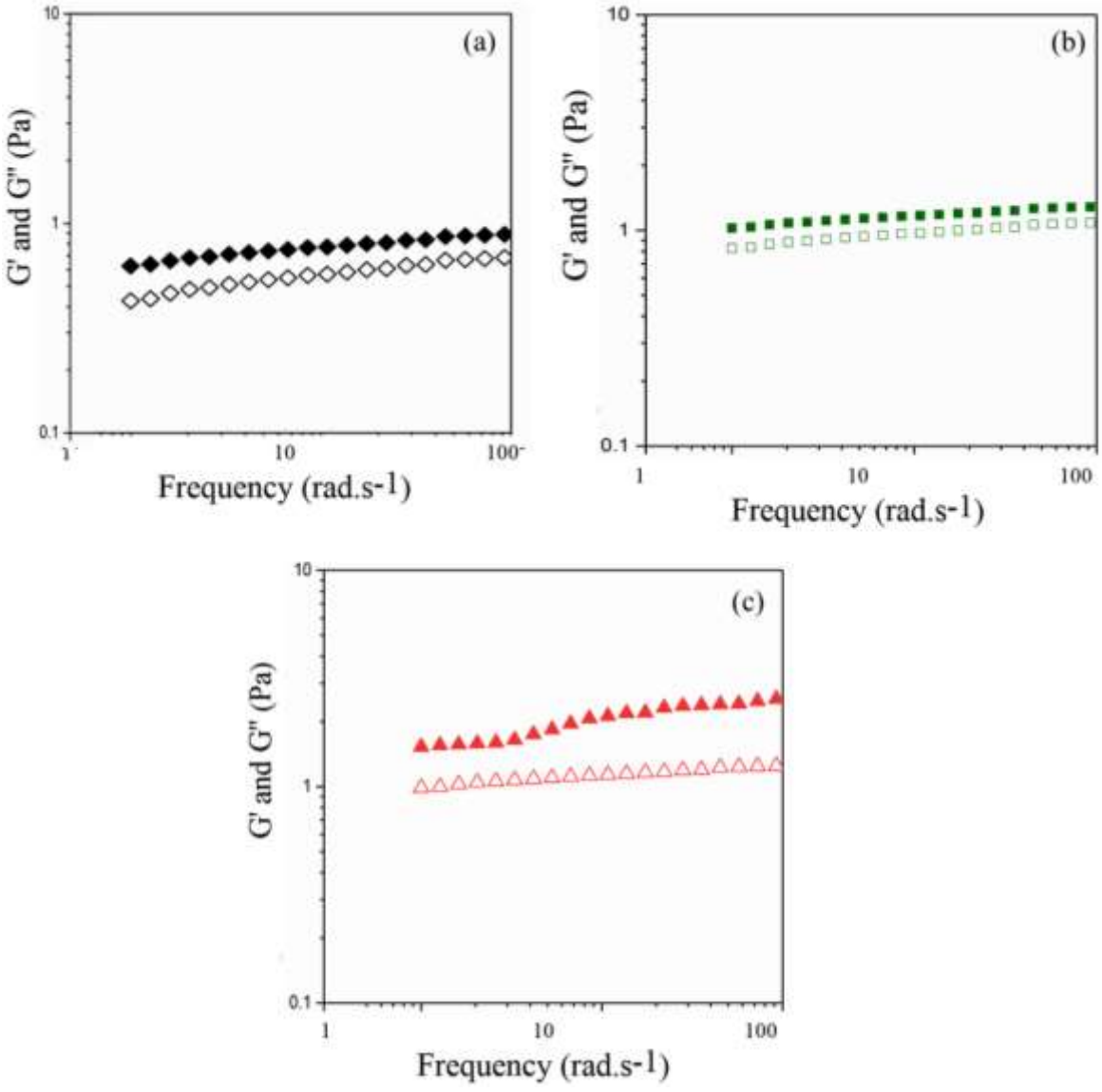

Figure 5.8: Frequency sweep analysis of prepared emulsions (a) n-pentane (b) n-hexane and (c) n-heptane emulsions. Solid symbols represent G′ (elastic moduli) and hollow symbols represent G″ (Viscous moduli). These tests were performed at 60˚C and ambient pressure.

At 30 ˚C, the n-pentane emulsion stabilized by natural surfactant at CMC value had a G′ value (2.3 Pa) that was higher than G″ (0.85 Pa) at 2.02 rad/s (Figure 5.7a). G′ was found to increase with increasing angular frequency, suggesting that an elastically dominant structure was formed between the SP solution and n-pentane. The n-pentane emulsion showed a G″ plateau over the frequency investigated, with the value of G″ hardly increasing. The G′ value (2.62 Pa) of the n-hexane emulsion stabilized by natural surfactant at CMC value was higher than G″ (0.92 Pa) (Figure 5.7b). The G′ value (3.06 Pa) of the n-heptane emulsion stabilized by natural surfactant at CMC value was higher than G″ (1.65 Pa) (Figure 5.7c). At 60 ˚C, the n-pentane emulsion had a G′ value (0.627 Pa) that was higher than G″ (0.42 Pa) at 2.02 rad/s (Figure 5.8a), for n-hexane emulsion G′ value (1.02 Pa) that was higher than G″ (0.82 Pa) (Figure 5.8b) and for n-heptane emulsion G′ value (1.527 Pa) that was higher than G″ (0.987 Pa) (Figure 5.8c). The storage modulus measures the elastic behavior of a material. When the value of G′ is significantly higher than the loss modulus (G"), it indicates that the material is exhibiting more solid-like behavior [273,274]. When the solid-like nature of a fluid dominates over its liquid-like nature, it typically means that the material exhibits more elastic behavior than viscous behavior. In other words, the material behaves more like a solid than a liquid under certain conditions. Frequency sweep analysis was also conducted at elevated temperature (90˚C) and shown in Figure 5.9. It was observed that for n-pentane emulsion G′ and G″ value was approximately aligned with each other that is ~ 0.45 Pa (Figure 5.9a) and similar observation was recorded for n-hexane emulsion where the value of G′ and G″ was ~0.72 Pa (Figure 5.9b). For n-heptane emulsion the value of G′ (0.85 Pa) was higher than that of G″ (1.8 Pa) as shown in Figure 9c. Materials with dominant solid-like behavior may exhibit characteristics like gels, such as forming a stable structure or resisting flow over time.

When subjected to deformation, materials with solid-like behavior tend to recover their original shape after the stress is removed, similar to how a solid behaves [163].

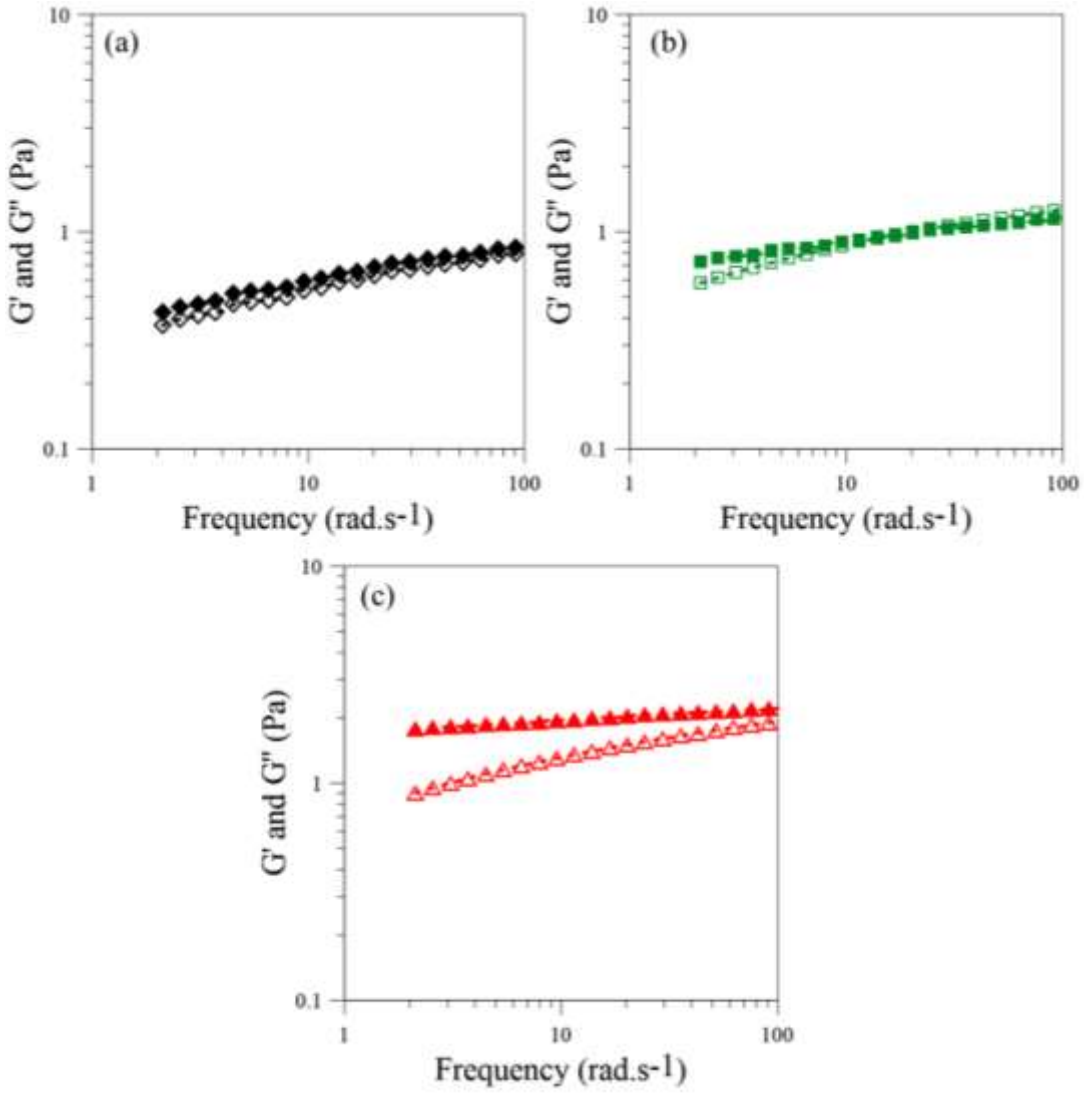

Figure 5.9: Frequency sweep analysis of prepared emulsions (a) n-pentane (b) n-hexane and (c) n-heptane emulsions. Solid symbols represent G′ (elastic modulii) and hollow symbols represent G″ (Viscous moduli). These tests were performed at 90˚C and ambient pressure.

This tendency to deform and recover their original shape, helps the emulsions access constricted pores in the reservoir, displacing oil and on bypassing the constrained pores, recover its original shape.

5.3.5 Dilution analysis

Emulsion formation is a frequently occurring phenomenon that occurs due to the interaction between the injected and produced fluids [275]. The stability of the emulsion formed within reservoir and the impact of the salinity of the injected water on the stability of emulsion needs to be assessed. The present study used microscopic results to examine how aqueous phase salinity affected emulsion stability. For this, saline solution as that of Cambay basin was prepared and diluted in 10 ml of emulsion (n-pentane, n-hexane and n-heptane separately) in the varying ratio (saline solution: emulsion), for say, 1:5, 2:5, 3:5, 4:5 and 1:1. Every test was performed at ambient conditions. Microscopic observation was performed for each of the diluted samples and shown in Figure 5.10 and Figure 5.11. The average size was in the range of 8 µm to 70 µm for n-pentane emulsion (1:5), and as the salinity increases from 2:5 to 1:1, bubble coalescence was observed, as a result large size droplet and a smaller number of droplets can be seen in Fig 5.10. Similarly, the average size was in the range of 2 µm to 40 µm for n-hexane emulsion (1:5) and 5 µm to 50 µm for n-heptane emulsion (1:5). Thereafter, with increase in dilution, coalescence of droplet was observed as shown in Fig 5.11. Emulsion behavior and stability in water-in-oil emulsions have been studied and the results indicate that the emulsion becomes less stable as the percentage of dilution increases within emulsion. From Figure 5.10 (dilution in n-pentane), it was evident that fairly packed oil droplet was present in case of 1:5. As the dilution increases to 2:5, coalescence of oil droplet was observed as large sized droplet was fairly packed over the area

analyzed. In case of dilution of 3:5, emulsion seems to lose its stability due to presence of few and large sized oil droplet, as a result of coalescence.

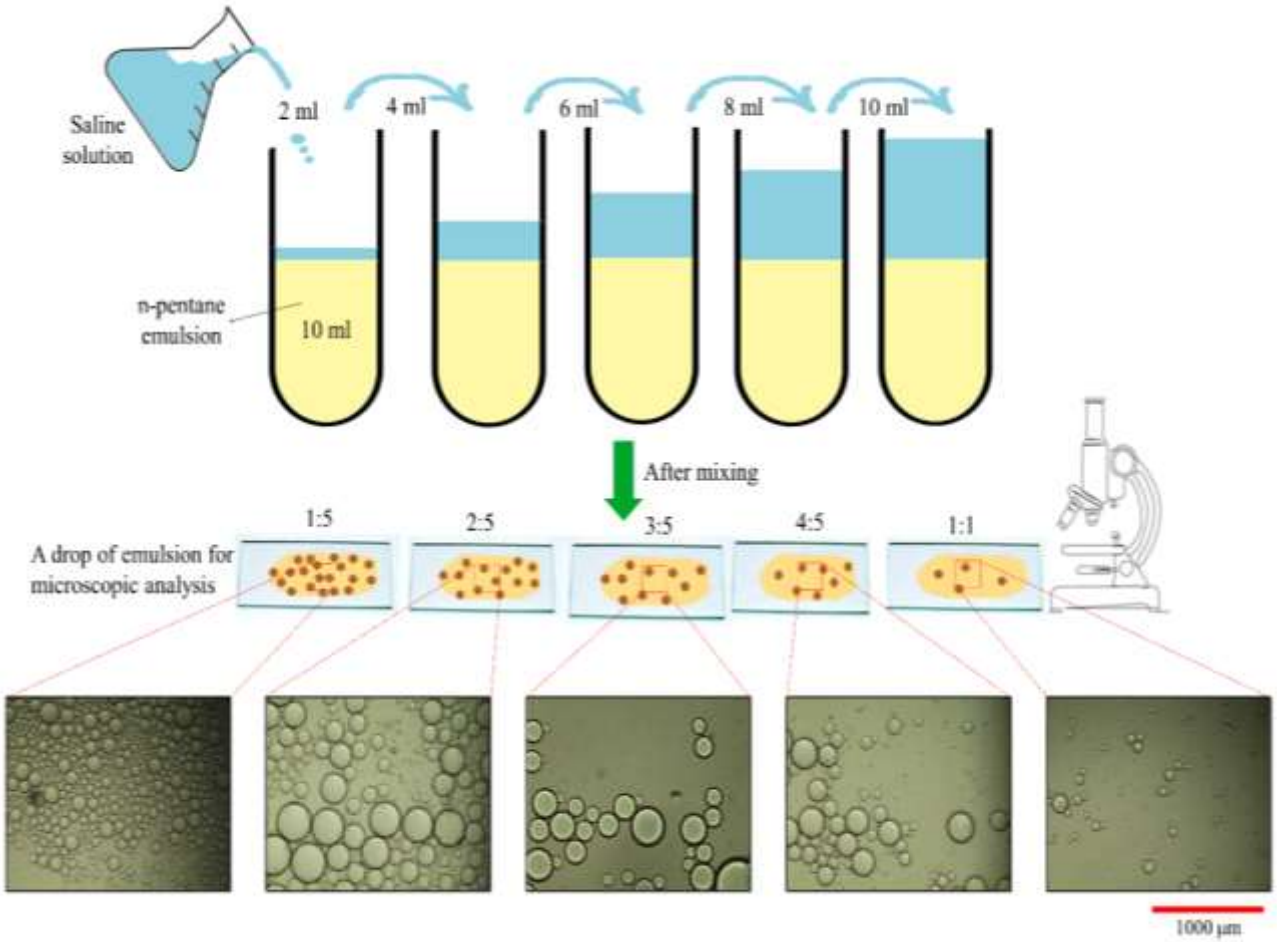

Figure 5.10: Schematic representation of dilution studies conducted for n-pentane emulsion. The ratio for dilution was varied from 1:5 to 1:1 and optical micrograph was recorded for each set of diluted emulsions.

Similar pattern was observed for 4:5 dilutions and finally at 1:1 dilution emulsion seems to destabilize completely as very few droplets of oil was observed during microscopic analysis. The coalescence step may be considered instantaneous, as suggested by a number of authors [276–278]. It is emphasizing that the two parameter governing in the phase separation are film drainage

and film strength [48]. However, regardless of how densely packed it appears in the micrograph, the emulsion with the smallest dilution shows limited coalescence. Similar dilution studies were conducted for n-hexane and n-heptane emulsion and their microscopic observation are shown in Figure 5.11.

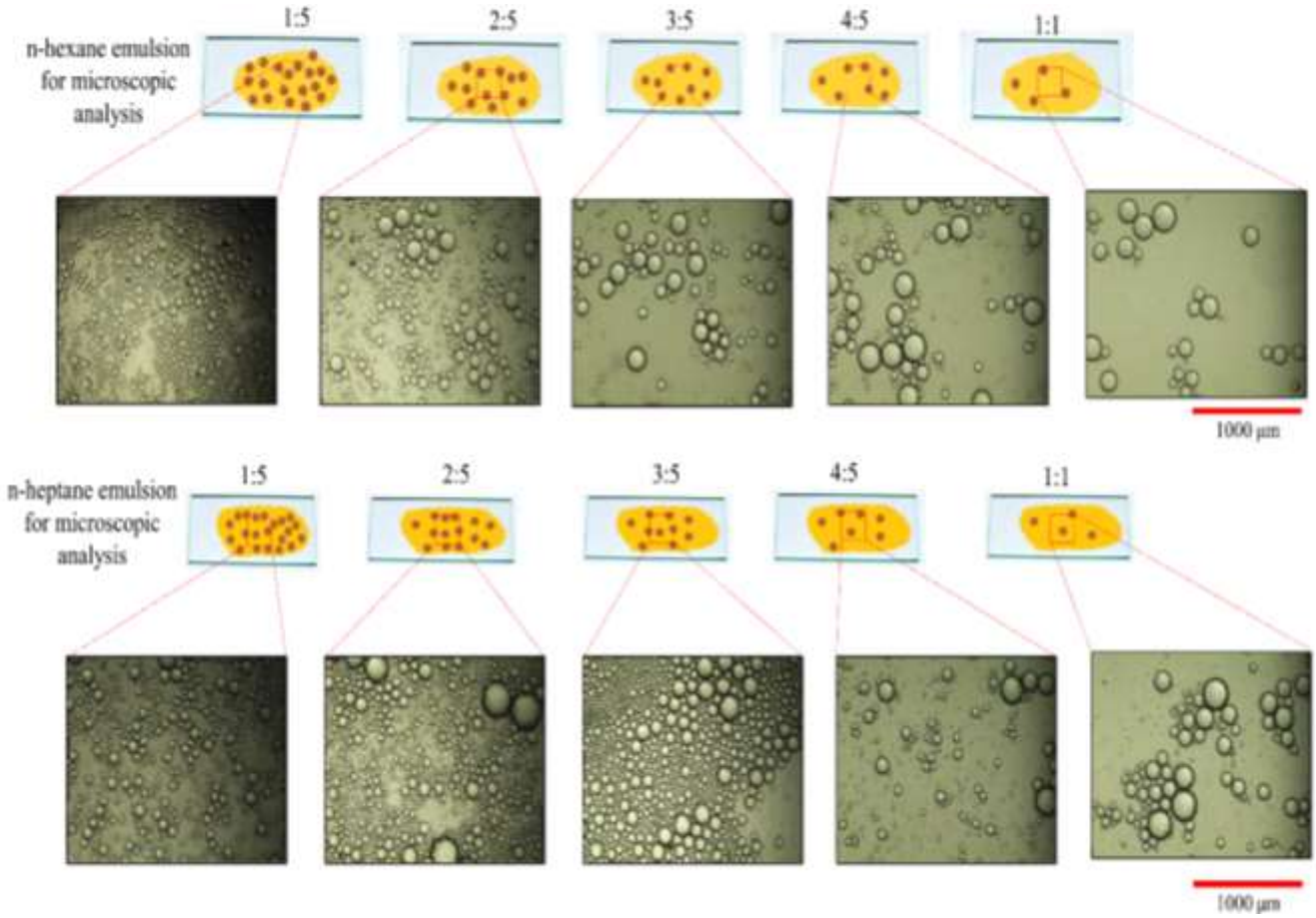

Figure 5.11: Optical micrograph of dilution analysis for n-hexane and n-heptane emulsion. Dilution ratio of saline solution and emulsion was varied from 1:5 to 1:1.

Microscopic observation of dilution in n-hexane emulsion was quite aligned as that of microscopic results of n-pentane dilution, as coalescence of oil droplet was observed from 2:5 and dominated in preceding dilutions. Microscopic analysis of dilution in n-heptane emulsion seems to be stable till ratio of 3:5 as moderately packed oil droplets were observed. Whereas, at dilution

ratio of 4:5 and 1:1, emulsion tends to destabilize and is evident from microscopic result, due to presence of large sized oil droplet. Performance of n-heptane emulsion was better than n-pentane and n-hexane emulsion and is fairly aligned with the IFT, rheological and microscopic results reported above. In emulsions, droplets are often stabilized by electrical charges that create repulsion between droplets, preventing them from coalescing. Adding salt (increasing salinity) can screen these electrostatic charges, reducing the repulsive forces between droplets. This can lead to increased droplet coalescence and a less stable emulsion. Furthermore, the presence of salts increases the ionic strength of the solution, which can affect the stability of emulsifying agents, such as surfactants. High ionic strength can lead to the collapse of the electrical double layer around the droplets, again promoting coalescence and phase separation. These findings are in line with literature study reported by Moradi et al. [158,159,279] who investigated the effect of salinity on the stability of w/o emulsions and showed that stability decreased as salinity increased. Few studies have examined the effect of water salinity on emulsion stability, and concludes that w/o emulsion stability can be enhanced by reducing water salinity and ionic strength up to a certain point [279–281].

5.3.6 Pore scale visualization

Through pore-scale analysis, microfluidics is gaining a lot of attention because it helps in visualizing the surfactant's potential for oil displacement. Traditionally, surfactant flooding is carried out in sand pack and core samples to ascertain the potential of surfactant [159,234,248,282]. While the laboratory sand pack and core samples closely resemble the rock formation, it is difficult to make real-time visual observations [250]. The micromodel setup, which utilizes glass microfluidic channels to simulate reservoir conditions, offers several advantages for evaluating oil recovery processes compared to traditional macroscopic experiments. Scale

Representation: Micromodels provide a scaled-down representation of reservoir rock formations, allowing researchers to observe and analyze fluid flow and displacement processes at the pore scale. This enables a more accurate depiction of the complex multiphase flow phenomena that occur in subsurface reservoirs. Glass microfluidic channels enable high-resolution imaging techniques such as microscopy which allow researchers to visualize fluid displacement and oil recovery processes in real-time, providing detailed information about pore-scale phenomena such as fluid trapping, mobilization, and displacement efficiency. Micromodel experiments facilitate quantitative analysis of fluid behavior and oil recovery performance metrics such as recovery factor, sweep efficiency, and residual oil saturation. This quantitative data enables researcher to assess the effectiveness of different recovery methods and compare the performance of various surfactants or additives.

Compared to field-scale experiments [283] or numerical simulations, micromodel experiments are relatively cost-effective and less time-consuming. Researchers can conduct multiple experiments under controlled conditions, allowing for rapid testing and optimization of oil recovery processes. Overall, the micromodel setup offers a more viable and efficient platform for evaluating oil recovery processes by providing a scaled-down, controlled environment for studying pore-scale phenomena. The visualization capabilities of micromodel experiments enhance our understanding of fluid flow dynamics in subsurface reservoirs and can contribute to the development of more efficient and sustainable oil recovery techniques. Numerous microfluidic investigations have been published in the literature studies, confirming our increased comprehension of the mechanism involved in surfactant flooding [251–253]. This work explores the microscopic analysis of oil (n-pentane, n-hexane and n-heptane) displacement through surfactant flooding. The microfluidic chip was originally flooded with brine, which has a salinity

like that of the Cambay basin and has characteristics of traditional oilfield formations. Brine was flooded in the chip until it reached most of the pore channels. This was followed by taking a microscopic image of the microfluidic chip from the inlet to the outlet as shown in Figure 5.12. To provide a clearer picture and comprehension of the uniform dispersion of brine, certain pore channels have been enlarged.

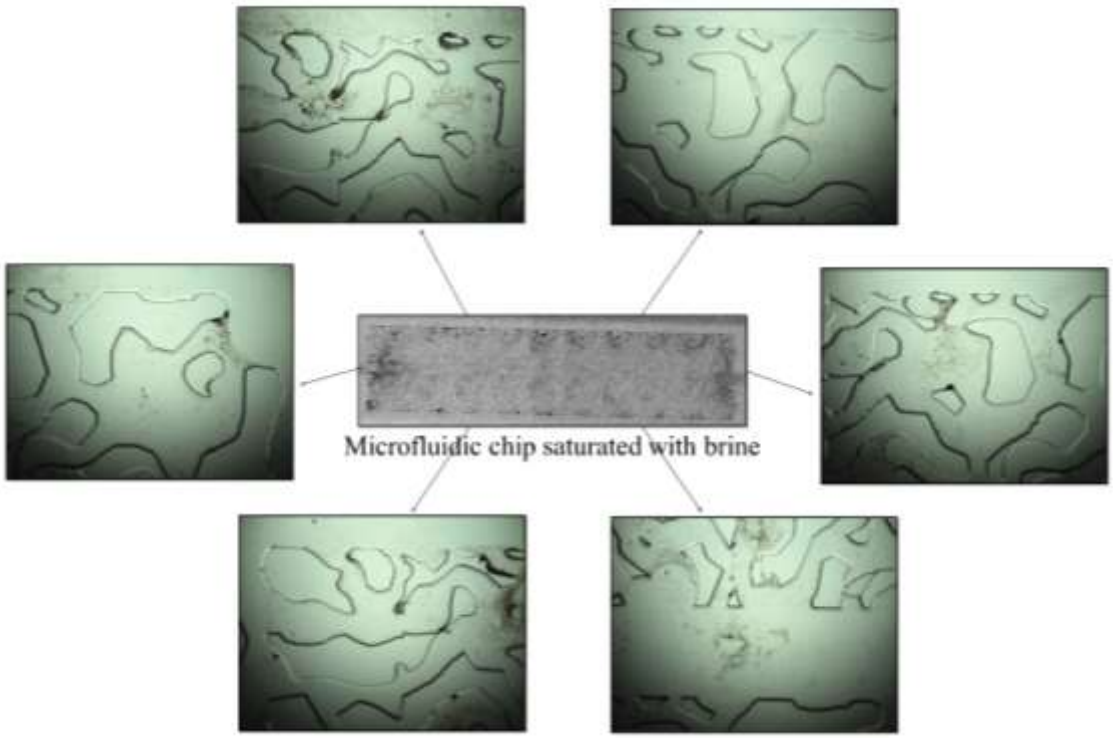

Figure 5.12: Optical micrographs of glass micromodel flooded with brine solution. The salinity of brine was kept equivalent to Cambay basin and no air bubble was encapsulated.

It can be seen from Figure 5.12 that there was no encapsulated air bubble within the pores. This was followed by the injection of n-pentane followed by flushing out of brine as shown in Figure 5.13a. The uneven distribution of the oil can be clearly seen by enlarging the view of the encapsulated oil at certain pore channels. A potential reason for the uneven oil distribution could be that some of the microfluidic setup's restricted pores are closed off to oil. To assess the natural

surfactant's potential for oil displacement, the surfactant was lastly flooded into the microfluidic chip that had been saturated with oil. The optical micrograph of microfluidic chip after the surfactant injection are shown in Figure 5.13b from the inlet to the outlet. Figure 5.13b, clearly entails that natural surfactant has shown its enormous potential in dislodging all the encapsulated oil (n-pentane).

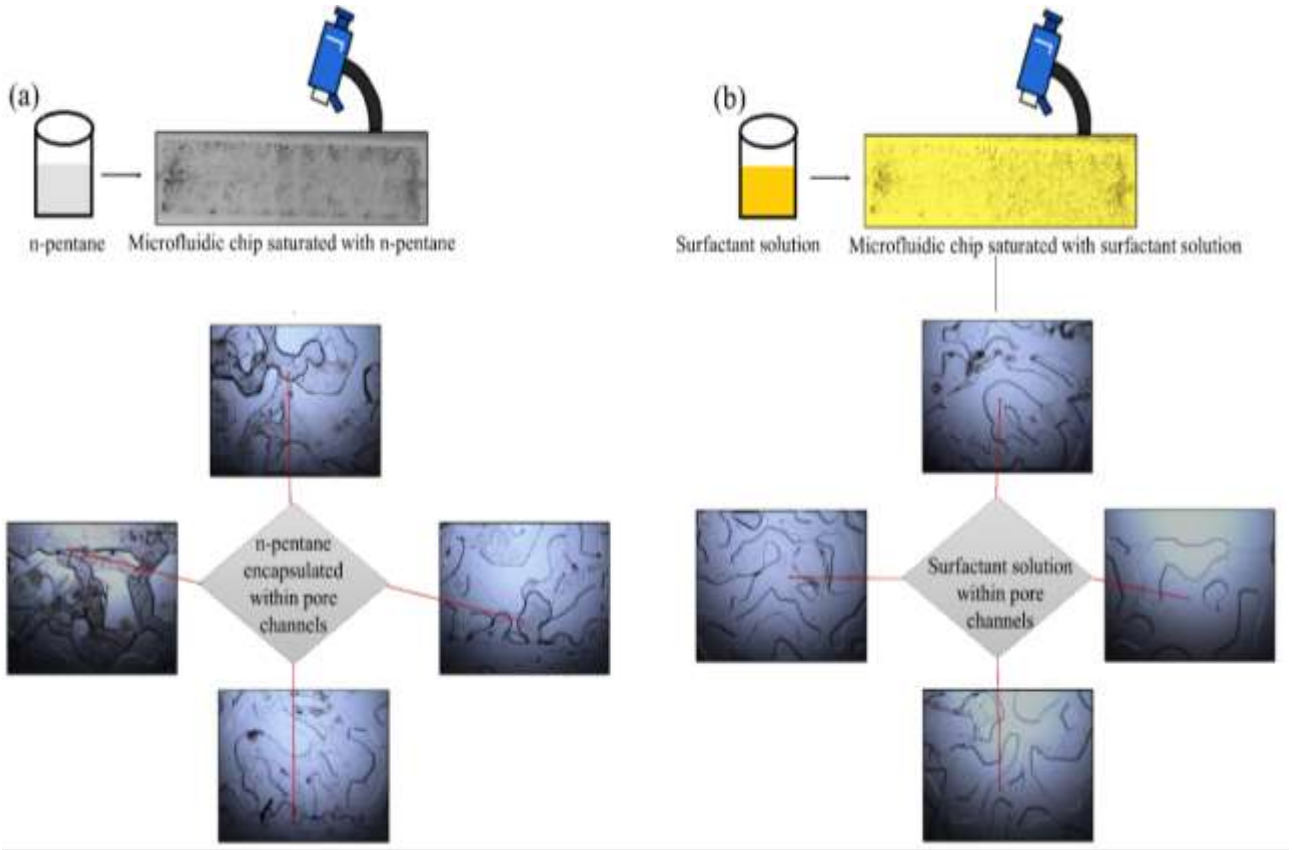

Figure 5.13: Optical micrographs of glass micromodel flooded with n-pentane (a) where trapped oil within pore channels can be clearly visualized and thereafter flooded with (b) surfactant solution.

Figure 5.13b shows enlarged view of a few pore channels shows that surfactant solution has been distributed throughout the microfluidic chip following oil displacement. Later, same set of experiments was performed for n-hexane followed by surfactant solution to visualize the

interaction between n-hexane and surfactant. For this, initially n-hexane was flooded in microfluidic chip and enlarged section of the trapped n-hexane within chip is shown in Figure 5.14a. Uneven distribution of n-hexane is quite similar as that observed for n-pentane. To visualize the surfactant potential, surfactant solution was flooded in microfluidic chip, as a result it tends to mobilize the trapped oil within the pore channels. Mobilizing of oil was done by means of emulsification and is clearly evident from the enlarged micrographs as shown in Figure 5.14b.

Lastly, the surfactant potential was visualized for its synergetic interaction with n-heptane within the micro channels of the chip. For this, microfluidic chip was initially saturated with n-heptane and trapped oil can be clearly seen in Figure 5.14c by means of optical micrograph taken after injection of n-heptane. The distribution of n-heptane was uneven and quite similar to that of the former one (n-pentane and n-hexane in Figure 5.13a and Figure 5.14a). This was followed by the injection of surfactant solution into microfluidic chip to visualize the surfactant potential. As a result, the trapped oil (n-heptane) in the pore channels tends to get mobilized. Also, it is quite imperative to visualize the emulsification within the pore channels of the chip as that observed in case of n-hexane. The surfactant solution displaces the oil and emulsification of n-heptane can be clearly seen as shown in Figure 5.14d. Moreover, emulsification in case of n-heptane was comparatively more than that in case of n-hexane. This may be attributed and aligned with the IFT results shown in Figure 5.4b and entails that lower IFT value is highly preferable for dislodging the oil. This could be explained by the different mechanisms that natural surfactants within the pores possess, such as IFT reduction, changing wettability, and emulsification, all of which are thoroughly explained in our previous research work [30,229,254]. Natural surfactants derived from agricultural products play a crucial role in enhancing oil recovery through their unique mechanisms.

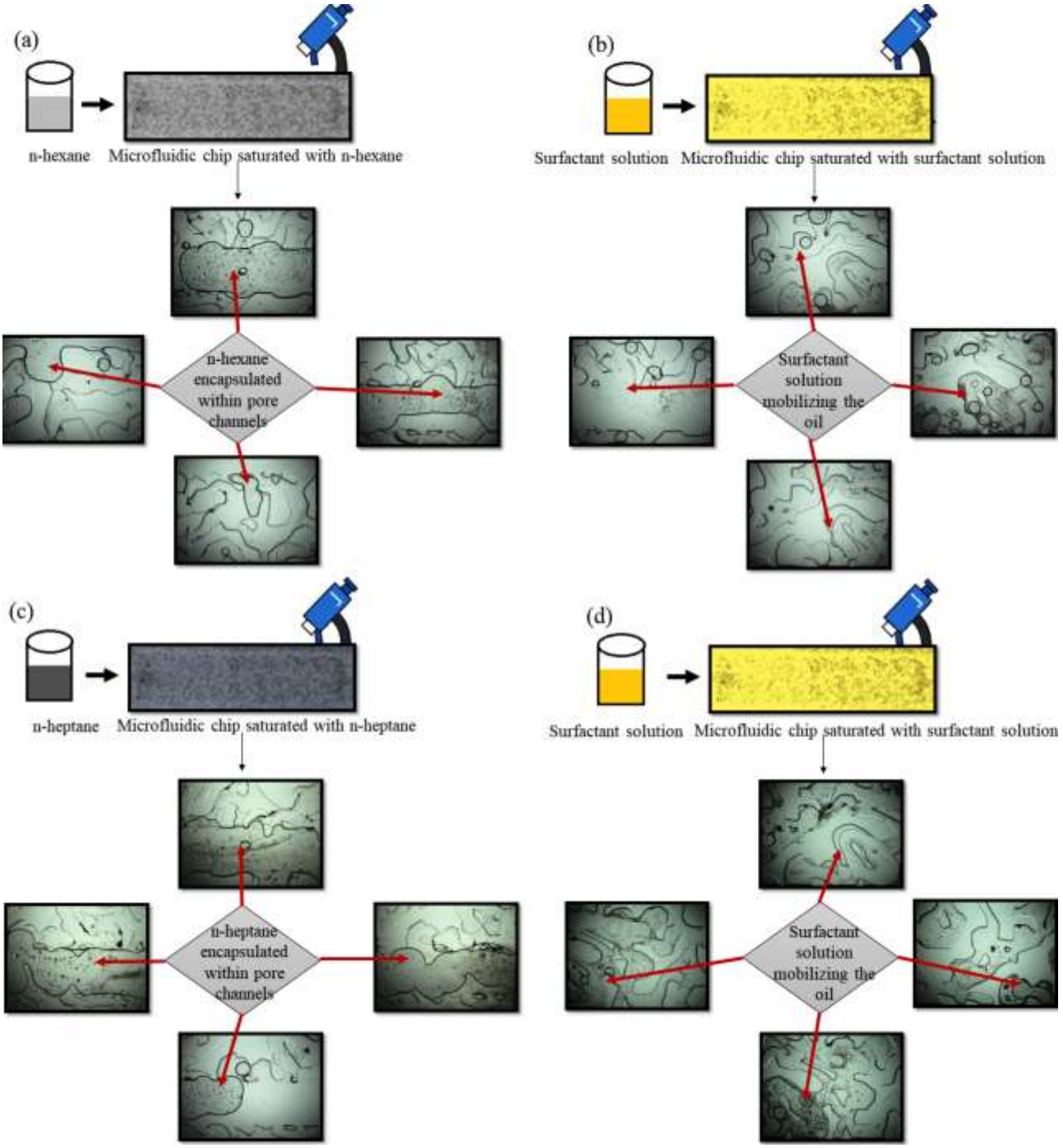

Figure 5.14: Microscopic view of glass micromodel flooded with n-hexane and n-heptane (in a and c respectively) where trapped oil within pore channels can be clearly visualized and thereafter flooded with surfactant solution (in b and d respectively) where surfactant solution emulsifying and mobilizing the trapped oil can be seen.

These natural surfactants reduce the interfacial tension between oil and water, thereby facilitating the displacement of oil trapped in reservoirs. These surfactants contain molecules that possess hydrophilic and hydrophobic ends, allowing them to effectively mobilize oil. Additionally, they can alter the wettability of the reservoir rock surfaces, making them more water-wet and promoting oil flow. The use of natural surfactants not only enhances oil recovery efficiency but also offers an eco-friendly and sustainable alternative to synthetic surfactants.

5.4 Conclusion

In conclusion, the evaluation of natural surfactants derived from agricultural products for oil recovery studies from a micromodel filled with paraffinic oil demonstrates promising results. The experiments conducted revealed that the natural surfactants exhibit competitive performance in reducing IFT at the interface of oleic phase and aqueous surfactant solution, that is, 14.2mN/m for n-pentane, 10.92mN/m for n-hexane and 9.8mN/m for n-heptane. Microscopic results showed n-heptane emulsion offered higher stability as compared to n-pentane and n-hexane emulsions and also modifying viscosity compared to conventional commercial surfactants. Additionally, oil mobilization studies conducted in the micromodel indicate the effectiveness of natural surfactants in enhancing oil recovery efficiency from paraffinic oil reservoirs. Lastly, dilution studies conducted demonstrates that, among three explored emulsions in this study, n-heptane emulsion offers higher stability till the dilution ratio of 3:5. These findings suggest that natural surfactants derived from agricultural products hold significant potential as sustainable alternatives for improving oil recovery processes in petroleum reservoirs. The utilization of renewable and environmentally friendly surfactants aligns with the industry's growing emphasis on sustainable practices and reduced environmental impact. Furthermore, the successful application of natural surfactants in enhancing oil recovery efficiency highlights the importance of exploring and

harnessing natural resources for innovative solutions in the petroleum industry. Moving forward, further research and development efforts should focus on optimizing the formulation and application of natural surfactants, considering factors such as scalability, compatibility with reservoir conditions, and cost-effectiveness. By continuing to explore the potential of natural surfactants, the petroleum industry can contribute to advancing sustainable practices and addressing environmental concerns while enhancing oil recovery efficiency.

Chapter 6

Hybrid Emulsion with Enhanced Thermal Properties Using Silica Nanoparticles and Plant-Derived Surfactants

Abstract

Emulsion-based systems offer a sustainable approach for enhancing fluid control and transport in subsurface environments, owing to their effectiveness in flow resistance, structural confinement, and interfacial modulation. However, the long-term stability of these emulsions is critical for ensuring reliable performance in practical mechanical and environmental applications. In this work, a novel formulation is reported for emulsions wherein they have been stabilized by natural surfactant extracted from fenugreek seed. In this work, two emulsion systems are reported, that is surfactant polymer and nanoparticle-surfactant-polymer emulsion. Surfactant-polymer emulsions are stabilized by natural surfactant whereas nanoparticle-surfactant-polymer emulsion are stabilized in presence of nanoparticle and natural surfactant. Both the emulsions exhibit shear thinning profile as observed from rheological studies. Nanoparticle-surfactant-polymer emulsions were found to be thermally stable than that of Surfactant-polymer emulsions as evident from microscopic and rheological studies. An increase in temperature has the unfavorable impact on surfactant-polymer emulsion as huge drop in viscosity profile was observed. The viscosity profiles of nanoparticle-surfactant-polymer emulsions were found to be best fitted by the Krieger-Dougherty model with the value of coefficient correlation $R^2 = 0.99$. The contact angle studies showed that NSP solution can reduce the contact angle to much lower value, which is 111˚ to 30˚

whereas surfactant-polymer solution was able to reduce from 116˚ to 57˚ only. Adsorption of silica nanoparticle was also observed in presence of sandstone and decrease in 27.32% of peak absorbance was observed in span of 20 days. Therefore, finding of the study indicates that nanoparticle-surfactant-polymer emulsions has potential to perform better than surfactant-polymer emulsions, even at elevated temperature, and can be a better and cost-effective alternative to the conventional emulsions used in thermal fluid applications in mechanical and subsurface systems.

6.1 Introduction

In thermal fluid transport systems involving porous media, water-based injection methods are often employed to enhance bulk fluid movement and improve sweep efficiency. However, due to the relatively low viscosity of water compared to other phases, its higher mobility can result in inefficient displacement [284]. Therefore, high molecular weight polymers are introduced to increase fluid viscosity, thereby reducing the mobility ratio and promoting more uniform heat and mass transfer. Polymers such as polyacrylamide (PAM) and partially hydrolyzed polyacrylamide (HPAM) are commonly used to improve the rheological properties of thermal fluids, particularly in heterogeneous or structurally complex flow environments [164,285]. Both have been widely used as thickening agents, even in reservoirs of high heterogeneity. While polymer-enhanced fluids offer substantial improvements in flow regulation and thermal distribution, the addition of surface-active agents (surfactants) can further optimize performance. These surfactants modify interfacial behavior, improving phase interaction and contact with solid surfaces within the system. By reducing interfacial tension, they lower the capillary resistance and enhance displacement efficiency, enabling better thermal penetration and energy delivery [286]. Surfactant plays vital role where residual oil is not able to be displaced due to the requirement of high energy, which can overcome the capillary pressure at nominal oil-water IFT [222]. It is due to the fact that, when IFT

is decreased, capillary number will significantly increase, which favors the displacement of oil. Various surfactants viz., alkoxy carboxylate, internal olefin sulfonate (IOS), alkoxyglycidylether sulfonates (AGES), sodium dodecyl sulfate (SDS), cetrimonium bromide (CTAB) have been used along with polymer [58,287], however, these surfactants were synthetic in nature. Previous study, that delves into the comparison of natural surfactant extract (SNS) *vs*. synthetic surfactant (SDS), reported that natural surfactant should be recommended over conventional surfactant as both were showing comparable results [98]. Natural surfactants are now in trend because of its affordability and wide availability. Various works have been performed on natural surfactants and they have been proven to be the great alternative to synthetic surfactants in terms of IFT reduction (from 60% to 96%), wettability alteration and improved oil recovery (from 25% to 58%) [32,38,39,229]. In addition, surfactants promote rupturing of droplets as well as they reduce the droplet coalescence during emulsification of oil in water [288]. However, the synergistic interaction of surfactant-polymer, that leads to emulsification/stabilization of oil, becomes weak and unstable at elevated temperatures and salinity. It indicates that the strength of surfactant-polymer film should be enhanced by incorporating better surface-active agent, that not only stabilizes the droplet against coalescence (a stable emulsion) but also makes them least dependent on field conditions.

Nanoparticles (NPs) are ultra-fine particles (size between 1-100 nm), that possess attributes similar to that of surface-active agents. As a result, it is adsorbed at oil surface and interact with existing surfactant-polymer chains. It further stabilizes the emulsified droplets by reducing the coalescence rate, which in turn makes them favorable for application due to enhanced thermal, rheological and mechanical properties [289]. In addition to this, application of surface-active NP is gaining attention as they have ability to enhance the rheological properties and decrease adsorption of surfactants within reservoir. Thus, the addition of surface-active NP play a critical

role in reducing surfactant adsorption, which can improve surfactant potential to influence IFT within porous media [290]. The inclusion of surface-active NP along with surfactant-polymer offers numerous advantages such as higher diffusivity, smaller size, availability of large surface area even at elevated temperature and higher salinity [291]. Moreover, surface-active NP also offers more stable emulsion, which is due to the fact that surface-active NPs adsorb at liquid-liquid interface and thereby decreases the free energy of system [292]. It has been established that particles tend to attach to the interface at higher rate when surfactants are present in emulsion systems [293]. Even in our previous work [294], it was reported that an additional recovery of 4.71% was possible during emulsion flooding when emulsion of polymer (1000 ppm PAM) and surfactant (0.22 wt%, SDS) stabilized by 1 wt% NPs (SiO_2; 15 nm) at 13.6 MPa and 313 K. Further investigation reported that inclusion of SiO_2 NPs drastically stabilized the emulsion even at elevated temperatures, resulting surfactant-polymer emulsion exhibited additional stability of 23 d with droplet size of 2.16 μm [295]. Zhou et al. [296] prepared a nanofluid by electrostatic mixing of silica NPs (SiNP-NH_2) and anionic surfactant *e.g.,* Soloterra 964. The prepared nanofluid showed remarkable potential in reducing IFT by 99.85% with Bakken crude oil. Though conventional surfactants were widely used as emulsifying agent but the application of natural surfactant in stabilizing emulsion of crude oil is limited and only few studies reported the use of natural surfactant in oilfield applications. For example, Pal et al. [8] used natural surfactant (sodium ethyl ester sulfonate, 23.53 mmol/l as CMC) in the emulsification of crude oil with ratio of 1:1. It was found that emulsion exhibited stability of 21 d thereafter, phase separation occurred. Another study reported formation of o/w emulsion with natural surfactant (Q-naturale) and medium chain triglyceride (MCT) oil, where prepared emulsion was found stable from 30 to 90˚C with salinity ≤ 300 mM NaCl and pH from 3-8 [54]. The application of another natural surfactant

(extracted from sunflower oil) in emulsification of heavy crude oil was reported by Kumar and Mahto [52]. Here, the emulsion (60% heavy crude oil and 2 wt% surfactant) was found stable at 25 ˚C. The application of a natural surfactant, extracted from Reetha (2 wt%), in IFT reduction of heavy crude oil was reported by Saha et al [68]. IFT value of crude oil reduced from 18.6 to 7.02 mN/m which further reduced to 3.3 mN/m after the inclusion of 0.3 wt% silica NPs. The contact angle measurements for an o/w emulsion of heavy crude oil and natural surfactant (Reetha)-polymer (Xanthan gum, 3000 ppm)-NP (silica NP, ~15 nm), was presented by Saha et al [68]. The prepared emulsion was remarkably stable with droplet size ranging from 7.48-5.45 μm. From the above studies, it is clear that the application of natural surfactant in stabilizing crude emulsions is important for environmental concerns however, the use of natural surfactant (*e.g.,* extracted from fenugreek seeds) in stabilization of crude oil is not reported in literature as far as we are aware.

Moreover, from previous studies, it was observed that commercial silica NPs were used in stabilization scheme of emulsions. NPs, when added externally, are prone to higher agglomeration and hence change their original form to large size clusters which usually prefer to stay in bulk phase than adsorbing at o/w interface [297]. For a favorable stabilization of crude oil droplet, it is essential that all NPs adsorb at the interface and facilitate greater stability and IFT reduction, so that more oil can be mobilized from the porous media. This seems to be possible when NP remains independent and shows least agglomeration as independent NP exhibits higher surface energy to interact with oil than large size NP cluster. Therefore, the novelty of this work lies in the application of single-step silica nanofluid for stabilizing crude emulsion of natural surfactant, extracted from fenugreek seeds [30]. The synthesis of single-step silica nanofluid is also detailed in our previous work [298] where NP of independent form and different sizes (34-142 nm) were developed. The nanofluid showed marginal change in size and zeta potential over the storage

period of 2 months. Thus, in this work, single-step silica nanofluid was used to stabilize crude emulsion of natural surfactant of fenugreek seeds and polymer PAM. O/w emulsion was prepared by silica nanofluid (34 nm) of 1 wt% in the base fluid of PAM (1000 ppm) and natural surfactant (at CMC ~ 0.2 wt%). The performance of prepared emulsion was compared with emulsions of crude oil-in-water stabilized by a natural surfactant and a polymer. IFT measurements were conducted for both surfactant-polymer (SP) solution/crude oil and NSP (nanofluid-surfactant-polymer) solution/crude oil at room and elevated temperature (90˚C). The visual appearance of SP and NSP emulsions were analyzed by microscopic images at room and elevated temperatures (60, 80, and 98 ˚C). For rheological properties of prepared emulsions, viscosity measurements were performed at ambient and higher temperature (90 ˚C). Furthermore, stored emulsions were tested to visualize recovery in viscosity profiles and values. Particle size and zeta potential of NSP solution were determined by dynamic light scattering (DLS) technique. For wettability studies, contact angle measurements were conducted for both cases (SP/crude oil and NSP/crude oil) followed by the discussion on emulsion stability at different pH levels. Finally, adsorption tests were conducted for SiO_2 NPs in presence of natural surfactant and the role of SiO_2 NP on surface adsorption of natural surfactant was discussed.

6.2 Materials and Methods

6.2.1 Materials

For this experimental study, natural surfactant extracted from fenugreek seeds was explored. The seeds were obtained from a retail store in Amethi (Uttar Pradesh). For extraction, methanol obtained from commercial vendor (SD Fine Chemicals, India) was used. The Soxhlet apparatus (used for extraction) as well as hot air oven (used for dying the samples) were utilized for surfactant preparation. Polymer (PAM) having molecular weight = 10^7 g/mol with 90 % purity

was supplied by SNF Floerger. Silica nanofluid of single-step origin were utilized and the method of their synthesis has been reported in prior work [298]. To weigh the chemicals', digital weighing balance was used (Mettler Toledo, ME204/A04; repeatability approximately 0.1 mg). All the aqueous solutions prepared in the study was done using deionized (DI) water, obtained from Millipore® Elix-10 water purification apparatus. For emulsion preparation, crude oil (pour point = 310 K, viscosity ranging from 5 to 2.9 mPa.s and density varying from 0.88-0.83 gm/cc) was used and obtained from Tarapur Oilfield, Ahmedabad, India. The properties of crude oil have been discussed in our previous studies [162,229]. The sand used in the study was obtained from a commercial vendor and to remove the impurities, sand was initially cleaned with toluene followed by oven drying at 250 ˚C for 96 hours.

6.2.2 Methodology of extracting Natural surfactant from fenugreek seeds

For extraction of natural surfactant from fenugreek seeds, detailed procedure has been elaborated in following points and schematic representation of the same is shown in Fig. S2 (supporting information). The detailed procedure of extraction has also been provided in our previous study [30]. The prepared surfactant is quite soluble in water and solubility studies have been conducted experimentally. Initially, 5 ml of DI water was taken in a clean glass vial and 0.1 gm of surfactant was added. The solution was shaken by vortex shaker. The surfactant was found to be easily soluble and no residue was left on filter paper during filtration. Next, same experiment was repeated with 5 ml of DI water and 0.2 gm of surfactant followed by filtration. The same set of experiments were repeated for increasing amount of surfactant (0.1-0.7 gm). It was observed that no residue was present on filter paper till 0.4 gm of surfactant in DI water. But, when 0.5 gm of surfactant was used for solubility, some residue was observed while filtration as evident from Figure 6.1. The amount of residue on filter paper increased with increasing weight of surfactant in

solution. Thus, it can be concluded that surfactant possesses the aqueous solubility, that is, till 0.4 gm in 5 ml of DI water at room temperature.

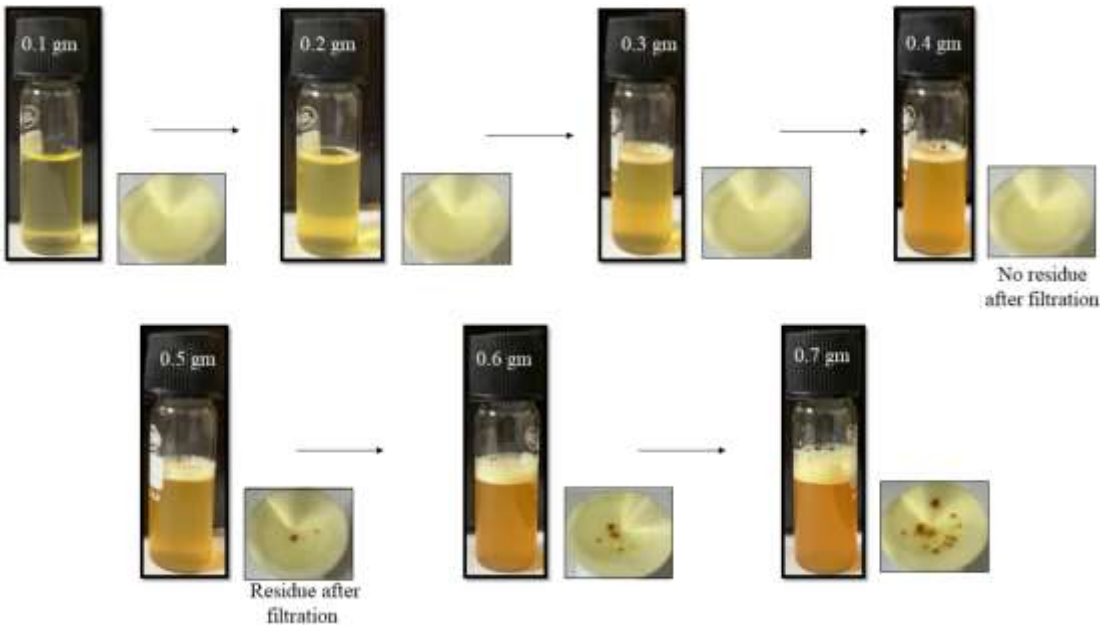

Figure 6.1: Detailed analysis used for depicting the aqueous solubility of natural surfactant extracted from fenugreek seeds.

6.2.3 Emulsion preparation by using natural surfactant, nanoparticle and polymer

For the study, two crude oil-in-water emulsion systems were prepared, that is, one stabilized by natural surfactant-polymer (SP) and other was stabilized by nanoparticle-natural surfactant-polymer (NSP). The schematic for preparation of emulsion system has shown in Figure 6.2.

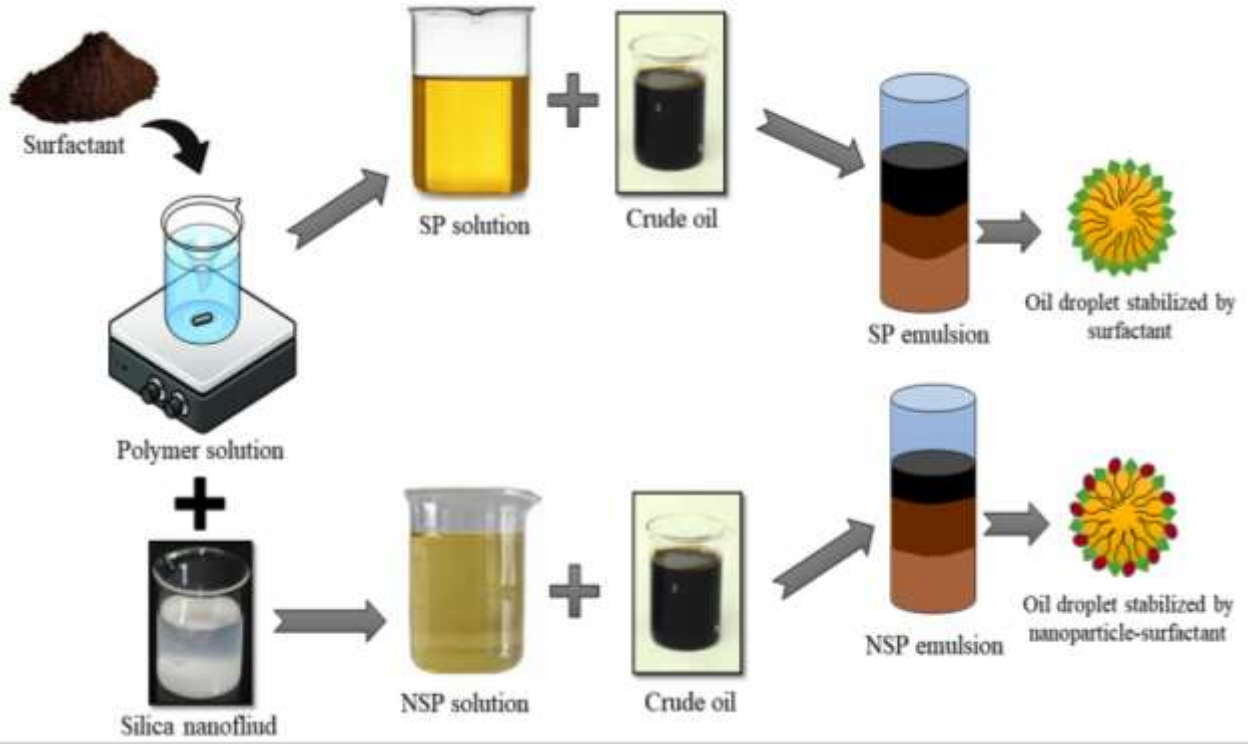

Figure 6.2: Schematic diagram showing the detailed procedure involved in the preparation of the SP and NSP emulsion. Emulsion was prepared by mixing crude oil (40%) and SP/NSP solution (60%).

For the SP and NSP solutions, the PAM solution (1000 ppm) was prepared by using magnetic stirrer (IKA-C-MAG-HS7) at 500 rpm for 7 hours. Natural surfactant was added in the polymer solution at CMC (0.2 wt%). Also, investigations for emulsions with alkane as an oil phase and nanoparticle/surfactant concentrations (lower than the CMC). We observed that the nanoparticle was able to stabilize the emulsions, though for not as long (less than 24 h). For preparing the first emulsion system, crude oil was added to the SP solution in ratio of 40:60 and shaken using Tarsons 1020 Spinix Vortex Mixer 2000 rpm for about 30 min till the single phase is achieved. For suspending nanofluid in surfactant-polymer solution, an industrial mixer grinder (Oster Grinder, MCPRO6-WSO) was used (speed 600 rpm for 30 min). Similarly, for the

preparation of other emulsion system stabilized by NSP, the ratio of crude oil and NSP solutions are taken as 40:60 and allowed to shake till the emulsion formation takes place. Silica nanofluid used in emulsion possess particle size ~34 nm and zeta potential value of -36 mV. Nanofluid used in the study was synthesized via single step method with a concentration of 1 wt%. Both the emulsion systems were kept for about two weeks at room temperature for investigating the creaming stability.

6.2.4 Stability and Microscopic Characterization of emulsion system

For thermal stability and microscopic investigation of the prepared emulsion system, an optical microscope (Motic, Hong Kong) was used. After the preparation of oil in water emulsion (both SP and NSP emulsion), a small amount of emulsion was taken by using laboratory pipette (Tarsons, United States) and placed on a clean glass slide for microscopic observation and images was recorded by using an inbuilt imaging tool (Moticam-10). Further, the thermal stability of both emulsions was investigated by using same optical microscope, equipped with electrical thermal stage (Novel Industries, India) with a thermocouple and images of emulsions were recorded at different temperatures, that is, at 40 ˚C, 60 ˚C, 80 ˚C and 98 ˚C. The pH of both SP and NSP slug was measured by using pH meter (Hanna Instruments, USA; Model: HI98129; range: 0-12 with an accuracy of ±0.02).

6.2.5 Rheological Characterization of emulsion system

To investigate the flow behavior of prepared emulsions, rheological studies were performed by using modular compact rheometer (MCR-52, Anton Paar, Austria). Freshly prepared emulsion (~20 ml) was poured in the cup and double gap system was used, where shear rate was varied from 1-1000 s^{-1}. Additionally, to investigate the flow behavior of emulsion at high

temperature (90 ˚C), same rheometer equipped with thermal jacket, circulation pump (ESCY IC 201) and a temperature unit (Peltier based, range -20-180 ˚C) was used to control the temperature as used in our previous studies [57,299]. Approximately a time of 15 min was given for attaining thermal equilibrium. Similarly, fresh emulsions were used for rheological studies at high temperature and shear rate was varied from 1-1000 s^{-1}. All the experiments were repeated thrice to observe the reproducibility in the obtained results and still uncertainty of ± 0.7-7.2% of obtained value was found.

6.2.6 Contact Angle measurements

For contact angle studies, a customized stainless steel pressure cell equipped with glass viewing ports supplied by D- CAM Engineering, India was used. For conducting contact angle measurement, mixture of sand and crude oil was prepared and evenly spread over the clean glass slide to form a uniform layer. This slide was then placed in a pressure cell, where a drop of SP and NSP slug were dropped on coated glass slide, separately. The pressure up to 12 bar was attained by using syringe pump (Teledyne ISCO, United States) and a gas compressor (Elephant, India). For recording the image of SP and NSP drop in presence of air, high quality camera was used (Phantom VCC, United States).

6.2.7 Interfacial tension measurements

For interfacial studies, dynamic tensiometer with Wilhelmy plate method (Model: K12 Kruss® Germany) was used [229,299]. For this study, IFT measurement was done between oil-SP slug and oil-NSP slug separately. The plate was fixed at one end and measurements were recorded automatically on measuring unit. The IFT measurements were conducted at 30˚C and 90˚C separately to analyze the effect of temperature.

6.2.8 Adsorption of nanoparticle on sandstone

For investigating particle adsorption, 20 ml of NSP slug was taken and poured in a glass culture tube and 10 gm of sand was added. The mixture was properly mixed by using an orbital shaker (Tarsons®, India) for about 20 min.

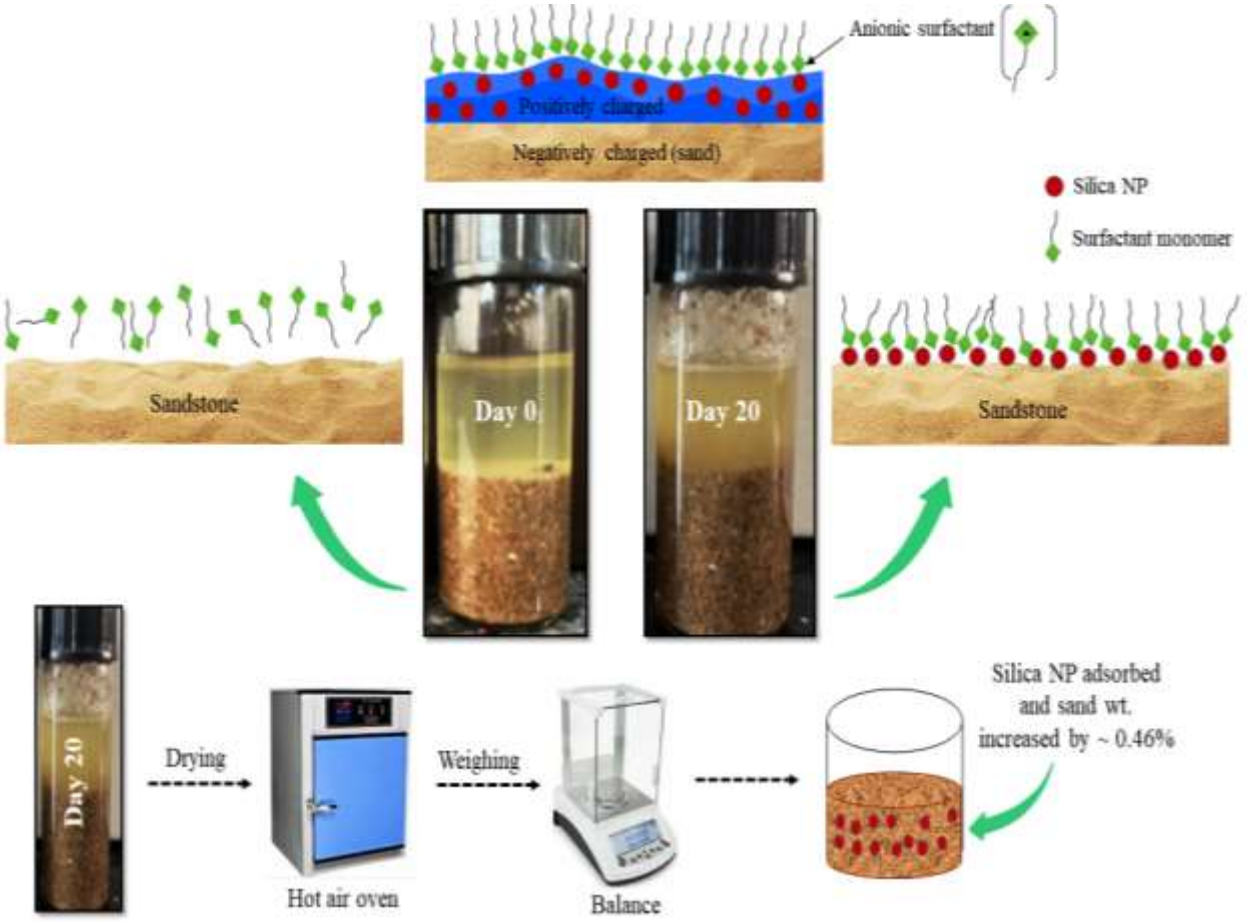

Figure 6.3: Illustrative representation of experimental investigations performed to study adsorption of surfactants and nanoparticles on sandstone media. Adsorption of nanoparticles analyzed by UV-vis analysis and adsorbed nanoparticles was confirmed by drying the solution followed by weighing the sand.

Later, 2 ml of NSP slug was extracted from the culture tube at day 0 and day 20 for analyzing in UV-vis Spectrophotometer (UV-vis 3200, Lab India®). The mixture was kept under observation for about 20 days to analyze particle adsorption on the sandstone surface. The dispersion was kept mixing twice a day and repeated the same for 20 days. After 20 days, the mixture was kept in hot air oven for complete drying. Later when the sand was completely dried, the weight of sand was measured to analyze any particle adsorption. The schematic of the detailed procedure is shown in Figure 6.3. All the studies were conducted at room temperature with wavelength ranging from 300-1100 nm with scan rate of 1 nm/s. The difference between both the peaks (at day 0 and day 20) was analyzed from the absorbance value obtained.

6.3 Results and Discussion

In this section, initially the IFT measurements between SP/NSP slug and crude oil have been reported. This was followed by the stability, microscopic and rheological characterization for both emulsion systems and effect of temperature was also explored. Next, particle size and zeta potential measurements were observed for NSP slug for exploring the effect of Si NPs. Later contact angle studies were performed for both SP and NSP slug on the rock surface. This was followed by the effect of pH on emulsion system. Finally, adsorption studies were conducted to observe the particle adsorption on rock surface.

6.3.1 Interfacial measurements

IFT measurements were performed to investigate the role of surfactant treated Si NPs (NSP slug) in mobilization of crude oil and compared it with without Si NPs (that is, SP slug). The effect of temperature was also analyzed in reducing interfacial tension at the interface of oil and SP/NSP slug. IFT measurements between crude oil-SP slug and crude oil-NSP slug is shown separately in

Figure 6.4. The IFT between crude oil and SP slug (at 30 ˚C) was observed to be 10.45 mN/m and is aligned with our previous study [229]. Reduction in IFT can be attributed to the orientation of surfactant at oil/water interface that contribute to decrease in surface free energy when comes in contact with crude oil [12]. When the temperature was increased to 90˚C, the rapid decrease in IFT was observed from 10.45 mN/m to 7.44 mN/m as evident from Figure 6.4. The reason for rapid decline in IFT can be attributed to the weak intermolecular forces at the interface of oil-aqueous phase due to rise in temperature.

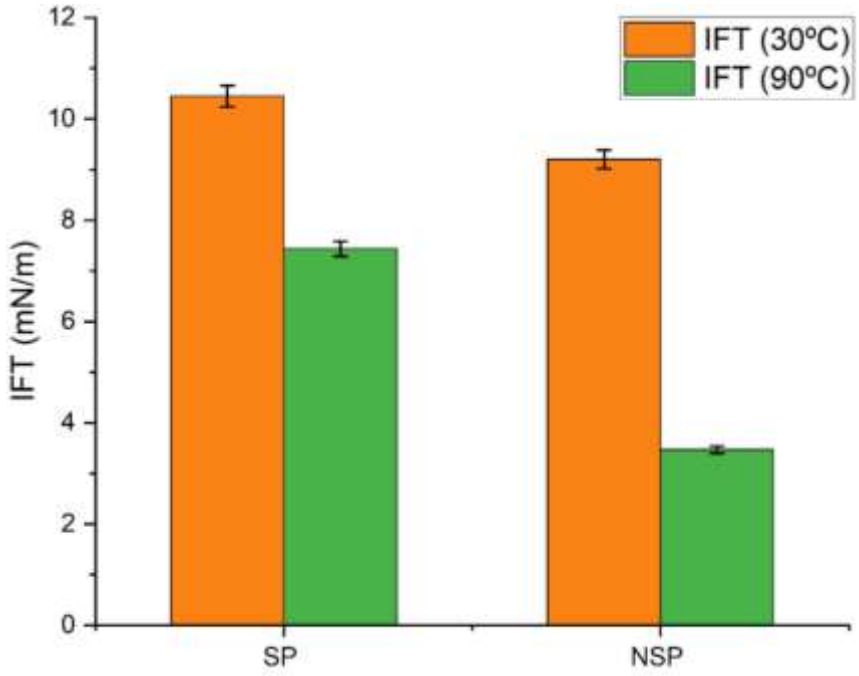

Figure 6.4: Observations of Interfacial tension (IFT) measurement between crude oil and SP/NSP solution at varying temperature 30˚C and 90˚C. The pressure was ambient, and surfactant used at CMC value (0.2wt%).

The IFT between crude oil and NSP slug was observed to be 9.2 mN/m (at 30˚C) and a reduction in IFT, more conducive for higher oil recovery was observed from 9.2 mN/m to 3.47 mN/m (at 90 ˚C), comparatively lowered than that of SP slug. Emulsions can alter the mobility of

injected fluids, improving sweep efficiency by providing a more uniform displacement front. Additionally, the emulsions can reduce the capillary pressure in the reservoir, aiding in the displacement of trapped oil. Furthermore, like surfactants, emulsions can lower the interfacial tension between oil and water, making it easier to mobilize residual oil. Emulsions can enhance the sweep efficiency by preventing the fingering of the displacing fluid through the oil. This mechanism differs from conventional surfactant or surfactant-polymer systems typically used in standard fluid displacement methods.

6.3.2 Stability and microscopic characterization

The crude oil emulsion stabilized by natural surfactant- polymer and nanoparticle-natural surfactant- polymer is shown in Figure 6.5.

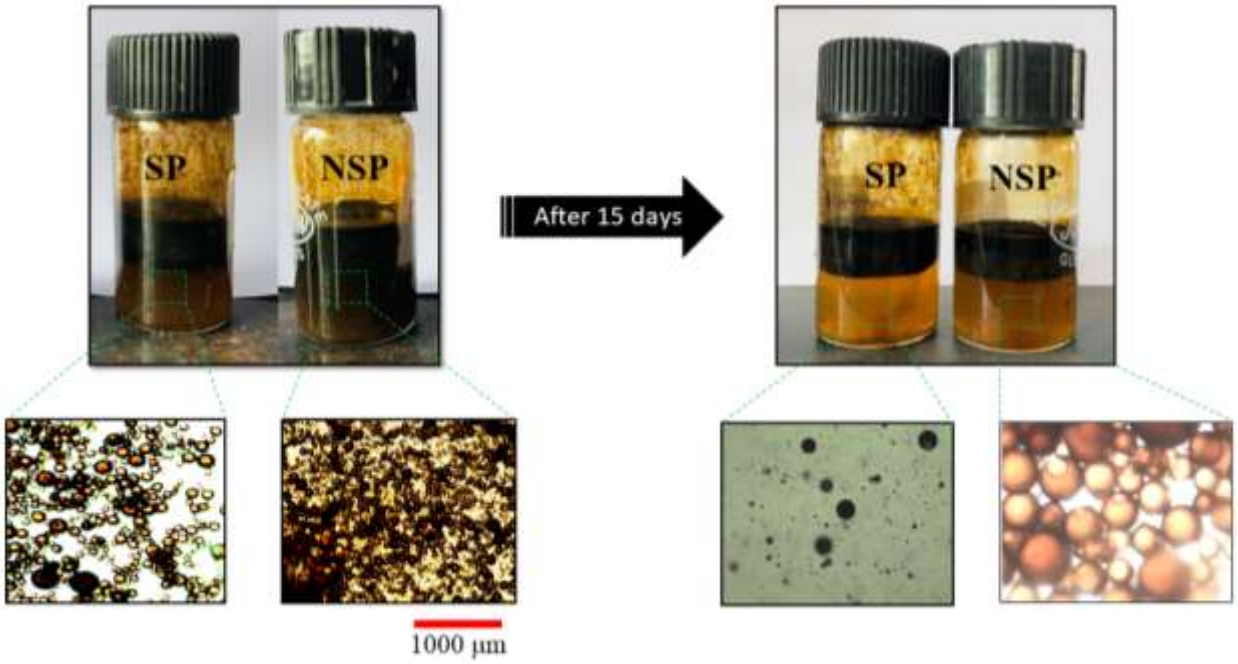

Figure 6.5: Visual appearance of SP and NSP emulsions taken immediately after preparation and after 15 days. The microscopic images were obtained from the liquid below the interface at day 0 and after 15 days.

The prepared emulsions were left undisturbed for about two weeks to visualize the creaming and phase separation with respect to time (Figure 6.5). It was observed that the phase separation as well as creaming was considerably higher in SP emulsion than that of NSP emulsion. This may be due to the presence of large-sized droplets in SP emulsion as evident from Figure 6.5. The size of droplet in SP emulsion influences the viscosity of emulsions and thereby large-sized oil droplets shifts towards the surface faster than NSP emulsion [68]. In NSP emulsion, small-sized oil droplets are observed as evident from the microscopic result (Figure 6.5). It is due to the presence of Si NPs deposition which contributes to higher density in NSP emulsion, as a result retarding the oil droplet movement in emulsion system.

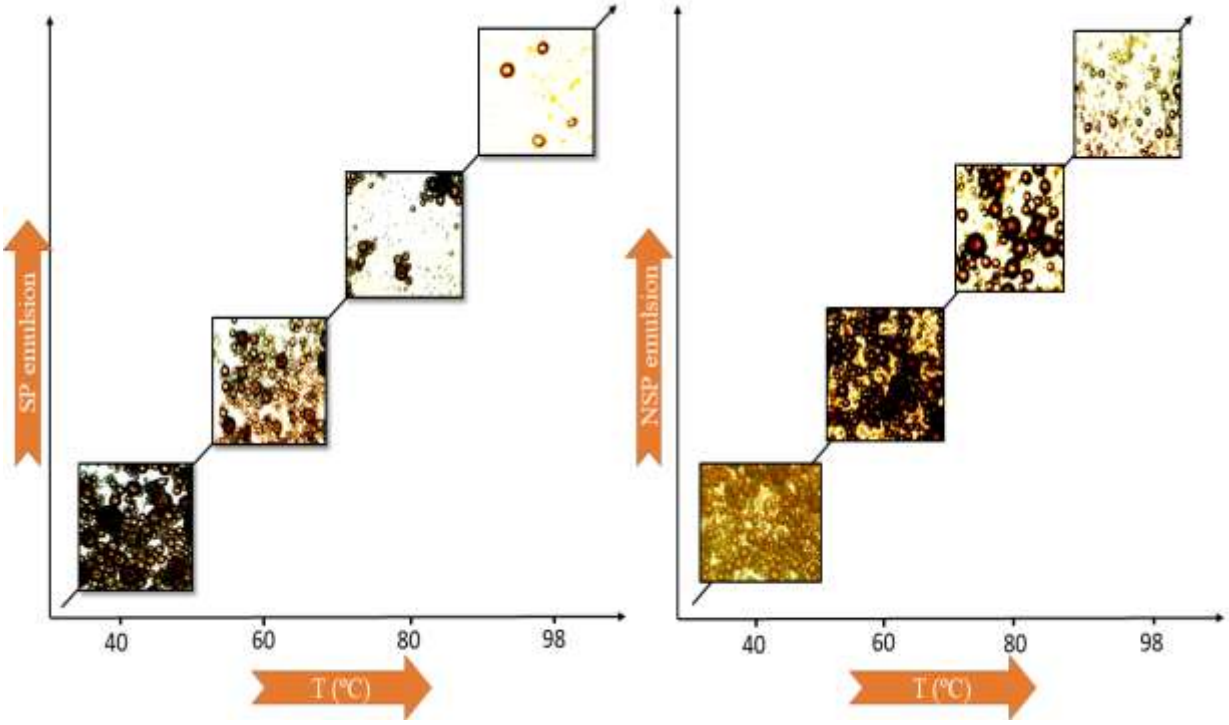

Figure 6.6: Microscopic observation of SP and NSP emulsions as a function of temperature (40˚C - 98˚C) viewed under optical microscope. The pressure was ambient, and emulsion is observed to become unstable with increasing temperature due to oil droplet coalescence.

To investigate the thermal stability of both SP and NSP emulsions, microscopic studies were conducted to observe coalescence at different temperatures, that is, 40˚C, 60˚C, 80˚C and 98 ˚C as shown in Figure 6.6. Separate emulsions were prepared, and the observations taken at different temperatures. SP emulsion was observed to be thermal stable from 40˚C to 60˚C as evident from microscopic results, where the coalescence of scattered oil droplets was observed. As the temperature reaches 80˚C, rapid coalescence of oil droplets was observed, thus affecting emulsion stability. With further rise in temperature (98˚C), complete coalescence of oil droplets occurred, rendering the emulsion completely unstable. The temperature at which emulsion becomes completely unstable is termed as higher range of thermal stability. Thus, it can be concluded that with increase in temperature, coalescence of oil droplet increases, and as a result emulsion becomes unstable. The thermal stability for NSP emulsion ranges from 40˚C to 80˚C. It is clearly observed from Figure 6.6 that NSP emulsion is strongly packed at 40˚C, finely packed at 60˚C with restricted coalescence of oil droplet against temperature and coalescence starts occurring from 80˚C. Thus, there is a significant shift or increase in temperature where the emulsion destabilizes when compared to SP emulsion as evident from microscopic results. Higher thermal stability of NSP emulsion is due to strong barrier offered by nanoparticle adsorption at the interface of crude oil-water [300]. Even at 98˚C, lesser coalescence of oil droplet was for NSP emulsion when compared to SP emulsion. Also the aqueous PAM solution acts as a thickener which further helps in preventing dislocation of surfactant molecules and nanoparticle from the interface of oil and water, as a result enhances the thermal stability [295].

6.3.3 Rheological analysis of emulsion systems

Rheological studies are one of the fundamental parameters to understand the flow behavior where stress is applied on some viscous sample and as a result change in flow behavior can be

observed [236,301]. Rheological studies are conducted for viscosity vs shear rate for both the SP and NSP emulsion at room and elevated temperature as shown in Figure 6.7. From figure, it was evident that both emulsions exhibited the non-Newtonian shear thinning behavior across the shear rate provided (1-1000 s^{-1}) and align with literature studies [57,238]. The viscosity of SP emulsion was found to be 6172.4 mPa.s at shear rate of 1 s^{-1} and shear thinning profile was observed, as viscosity consistently decreased with increase in shear rate, that is, 792.13 mPa.s at shear rate of 10 s^{-1}, ~101 mPa.s at shear rate of 100 s^{-1} and 18.41 mPa.s at 1000 s^{-1} (Figure 6.7 (a)).

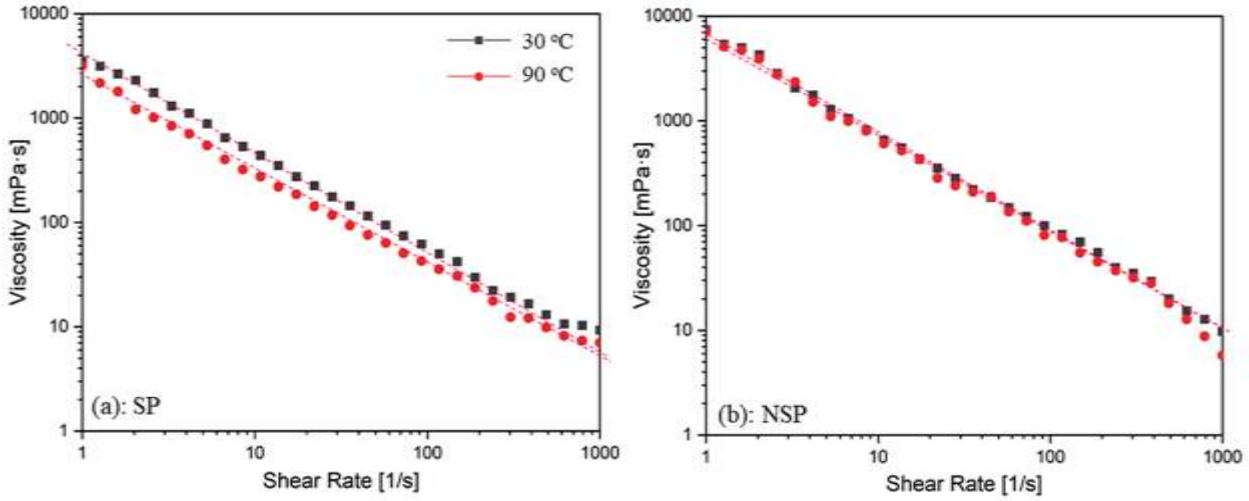

Sample	T (°C)	Correlation coefficient, R^2	Coefficient, a
SP	30	0.93	4.35
SP	90	0.91	4.48
NSP	30	0.96	5.41
NSP	90	0.97	5.58

Figure 6.7: Graphical plot for viscosity results of (a) SP and (b) NSP emulsion against varying shear rate (1-1000 s^{-1}). Red lines show the best mathematical model fit (Krieger-Dougherty Model) for the (a) SP and (b) NSP solutions and the below table shows the obtained values of model parameters. These observations were performed at ambient pressure and two temperatures (30/90˚C).

As the SP emulsion was stabilized by natural surfactant, that was anionic in nature as reported in our previous study [30], the surfactant tend to cover the oil droplet completely and provides repulsive energy barrier [302]. The effect of temperature on viscosity of SP emulsion were explored and shown in Figure 6.7 (a). It is evident from Figure 6.7 (a), that there is considerable decrease in viscosity of SP emulsion at high temperature (90˚C), that is, from 5585 mPa.s (at 1 s^{-1}), 493.87 mPa.s (10 s^{-1}), ~75 mPa.s (100 s^{-1}) to 13.871 mPa.s (1000 s^{-1}). Rise in temperature may lead to significant changes in the viscosity in both the phases (oil and water). Moreover, the decrease in viscosity with increase in temperature, illustrate that at high temperature coalescence of oil droplets occurs and oil droplets completely gets vanished [303] and are aligned with microscopic results as shown in Figure 6.6.

The viscosity profile for NSP emulsion was also investigated at room temperature (30˚C) as well as high temperature (90˚C) as shown in Figure 6.7 (b). From Figure 6.7 (b), it is clearly evident that addition of nanoparticle leads to enhancement of viscosity as compared to SP emulsions. The reduction in viscosity was observed decrease from 7382.4 mPa.s (30˚C) to 7184.6 (90˚C) at shear rate of 1 s^{-1} and 9.756 mPa.s (30˚C) to 5.748 mPa.s (90˚C) at shear rate of 1000 s^{-1}. Shear thinning profile was observed for NSP emulsion even at elevated temperature as clearly seen from fig that viscosity tends to decrease as shear rate increases and is aligned with literature [295]. Moreover, very slight reduction in viscosity of NSP emulsions was observed, and it is attributed to the fact that in presence of nanoparticle, emulsion remains thermally stable, and coalescence of oil droplet occurs at slower rate than that of SP emulsions. This may be due to the presence of surfactant which helps in altering the wettability of nanoparticle as well as modifying nanoparticle's adsorption at the interface of oil and water and thus restricts coalescence of oil

droplet [304]. These results are aligned with the microscopic findings of NSP emulsion as shown in Figure 6.6.

Also modelling analysis was investigated to get the best fit model. The model best fitted that explains the colloidal system of both SP and NSP emulsion is Krieger-Dougherty Model as provided in equation (1)

$$y = (y^0 - y^\infty)/\,(1 + a.x) + y^\infty \qquad (1)$$

The value of coefficient correlation R^2 is 0.88 for SP emulsion at room temperature whereas 0.91 for SP emulsion at high temperature with coefficient 'a' is 4.35 and 4.48 respectively. Whereas for NSP emulsion, coefficient correlation R^2 was around 0.96 (30˚C) and 0.99 (90˚C) with the value for coefficient 'a' are 5.41 and 5.58 respectively. The model is said to be fitted best if the value of R^2 ranges above 0.95. Thus, it can be concluded that the Krieger-Dougherty Model was best fitted for NSP emulsion (90˚C) with highest value of R^2, that is, 0.99 as shown in Figure 6.7.

In addition to this, SP and NSP emulsion were kept for about 15 days (as shown in Figure 6.8 and 6.9) to visualize the changes in their characteristics. For the same, rheological studies were conducted for both emulsion systems after 15 days to observe the viscosity profiles. It can be clearly seen in Figure 6.8, that there is huge drop in viscosity profile of SP emulsion after 15 days and also supported along with the microscopic images of the same. Viscosity was observed to decrease from 6172.4 mPa.s (day 0) to 2753.4 mPa.s (day 15) at shear rate of 1 s^{-1} and 18.41 mPa.s (day 0) to ~6 mPa.s (day 15) at shear rate of 1000 s^{-1}. As evident from microscopic results, very few oil droplets were observed when compared to the microscopic results of fresh SP emulsion as seen in Figure 6.6, where a tight packet of oil droplets can be seen. This may be due to the fact that

oil droplets tend to grow with time, lead to increase in coalescence and thereby emulsion instability.

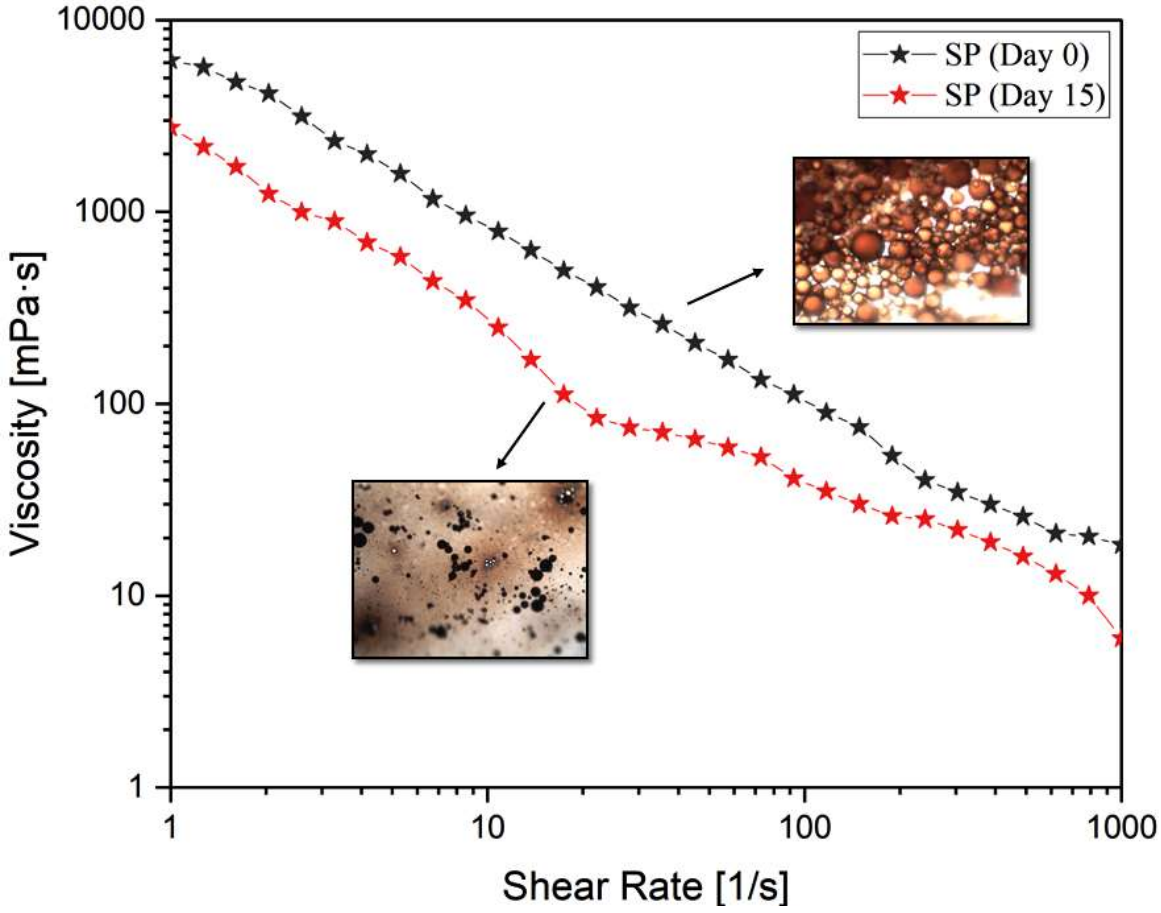

Figure 6.8: Viscosity results obtained as a function of shear rate for freshly prepared and stored SP emulsion (after 15days) at temperature 30˚C and pressure 1 bar. Microscopic observation for both fresh and stored emulsions has been provided to support the viscosity results.

The viscosity profile for both NSP emulsions, that is, fresh emulsion and emulsion after 15 days is shown in Figure 6.9 and supported along with microscopic investigation of the same reported in Figure 6.9.

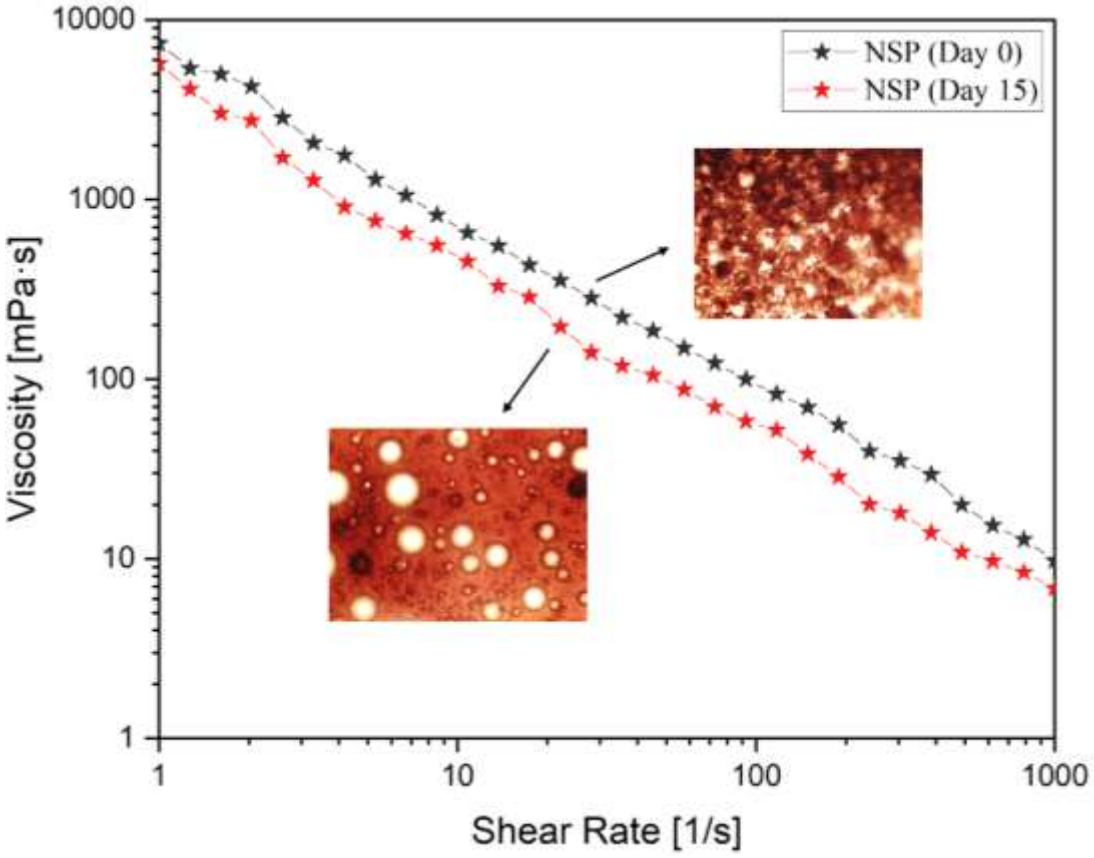

Figure 6.9: Viscosity profiles for freshly prepared NSP emulsion and stored NSP emulsion (after 15 days) obtained as a function of shear rate at temperature 30˚C and pressure 1 bar. Viscosity profiles are supported with the optical micrograph provided for both emulsions.

There is relatively lesser reduction in viscosity of NSP emulsion even after 15 days, that is, 22.6% reduction at shear rate of 1 s^{-1} and 29.7% reduction at 1000 s^{-1}. In addition, microscopic investigation of NSP emulsion at day 15 result in presence of large size oil droplet and complete coalescence does not occur as that of SP emulsion (day 15). Thus, it can be concluded that performance and stability of NSP emulsion is better than that of SP emulsions as inferred from microscopic as well as rheological studies. Therefore, NSP emulsions stabilized with natural surfactants show strong potential as efficient and sustainable alternatives for advanced fluid transport and thermal flow applications in porous media systems

6.3.4 Particle size and zeta potential measurements

Due to higher surface energy, nanoparticles tend to agglomerate and settle down with time in aqueous phase [175]. Due to this behavior of nanoparticle, it is not considered as a viable option for industrial applications. Conventionally, the use of surfactant helps in improving nanofluid stability through two main mechanisms, which include steric stabilization *i.e.,* surfactant molecules adsorb onto the surface of nanoparticles, creating a steric barrier that prevents agglomeration by repelling particles from each other and via electrostatic stabilization in which surfactants can impart charges to nanoparticles which leads to electrostatic repulsion between particles of same charge. Thus, it prevents particles from aggregation [44]. Therefore, surfactant was added to enhance the surface properties of nanoparticles. The nanoparticle used in NSP emulsion was SiO_2 (~34 nm) is most widely used as it is ecofriendly and cost effective when compared to other nanoparticles [305]. A smaller particle size indicates the presence of higher number of particles per unit area which further leads to enhanced particle collision. As a result, charge depletion area is formed on the surface of SiO_2 and tends towards to more agglomeration [175]. Average particle size and zeta potential of the silica nanoparticles in surfactant solutions was also conducted and the particle size was 45.51 nm and zeta potential value was -44 mV. For understanding the stability of NSP slug by means of electrophoretic behavior, zeta potential measurements were done. From table 1, the value of zeta potential was observed to be -36 mV and lying in stable region, that is, $\geq \pm$ 30 mV [306]. When the value of zeta potential ranges in ±30mV, the solution is said to be unstable [307]. All the measurements were performed at ambient conditions and result listed in Table 6.1. Table 6.1 provides the information on particle size and zeta potential of nanofluid without surfactant. Additionally, it also provides the detail of concentration of surfactant and polymer used in the preparation of NSP solution.

Table 6.1: Details of chemicals utilized in this study.

Nanofluid (without surfactant)	
Average particle size	34 nm
Zeta-potential	-36 mV
Base fluid	**1000 ppm PAM**
Surfactant	**0.2 wt%**

6.3.5 Contact Angle studies

To ascertain the wetting property of any solution by means of alteration at liquid-air interface, contact angle measurements play a crucial role. Contact angle studies help in analyzing the wetting characteristics of a solution in presence of air and is performed from heavier to lighter phase. As the contact angle increases, wetting characteristics of solution is said to be increased whereas decrease in contact angle means reduction in wetting characteristics of solution [165]. The contact angle measurements were conducted for both SP solution and NSP solution in presence of air at ambient conditions. It is clearly seen from Figure 6.10 that contact angle for NSP solution is fairly lower than SP solution over the complete span of time (min) explored. For SP solution, initially contact angle was observed to be 116˚ and it tend to reduce tremendously with time, that is, 104˚ at 4 min, 91˚ at 8 min, 77˚ at 12 min, 68˚ at 16 min and 57˚ at 20 min. Total reduction in contact angle was observed to be ~50% in span of 20 min for SP solution. Smaller values of contact angle signify that surface if more wetted by the SP solution and the SP droplet

seems to cover more surface area and has ability to displace the oil from that surface. The wetting characteristics of SP solution seem to be much more improved in presence of nanoparticles as the contact angle profile for NSP solution is quite lower than that of SP solution as shown in Figure 6.10.

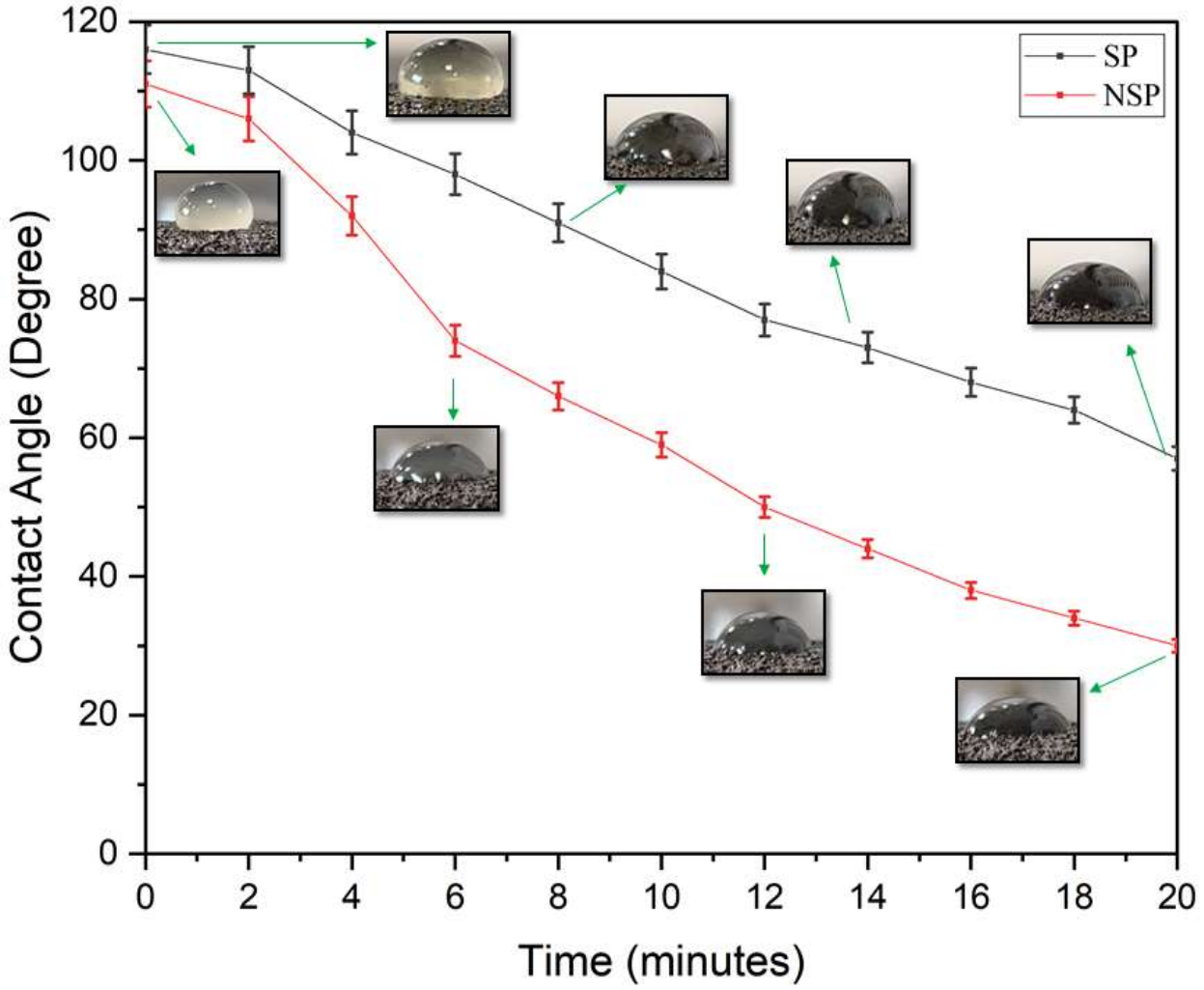

Figure 6.10: Contact angle measurement for both SP and NSP solution performed at ambient pressure and temperature. Contact angle study was conducted between sand saturated with crude oil and SP/NSP solution.

To understand the synergy of nanoparticle with surfactant-polymer, the contact angle studies for NSP solution were conducted and initially it was recorded as 111˚. Later the contact

angle seems to reduce enormously and observed to be 92˚ at 4 min, 66˚ at 8 min, 50˚ at 12 min, 38˚ at 16 min and finally 30˚ at 20 min and aligned with literature studies [66,165,308]. The total reduction in contact angle was ~73% over the explored time (20 min) which is much lower than that of contact angle for SP solution. This reduction in contact angle may be attributed to the presence of nanoparticle that offers water wet conditions [179]. As the particles tend to get adsorbed on surface, surfactant plays its role in detaching from the interface of solid surface and gets adsorbed, thereby enhances physical adsorption [309]. This leads to reduction in surface free energy that restricts particle agglomeration which in return offers strong water wet conditions by reducing the contact angle [310]. Therefore, the comparison of SP and NSP slug illustrates that NSP formulation offers better performance in enhancing the wettability and same can be inferred from the rheological as well as microscopic analysis. Also, the substrate surface seems very coarse and not smooth, the quick drop in contact angle may be attributed due to the penetration of the droplets inside the substrate due to surfactant adsorption, or by the wettability alteration offered by natural surfactant and require further validation.

6.3.6 Effect of particle adsorption on rock surface using UV-Vis method

The most reliable method to ascertain the stability of nanoparticle within a colloidal system by means of absorbance is UV-vis spectroscopy [299]. The value of absorbance refers to the amount of nanoparticle and its dispersion within a colloidal system. Denser the concentration of nanoparticle, higher peak in UV-vis spectrum will be observed whereas lesser the concentration of nanoparticles results in lower peak [311]. For analyzing the adsorption of nanoparticle onto the rock surface (sandstone), UV-vis analysis was conducted for NSP solution submerged in sand at day 0 and day 20 as shown in Figure 6.11. NSP solution at day 0 had a peak absorbance value of 0.2752 and after 20 days the peak absorbance value was observed to decrease to 0.2 from 0. 2752.

Also evident from fig that initially the absorbance value increases and later tends to decrease after attaining the peak at certain wavelength (400 nm).

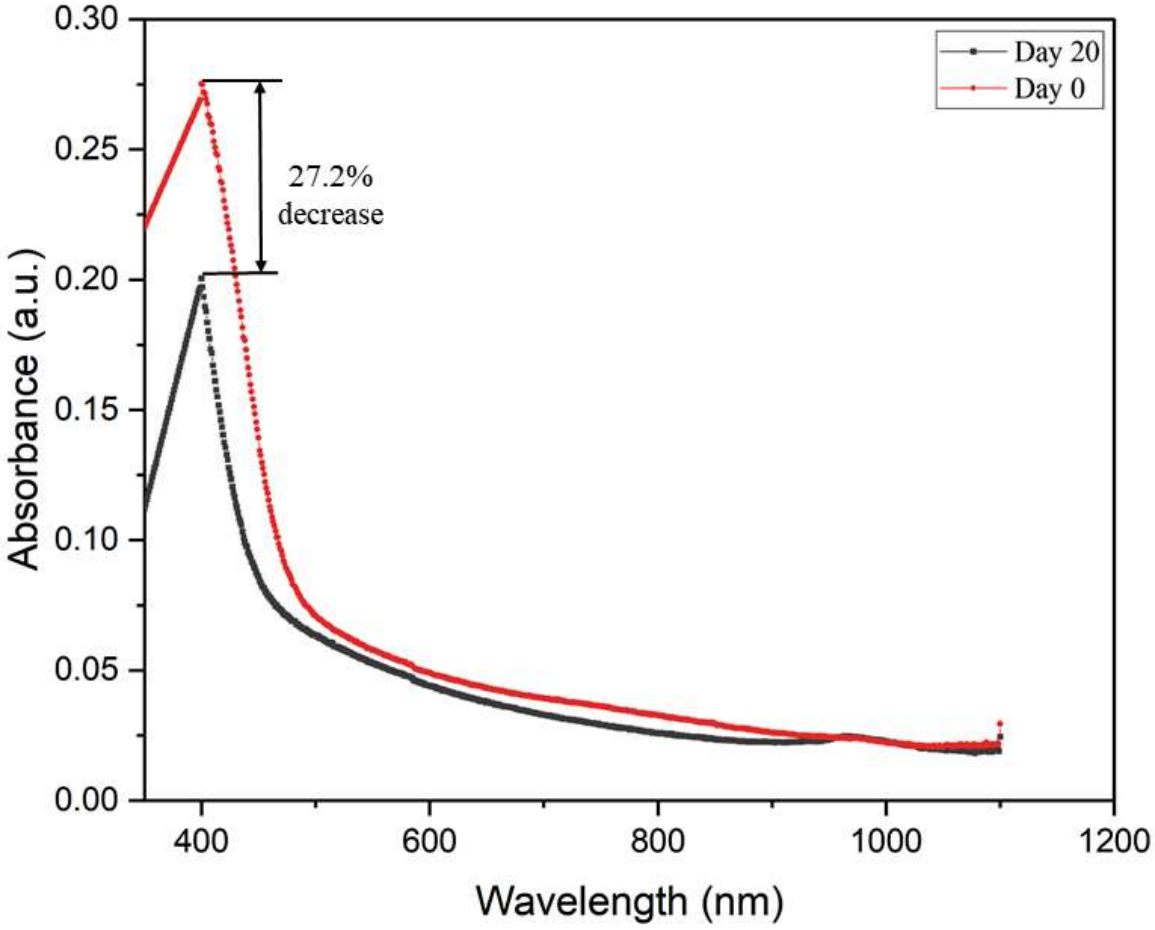

Figure 6.11: UV-Vis results obtained for the NSP solution (at day 0 and day 20). NSP solution was poured in glass culture tube with sand and solution was extracted at day 0 and day 20 for analyzing the adsorption of nanoparticle with respect to time.

This clearly indicates that within the time span of 20 days some particles were adsorbed onto the rock surface. A fall in absorbance value of UV typically relates to decrease in the concentration of absorbing species in solution [67]. This could be due to various factors such as dilution, chemical reaction, or removal of the absorbing species from the solution. The increase in

nano absorbance at first place refers to UV of NSP solution at day 0 (indicated by red color in Fig. 8). After 20 days, there was a drop in nano absorbance (indicated by black color in Figure 6.11). The drop in the values of absorbance can be attributed to reduction in the amount of nanoparticles and its dispersion within a colloidal system. Denser the concentration of nanoparticle, higher is peak of UV-vis spectrum. The percentage change in adsorption of nanoparticles can be obtained from equation (2) below:

$$\%\ Change\ in\ adsorption = \frac{N_0 - N_{20}}{N_0} \times 100 \qquad (2)$$

where, N_{20} is the peak absorbance value after 20 days and N_0 is the peak absorbance value at day 0. In order to confirm the deposition of nanoparticle with respect to time, further studies were conducted, that is, the culture tube containing NSP solution and sand was kept in oven to get completely dried and left over sand in the culture tube was measured using a weighing balance. In this part of the study, initially NSP solution and sand were thoroughly mixed in a culture tube and same was left undisturbed for 20 days. After 20 days, a drop of NSP solution was taken for UV-*vis* measurement where a drop in peak absorbance value was observed. This may be due to lower concentration of nanoparticles in NSP solution after span of 20 days. Thereafter, the solution containing sand and NSP solution was oven dried and sand was measured. Here, a small increment in the weight of sand was observed. To prevent the escape of water vapor and nanoparticle/surfactant in NSP solution, the culture tube was isolated with the help of an aluminum foil. Given these experiments were not performed in the presence of oil, it can be concluded that the incremental weight of sand was the result of nanoparticle adsorption. As a result, an incremental weight of ~0.46 wt% in sand was observed. This study was conducted in order to observe the adsorption of nanoparticle over the course of time and change in ~27.32% of adsorption was observed.

6.3.7 Effect of pH on emulsion system

pH has huge impact on the adsorption of surfactant, and the charge carried by solid surface varies with the pH alteration. Magnitude of surfactant adsorption varies with the changing pH. Increase in pH of surfactant solution results in decreasing the hydroxyl groups, responsible for affecting hydrogen bond formation [218]. The effect of pH on stability of both SP and NSP emulsion is investigated as shown in Figure 6.12.

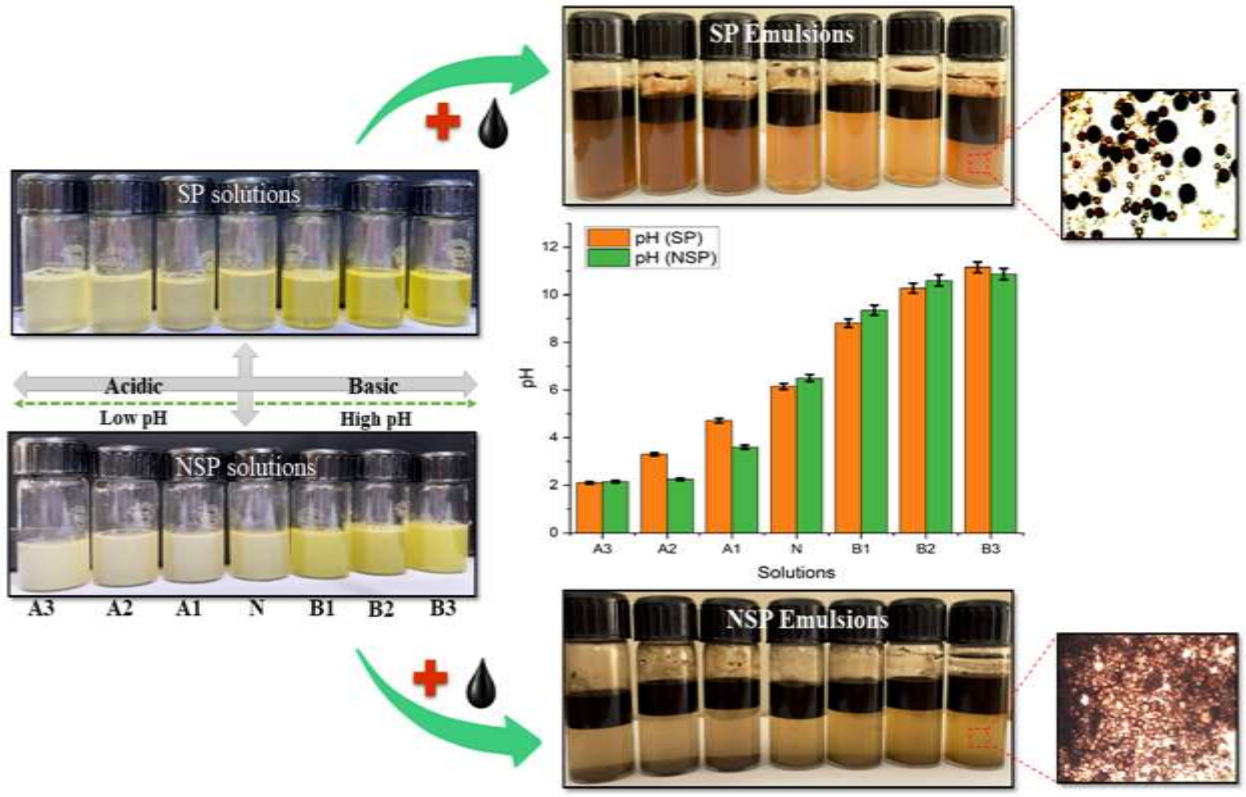

Figure 6.12: Graphical representation showing the effect of varying pH on emulsification of crude oil stabilized via SP/NSP solution and observed by visual and microscopic images. Values of varying pH for SP/NSP solution is shown in bar graph and emulsions was found to be basic in nature.

It can be observed from the fig that initially SP and NSP solution were taken separately and HCl was added to attain low pH, whereas NaOH was added to attain high pH solutions. Apart from neutral solution (N), three formulations were prepared with decreasing pH (A_1, A_2 and A_3) and three different formulations with increasing pH (B_1, B_2 and B_3). The neutral (N) SP and NSP solution has the pH value of 6.15 and 6.5 respectively. Solution is said to be neutral if pH lies between 5-7, acidic if pH value is lesser and basic if pH value of higher than former [312]. The values at lower pH for SP formulation was recorded as $A_1 = 4.71$, $A_2 = 3.3$ and $A_3 = 2.1$ whereas for NSP formulation the values are $A_1 = 3.6$, $A_2 = 2.25$ and $A_3 = 2.15$. Contrary, for basic range, pH values are observed to be $B_1 = 8.1$, $B_2 = 10.28$ and $B_3 = 11.15$ for SP formulation whereas $B_1 = 9.35$, $B_2 = 10.6$ and $B_3 = 10.87$ for NSP formulation and plotted on a graph as shown in Figure 6.12. Later, addition of equal quantity of crude oil to all formulations were done, emulsions was prepared. The emulsion for both SP and NSP with high pH formulation seems to be much more stable by the visual results. The change in pH can also influence the adsorption of surfactants onto particle surfaces. At different pH levels, both the surfactant and particle surface charges can change, affecting the strength and nature of adsorption. The pH affects the charge on particles (e.g., through ionization of surface groups), influencing electrostatic interactions with surfactants. This can impact the stability of colloidal dispersions, flocculation, and aggregation behaviors. By adsorbing onto particle surfaces, surfactants can modify the surface properties (e.g., hydrophobicity or hydrophilicity), which is pH-dependent. This can be crucial in processes like flotation, sedimentation, and wetting. Overall, understanding the pH-dependent behavior of surfactants is essential in applications like detergency, emulsification, pharmaceuticals, and environmental remediation, where precise control over surface and interfacial phenomena is required. To confirm these visual results, microscopic investigations were done, as a result,

microscopic images also confirm stable emulsion formation at high pH. As shown in Figure 6.12, a fine package oil droplets are observed for SP emulsion whereas a tight packet of very fine oil droplets is observed for NSP emulsion at higher pH. Thus, it can be concluded that prepared emulsions are basic in nature.

6.4 Conclusion

Study deals with the application of natural surfactant extracted from fenugreek seeds in emulsification of crude oil. Moreover, the effect of single step silica nanofluid was explored in emulsification. For successful industrial application of the prepared emulsion (SP and NSP), rheological behavior as well as microscopic investigation plays a crucial role. Findings of the study are summarized in key points as below:

- Initially the interfacial behavior of both SP and NSP solutions are investigated in presence of crude oil and observed that NSP solution can reduce the IFT to lower value (9.2 mN/m) than that of SP solution (10.45 mN/m) at ambient condition.
- IFT was also investigated at elevated temperature (90˚C), where NSP solution shown its potential in reduction of IFT to 3.47 mN/m value that is much lower than that of SP solution (7.44 mN/m).
- Microscopic investigations for both SP and NSP emulsions were performed, and it was found that NSP emulsions were thermally stable even at high temperature (80˚C) whereas SP emulsions were only stable till 60˚C.
- Rheological observation was made with the viscosity results of SP and NSP emulsion at 30˚C and 90˚C. It was observed that both the emulsions have shear thinning profile but NSP emulsions were thermally stable as only marginal reduction in viscosity profile was

observed at high temperature and best fitted with Krieger-Dougherty Model with R^2 = 0.99.

- Emulsions were kept under observation for about 2 weeks and rheological investigations were performed for kept emulsions. It was found that there was huge reduction in viscosity profile of SP emulsion than that of NSP emulsion and same was also confirmed from microscopic results.

- For the wettability analysis of SP and NSP solution, contact angle measurements were conducted. It was observed that NSP solution can reduce the contact angle from 111˚ to 30˚, whereas SP solution was able to reduce the contact angle from 116˚ to 57˚.

- The prepared emulsions were found to be basic in nature as evident from the pH results.

- Adsorption of Si NP was analyzed in presence of sandstone was found that nanoparticle tends to get adsorbed with respect to time as evident from the UV-vis studies.

Based on above observations, it can be concluded that NSP emulsion has the better potential in emulsification of crude oil than that of SP emulsions as evident from IFT, microscopic, rheological and wettability results. Stable nanofluids act as stabilizers in emulsions by preventing coalescence of oil droplets, leading to a more uniform distribution. This approach improves the efficiency of fluid displacement processes by enhancing the interfacial contact between immiscible phases, thereby promoting more effective phase transfer and overall system performance. Maximizing displacement efficiency is essential for optimal resource utilization and sustained functionality of subsurface flow systems. Additionally, it contributes to the extended operational life of engineered porous structures and supports efficient management of thermal or multiphase transport processes. Therefore, emulsions formulated with nanoparticle-surfactant-polymer (NSP)

systems using natural derivatives can be recommended as a sustainable and cost-effective solution for advanced fluid transport and thermal regulation applications.

Chapter 7

Stable nano- enhanced Phase Change Material Emulsions of Natural Surfactant and Single-Step Silica Nanofluid for Enhancing Thermal Energy Storage Potential of an Organic Phase Change Material

Abstract

The study investigates the stabilization of n-PCM (nano phase change material) emulsions using natural surfactants combined with silica nanofluid of single step origin at concentrations of 0.5 and 1 wt%. The novelty of study lies in application of natural surfactant used to enhance the emulsification process, ensures a sustainable and non-toxic stabilization method. Silica nanofluid of single step origin was incorporated to improve stability and performance, making these advanced emulsions a practical choice for various industrial applications. The emulsions were characterized through various techniques, including differential scanning calorimetry to assess thermal properties, interfacial tension measurements to evaluate emulsification efficiency, microscopic analysis for droplet distribution, and rheological testing to determine viscosity changes. Corrosion tests were conducted to investigate the protective effects of the stabilizers, while scanning electron microscopy and energy dispersive x-ray spectroscopy provided insight into the structural characteristics and distribution of nanoparticles within the emulsion. The results demonstrated that the addition of 0.5 wt% silica nanofluid significantly improved the stability and thermal characteristics of the n-PCM emulsion without adversely affecting its phase change behavior, with melting point of 21.08°C, enthalpy of melting 1205.171 J/g, freezing point of

15.46°C and enthalpy of crystallization 1284.825 J/g. In contrast, the emulsion with 1 wt% silica nanofluid led to alterations in thermal properties and viscosity, suggesting a more complex interaction with the n-PCM matrix. Overall, the study highlights that a lower concentration of silica nanoparticles (0.5 wt%) is preferable for optimizing the stability and thermal performance of n-PCM emulsions, making it a viable approach for applications requiring efficient thermal energy management.

7.1 Introduction

Thermal energy storage (TES) plays a crucial role in modern energy systems, particularly in enhancing energy efficiency and sustainability [313]. TES systems enable the capture and storage of thermal energy for later use, allowing for better management of supply and demand in various applications, including heating, cooling, and power generation [314]. The development of efficient TES systems is critical for enhancing energy efficiency and supporting sustainable energy solutions [315]. Among various TES technologies, Phase Change Materials (PCMs) have gained considerable attention due to their high latent heat storage capacity and ability to regulate temperatures during phase transitions [316]. PCMs are essential for TES due to their ability to absorb, store, and release large amounts of latent heat during phase transitions, typically from solid to liquid and vice versa [317,318]. This characteristic makes PCMs highly effective in applications requiring temperature regulation, such as in building materials, electronics cooling, and solar energy systems [319–321]. However, conventional PCMs often face challenges related to low thermal conductivity, leakage during phase change, and stability issues, which limit their practical applications [322]. To overcome this challenge, nano-enhanced PCMs (n-PCM) emulsion have emerged as a promising approach by incorporating nanoparticles to improve thermal conductivity, stability, and overall performance.

n-PCM emulsions provide a more efficient and versatile solution for TES, addressing some of the limitations associated with traditional n-PCMs and offering enhanced performance, stability, and flexibility. Chen et al. [72] prepared the phase change emulsion by employing phase incursion method. Emulsion was prepared using microparticles of tetradecane and water having melting point 277.7 K and heat of fusion 73.47 KJ/kg. Zhang et al. [73] prepared the PCM in water emulsion for solar thermal applications by using n-octacosane as PCM with melting point at 60°C. For preparing the emulsion, binary mixture of synthetic surfactant (Span and Tween) in 1:1 mass ratio was used and SiO_2 particles (7-40 nm) was used as nucleating agent. Zhang et al. [323] prepared n-PCM emulsion for TES applications by using sonication method. Various paraffins were explored in the study with OP-10 as an emulsifier and nucleating agents as nano-metal oxide (ZnO, Al_2O_3). As a result, emulsions were found stable and possess great stability as well as lower viscosity. Liu et al. [324] formulated PCM-water nano emulsion using phase inversion method. Various surfactants explored as stabilizers, that is, binary mixture of Brij L4 and Tween 60 or Tween 80 in 6:4 ratio. As a result, PCM nano emulsion offers higher stability with a droplet size of 60 nm and low viscosity of 50 mPa.s. Further addition of nucleating agent (n-octadecane; 2wt%) results in promising stability of emulsion till 120 d with a latent heat of 50 J/g and supercooling of 5°C. n-PCM emulsions offer significant advantages for TES, they also come with several drawbacks that can limit their widespread application. Significant drawback is the cost associated with synthesizing n-PCMs and incorporating nanoparticles and stabilizing agents can be relatively high compared to conventional PCMs [325]. This increased cost could hinder the large-scale adoption of n-PCM emulsions, particularly in applications where cost-effectiveness is a key consideration. In addition to this, n-PCM emulsions stabilized by synthetic surfactants have been extensively explored for TES applications, they present several drawbacks that can limit their

practical utility and sustainability. Significant issue is the potential environmental and health risks associated with synthetic surfactants [326]. These chemicals are often non-biodegradable and can persist in the environment, leading to bioaccumulation and toxicity concerns [327,328]. The release of synthetic surfactants into water bodies and ecosystems can adversely affect aquatic life and disrupt ecological balance [7,329]. Addressing these challenges is essential for advancing n-PCM emulsions toward practical and sustainable TES applications, necessitating further research into optimizing formulation, stability, safety, and cost-effectiveness. Thus, there is the need for alternative stabilizing and nucleating agents, such as natural surfactants and nanofluid of single step origin, that offer better environmental compatibility, low cost, stability and performance to advance n-PCM emulsions for sustainable thermal energy storage solutions.

Natural surfactants, derived from renewable sources, are increasingly being used to stabilize emulsions due to their biodegradability, low toxicity, and compatibility [19]. The use of natural surfactants aligns with sustainability goals by reducing reliance on synthetic chemicals [18]. Natural surfactants are biodegradable and less harmful to the environment, making the emulsions more environmentally friendly compared to those stabilized with conventional synthetic surfactants. Natural surfactants facilitate the formation of stable emulsions by reducing interfacial tension [229,272,330]. This results in a more homogeneous distribution of droplets within the emulsion, which is essential for maintaining consistent thermal performance. Various natural surfactants have been reported in literature [30,32,39,41,331] but none of them have been explored in TES. In conjunction with natural surfactants, silica nanoparticle have shown great potential as stabilizing agents due to their ability to form robust interfacial layers around emulsion droplets, thereby preventing coalescence and phase separation [332,333]. Silica nanoparticles are known for their excellent surface properties, high thermal conductivity, and stability, making them ideal

for TES applications [334]. The incorporation of silica nanoparticles in PCM emulsions not only enhances thermal conductivity but also prevents phase separation and improves the overall stability of the emulsion [73]. Various studies reported in literature have utilized the commercial silica nanoparticle for TES applications [335–338]. Commercialized silica nanoparticles face several challenges that limit their widespread application. One of the main issues is the high production cost associated with their synthesis [62,339]. In addition to this, they are prone to agglomeration due to their high surface energy and strong intermolecular forces [340,341]. Overcoming these challenges require the use of sustainable and greener alternative for industries looking to adopt eco-friendly and efficient manufacturing practices. Single-step silica nanoparticle synthesis is vital to address the limitations of commercialized silica nanoparticles, such as high cost, time-consuming production, and inconsistent quality [164,298]. The single-step synthesis method simplifies the preparation process, potentially reducing costs and making the technology more scalable for industrial applications [342]. Additionally, a streamlined synthesis method can improve the reproducibility and functionality of silica nanoparticles, allowing for more controlled interactions with other materials, including natural surfactants and stabilizers in emulsions. The combination of these two stabilizing agents not only provides enhanced thermal conductivity but also offers environmental benefits by reducing the use of synthetic materials. Overall, the integration of natural surfactants with n-PCM represents a significant leap forward in the development of advanced thermal management materials. This approach not only improves performance but also supports sustainable practices, paving the way for innovative solutions in energy storage and management.

This research focuses on the formulation of an n-PCM emulsion stabilized by natural surfactant (extracted from fenugreek seeds) and silica nanoparticles synthesized through a single-

step process (sol-gel method), which offer improved stability and heat transfer properties as well as ecofriendly. This study explores the synthesis of n-PCM emulsions using silica nanofluid at 0.5 wt% and 1 wt% concentrations to enhance emulsion stability and thermal performance, presenting a sustainable and efficient approach for energy storage solutions. This approach simplifies the preparation method and potentially reduces production costs while maintaining the desired stability and thermal performance. The research aims to investigate the thermal properties, rheological behavior, and stability of the prepared n-PCM emulsion, along with an evaluation of its corrosion resistance and morphological characteristics using techniques such as Interfacial Tension (IFT) measurements, Differential Scanning Calorimetry (DSC), UV- visible spectrophotometer, rheological measurements, Scanning Electron Microscopy (SEM), and Energy-Dispersive X-ray Spectroscopy (EDX). The findings from this research will contribute to the advancement of sustainable and efficient TES systems, offering insights into the potential of natural surfactants and nanoparticles in enhancing PCM applications.

7.2 Materials and Methods

7.2.1 Materials

For the study, n-hexadecane was used as a PCM obtained from Spectrochem, India (99% pure). Single step silica nanofluid used in the study and its preparation methodology has been reported in our previous work [164]. DLS measurements of nanofluid is shown in Table 7.1 [343]. Natural surfactant used to stabilize the emulsion and was obtained from fenugreek seeds. Extraction of surfactant was done via Soxhlet apparatus and dried by using hot air oven (Jain Scientific Glassworks, India). Detailed procedure of extraction of surfactant from fenugreek seeds has been reported in our previous study [30]. Magnetic stirrer (Model: IKA-C-MAG-HS7) was used for uniform mixing of all the aqueous solutions. For measuring the samples, digital weighing

balance (ME204/A04) was used. All the glassware used in this study was properly cleaned and dried to avoid any possible contamination.

Table 7.1: Average particle size and zeta potential of silica nanofluid prepared *via* single-step.

Silica concentration (wt%)	Average Size	Zeta Potential
0.5	5-10 nm	-48 mV
1	10-20 nm	-42 mV

7.2.2 *Synthesis of emulsion using natural surfactant*

n-PCM emulsion was prepared by using n-hexadecane (oil phase) and single step silica nanofluid (aqueous phase), whereas natural surfactant was used to stabilize the emulsion. The ratio oil phase to aqueous phase was taken as 40:60 [330]. Two different concentrations (0.5 wt% and 1 wt%) of nanofluid of single step origin was explored in this study as mentioned in Table 7.2.

Table 7.2: Nomenclature and composition of emulsions with varying concentrations of silica nanofluid and natural surfactants.

Oil phase (PCM)	Aqueous phase	Nanoparticle concentration (wt%)	Stabilizer	Emulsion ratio	Emulsion nomenclature
n-hexadecane	Single step silica nanofluid	0.5	Natural surfactant (fenugreek seeds)	oil phase: aqueous phase (40:60)	PCM1
		1.0			PCM2

Initially, n-hexadecane and nanofluid (0.5 wt%) was allowed to mixed in a beaker using magnetic stirrer, but both the oil as well as aqueous phase remain separated until the addition of natural surfactant as shown in Figure 7.1.

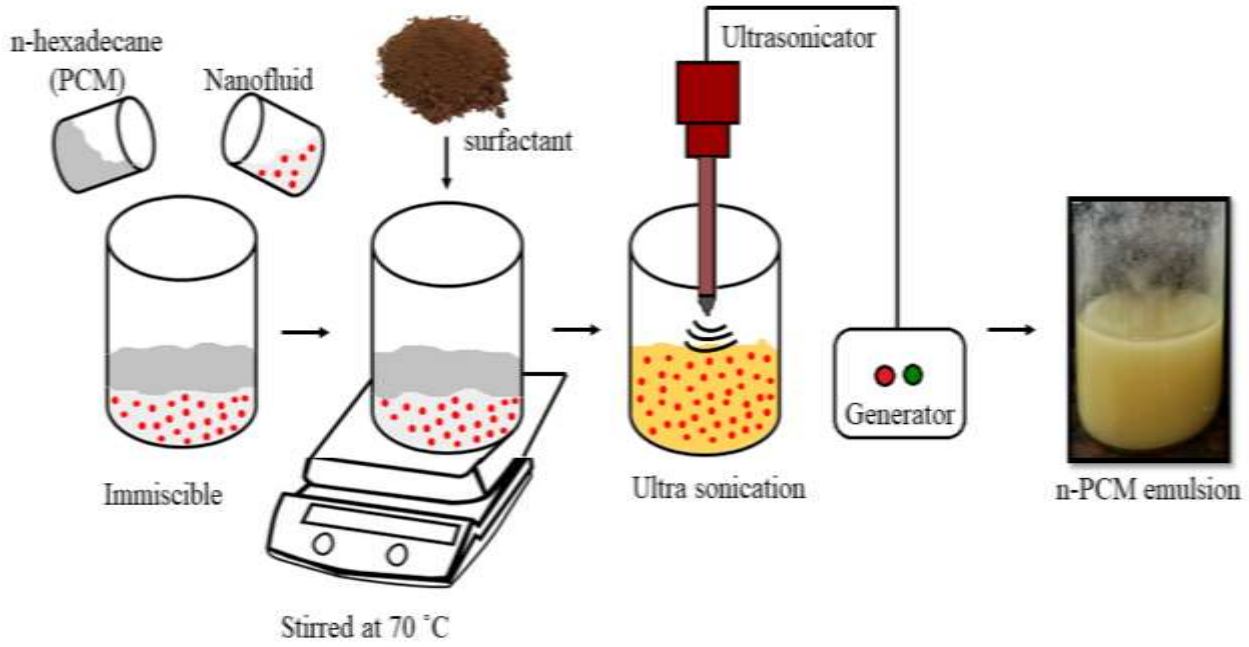

Figure 7.1: Schematic representation of the preparation of n-PCM emulsion stabilized by natural surfactants and silica nanoparticles.

Natural surfactant was added at CMC value of 0.2 wt%. CMC of the natural surfactant was calculated by using electrical conductivity measurements as well as surface tension measurements [30]. After addition of surfactant, sample was allowed to stir at 400 rpm for 1 h at 70°C. Further, for uniform mixing and even distribution of particles within the emulsion system, emulsion was sonicated by using ultra sonication (frequency 24kHz; time 30 min). Same procedure was repeated for preparation of 1 wt% n-PCM emulsion. During sonication, the temperature was carefully monitored using a digital thermometer to ensure that it remained consistent. To prevent overheating caused by prolonged sonication, the process was conducted in cycles, with intermittent

pauses allowing the system to cool when necessary. Additionally, the equipment used was placed in an environment maintained at 70ºC to ensure uniformity in temperature during mixing and sonication. The n-PCM emulsion with 0.5 and 1 wt% silica nanofluid will now be abbreviated as PCM1 and PCM2 respectively as shown in Table 2. The entire procedure of synthesis of n-PCM emulsion is shown in Figure 7.1.

7.2.3 Characterization of n-PCM emulsion

After emulsion preparation, UV-vis studies were conducted for both emulsion system (PCM1 and PCM2) by using UV-vis Spectrophotometer (UV-vis 3200, Lab India®) [344]. The wavelength range was set from 300 nm to 800 nm to cover the full spectrum of interest. The samples were diluted prior to performing the UV-Visible analyses. A dilution ratio of 1:10 was used, where one part of the emulsion was mixed with nine parts of deionized water. This step ensured that the optical density of the samples fell within the measurable range of the UV-Visible spectrophotometer and minimized potential scattering effects caused by the concentrated emulsion. Both n-PCM emulsions were loaded into quartz cuvettes with an appropriate path length (typically 1 cm). The cuvettes were carefully sealed to prevent any contamination or evaporation during the measurement process. Both samples were scanned across the wavelength range (300-800 nm). The absorbance spectra were recorded to identify the characteristic peaks associated with the nanoparticles dispersed in the PCM matrix.

For determination of interfacial properties, dynamic tensiometer was used (K-12, Kruss, Germany) between n-hexadecane and surfactant solution at CMC. IFT investigations were done by using Wilhelmy plate method [229,330]. Wilhelmy plate is a flat and thin plate used in IFT measurements. The Wilhelmy plate was thoroughly cleaned and attached to a sensitive balance. The plate was then partially immersed in the n-hexadecane layer, which was carefully placed above

the surfactant solution in a specially designed vessel to ensure a stable interface. As the plate contacts the interface between the n-hexadecane and the surfactant solution, the IFT value was recorded automatically. The IFT measurements were conducted both at 30 and 90°C.

7.2.4 Microscopic observations of n-PCM emulsion

Microscopic analysis was conducted to observe the distribution and stability of the PCM droplets and nanoparticles within the emulsion system. The prepared sample was observed under an optical microscope (Motic, Hong Kong) equipped with a digital camera (Moticam-10) as reported in previous study [272]. The microscope was set to an appropriate magnification level to clearly visualize the PCM droplets and nanoparticles. Images were captured to analyze the size distribution of the PCM droplets and the dispersion of nanoparticles within the emulsion. In order to investigate the thermal stability of both the prepared emulsion, same set up was used along with the electrical heating stage (Novel industries, India). Heating stage allowed for precise temperature control, enabling the observation of the emulsion at 60 and 90°C. The temperature was monitored using a built-in thermocouple to ensure accurate control and consistency throughout the experiment.

7.2.5 SEM and EDX of n-PCM emulsion

The n-PCM emulsion samples thus prepared was allowed to place onto a conductive adhesive tape mounted on an aluminum stub. To enhance the conductivity of the samples, a thin layer of gold was sputter-coated for 60 seconds using a sputter coater (DII-29030SCTR). The samples were then examined under a scanning electron microscope (JEOL, JSM-7900F) at an accelerating voltage of 5-15 kV. SEM micrographs were captured at varying magnifications to analyze the surface morphology and particle size distribution within the emulsion. Elemental

analysis was conducted simultaneously using an EDX detector (Z2-i7 Analyzer) attached to the SEM instrument. The EDX spectra were obtained from specific regions of interest to determine the elemental composition and to verify the presence of key elements associated with the n-PCM emulsion formulation.

7.2.6 Rheological studies of n-PCM emulsion

To understand the rheological properties and stability of n-PCM emulsions, a modular compact rheometer (MCR-52, Anton Paar, Austria) was used. The rheometer used was equipped with a bob and cup geometry. Specifically, the cup has an outer diameter of 3.9 cm and a length of 6.5 cm, and it was fixed securely on the base of the rheometer. The bob, which has a diameter of 3.4 cm, was mounted on a moving arm. This geometry was selected for its effectiveness in handling fluid systems with complex flow behaviors, such as emulsions, providing high precision in viscosity and shear stress measurements. The bob (also known as the inner cylinder) is immersed in the sample, which is contained within the stationary cup (outer cylinder). The rotational motion of the bob induces shear flow within the emulsion, allowing for the measurement of shear and dynamic viscosities. Rheological analysis was conducted in both shear and dynamic modes. In shear rheology, shear rate was varied from 1 -1000 s^{-1} whereas in dynamic rheology, shear strain was varied from 1-100%, keeping the frequency constant at 10 rad s^{-1}. Each measurement was repeated thrice in order to get reproducibility in the results and uncertainty of ± 0.6 – 8.4 % of the mentioned values. In addition to this, rheological behavior of prepared emulsion was also observed at elevated temperature, that is, 90°C. The temperature was controlled using the same rheometer that was used in our previous research [57,332], which was provided with a thermal jacket, a circulation pump (ESCY IC 201), and a Peltier-based temperature unit with a range of 20-180 °C.

7.2.7 Thermal analysis and stability of n-PCM emulsion

DSC analysis was performed using 4000 PerkinElmer model (DSC7020), calibrated with standard materials to ensure accuracy. A small quantity of sample ~10 mg of the n-PCM emulsion was placed in an aluminum pan for the observation. The DSC measurements were conducted under a nitrogen atmosphere to prevent oxidation, with a heating and cooling rate of 5 °C/min across a temperature range of -20°C to 50°C. The thermal data thus obtained was analyzed and plotted by using Origin software. The onset and peak temperatures of melting and crystallization, as well as the enthalpies of these transitions, were recorded. In addition, thermal properties, after various cycles, were analyzed for these emulsions, to assess any degradation or shift in phase change behavior. The n-PCM emulsion was subjected to accelerated thermal cycling using a DSC between temperature range, -20°C to 50°C. The emulsion was exposed to 25 and 50 cycles. Each cycle consisted of a rapid heating phase followed by a cooling phase to ensure complete phase change.

7.2.8 Corrosion test

Corrosion test was conducted to determine the feasibility of the n-PCM emulsion with the three frequently used heat exchanger building materials, that is, copper (Cu), aluminum (Al), and stainless steel 316 (SS). Initially, metal samples were cleaned according to standard procedures to remove any oxide layers, dirt, or contaminants. The samples were cleaned in acetone for 10 min to ensure all surface contaminants were removed. The samples were then rinsed with deionized water and dried completely. The metal samples were carefully placed in a container carrying the PCM1 and PCM2 separately and was wrapped completely to prevent any contact with air. The metal sample was in liquid state at room temperature for 45 d and after that metal samples were taken out to calculate the corrosion. Weight loss method was used to determine the corrosion rate.

Each sample was weighed before and after exposure to the n-PCM emulsion using an analytical balance (Metler Toledo, ME204/A04) with an accuracy of 0.1 mg.

7.3 Results and Discussion

Primarily, IFT measurements were conducted between PCM and natural surfactants to understand the potential of natural surfactant in stabilizing the emulsions. UV-Vis spectroscopy was used to monitor the stability and homogeneity of the n-PCM emulsions. This was followed by optical microscopy, which revealed well-dispersed droplets of n-PCM emulsions, indicating successful emulsification. SEM and EDX provided insights into the microstructure and composition of the emulsions. Rheological was done to understand the flow behavior under different shear rates. DSC analysis provided valuable information on the thermal properties of the n-PCM emulsions. Lastly, corrosion tests conducted on metal substrates in contact with the n-PCM emulsions.

7.3.1 Interfacial tension investigations

PCMs are extensively used in thermal energy storage systems due to their high latent heat capacity and ability to store and release thermal energy during phase transitions [345]. Understanding the interfacial properties between PCMs and surfactants is crucial for enhancing the thermal performance and stability of PCM emulsions [346]. Natural surfactants, derived from renewable resources, have gained significant interest due to their biodegradability and minimal environmental impact [113]. IFT measurements were performed between n-hexadecane (PCM) and natural surfactant from fenugreek seeds at both 30 and 90°C as shown in Figure 7.2. Natural surfactant was used at CMC value (0.2wt%). CMC is the concentration above which surfactant molecules begin to form micelles in the solution, significantly altering the interfacial properties

[193,237]. The results showed a significant decrease in IFT between n-hexadecane and surfactant solution, that is, 9.8 mN/m at 30°C (Figure 7.2). This reduction may be attributed to the adsorption of surfactant molecules at the interface, lowering the free energy and reducing interfacial tension [12]. Moreover, at higher temperature (90°C) the IFT value seems to decline and was observed to be 6.4 mN/m as shown in Figure 7.2.

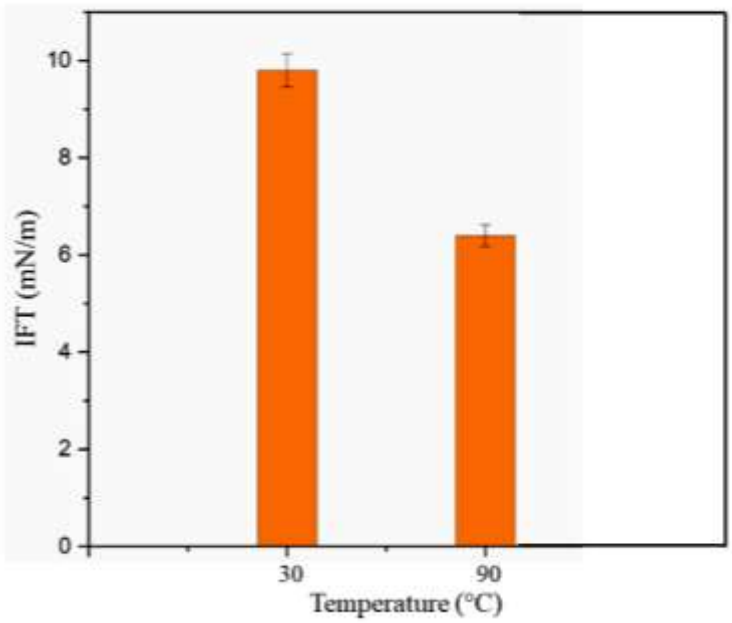

Figure 7.2: Interfacial tension (IFT) measurements between PCM (n-hexadecane) and natural surfactant solution at 30 and 90°C. The graph illustrates the variation in IFT as a function of temperature, highlighting the impact of the natural surfactant on the interfacial properties of PCM.

This reduction in IFT with increasing temperature is consistent with the general behavior of liquid-liquid interfaces, where higher temperatures typically lead to a decrease in IFT due to increased molecular motion and reduced intermolecular forces [242]. The results demonstrated that temperature has a significant impact on IFT, with higher temperatures leading to lower IFT values. These findings have important implications for applications in formulation of stable

emulsions, where controlling IFT is crucial. Additionally, the eco-friendly nature of the natural surfactant presents a compelling case for its use in industrial applications where environmental considerations are paramount. The study demonstrates that natural surfactants can effectively reduce the IFT between n-hexadecane and water, similar to synthetic surfactants. This suggests that natural surfactant effectiveness in reducing IFT may be enhanced under higher temperature conditions, relevant to thermal storage applications.

7.3.2 Characterization of n-PCM emulsion

Characterization of the synthesized n-PCM emulsions stabilized by natural surfactants was done using UV-Vis spectroscopy. These techniques provide insights into the optical properties and particle size distribution, which are essential for evaluating the stability and performance of the emulsions [347]. UV-Vis spectroscopy analysis provided insights into the optical behavior of n-PCM emulsions. This methodology serves as a reliable approach for characterizing the interaction between nanoparticles and the PCM, which is crucial for optimizing the performance of these materials in thermal energy storage applications [348]. The UV-Vis spectra indicated characteristic absorption peaks corresponding to the nanoparticles, confirming their presence and dispersion in the emulsion matrix. Figure 7.3 represent the absorbance peak for both the prepared n-PCM emulsions, that is, PCM1 and PCM2. From Figure 7.3, it can be seen that the peak for both the emulsions are at wavelength of 400 nm with peak values of 2.3119 and 1.4336 for PCM1 and PCM2 respectively. The high absorbance value typically reflects a stable dispersion of nanoparticles within PCM1. This stability ensures that nanoparticles are uniformly distributed, which is crucial for enhancing the thermal and optical properties of the n-PCM. The effective interaction of nanoparticles with light at this concentration suggests optimal dispersion and minimal aggregation. Conversely, the lower absorbance value of PCM2 may indicate that

nanoparticles have begun to aggregate or form larger clusters, reducing their effective surface area and interaction with light. Aggregation can result from exceeding the optimal concentration, leading to a non-uniform dispersion and potential sedimentation of nanoparticles [349]. These aggregated nanoparticles can decrease the emulsion's overall performance, making it less efficient for its intended applications. Thus, PCM1 signifies effective nanoparticle dispersion and strong light interaction, which is beneficial for maintaining the emulsion's desired properties.

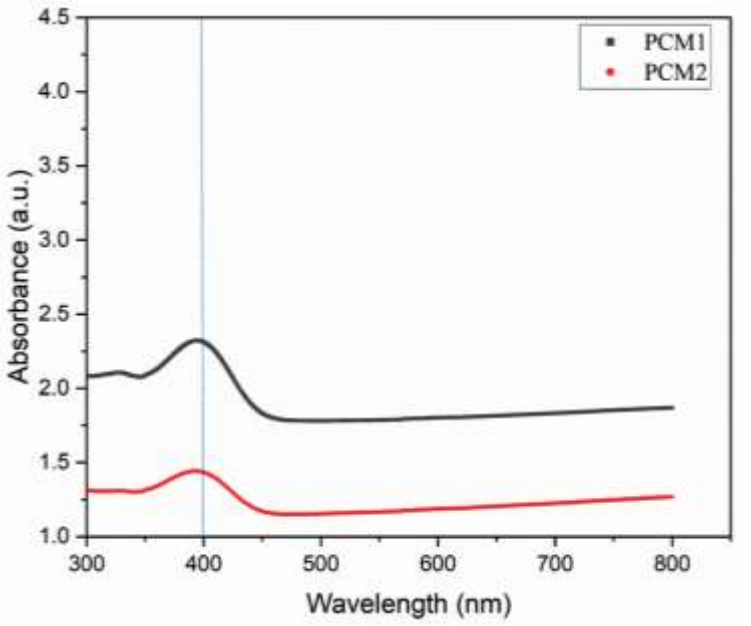

Figure 7.3: UV-*vis* spectra of PCM1 and PCM2 with varying concentrations of silica nanoparticle. All the measurements were conducted at ambient conditions.

7.3.3 Stability and microscopic investigations of n-PCM emulsion

The two n-PCM emulsions (PCM1 and PCM2) stabilized by single step silica nanofluid and natural surfactant (at CMC) is shown in Figure 7.4. Both the prepared emulsions were left undisturbed and kept under observation for 30 d to observe the phase separation as shown in Figure 7.4. From Figure 7.4, it can be clearly seen that PCM1 was highly stable with lesser water release as compared to PCM2.

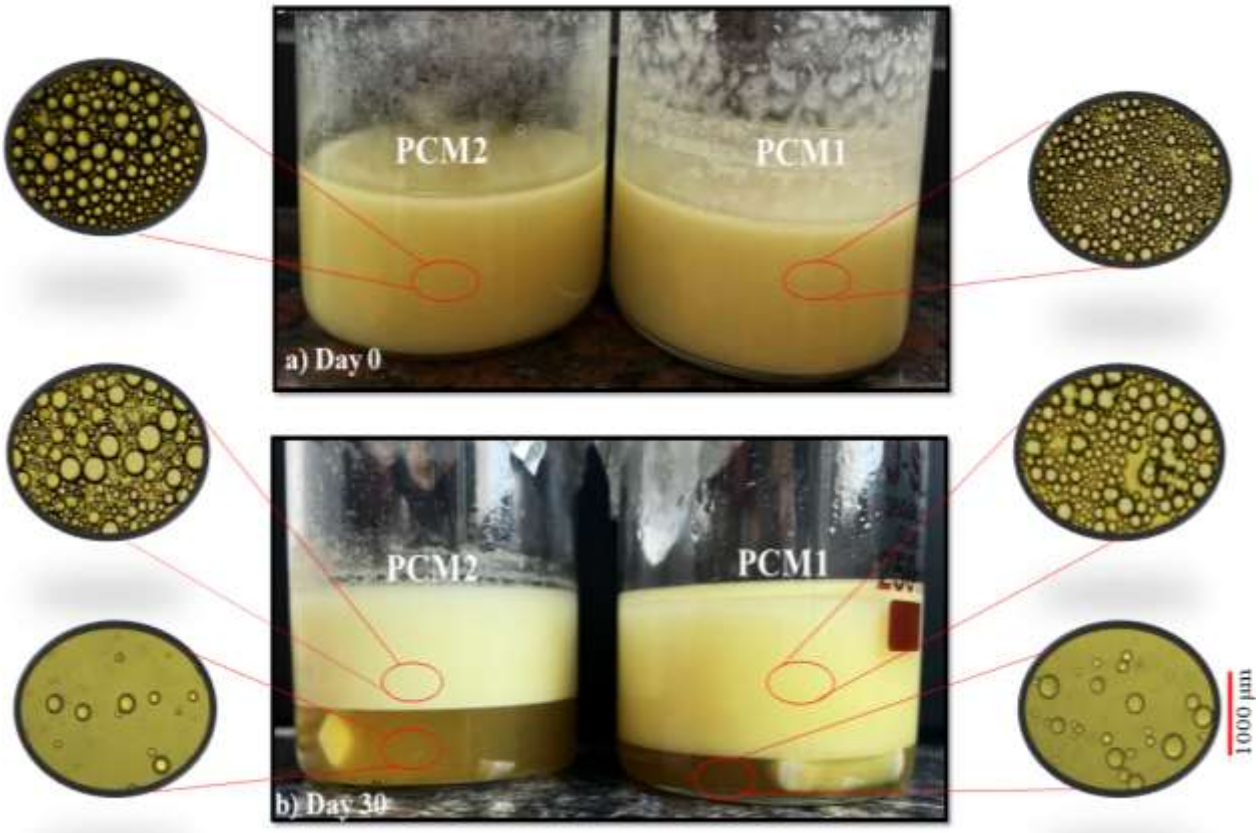

Figure 7.4: Visual representation and optical graph of PCM1 and PCM2 at Day 0 and Day 30, showing initial clarity and potential phase separation over time.

The increased phase separation in PCM2 compared to the PCM1 may be primarily due to enhanced particle interactions and increased viscosity, which collectively results in weakening emulsion's stability and lead to greater phase separation. This may be also attributed to presence of large sized droplet in freshly prepared PCM2 as shown in Figure 7.4. In PCM2, larger droplet sizes and a higher degree of aggregation were observed over time, suggesting increased particle interactions that promote coalescence and phase separation [17]. Conversely, PCM1 maintained a more consistent droplet size distribution, with fewer occurrences of droplet fusion, indicating greater stability. In addition to this, surfactant used at CMC results in the formation of micelles to stabilize the n-PCM emulsion droplets in the aqueous phase, preventing coalescence and

enhancing dispersion [266]. This effect is crucial for applications where uniform distribution of n-PCM emulsion is required for efficient thermal management. Thus, PCM1 likely allowed the natural surfactant to more effectively cover the surface of the droplets and nanoparticles, preventing aggregation and maintaining the emulsion's stability as evident from Figure 7.4. Moreover, microscopic observations were carried out for the aqueous phase left after phase separation, as a result loose packaging of droplets were observed as shown in Figure 7.4.

Furthermore, the thermal stability of both PCM1 and PCM2 was observed via optical microscope at 30, 60 and 90°C as shown in Figure 7.5. From Figure 7.5, it can be observed that at 30°C, PCM1 possess the tight and uniform packing of oil droplet whereas in PCM2, the packaging of oil droplet was comparatively lesser denser and uniform. The stability of n-PCM emulsions is significantly influenced by the choice of surfactant used to prevent droplet coalescence and particle aggregation. Natural surfactants have gained attention due to their biodegradability, biocompatibility, and low toxicity [28]. These surfactants adsorb at the oil-water interface, reducing interfacial tension and forming a protective barrier around the droplets or nanoparticles, thereby enhancing the stability of the emulsion [41]. As the temperature reaches to 60°C, coalescence of droplets was observed and more coalescence was visualized in PCM2 as compared to PCM1. This may be attributed to the higher concentration of nanoparticle in PCM2 leads to increased particle density, enhances particle-particle interactions, leading to a greater tendency for aggregation and flocculation [239]. Lastly, when the temperature reaches to 90°C, fairly dense packet of oil droplet was observed for PCM1 whereas in PCM2, more coalescence of oil droplet was observed and was thermally less stable. Natural surfactant used at CMC has shown its potential in emulsification and found effective at reducing IFT and stabilizing individual droplets for PCM1 but may become insufficient to fully counteract the destabilizing effects caused by the increased

nanoparticle loading in case of PCM2 [4]. As a result, PCM1 was found to possess greater thermal stability than that of PCM2.

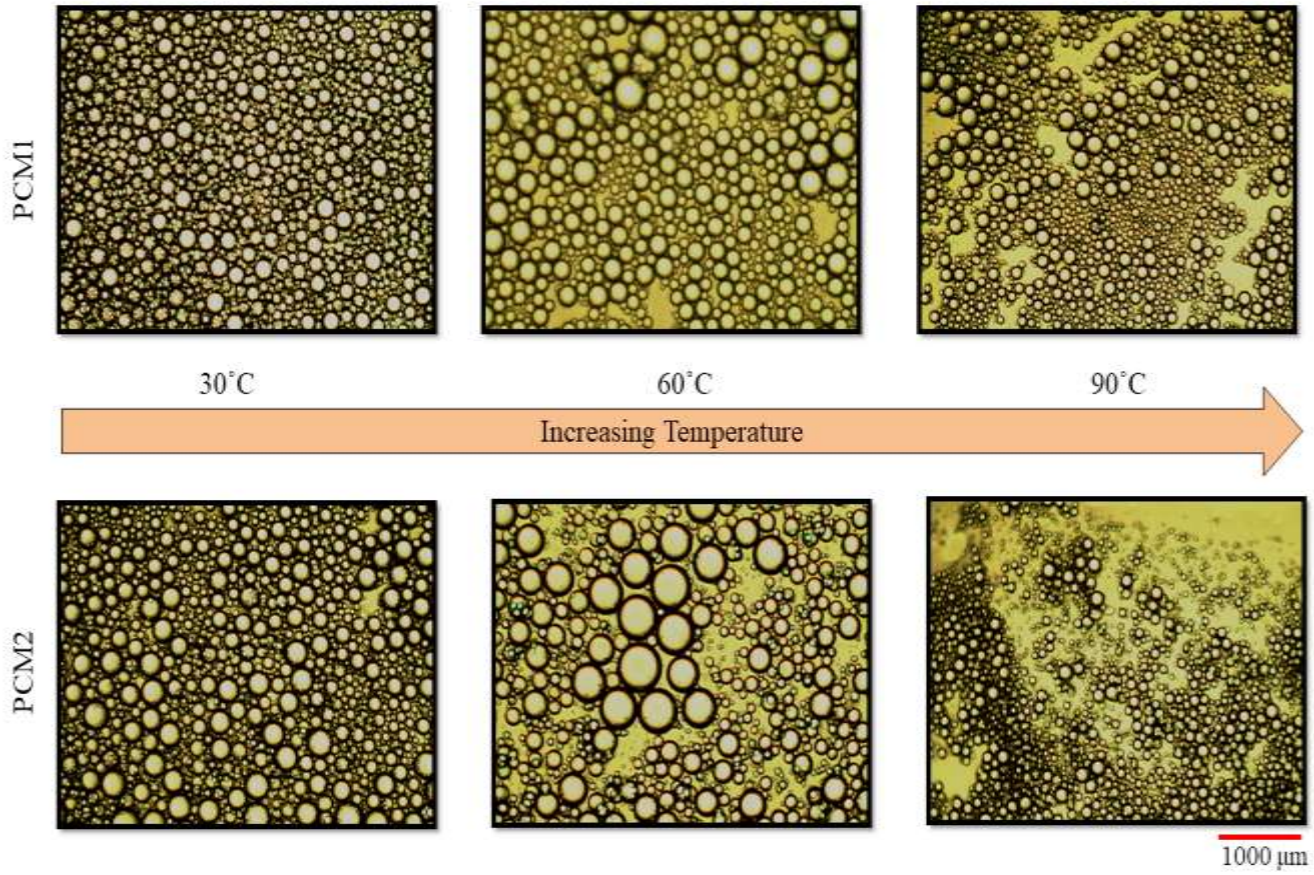

Figure 7.5: Microscopic images of PCM1 and PCM2 at 30, 60, and 90°C. The images illustrate the variation in droplet distribution and emulsion stability with changing weight percentages and varying temperature.

7.3.4 SEM and EDX measurements

SEM analysis was employed to investigate the morphology and structural characteristics of the prepared n-PCM emulsion. The SEM micrographs prepared emulsions are shown in Figure 7.6.

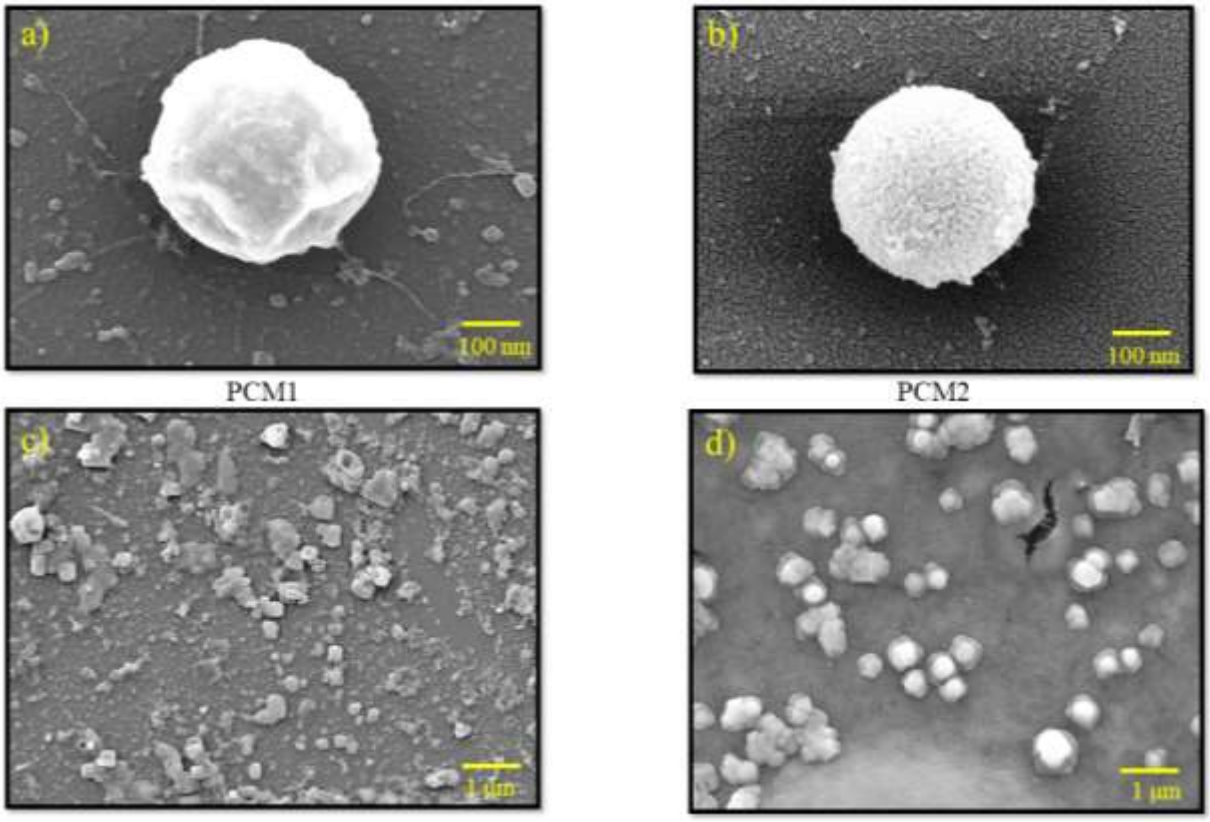

Figure 7.6: SEM images illustrating the morphology of emulsion droplets in (a) PCM1 and (b) PCM2; (c) PCM1 showcasing the dispersion and uniformity of particles within the emulsion matrix and (d) Noticeable particle aggregation in PCM2, illustrating clustering and reduced uniformity at higher concentration.

Figure 7.6 (a) and 7.6 (b) shows the micrograph of emulsion droplet of PCM1 and PCM2 respectively and are found to possess spherical shape as reported literature [73]. Moreover, Figure 7.6 (c) and 7.6 (d) are the SEM micrographs of PCM1 and PCM2 respectively showing the dispersion of the particle within the PCM matrix. The distribution of the particles in PCM1 are observed to be uniform and are prone to less agglomeration as evident from Figure 7.6 (c). In contrast, agglomeration of particles can be clearly visualized from Figure 7.6 (d) for PCM2. This behavior may be attributed to the increased concentration of particles in silica nanofluid, which

may lead to greater particle-particle interactions and destabilization of the emulsion as compared to PCM1 [350]. The evenness of particle distribution within PCM1 was observed and good dispersion is crucial for ensuring consistent thermal performance across the material. SEM images provided in Figure 7.6 capture the morphology of the dried sample rather than the in-situ distribution within the emulsion. However, obtaining high-resolution imaging of in-situ state presents significant challenges due to liquid nature of the emulsion. To address this concern, our analysis is supplemented with optical microscopy as well as *UV-vis* spectroscopy results to better illustrate the dispersion of particles within PCM matrix.

Along with the SEM analysis, EDX spectrum of both PCM1 and PCM2 is shown in Figure 7.7 and Figure 7.8 respectively. In PCM1, main elements observed during the analysis were silicon (Si), oxygen (O) and carbon (C) as shown in Figure 7.7. Oxygen was observed to be the dominating element (56.6%) in the PCM matrix. This may be due to selection of organic PCM (n-hexadecane) for this study which often include oxygen-rich compounds such as esters, alcohols, or acids and the presence of these compounds in the emulsion can result in a higher concentration of oxygen. The other two elements found were comparatively lower, that is, 30.3% silicon and 13.1% carbon. The lesser concentration of carbon may be attributed to the presence of natural surfactants which might contribute to the carbon content, but these are typically present in smaller amounts compared to the inorganic silica nanoparticles and organic PCM used [30,217]. In PCM2, main elements observed are silicon (Si), oxygen (O), carbon (C), nitrogen (N), sodium (Na) and sulfur (S) as shown in Figure 7.8. The dominance of oxygen (49.1%) followed by silicon (25.1%) and carbon (16.6%) are observed and resembles same as in case of PCM1. The other element detected Na, N and S are in vey lower amount, that is, 7.4%, 1.2% and 0.6 %. These minor elements detected may be attributed to presence of natural surfactant as reported in previous study [30].

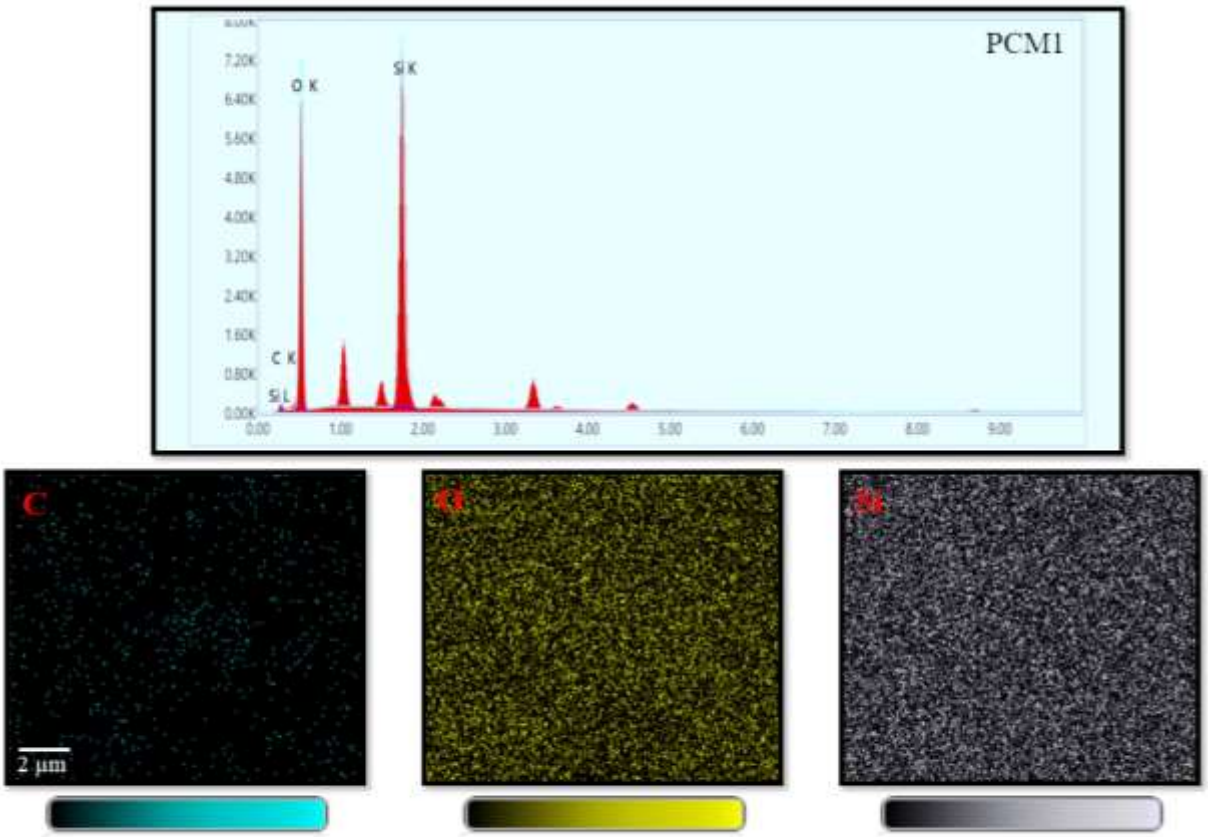

Figure 7.7: EDX analysis of PCM1 highlighting the elemental composition and distribution within the emulsion matrix.

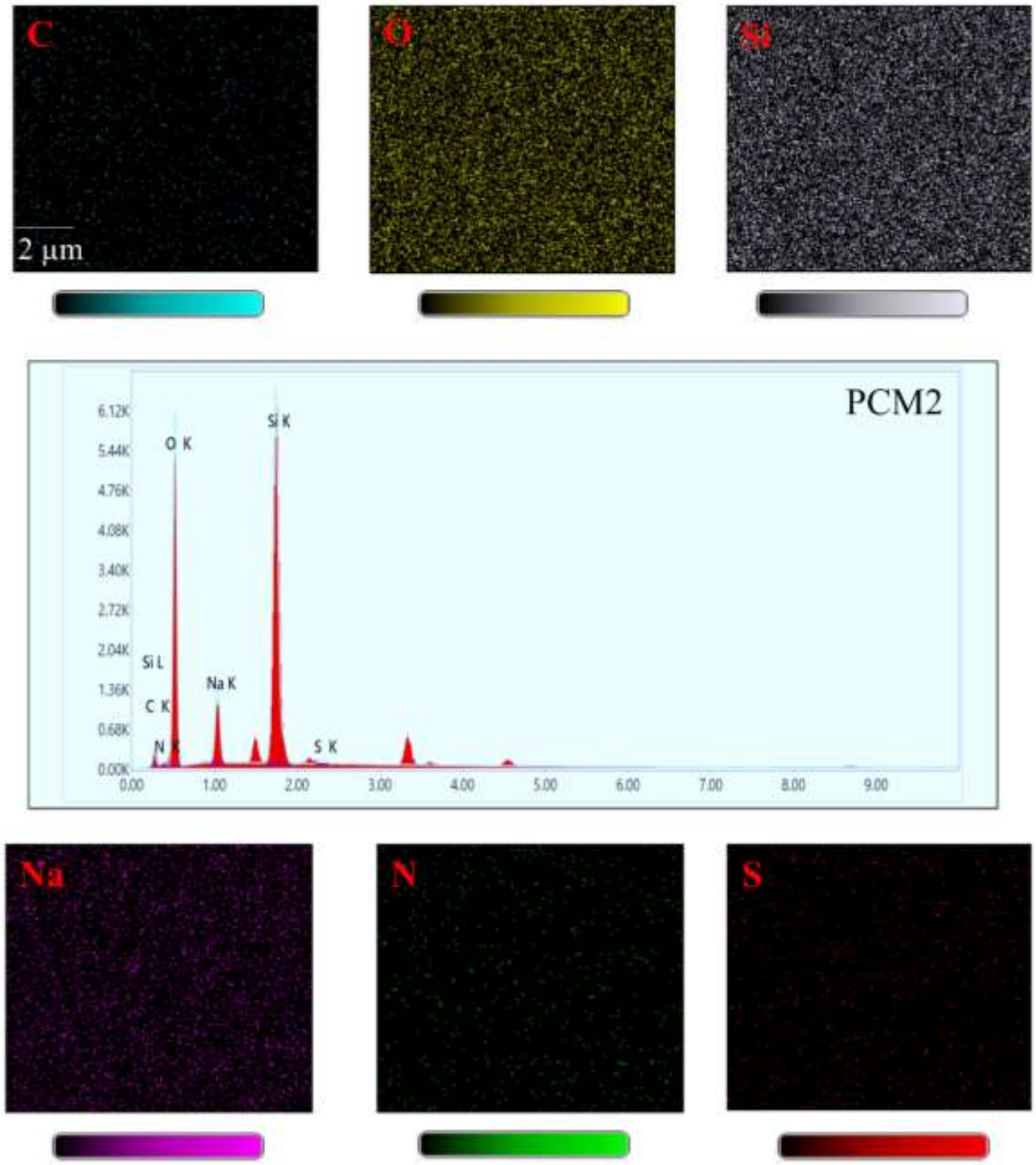

Figure 7.8: EDX analysis of PCM2 revealing the elemental composition.

7.3.5 Rheological investigation of n-PCM emulsions

Rheological properties are critical for understanding the flow behavior and stability of n-PCM emulsions, which are increasingly used in energy storage and thermal management

applications. Rheological properties help in understanding the stability of emulsions by indicating how particles are dispersed within the continuous phase [303].

7.3.5.1 Shear rheology results

Rheological measurements can provide insights into the microstructural interactions within the emulsions, such as particle-particle interactions and the effects of surfactants [309]. These interactions influence the overall performance and efficiency of the emulsion in various applications. Rheological measurements were conducted for both PCM1 and PCM2 at 30 and 90°C as shown in Figure 7.9.

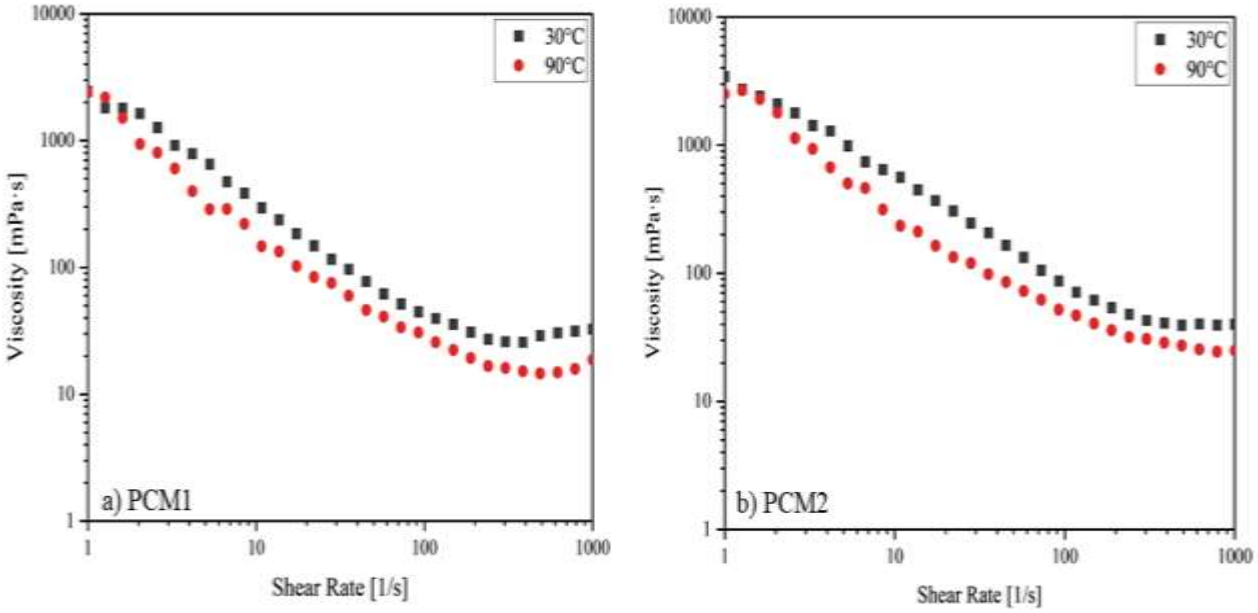

Figure 7.9: Rheological analysis of PCM1 and PCM2 at 30 and 90°C, illustrating the viscosity and flow behavior of the emulsions under varying conditions. highlighting the effect of concentration and temperature on their rheological properties.

The rheological analysis of both the n-PCM emulsions reveals a pronounced shear-thinning behavior across a range of shear rates (1-1000 s^{-1}) [55,229]. The viscosity of the emulsions decreases with increasing shear rate, indicating that the emulsion transitions from a more viscous

state at low shear rates to a less viscous state at high shear rates. This behavior is characteristic of non-Newtonian fluids and can be attributed to the microstructural reorganization of n-PCM particles within the emulsion matrix as per literature studies [323,351]. The viscosity of PCM1 was observed to be 2441 mPa.s at shear rate of 1 s^{-1}, 295 mPa.s at shear rate of 10 s^{-1}, 42 mPa.s at 100 s^{-1} and 32 mPa.s at 1000 s^{-1} as shown in Figure 7.9 (a). The shear-thinning properties of n-PCM emulsions are advantageous in practical applications where varying flow conditions are encountered. For instance, in cooling systems or thermal energy storage, the ability of the emulsion to decrease viscosity under high flow rates can lead to reduced pumping costs and improved energy efficiency. Further the flow behavior of PCM1 was investigated at elevated temperature (90°C) as shown in Figure 7.9 (a). From Figure 7.9 (a), it can be seen that the viscosity was 2398 mPa.s at 1 s^{-1}, 147 mPa.s at 10 s^{-1}, 29 mPa.s at 100 s^{-1} and 19 mPa.s at 1000 s^{-1}. By comparing both data obtained at 30 and 90°C, it can be concluded that the emulsion was highly stable at 90°C at lower shear rates whereas at higher shear rate a fair reduction in viscosity profile was observed. This may be attributed to presence of natural surfactants, which are surface-active agents, play a pivotal role in maintaining the stability of these emulsions by reducing IFT and forming protective barriers around the dispersed n-PCM particles within the emulsion matrix.

Furthermore, the flow behavior of PCM2 was also investigated at 30 and 90°C as shown in Figure 7.9 (b). The viscosity at 30°C was observed to be 3429 mPa.s at 1 s^{-1}, 562 mPa.s at 10 s^{-1}, 85 mPa.s at 100 s^{-1} and 40 mPa.s at 1000 s^{-1}. The viscosity at 90°C was observed to be 2506 mPa.s at 1 s^{-1}, 235 mPa.s at 10 s^{-1}, 50 mPa.s at 100 s^{-1} and 25 mPa.s at 1000 s^{-1}. The viscosity values have been rounded off in accordance with the estimated uncertainty (±0.6–8.4%) to ensure consistency with the precision of the measurements. By comparing both the data 30°C and 90°C of PCM2 as shown in Figure 7.9 (b), it can be clearly seen that drop in viscosity profile at higher

temperature (90°C) was significant as compared to 0.5 wt% n-PCM emulsion. This may be attributed to increased concentration of silica nanoparticles, that have a greater tendency to aggregate due to stronger van der Waals forces and increased particle-particle interactions [352]. This aggregation can lead to the formation of larger clusters, which reduces the effective surface area available for stabilizing the emulsion [353]. As a result, the emulsion becomes less stable under thermal conditions, leading to a more significant drop in viscosity at elevated temperatures. The reduced thermal stability of PCM2 compared to PCM1, as indicated by their viscosity profiles (Figure 7.9), is primarily due to particle aggregation, interference with surfactant stabilization, and thermodynamic limits. These factors collectively result in a less stable emulsion at higher temperatures, leading to a more significant reduction in viscosity. Understanding these effects is crucial for optimizing the formulation and ensuring the effective use of n-PCM emulsions in thermal management applications. Shear-thinning fluids exhibit high viscosity at low shear rates and reduced viscosity at high shear rates. In subsurface recovery processes, this property is advantageous during injection and flow through porous media. The higher viscosity at low shear helps in improving mobility control, reducing fingering effects and enhancing sweep efficiency. As the fluid experiences higher shear while being pumped, its viscosity decreases, allowing easier injection with lower energy requirements. Once inside the reservoir, viscosity increases again under low shear conditions, supporting better displacement of trapped fluids. In heat-transfer systems, shear-thinning behavior improves pumping efficiency while maintaining sufficient viscosity for stable suspension of nanoparticles or PCM droplets. This ensures uniform dispersion, reduced sedimentation and consistent thermal performance. Thus, shear-thinning rheology enhances operational efficiency, stability and performance in both applications.

7.3.5.2 Dynamic rheology results

Dynamic rheology helps in understanding the viscoelastic nature of n-PCM emulsions, which exhibit both solid-like (elastic) and liquid-like (viscous) behavior [354]. By measuring parameters such as the storage modulus (G'), which indicates the elastic or solid-like behavior, and the loss modulus (G''), which reflects the viscous or liquid-like behavior [61], researchers can gain insights into the material's ability to store and dissipate energy. This information is crucial for applications where both flow and structural stability are important, such as in thermal energy storage systems. Strain-sweep measurements were conducted for both PCM1 and PCM2 at 30 and 90°C as shown Figure 7.10 and 7.11 respectively and the frequency was kept constant at 10 rad. s^{-1} as mentioned in literature studies [56,174,263].

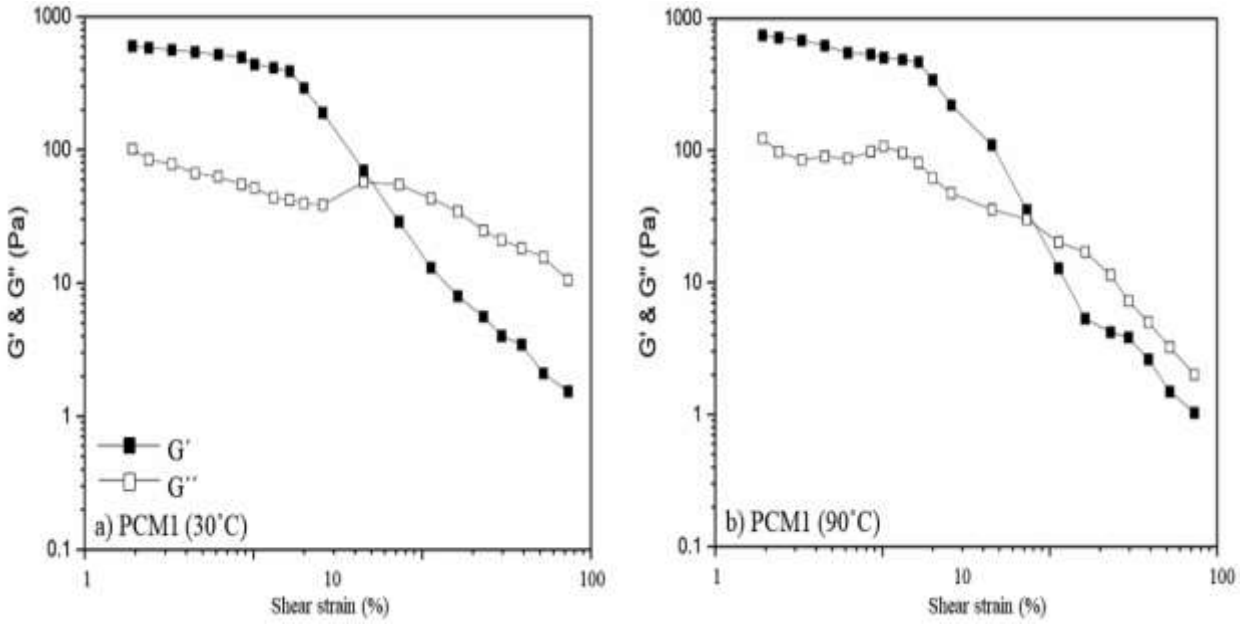

Figure 7.10: Oscillatory rheological analysis of PCM1 conducted at 30 and 90°C. The data illustrate the emulsion's viscoelastic properties over a range of shear strain.

For PCM1 at 30°C, storage modulus was observed to fall from 600 Pa to 1 Pa when shear strain was varied from 1-100% whereas the reduction in loss modulus was from 103 Pa to 7 with

a cross over point at ~ 60 Pa with 28% shear strain (Figure 7.10 (a)). Same emulsion was investigated at elevated temperature (90°C) where the storage modulus was observed to fall from 879 Pa to 1 Pa whereas 146 Pa to 2 Pa reduction was observed in loss modulus shear strain was varied from 1-100% (Figure 7.10 (b)). The experimental results have been rounded off appropriately based on the estimated uncertainty to ensure clarity and alignment with the accuracy of the measurements. These rounded values fall within the reported uncertainty range (±0.6-8.4%) and maintain the precision required for reproducibility. Also, a shift in cross over point was observed from ~60 Pa (at 30°C) to ~ 29 Pa at 40 % shear strain (at 90°C). A shift in the crossover point towards higher strain indicates a robust network with stronger interparticle and surfactant interactions, which enhances the emulsion's ability to resist deformation and maintain stability [355]. This may be also attributed to addition of effective surfactant and optimized particle concentration (0.5 wt%) that result in shift the crossover point to a higher strain, reflecting improved stability and a more cohesive internal structure [356].

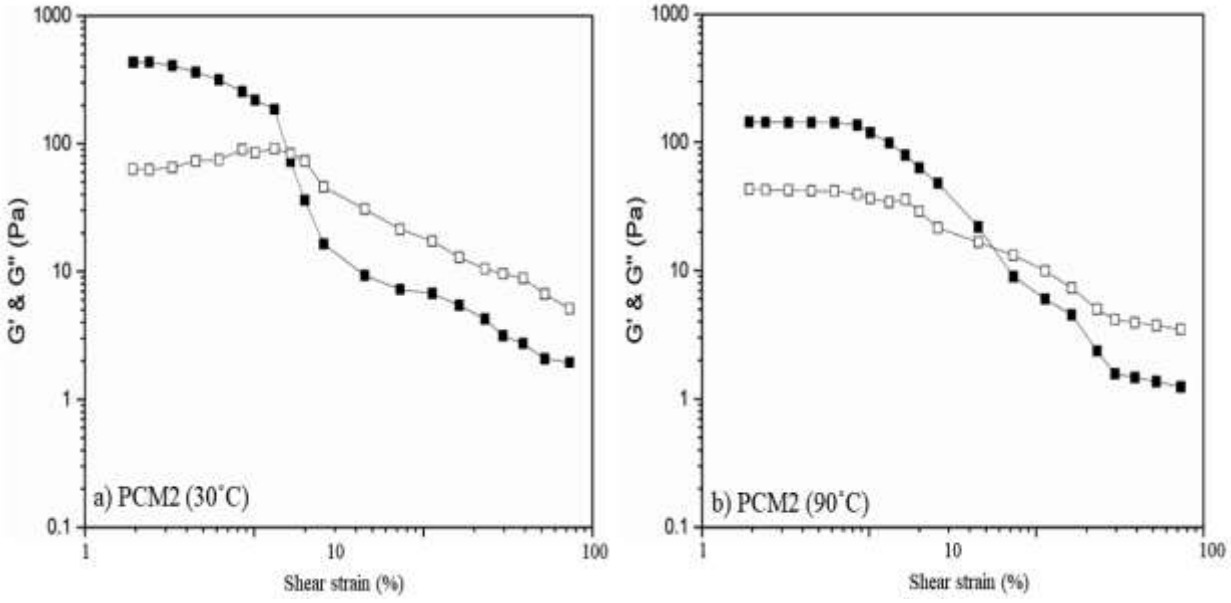

Figure 7.11: Oscillatory rheological analysis of PCM2 demonstrating shear strain dependence at a constant frequency, highlighting changes in viscoelastic behavior with temperature.

Similarly, for PCM2 at 30°C, the storage modulus was observed to fall from 622 Pa to 1 Pa whereas 67 Pa to 4 Pa reduction was observed in loss modulus shear strain was varied from 1-100% (Figure 7.11 (a)) with a cross over point at 83 Pa at 8.5% shear strain. Conversely at 90°C, storage modulus was observed to fall from 156 Pa to 1 when shear strain was varied from 1-100% whereas the reduction in loss modulus was from 49 Pa to 3 Pa with a cross over point at ~ 15 Pa with 21% shear strain (Figure 7.11 (b)). The shift in crossover point has been slightly increased as compared to PCM1 as shown in Figure 7.10. This may be primarily attributed to presences of higher silica content (1 wt%), where the potential of surfactant layers that stabilized the emulsion might become more strained or disrupted at elevated temperatures [357]. This disruption can lead to a more breakdown of the emulsion's structural network at high temperatures in PCM2, causing a larger shift in the crossover point. Also, the viscoelastic properties are more affected in the higher silica concentration due to changes in the particle interactions, resulting in a more substantial shift in the crossover point at higher temperature [358].

7.3.6 DSC analysis

DSC analysis is vital for evaluating the thermal properties, stability, and overall performance of PCM emulsions, which are widely used in energy storage, thermal management, and other applications [323,337]. DSC can accurately measure the temperatures at which PCMs undergo phase changes (e.g., melting and solidification) [338]. This information is essential for evaluating the effectiveness of PCM emulsions in thermal energy storage applications, as it helps determine the operational temperature range. DSC can also provide insights into the crystallization behavior of PCMs, including supercooling effects [359]. The plot of DSC for PCM1 and PCM2 is shown in Figure 7.12 (a) and 7.12 (b) respectively. Heat flow is measured as a function of temperature to study the thermal properties of materials. The heat flow can be either positive or

negative, and these directions indicate different thermal processes occurring in the n-PCM emulsion matrix. In this study, it was assumed that a positive heat flow in DSC indicates that the system is absorbing heat from its surroundings, corresponding to an endothermic process. [360]. Both the prepared n-PCM emulsion absorbs heat from the surrounding when temperature was varied from -20°C to 50°C witnessing the endothermic event. As a result, positive heat flow was observed during the melting of the n-PCM emulsions. During this process, the material absorbs heat to overcome intermolecular forces or break chemical bonds. The melting point and enthalpy of melting was observed to be 21.08°C and 1205.171 J/g respectively for PCM1 (Figure 7.12 (a)). Similarly, for PCM2 the melting point of 22.65°C and enthalpy of melting 1627.145 J/g was observed (Figure 7.12 (b)).

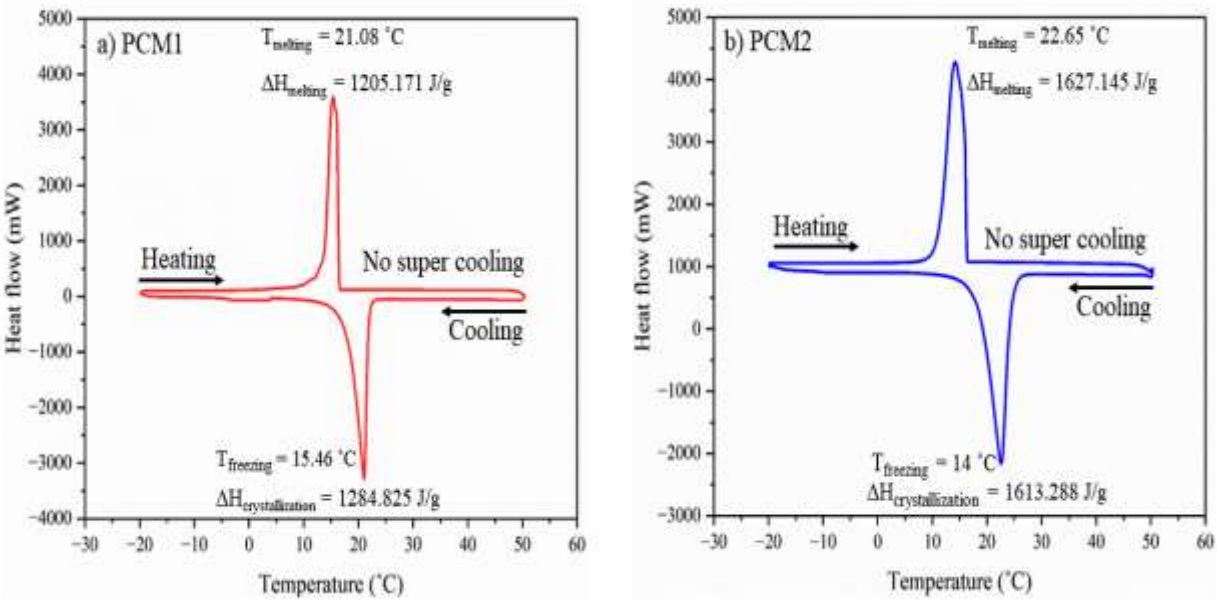

Figure 7.12: DSC thermograms of PCM1 and PCM2. The analysis highlights the thermal behavior of the emulsions, including phase transitions. Peaks corresponding to the melting and crystallization temperatures of n-PCM emulsions are shown, demonstrating how concentration affects the thermal properties of the emulsion.

Both tested n-PCM emulsions did not exhibit supercooling, confirming the stability and reliable thermal response of the system under the experimental conditions. Conversely, a negative heat flow indicates that the system is releasing heat to its surroundings and referred to as exothermic process. Both the prepared n-PCM goes through the exothermic events that result in negative heat flow and crystallization was observed. During this process, the material releases energy as it forms new bonds or crystallizes from a disordered state. The freezing point and enthalpy of crystallization was observed to be 15.46°C and 1284.825 J/g respectively without any supercooling for PCM1. Similarly, no supercooling was observed for PCM2 with the freezing point of 14°C and enthalpy of crystallization as 1613.288 J/g. The enthalpy of phase change for the emulsion appears significantly higher than that of pure n-hexadecane. The observed increase in enthalpy may be attributed to unique characteristic of the material used in this study. Unlike previous works where enhancement was achieved using externally added commercial nanoparticles, which are susceptible to agglomeration, whereas present approach utilized a single-step based synthesized silica nanofluid. This nanofluid offered superior dispersion stability, reducing the likelihood of agglomeration and ensuring better integration within PCM matrix. Additionally, present study is aligned with the trends reported in literature to validate the observations. A study by Murugan et al. [361] reported that the latent heat of pure paraffin during melting and freezing cycles was 131.8 J/g and 139.2 J/g, respectively. The addition of 0.9 wt% nanofluid (MWCNTs) resulted in an increase to 148.3 J/g and 150.7 J/g, respectively. This study observed a maximum enhancement in latent heat of approximately 7.6% and 11%, respectively, compared to pure PCM.

The DSC curves showed that the melting and crystallization temperatures of n-PCM emulsions were affected by the presence of silica nanofluid. PCM2 generally exhibited slightly

higher melting points compared to PCM1. This could be attributed to enhanced nucleation effects and altered thermal dynamics [362]. The incorporation of silica nanofluid into PCM leads to modified thermal properties, including phase transition temperatures and enthalpy values [363]. The increase in silica concentration impacted the stability of the emulsions (as evident from SEM, microscopic and rheological results), leading to observable changes in the DSC curves. The results suggest that silica additives can enhance the performance of PCM by influencing their thermal behaviors, making them potentially more effective for thermal energy storage applications. In addition to this, an increase in enthalpy of PCM1 and PCM2 compared to pure n-hexadecane (236 J/g) is beneficial for thermal storage applications because it enhances the material's capacity to store and release thermal energy, improves phase change efficiency, reduces supercooling, and increases stability. These improvements make the n-PCM emulsions more effective and reliable for various thermal management and energy storage applications. DSC analysis revealed that the thermal properties of n-PCM emulsions are significantly affected by the addition of silica nanofluid. Both 0.5 wt% and 1 wt% silica concentrations altered the phase transition characteristics, with notable differences in melting and crystallization temperatures as well as enthalpy values. These findings provide valuable insights for optimizing PCM emulsions for various thermal management and energy storage applications. In our subsequent studies, it was consistently observed that a lower nanoparticle concentration, around 0.5-1 wt%, proved to be the most effective in balancing performance, cost efficiency, and stability, outperforming higher concentrations [99,165,274]. This trend highlights that beyond a certain threshold, increasing nanoparticle concentration does not necessarily yield proportional benefits and may even lead to challenges such as aggregation or increased viscosity. Therefore, in this study, lower concentration

range (0.5–1.0 wt%) was explored to maintain an optimal balance between effectiveness and practicality.

Furthermore, thermal cycling tests were conducted to evaluate the stability and performance of PCM1 and PCM2 under repeated heating and cooling conditions as shown in Figure 7.13. The test was conducted over 25 and 50 cycles, with each cycle consisting of heating the sample to the melting point and then cooling it back to the solidification point [364]. The thermal cycling tests demonstrated that both the prepared n-PCM emulsions remained thermally stable throughout the cycling process. Specifically, there were no observed changes in the melting and solidification points of the emulsions after 25 and 50 cycles. This stability indicates that the emulsions retained their phase change characteristics and performance over repeated thermal stress. Thermal cycling tests showed that the emulsions retained their homogeneity, with no visible phase separation after multiple heating and cooling cycles. Presence of silica nanoparticles provided structural reinforcement to emulsion droplets, while natural surfactant maintained interfacial stability by preventing coalescence. DSC analysis confirmed that the latent heat storage capacity and melting-freezing temperatures remained nearly unchanged after cycling, indicating thermal reliability of the PCM system. The enthalpy of crystallization/ melting and the phase transition temperatures of PCM1 and PCM2 was consistent with their initial values. This suggests that the single step silica nanofluid and the natural surfactant effectively stabilized the n-PCM emulsion, preventing any significant degradation or alteration in phase change properties. This demonstrates the robustness of these emulsions for practical use in thermal energy applications. Temperature influences both surfactant performance and emulsion integrity. At elevated temperatures beyond the optimal range, reduced interfacial strength and increased droplet mobility may promote coalescence. Thermal cycling tests indicated stability within the studied range, but

very high temperatures may weaken the protective surfactant layer. Salinity may significantly affect electrostatic interactions. Increased ionic strength compresses the electrical double layer, which can lead to droplet aggregation and nanoparticle clustering. Nanoparticle concentration is also critical. While silica nanoparticles improve structural stability, excessive loading promotes agglomeration and increases viscosity, affecting flow behaviour. Therefore, an optimum balance between surfactant concentration and nanoparticle loading is necessary to maintain emulsion stability and practical usability.

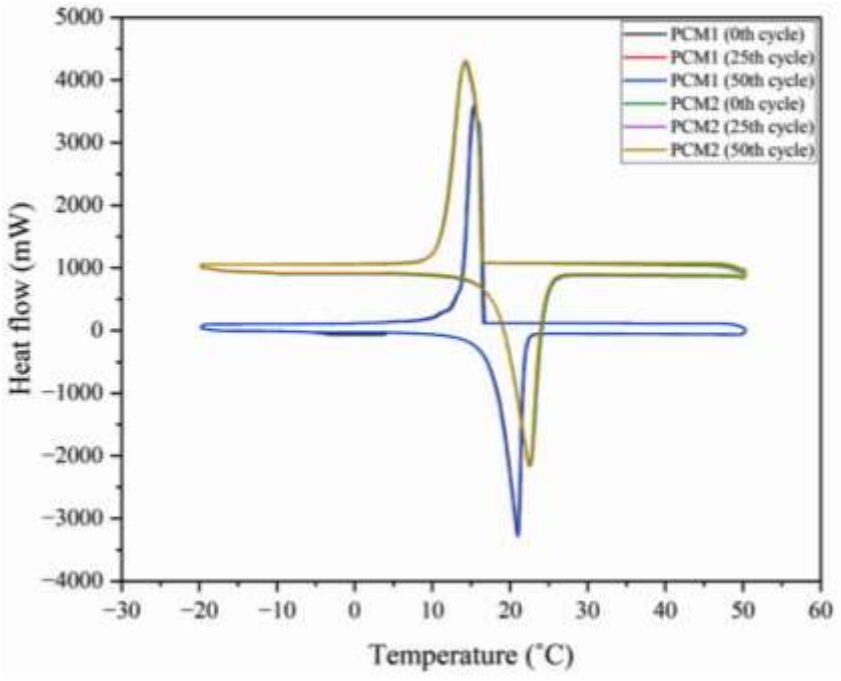

Figure 7.13: DSC analysis of PCM1 and PCM2 subjected to 0, 25, and 50 thermal cycling tests. Prepared emulsions seem to be thermally stable.

Under high-salinity conditions, stability may be influenced by ionic strength; however, optimized surfactant concentration and nanoparticle loading minimized aggregation. DLS and zeta potential measurements can indicate acceptable particle size distribution and electrostatic stability even in

saline media. These observations demonstrate that combined action of surfactant and silica nanoparticles ensures resistance to thermal stress and salt-induced destabilization, supporting the suitability of these systems for long-term thermal energy storage applications.

7.3.7 Corrosion test results

Stabilization of n-PCM emulsion (PCM1 and PCM2) using natural surfactants and nanoparticles has shown promising results in enhancing the stability. However, the corrosion effects of these emulsions on different metals are a concern for long-term application. This study focuses on evaluating the corrosion rates of Al, Cu and SS when exposed to PCM1 and PCM2 and the detailed corrosion analysis is shown in Figure 7.14.

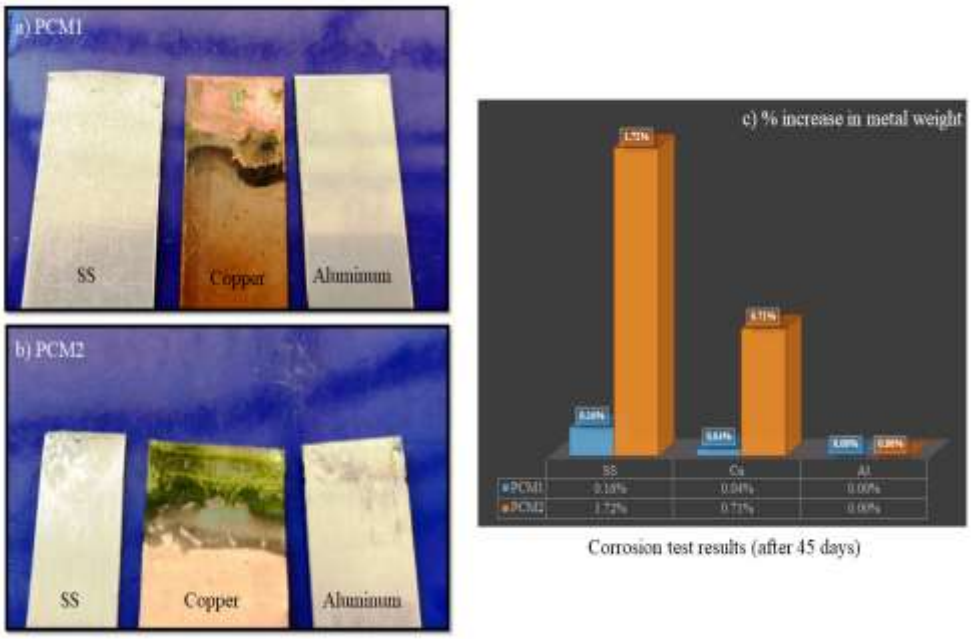

Figure 7.14: Corrosion test results showing the visuals of metal samples (stainless steel, aluminum, and copper) immersed in (a) PCM1 and (b) PCM2 for 45 days. (c) Increase the weight of all metal samples over time, reflecting the corrosion effect of the emulsion.

From the Figure 7.14, it can be clearly seen that SS plate gets corroded in PCM2 with 1.72% increase in the weight of the plate as compared to PCM1 with 0.16% increase in weight of plate. The presence of both organic (natural surfactants) and inorganic (silica nanoparticles) compounds in the emulsion may lead to the formation of complex compounds on the SS surface [365]. These compounds can integrate into the corrosion product layer, resulting in additional weight gain. A little corrosion in Cu plate was observed with increase in weight of plate ~ 0.04% for PCM1 and fairly increase in corrosion was observed for PCM2 with 0.71% increase in weight. When copper is exposed to an environment containing an n-PCM emulsion, it can react with oxygen and water to form corrosion products such as copper oxides and are typically adherent and accumulate on the copper surface, resulting in an increase in weight [366]. The emulsion environment may also influence the rate and type of oxides formed, leading to variations in the extent of weight gain. No corrosion was observed in Al plate when exposed to both the prepared emulsions as shown in Figure 7.14. This may be attributed to the ability of Al to form a thin, dense oxide layer (aluminum oxide, Al_2O_3) on its surface when exposed to air or moisture. This oxide layer acts as a passive barrier that prevents the underlying metal from reacting with its environment [367]. In the presence of an n-PCM emulsion, this protective oxide layer remains intact, effectively blocking the emulsion components from causing any further corrosion. Thus, aluminum metals can be used for the long term storage of the prepared emulsions as mentioned in literature [364].

7.4 Conclusion

The stability and performance of n-PCM emulsions stabilized by natural surfactants and silica nanofluid (PCM1 and PCM2) have been comprehensively evaluated through various analytical techniques.

- The IFT between natural surfactants and organic PCM (n-hexadecane) was 9.8 mN/m at 30°C and reduced to 6.4 mN/m at 90°C underscores its potential utility in applications that involve varying thermal conditions.
- Microscopic observations revealed a more uniform distribution of droplets and enhanced emulsion stability was observed for PCM1 as compared to PCM2 (30°C). PCM1 offers superior thermal stability compared to PCM2 at elevated temperature (90°C).
- SEM images confirmed the presence and even distribution of silica nanoparticles within the PCM1 matrix than PCM2, showing their role in stabilizing the emulsion. EDX analysis provided further evidence of the silica nanoparticles' integration and their interaction with the PCM and surfactants.
- UV-vis findings indicates that PCM1 provides better optical performance in terms of absorbance, potentially due to more uniform distribution and fewer particle-particle interactions compared to PCM2.
- PCM1 exhibited better rheological performance in both shear and oscillatory measurements. This concentration provides a more favorable balance of viscosity and viscoelastic properties, making it preferable for applications requiring optimal flow behavior and structural stability.
- DSC result indicate that silica nanoparticles do contribute to the stabilization of n-PCM emulsions, excessive concentration (1 wt%) may lead to alterations in the thermal behavior, potentially affecting the performance of the PCM in applications where precise thermal control is critical. Thus, PCM1 is recommended for practical applications with long term storage in aluminum metals.

In summary, results suggest that natural surfactant could be a viable option for formulating stable emulsions in both ambient and elevated temperature environments. In addition, the incorporation of natural surfactants and silica nanofluid (at 0.5 wt%) into n-PCM emulsions enhances their stability, improves rheological properties, and contributes to better corrosion resistance. Thus, optimizing the silica concentration is crucial for achieving desired in n-PCM emulsions. The results support the potential application of these stabilized emulsions in various industries, including energy storage and thermal management.

Chapter 8

Sustainable Biomass derived Natural Surfactant in Fly Ash Industrial Waste Utilization for Carbon Storage: Evaluation of Environmental Impact

Abstract

The rising carbon emissions challenge global environmental sustainability and climate stability. This study aims to advance climate change mitigation by integrating fly ash and natural surfactant into CO_2 sequestration strategies. Fly ash, a by-product of industrial processes, presents an opportunity for innovative reuse. By integrating fly ash along with natural surfactant into CO_2 sequestration strategies, two pressing environmental issues can be addressed simultaneously: the management of industrial waste and the reduction of greenhouse gas emissions. The novelty of this work explores the application of fly ash along with natural surfactant in carbonation and CO_2 sequestration, aiming to contribute to the development of sustainable and effective climate change mitigation technologies Pressure decay studies revealed that a (5 wt% fly ash + FS) demonstrated the highest CO_2 absorption, supported by microscopic analysis. Further research on optimizing reaction conditions and kinetics of mineralization could enhance this method's efficiency and scalability for broader application.

8.1 Introduction

The increasing levels of carbon dioxide (CO_2) in the atmosphere has become a major concern due to its significant impact on global climate change. The global imperative to minimize CO_2 emissions has never been more critical as we confront the escalating challenges of climate

change [74]. International accords, such as the Paris Agreement, aim to limit global warming to well below 2°C above pre-industrial levels, with aspirations to cap the rise at 1.5°C [368]. Achieving these targets necessitates a substantial reduction in CO_2 emissions, which is the primary driver of anthropogenic climate change. India, as one of the world's fastest-growing economies, faces significant challenges in minimizing CO_2 emissions while sustaining its development trajectory [369]. The country's heavy reliance on coal for energy generation contributes to greenhouse gas (GHG) emissions, necessitating urgent and effective mitigation strategies. In 2007, CO_2 accounts for 70.72% of India's net GHG emissions. The country's GHG emissions is mostly caused by the energy sector (57.8%), with the production of electricity making up the greatest portion (65.4%) of these emissions [370]. Thus, CO_2 emissions in India is predicted to rise sharply. To address this issue, it requires innovative and effective strategies to reduce CO_2 emissions. Various approaches have been explored, including enhancing energy efficiency, transitioning to renewable energy sources, and implementing carbon capture and storage (CCS) technologies. By focusing on these strategies, nations worldwide are working collectively to mitigate the adverse effects of climate change and promote a sustainable future. Among these, CCS has gained considerable attention as it allows for the direct capture of CO_2 from industrial processes and its subsequent storage or utilization.

In this endeavor, mineral trapping is a promising method for CCS that involves the sequestration of CO_2 through chemical reactions with naturally occurring minerals. This process ensures long-term storage and minimizes the risk of leakage as well as quite simple to perform. As a crucial component of CCS strategies, mineral trapping offers a viable solution for mitigating climate change by permanently removing CO_2 from the atmosphere and reducing GHG concentrations. Direct mineral carbonation is a promising method for CO_2 sequestration,

addressing the urgent need to mitigate GHG emissions. This process involves the chemical reaction between CO_2 and naturally occurring minerals. In single step method, CO_2 reacts with alkaline metal oxide either by gas-solid method (dry) or aqueous method (wet) [342]. Among these two methods, aqueous method is considered as the most promising alternative for mineral carbonation. Annually, a large amount of CO_2 ~ 4.02 Giga tons is thought to be directly fixed and indirectly avoided by the means of CO_2 mineralization of alkaline wastes, as a result 12.5% reduction in global human CO_2 emissions [371]. Waste product like metallurgical slag from steel industry accounts for 325.2 – 407.1 g/kg of CO_2 sequestration. Various carbonation studies using metallurgical slag was reported in literature review due to its higher calcium content of ~ 23.66% and when exposed to CO_2 for 4 weeks in closed chamber, result in 9.32% of calcium carbonate ($CaCO_3$) [372–374]. A wide range of waste products were explored in literature, for instance, steel slag [75], basic oxygen furnace slag [76], blast furnace slag [77], concrete [78], fly ash [79], Sugarcane bagasse fly ash [80]. Out of these, fly ash can be considered as most promising waste material for sequestering CO_2 and a popular feedstock for CO_2 mineral carbonation due to its enormous yearly production [375].

Fly ash, a byproduct of coal combustion in power plants, is abundant and often considered a waste material, posing environmental disposal challenges. However, its rich content of calcium, silicon, aluminum, and iron oxides makes it a viable candidate for carbonation reactions. In these processes, fly ash reacts with CO_2 to form stable carbonates, effectively sequestering CO_2 and mitigating its release into the atmosphere. This dual benefit of reducing industrial waste and capturing CO_2 aligns with global efforts to combat climate change. Recent studies have focused on optimizing the carbonation conditions, enhancing the reactivity of fly ash, and understanding the underlying mechanisms to maximize CO_2 uptake. The method of coal burning along with the

mineralogy of the parent coal heavily influence the physical and chemical characteristics of coal fly ash [376]. Nonetheless, the majority of coal fly ashes produced worldwide are alkaline and include significant levels of calcium oxide (CaO) [377]. Reddy et al., (1986) was the first to investigate the improvement of fly ash's natural mineralization process using aqueous carbonation [81]. Sun et al., (2012) used brown coal fly ash (obtained from Latrobe Valley, Australia) for CO_2 sequestration via indirect mineralization under mild conditions. It was observed that maximum 264 kg of CO_2 per tonne of fly ash can be captured [82]. Ji et al., (2017) employed the application of fly ash from Chinese Shenfu coal for sequestration of CO_2 via direct mineralization. It was concluded from the study that addition of sodium carbonate (Na_2CO_3) (0.5 mol/L) leads to enhance the carbonation efficiency and performed the experiment in batch reactor at high temperature (140-220°C) and pressure (10-20 bar), as a result formation of $CaCO_3$ precipitates was observed [375]. Similarly, many studies of mineral carbonation using fly ash are reported in literature [378–380]. Moreover, for further enhanced carbonation efficiency, researchers introduce the addition of additives, for instance, brine solution [381]. Soong et al., (2006) conducted a carbonation study by using fly ash and brine for CO_2 sequestration under mild operating conditions. It was observed that when fly ash and brine solution reacts with CO_2, the major content of fly ash (CaO) gets converted into calcium hydroxide ($Ca(OH)_2$). Further, addition of sodium hydroxide (NaOH) leads to more CO_2 sequestration [377]. Yaumi et al., (2013) modified the surface of oil fly ash for selective capturing of CO_2. In this study, activation of fly ash was done by ~ 30% of ammonium hydroxide (NH_4OH), as a result surface area was enhanced from 59-318 m^2/g and leads to capture 240 mg/g of CO_2 [382]. Qian et al., (2005) performed the modification of municipal solid waste (MSW) fly ash by anionic chelating surfactant (ethylenediaminetriacetic acid lauryl and monolauryl phosphate). It was observed that fly ash activated by ethylenediaminetriacetic acid lauryl offers

higher active ratio (> 95%) than that of monolauryl phosphate [83]. Recent studies have explored the enhancement of fly ash's properties through various modifications. One promising approach involves the use of natural surfactants, which are environmentally benign and derived from renewable resources [32,40,41,59]. Our previous study deals in the extraction of natural surfactant from fenugreek seeds and its potential of CO_2 absorption was observed to be 9-15% higher than that of water [30]. In addition, the synergy of natural surfactant along with natural polymer was explored for CO_2 mobility control [167]. Moreover, the natural surfactant was used to stabilize the 0.1 wt% silica nanofluid, as a result more CO_2 absorption was observed in comparison to conventional nanofluid. Enhanced CO_2 absorption can be attributed to inclusion of natural derivative that offers enhanced surface area [333]. Natural surfactants can modify the surface characteristics of fly ash, increasing its active sites and improving its interaction with CO_2 molecules [383]. Despite the potential advantages, the integration of natural surfactants with fly ash for CCS applications remains underexplored. The novelty of integrating fly ash with natural surfactants for CO_2 entrapment lies in combining two sustainable materials to enhance the efficiency of CO_2 capture while addressing limitations of existing methods. Traditional CO_2 sequestration using fly ash relies primarily on direct carbonation, where CO_2 reacts with calcium and magnesium oxides in the ash to form stable carbonates. While effective, these methods often suffer from slow reaction rates and incomplete carbonation due to poor dispersion of fly ash particles and limited surface area exposure. The introduction of natural surfactants presents a novel solution by improving the dispersion and stabilization of fly ash particles in aqueous environments, maximizing the surface area available for CO_2 entrapment. Unlike synthetic surfactants, which can be harmful to the environment, natural surfactants are biodegradable and non-toxic, ensuring a more sustainable approach. These surfactants form micelles that prevent particle agglomeration,

allowing for better interaction between CO_2 and the reactive components of the fly ash. The approach differs from previous studies on CO_2 sequestration using fly ash is the synergistic use of natural surfactants to simultaneously enhance CO_2 solubility and promote the reaction with fly ash. In conventional methods, the focus has been predominantly on either improving the reactivity of fly ash through chemical treatments or capturing CO_2 using synthetic agents. The proposed integration of natural surfactants can also facilitate the absorption of CO_2, as surfactants improve gas-liquid interaction and mass transfer rates. This could lead to higher CO_2 capture efficiency compared to existing sequestration techniques that rely solely on the mineral content of fly ash. Overall, the innovation lies in the dual function of natural surfactants-enhancing the reactivity of fly ash and promoting CO_2 solubility; thereby providing a more efficient, eco-friendly solution for CO_2 entrapment.

This research aims to address this gap by systematically investigating the synergistic effects of natural surfactants on the CO_2 capture efficiency of fly ash via direct mineralization. This study explores the synergistic potential of fly ash and natural surfactants extracted from fenugreek surfactant (FS) [30] in CO_2 capture. The integration of these materials aims to create a high-performance, sustainable solution for mitigating CO_2 emissions from industrial sources. Carbonation mechanism was analyzed by pressure drop studies followed by microscopic observation. Finally, characterization of carbonated fly ash sample was done by using FTIR studies. This research contributes to the advancement of green technologies against climate change. Through this, we seek to develop a more effective and eco-friendly solution for CO_2 capture, contributing to the advancement of CCS technologies.

8.2 Materials and Methods

8.2.1 Materials

Fenugreek seeds were obtained from nearby grocery store from Jais, India. Methanol was used as a solvent for extraction of surfactant and obtained from SD Fine Chemicals. Deionized (DI) water was used to prepare the aqueous solutions and obtained from Millipore® Elix-10 water purification apparatus. Extraction of natural surfactant was done by using Soxhlet apparatus and dried in hot air oven obtained from Jain Scientific Glassworks, India. The coal fly ash was obtained from ACC cement factory, Gauriganj, India. For absorption studies, CO_2 (purity~99.95%) was used and procured from Sigma gases, India.

8.2.2 CO_2 absorption studies by using coal fly ash

CO_2 absorption is a process where carbon dioxide gas is captured by a liquid or solid absorbent material. Figure 8.1 shows the experimental setup used for the absorption test. CO_2 absorption studies were conducted on the aqueous solution of fly ash. Following the fly ash solution preparation, 25 mL of the sample was measured and added to a high-pressure equilibrium cell with a 50 mL holding capacity. After adding a magnetic bead, the compartment was sealed. Using a small vacuum pump (SSU VE 115/125, flow rate = 50 L/min), the remaining area was sucked. First, a sensitive pressure transducer (DiGi gauge TX-430, range 0−65 bar, accuracy value = 0.25%) is used to continually monitor the pressure inside the cell when CO_2 from the cylinder is injected under controlled pressure (by gently opening a flow valve). A magnetic stirrer (IKA-C-MAG-HS7) was used to continually agitate the fly ash solution inside the cell at speed of 600 rpm in order to guarantee the uniform and steady diffusion of CO_2 in fly ash solution. Recorded pressure readings were also taken throughout this process. Pressure gradually decreases as CO_2 is absorbed in fly ash solution until no more CO_2 can be absorbed, at which point pressure reaches

an equilibrium state. The CO_2-laden fly ash solution was decanted into a glass vial for additional research when the equilibrium pressure was reached and the residual pressure was released by releasing a valve.

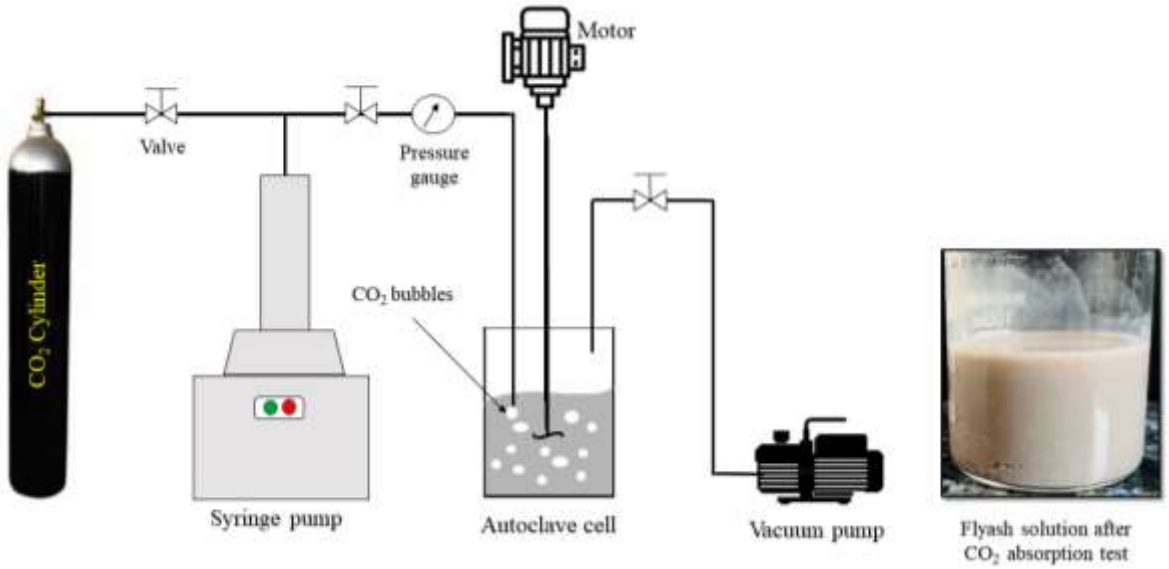

Figure 8.1: Detailed representation of experimental setup used for CO_2 capturing. The experiments were performed at room temperature.

8.2.3 Microscopic investigation of CO_2 absorbed

After CO_2 was absorbed, the fly ash solution was taken for microscopic studies. Microscopic characterization was done by using an optical microscope (Motic® microscope, Hong Kong) with built-in imaging software (Motic Images Plus 2) in an ambient environment. A digital camera (Moticam-10) coupled to an optical microscope was used to track and record the stability of CO_2 bubbles in fly ash solution.

8.2.4 Post characterization of carbonated fly ash

After the CO_2 absorption studies, FTIR analysis (PerkinElmer®, USA) of carbonated fly ash solution was done. Fly ash, a byproduct of coal combustion in power plants, contains various

crystalline phases. FTIR was conducted of fly ash before after the CO_2 absorption to confirm and visualize the change in peaks or functional groups present which ensure the absorption process.

8.3 Results and Discussion

Initially, for carbonation of fly ash, various samples were prepared with and without natural surfactant and pressure drop studies were conducted. Capturing of CO_2 in the prepared carbonated samples was analyzed by microscopic studies. Lastly, characterization of carbonated fly ash sample was done via FTIR analysis.

8.3.1 Trapping Mechanism for Carbon Storage

CO_2 storage is a critical component of CCS technologies aimed at reducing atmospheric CO_2 levels and mitigating climate change. The effectiveness of CO_2 storage can be enhanced through several mechanisms: mineral trapping, solubility trapping, residual trapping, and stratigraphic trapping as shown in Figure 8.2. Mineral trapping involves the chemical reaction of CO_2 with minerals in the storage formation, leading to the formation of stable carbonate minerals. This is one of the most secure forms of CO_2 storage because the CO_2 is permanently converted into solid minerals. For example, CO_2 reacts with calcium, magnesium, and iron-bearing silicate minerals to form calcite ($CaCO_3$), magnesite ($MgCO_3$), and siderite ($FeCO_3$). This process occurs naturally in basaltic rocks and ultramafic formations, where the mineral content is favorable for these reactions. Solubility trapping involves the dissolution of CO_2 in the formation water (brine) present in the storage reservoir. Once injected, CO_2 dissolves into the brine, forming a weak carbonic acid (H_2CO_3). Over time, the dissolved CO_2 becomes less mobile and more securely stored as part of the aqueous phase. This method relies on the solubility of CO_2 in water and is more stable at higher pressures and lower temperatures typically found at greater depths.

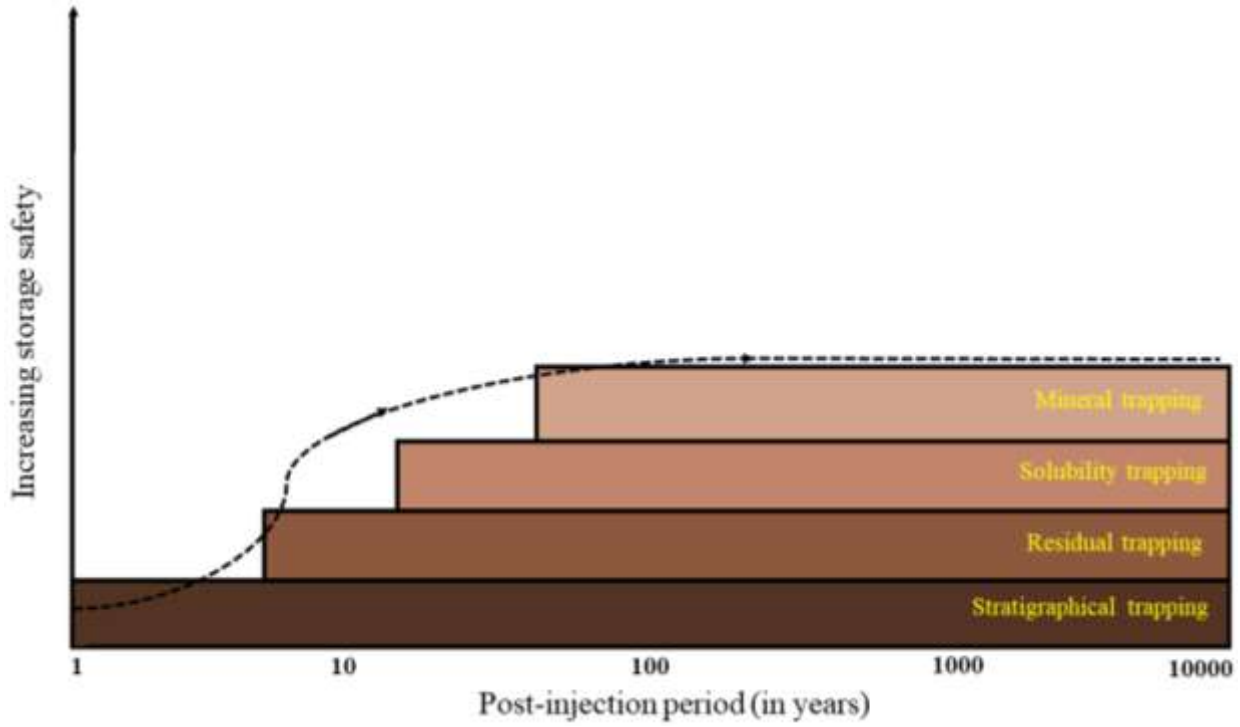

Figure 8.2: Schematic representation of CO_2 storage mechanism as a function of time. Each storage mechanism highlights different pathways and processes essential for the effective long-term containment of CO_2.

Residual trapping, also known as capillary trapping, occurs when CO_2 is immobilized in the pore spaces of the reservoir rock by capillary forces. After the bulk of the CO_2 has migrated, small amounts remain trapped in the pore spaces as isolated bubbles or ganglia, held in place by the surface tension of the fluids. This method enhances the security of CO_2 storage because the trapped CO_2 is unable to migrate, even if there is a failure in the structural seal. Stratigraphic trapping involves the use of impermeable rock layers (caprocks) that act as a physical barrier to prevent the upward migration of CO_2. These caprocks, typically composed of shale or claystone, create a structural trap overlying the CO_2 injection site. Additionally, CO_2 can be trapped in structural features like anticlines and fault traps. The effectiveness of stratigraphic trapping depends on the integrity and continuity of the caprock and the geological structure of the storage

site. In practice, CO_2 storage projects often benefit from a combination of these trapping mechanisms. For instance, initial CO_2 injection may primarily rely on structural and residual trapping, with solubility and mineral trapping becoming more significant over longer timescales as CO_2 dissolves in brine and reacts with minerals. This, effective CO_2 storage requires a comprehensive understanding and utilization of various trapping mechanisms to ensure long-term stability and security. Each method mineral, solubility, residual, and stratigraphic trapping; contributes uniquely to the overall effectiveness of CO_2 sequestration efforts, enhancing the capacity to mitigate GHG emissions and combat climate change.

8.3.2 Carbonation studies by using coal fly ash

Carbonation using fly ash involves the reaction of CO_2 with the alkaline components of fly ash to form stable carbonates. This process not only helps in capturing and storing CO_2 but also in utilizing a waste byproduct from coal combustion, contributing to environmental sustainability. The schematic representation of carbonation plant starting from generation fly ash as a waste product of industries to it reuse or disposal is show in Figure 8.3. Carbonation of fly ash possess various advantages for instance, CO_2 Sequestration, waste utilization and material improvement. Carbonation process helps in sequestering CO_2, reducing the amount of GHGs in the atmosphere. Fly ash, a byproduct of coal combustion, is often considered a waste material. Utilizing it for CO_2 capture turns waste into a resource, promoting waste management and recycling. The formation of carbonates can improve the physical properties of fly ash, making it more suitable for use in construction materials like concrete, enhancing their strength and durability.

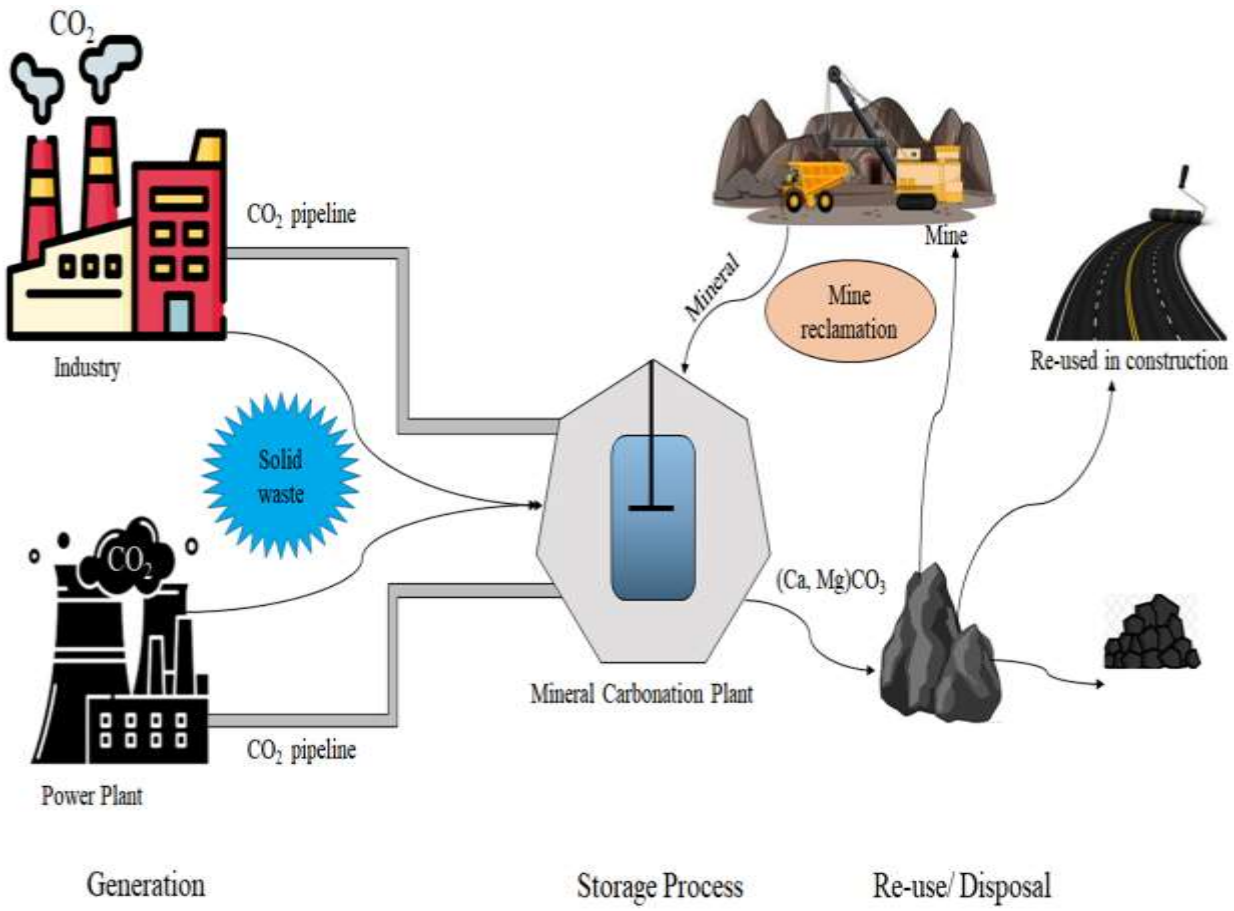

Figure 8.3: Schematic representation of Life Cycle of fly ash from Generation to Re-use/disposal. Various re-use applications emphasizing the sustainable management and environmental benefits of repurposing fly ash.

Carbonated fly ash has various application including **c**onstruction Materials, Soil Amendment and Environmental Remediation. Carbonated fly ash can be used in the production of concrete and other building materials. The carbonates formed during carbonation enhance the binding properties of fly ash, improving the strength and durability of the materials. Treated fly ash can be used to improve soil properties, providing essential nutrients and helping in soil stabilization efforts. Carbonated fly ash can be used in environmental applications, such as neutralizing acidic soils and waters.

The carbonation of fly ash, which involves the reaction of CO_2 with the materials in fly ash, can occur through both direct and indirect mechanisms as shown in Figure 8.4. Direct carbonation of fly ash involves a chemical reaction between the calcium compounds in the fly ash and CO_2 to form stable carbonates.

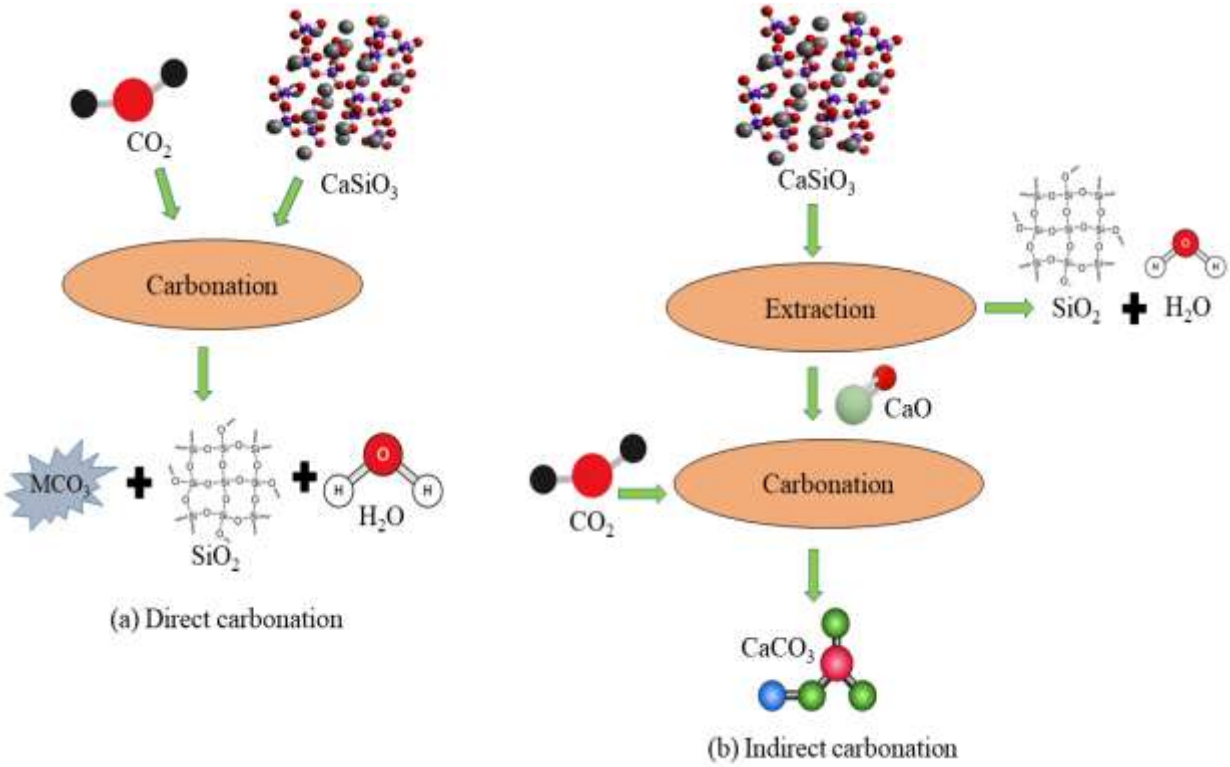

Figure 8.4: Schematic illustration of direct and indirect carbonation mechanisms. The key steps and chemical reactions involved in each mechanism, illustrating the pathways for CO_2 sequestration.

This process is a promising method for sequestering CO_2 and utilizing industrial waste. This process primarily targets the calcium (Ca) and magnesium (Mg) oxides present in fly ash. When fly ash, which is a byproduct of coal combustion, is exposed to CO_2 under controlled conditions of temperature and pressure, the calcium and magnesium oxides react with CO_2 to form $CaCO_3$ and $MgCO_3$. This carbonation process not only sequesters CO_2 but also stabilizes fly ash

by reducing its alkalinity and leachability, making it more environmentally benign and suitable for various applications, such as in construction materials. On the other hand, indirect carbonation using fly ash involves a two-step process to capture and sequester CO_2. Initially, fly ash, which is a byproduct of coal combustion, undergoes an extraction phase where calcium and magnesium silicates are leached out using an acidic solution, typically containing acids like hydrochloric or acetic acid. This step aims to dissolve the reactive components of the fly ash, forming soluble calcium and magnesium ions in the solution. This method not only sequesters CO_2 but also utilizes industrial waste, thereby contributing to waste management. The resulting carbonates are stable and can be used in various applications, including construction materials. This approach is advantageous as it leverages abundant industrial byproducts and converts them into useful products while mitigating GHG emissions.

8.3.3 CO_2 absorption studies

Fly ash, a byproduct of coal combustion in power plants, has shown promising potential for CO_2 absorption. This material is primarily composed of silica, alumina, and other oxides, giving it unique properties suitable for capturing CO_2. Fly ash absorbs CO_2 through a process known as chemisorption, where CO_2 molecules react with the alkaline components in the fly ash, forming carbonates. The presence of CaO, magnesium oxide (MgO), and other reactive compounds in fly ash enhances its capacity to chemically bind with CO_2. Fly ash is a readily available waste product from coal-fired power plants, making it an economical option for CO_2 capture. Using fly ash for CO_2 absorption provides a valuable application for a material that is otherwise considered an environmental pollutant. Additionally, combining fly ash with other materials to form composites can improve its effectiveness in capturing CO_2. Fly ash offers a cost-effective and abundant material for CO_2 absorption, with applications that could help mitigate the

impacts of industrial CO_2 emissions. Thus, in this work various aqueous solution of fly ash of varying concentration 2-15 wt% were prepared and CO_2 absorption studies were conducted (Figure 8.5). Initially for DI water, the pressure drop of ~ 39% was observed. This was followed by the addition of fly ash in DI water, where in 2 wt% of fly ash solution only ~27.14% of pressure drop was observed. In addition to this, ~35.7% in 5 wt% fly ash solution, ~ 27.8% 10 wt% solution and ~ 27.14% in 15 wt % solution was observed. From CO_2 absorption studies, the pressure drop as well as the CO_2 capturing was more in DI water and 5 wt% fly ash solution as shown in Figure 8.5. The CO_2 absorption in water is a reversible process therefore, 5 wt% fly ash solution was considered for further studies. For further improvement in CO_2 absorption, fenugreek based natural surfactants was explored [30] and added at CMC value of 0.2 wt% in 5 wt % fly ash solution. From Figure 8.5, maximum pressure drop (~37.8%) was observed for fenugreek surfactant (FS). The natural surfactants serve to improve the wettability and dispersion of fly ash in aqueous solutions, preventing particle aggregation. This increases the surface area of fly ash exposed to CO_2, facilitating more efficient carbonation reactions. In particular, surfactants can form micelles that assist in the adsorption of CO_2, allowing for better interaction between the gas and the reactive sites on the fly ash. CO_2 is absorbed into the surfactant-stabilized fly ash suspension. This approach not only captures and sequesters CO_2 but also adds value by converting industrial waste (fly ash) into a material with potential for use in construction and other industries. By using natural, biodegradable surfactants, the process remains environmentally friendly, aligning with sustainable development goals for carbon management. The pressure decay method is a widely used technique for assessing the absorption of CO_2 in various fluids, particularly in the context of storage, and capture technologies. This method involves monitoring the pressure change in a closed system as CO_2 is absorbed by the material under study. Uncertainty in the measurements may arise primarily

from instrumental precision in pressure and temperature sensors, volume calibration of the autoclave cell and repeatability of experimental runs. Error propagation analysis was performed to estimate the overall uncertainty in the calculated CO_2 uptake. The combined uncertainty was found to be within an acceptable range, confirming the reliability of the reported values. Additionally, all experiments were conducted in triplicate, and the average values with error bar are now reported to enhance statistical confidence.

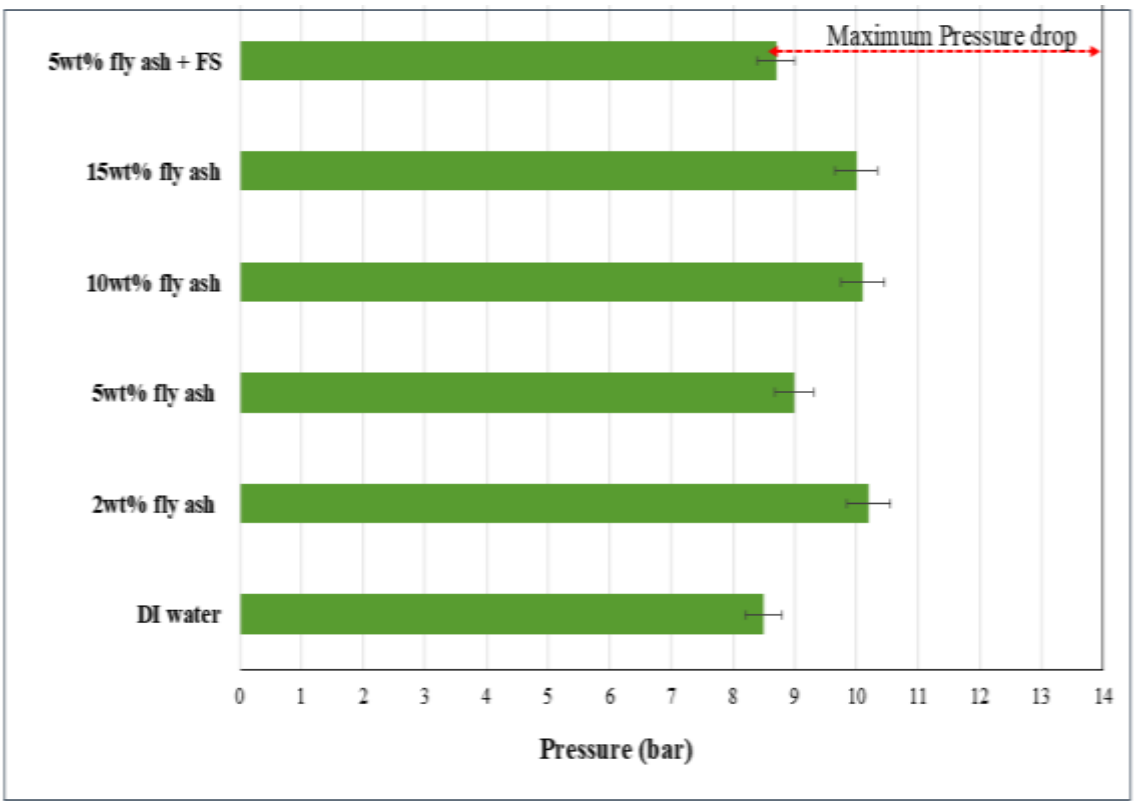

Figure 8.5: Pressure drop variation during CO_2 entrapment process for various fly ash solutions. The observed pressure drop indicates the system's efficiency in capturing CO_2.

Pressure decrease during the absorption experiment signifies that gas has been absorbed by the fluid. The fluid's saturation of CO_2 absorption was verified by the absence of any more pressure

reduction, which was kept for six hours to make sure no more CO_2 was absorbed. In order to calculate number of moles (n) of CO_2 for sample (5wt% + FS), using Ideal gas equation

$$PV = nRT$$

where,

P = 5.3 bars

V = 0.05 L

R = 0.08314 L.bar.$K^{-1}mol^{-1}$

T = 303.15 K

Thus, n = 0.01052 moles

The molar mass of CO_2 is approximately 44.01 g/mol. Therefore, the mass of CO_2 captured can be calculated as:

$$Mass\ of\ CO_2 = 0.01052\ \times 44.01$$

$$= 0.4629\ grams$$

So, 0.4629 gm of CO_2 was absorbed in 1.25 gm of fly ash used in aqueous solution.

Mass of fly ash = 1.25 g =0.00125 kg

$$Capacity = \frac{0.4629\ g}{0.00125 kg}$$

$$Capacity = 370.38\ \text{g} - CO_2/\ \text{kg} - \text{FA}$$

Thus, the capacity of CO_2 sequestration is approximately 370.38 g-CO_2/kg-fly ash.

The amount of CO_2 absorbed was calculated using ideal gas law, which relates pressure, volume, temperature and number of moles in gas phase. This approach is appropriate under the experimental conditions employed, where the gas behaves close to ideal due to moderate pressures

and controlled temperatures. Equation of state was applied to convert the observed pressure decay into corresponding moles of CO_2 sequestered by the solid-liquid system. Assumptions associated with the ideal gas model, includes negligible gas-gas interactions and uniform temperature distribution within the autoclave cell. These assumptions were considered reasonable for the selected operating conditions. However, it is also acknowledged that deviations from ideal behavior may occur at higher pressures. This discussion may improve the transparency of calculation method and strengthens scientific rigor of the sequestration capacity analysis.

8.3.4 Microscopic investigations of carbonated fly ash

CO_2 absorption in fly ash solution involves the dissolution of carbon dioxide into an acidic solution containing extracted components from fly ash. Microscopic investigation of CO_2 bubbles in fly ash solution reveals a similar process of gas dissolution and chemical reactions. After CO_2 absorption test, each sample was taken for microscopic observation to visualize the CO_2 absorbed. Figure 8.6 shows the presence of CO_2 bubbles absorbed during the absorption studies. Figure 8.6-a represents the existence of CO_2 bubble in DI water. When a CO_2 bubble is introduced into pure water, the CO_2 molecules at the gas-water interface begin to dissolve into the surrounding water. This dissolution occurs because of the difference in partial pressure between the CO_2 in the bubble and the water, leading to the diffusion of CO_2 molecules into the liquid. The CO_2 bubble's size will decrease over time as CO_2 continues to dissolve and diffuse into the water. Similarly, Figure 8.6-b, Figure 8.6-c and Figure 8.6-d shows the CO_2 bubble absorbed in the aqueous fly ash solution. The CO_2 bubbles appear to be smaller in size as compare to the bubbles in pure water. Small sized and evenly scattered CO_2 bubbles increase the surface area available for CO_2 dissolution into solution. This facilitates faster dissolution of CO_2 into the solution, enhancing the efficiency of carbon capture processes. Smaller bubbles also reduce buoyancy effects, allowing

them to remain in contact with the solution longer and maximize the interaction time between CO_2 and reactive agents. This improves the overall effectiveness of converting CO_2 into stable carbonate minerals, thereby contributing to effective carbon sequestration strategies to mitigate GHG emissions.

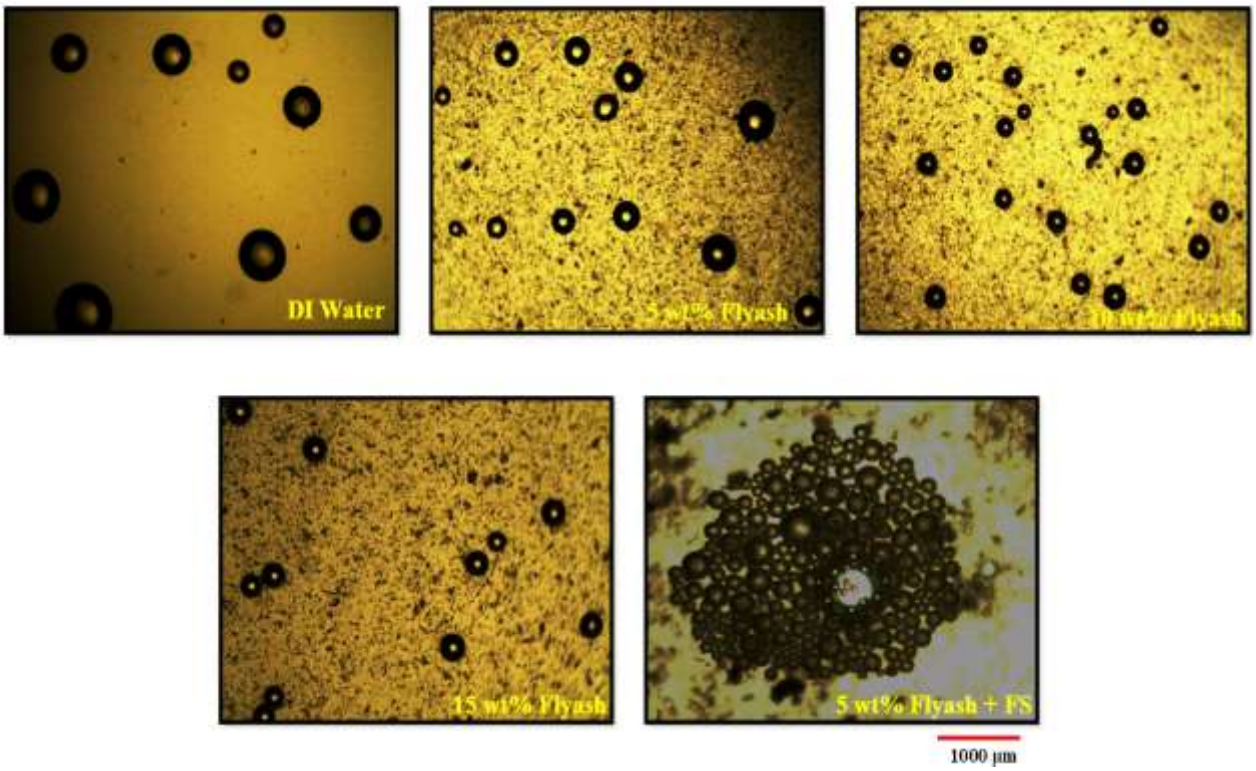

Figure 8.6: Microscopic observations showing CO_2 entrapment in fly ash solutions. The enhanced adsorption capacity of fly ash when treated with natural surfactants, highlights the microstructural changes and increased surface area that facilitate efficient CO_2 capture.

After introducing the natural surfactants in fly ash solution more pressure reduction was observed (as evident from Figure 8.5). The microscopic investigation also confirms the absorption studies as more denser packing of CO_2 bubbles was observed as shown in Figure 8.6-e for FS in 5wt% fly ash solution. Additionally, the use of natural surfactants can stabilize these bubbles, preventing their coalescence and maintaining their high surface area. Moreover, all the samples

were kept under observation for one week post CO_2 absorption test and microscopic analysis were conducted as shown in Figure 8.7. For DI water as shown in Figure 8.7-a, revealing no visible CO_2 bubbles. This observation suggests that DI water has limited capacity for retaining CO_2 in bubble form under the tested conditions. The results underscore the differences in CO_2 absorption capabilities between DI water and other potential absorbents, such as fly ash, highlighting the need for more efficient materials in CO_2 capture and storage applications. Among aqueous fly ash solution shown in Figure 8.7-b, 8.7-c and Figure 8.7-d, the CO_2 bubbles were lesser and comparatively bigger in size that the samples just after absorption tests (Figure 8.6). Significant reduction in the number of CO_2 bubbles within the fly ash may be attributed to lower density of CO_2 bubbles within the fly ash matrix, suggesting effective adsorption and sequestration of CO_2 by the fly ash. Microscopic observations in Figure 8.7-e indicates the presence of CO_2 bubbles within the solution, demonstrating the interaction between CO_2 and the fly ash-natural surfactant matrix.

The analysis reveals the potential of natural surfactant in enhancing the fly ash's capacity to capture CO_2, resulting in visible CO_2 bubble. These findings highlight the potential of using a fly ash-natural surfactant blend to improve CO_2 absorption efficiency, providing a viable strategy for CCS applications. Integrating fly ash and natural surfactants for CO_2 entrapment presents an economically viable solution by utilizing industrial by-products and low-cost, renewable resources. Fly ash, a waste product from coal-fired power plants, is abundantly available at low cost. Its aluminosilicate composition makes it a suitable material for carbonation, where CO_2 is chemically trapped as stable carbonates. The cost of natural surfactants extracted from fenugreek seeds are approximate to that of synthetic surfactants but offer several advantages, including

biodegradability, low toxicity, and environmental compatibility, making them valuable in various applications.

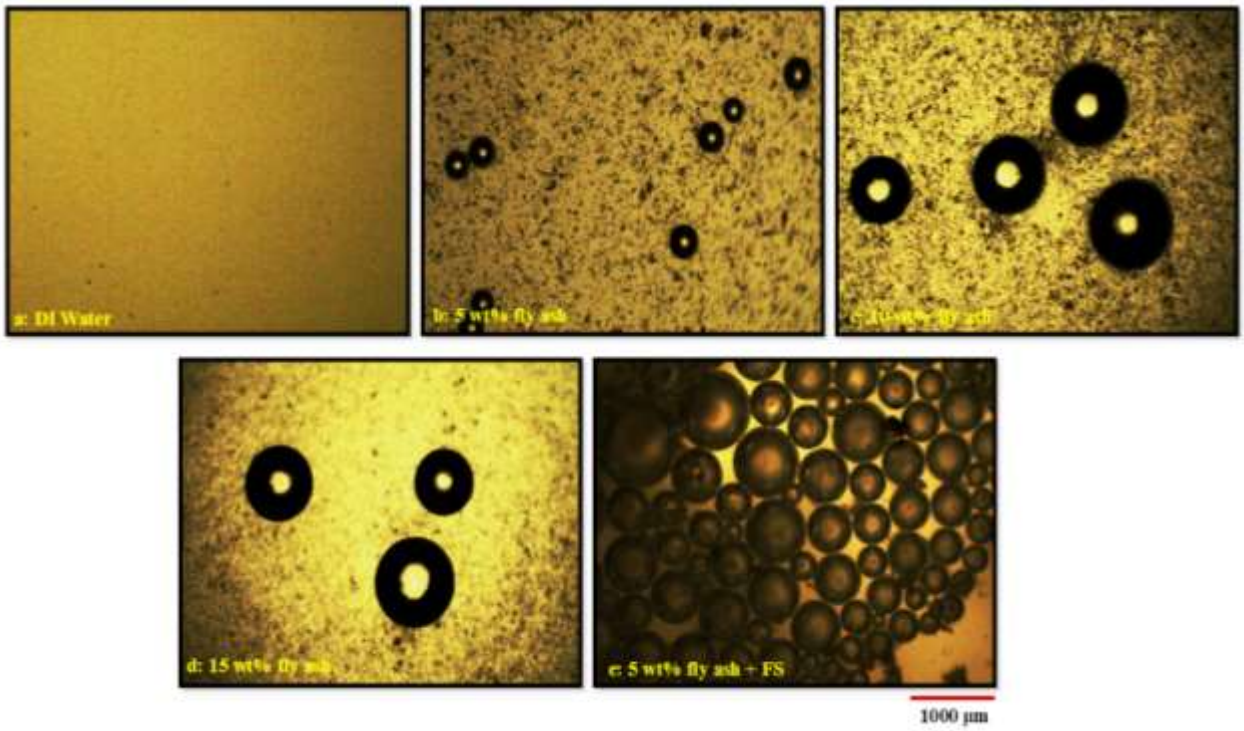

Figure 8.7: Microscopic analysis showing captured CO_2 post one week of absorption test in various fly ash solutions. Post-absorption analysis reveals the presence and distribution of CO_2 bubbles within the fly ash matrix, offering insights into the efficiency and capacity of fly ash as a CO_2 adsorbent.

For commercial implementation, the cost-effectiveness of this technology lies in the minimal processing required for fly ash and the natural surfactants. Fly ash can be directly sourced from industrial sites, reducing transportation and raw material expenses. Natural surfactants can be produced at scale from existing agricultural industries, keeping costs low. The potential savings from CO_2 capture, coupled with government incentives for carbon reduction, further enhance the economic appeal. Scaling this technology would also provide a dual benefit: utilizing waste

materials and reducing CO_2 emissions, aligning with the circular economy principles. As industries face increasing regulatory pressures to lower carbon footprints, this integrated solution offers a commercially feasible and environmentally sustainable option for large-scale CO_2 entrapment.

Fenugreek-derived surfactant is biodegradable, renewable and obtained through low-energy extraction processes, unlike synthetic surfactants that rely on petrochemical feedstocks and energy-intensive synthesis. This reduces the embodied carbon associated with material production. In CO_2 entrapment experiments, natural surfactant enhanced gas-liquid interaction and mineralization efficiency, allowing higher CO_2 uptake with lower chemical input. This improves the overall carbon mitigation performance of system. In thermal energy storage and nanofluid applications, surfactant promotes stable dispersion at low concentrations (near CMC), which reduces material usage and pumping energy due to favorable rheology. The combination of lower production emissions, improved entrapment efficiency and energy savings during operation indicates a meaningful reduction in environmental footprint compared to systems employing synthetic surfactants.

8.3.5 Characterization of carbonated fly ash samples

FTIR is significant in analyzing carbonated fly ash because it can identify and quantify carbonate minerals formed during carbonation processes. It provides detailed information about chemical bonds present in the carbonates, confirming successful CO_2 sequestration. Figure 8.8 shows the FTIR spectrum of untreated fly ash, 5 wt% and 10 wt% carbonated fly ash along with the 5 wt% fly ash with natural surfactants (FS). In raw fly ash, peak 1074 cm^{-1} corresponds to Si-O-Si asymmetric stretching and peak at 794 cm^{-1} is associated with the absorbance due to symmetric of Si-O-Si bond [384]. After carbonation studies, some new peaks (in 5 wt% fly ash +

NS sample) are found during FTIR analysis. Peak at 457 cm^{-1} corresponds to the existence of Si-O stretching band vibrations [385].

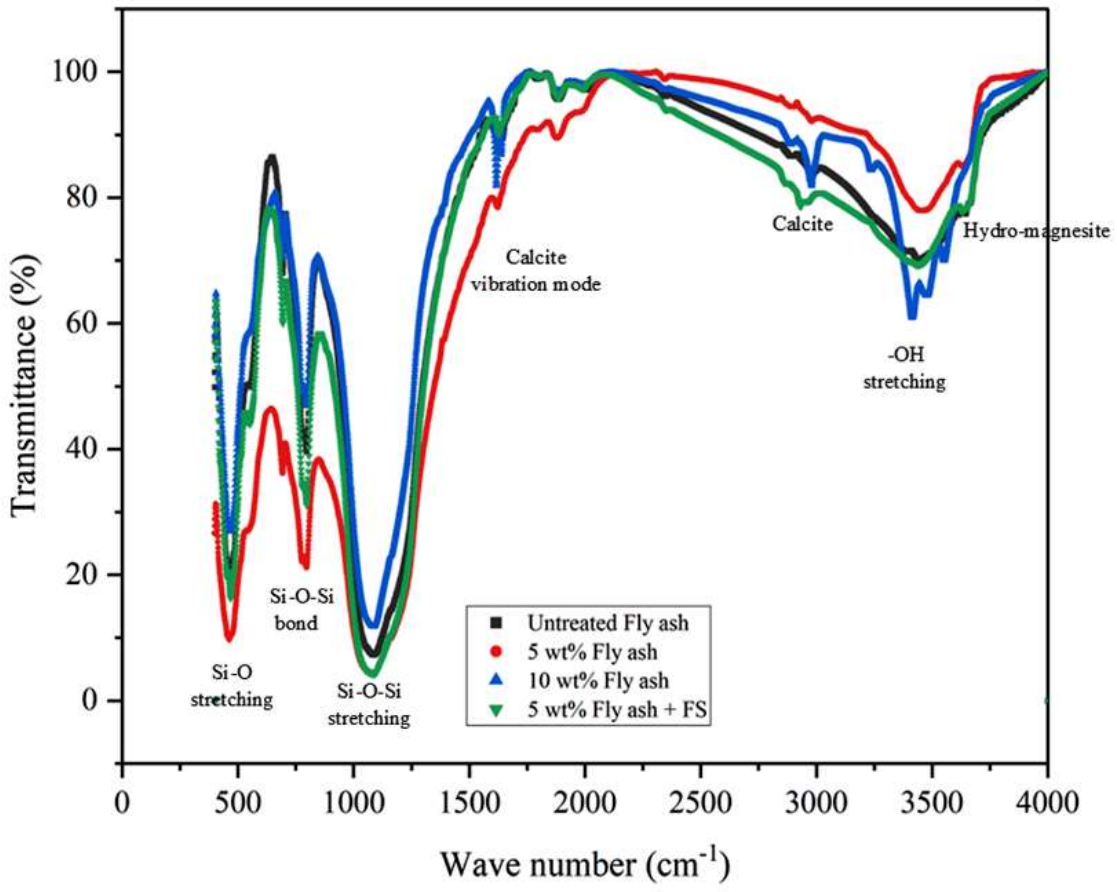

Figure 8.8: FTIR spectra of fly ash solutions after CO_2 absorption. Key peaks corresponding to functional groups such as hydroxyls, carbonyls, and silicates are highlighted, demonstrating the chemical modifications and enhanced surface activity resulting from the addition of natural surfactants.

In addition to this, peak at 1406 cm^{-1} corresponds to CO_3^{2-} [386] along with peak at 1462 cm^{-1} refers to formation of calcite [387]. Peak at 1795cm^{-1} attributed to calcite vibration mode [388]. Further, peak observed in the range of 3200cm^{-1} to 3600 cm^{-1} is attributed to -OH group [376]. Additional peak was observed at 3647 cm^{-1} correspond to existence of hydro magnesite in

(5wt% fly ash + FS) and confirms the presence of Mg precipitates [389]. FTIR helps assess the effectiveness of carbonation reactions, aiding in optimizing conditions for enhanced CCS in fly ash, crucial for mitigating GHG emissions. The integration of fly ash and natural surfactants for CO_2 entrapment holds promising potential for large-scale applications, particularly in industries that are significant contributors to carbon emissions. One of the key implications of this technology is its ability to provide a sustainable, cost-effective method for capturing CO_2 while utilizing industrial by-products, such as fly ash from coal combustion. On a larger scale, this technology could be incorporated into existing CCS systems, serving as a supplementary or alternative material to traditional chemical absorbents. In terms of scalability, power plants and cement industries, both significant sources of fly ash, could implement this technology directly at the point of emission. The use of natural surfactants, which are biodegradable and non-toxic, enhances the environmental appeal of the process. These industries could modify their exhaust systems to include fly ash-surfactant mixtures as a filtration medium, trapping CO_2 before it is released into the atmosphere. This would help reduce the carbon footprint of industrial processes while simultaneously repurposing waste materials, creating a closed-loop system. Another potential application could be in carbon-negative construction materials. Fly ash is already used in concrete production, and CO_2-enriched fly ash could be further integrated into building materials, locking in captured carbon for extended periods. This could transform construction industries by creating carbon-storing infrastructure, leading to more sustainable urban development. In addition, the process could be adapted for use in other sectors, such as agriculture, where CO_2-enriched fly ash could be utilized to enhance soil properties, improving crop yield while sequestering carbon in the ground. Implementing this technology on a broader scale offers a multi-functional approach to

mitigating climate change, fostering circular economy principles while addressing industrial waste and CO_2 emissions.

The mechanistic interaction between CO_2 and surfactant-fly ash composite involves a combination of dissolution, interfacial enhancement and mineralization processes. When CO_2 is introduced into aqueous suspension, it first dissolves to form carbonic acid, which further dissociates into bicarbonate and carbonate ions. Fly ash contains reactive oxides such as CaO and MgO that readily react with these ions to form stable carbonate minerals (e.g., $CaCO_3$ and $MgCO_3$). This mineralization pathway ensures permanent and stable sequestration of CO_2. Natural surfactant plays a crucial supporting role by reducing surface tension and improving the wettability and dispersion of fly ash particles. Enhanced dispersion increases the available reactive surface area and promotes better contact between dissolved CO_2 and active mineral sites. Surfactant also improves gas-liquid mass transfer, facilitating greater CO_2 dissolution into aqueous phase. Microscopic observations confirmed improved particle distribution and interaction in presence of surfactant. From scalability perspective, both fly ash and natural surfactant are inexpensive, abundant, and environmentally safe materials. The process operates under moderate conditions and offers dual benefits of industrial waste utilization and carbon capture, making it suitable for large-scale and sustainable CO_2 mitigation applications.

8.4 Conclusion

This study focuses on potential of natural surfactant in industrial waste utilization for carbon entrapment applications. Fly ash, a byproduct of coal combustion, was combined with the natural surfactant to enhance CO_2 capture efficiency. The use of fly ash, a low-cost waste material close to CO_2 emission sources, presents a feasible option for carbon capture. By improving CO_2 adsorption through natural surfactant modification, this approach offers both economic and

environmental benefits. Pressure drop studies demonstrated that (5 wt% fly ash + FS) sample achieved the highest CO_2 absorption, as confirmed by microscopic analysis showing the maximum number of CO_2 bubbles. Characterization of the carbonated fly ash with FTIR and XRD revealed new peaks, indicating successful CO_2 entrapment. The natural surfactant increases active sites on the fly ash surface, enhancing its CO_2 adsorption capacity. This method not only addresses the challenge of industrial waste management but also contributes to environmental protection by mitigating CO_2 emissions. The integration of fly ash with natural surfactants offers a sustainable and cost-effective solution for carbon capture. Ongoing research aims to optimize the CO_2 entrapment process, including reactor design and process conditions, to further enhance the efficiency of CO_2 capture and the quality of carbonated fly ash. This innovative approach supports both environmental sustainability and industrial efficiency.

The integration of fly ash and natural surfactants for CO_2 entrapment presents a promising avenue for reducing atmospheric carbon levels. However, several potential research directions could enhance the efficiency and feasibility of this approach. One area of focus is optimizing reaction conditions, such as the temperature, pressure, and concentration of CO_2, which can significantly influence the carbonation process. Fine-tuning these parameters could lead to faster and more efficient carbon entrapment within fly ash particles. Further research could also explore the role of different types of natural surfactants and their interactions with various compositions of fly ash, aiming to identify the most effective combinations for maximum CO_2 capture. Investigating the long-term stability of carbonated fly ash is another important consideration. Studies could evaluate the durability of the sequestered carbon over time, including its resistance to environmental factors such as moisture, temperature fluctuations, or acidic conditions. Understanding the long-term behavior of carbonated fly ash could provide insights into its

potential use in construction materials, offering a dual benefit of carbon storage and material recycling. These future directions are key to developing a scalable, sustainable solution for CO_2 mitigation using fly ash and natural surfactants.

In addition, a detailed comparison between the results of present study and those reported in literature has been summarized in Table 8.1. Table 8.1 shows a consolidated comparison between the outcomes of present study and those reported in literature. The fenugreek-based surfactant developed in this work demonstrates a significantly lower CMC, effective surface and interfacial tension reduction and competitive cost when compared with previously reported natural and synthetic surfactants. These results indicate strong surface activity at low concentration, which is desirable for large-scale applications. In terms of thermal energy storage, surfactant-incorporated PCM emulsion exhibits very high phase change enthalpy values. Although nature of systems differs, but observed enhancement trend is consistent with earlier studies, thereby validating the present observations. Unlike most previous works that focus on a single application, the present study demonstrates a multifunctional material suitable for emulsification, carbon entrapment, and thermal energy storage. This integrated performance highlights the novelty and practical relevance of the proposed system.

Table 8.1: Summary comparison of outcomes from the present study and literature-reported surfactants.

Parameters	**Literature Reports**	**Present Study (Fenugreek-based surfactant)**	**Significance of present work**
Surfactant Source	Mostly synthetic and some plant based natural surfactants [37–39,259]	Derived from fenugreek seeds	Renewable and ecofriendly

CMC	0.8-8wt% for plant based surfactants [35,38,39,41,227,390]	0.2wt%	Less quantity required
SFT	25-40 mN/m for bio-surfactants [166,212,331,391]	22 mN/m	Strong surface activity
IFT	48-2.5 mN/m depending on source [26,32,34,35,39]	~10 mN/m	Effective for oil water interaction
Emulsification ability	Moderate to good and also concentration dependent [52,309,392]	Stable emulsion at low concentration (0.2wt%)	Improved performance
Salt Tolerance	Destabilization reported for high salinity for conventional surfactants [57,158,194,268]	Stable under saline environment (up to 3 wt% salinity)	Suitable for practical application
Cost of surfactant	Not reported for natural surfactant	Economical competitive as of conventional surfactant	Ecofriendly alternative
Surfactant Yeild	Rarely reported for natural surfactant	12.76 ±11% g from 100 g fenugreek seeds	Scalable extraction
Environmental impact	Mostly synthetic surfactants are toxic [18,256]	Biodegradable and natural	Environmentally safer
PCM latent heat (melting)	131.8 J/g (for pure PCM); 148.3 J/g with additives [361]	1205.171 J/g (PCM emulsion)	High energy storage
PCM latent heat (freezing)	139.2 J/g (for Pure PCM; 150.7 J/g with additives [361]	1284.825 J/g (PCM emulsion)	Enhanced TES capacity
Enthalpy enhancement trend	Conventional additives improve TES performance (natural additive rarely reported) [393,394]	Same trend observed	Validates present results

Application focus	Mostly single function [224,227,395]	Emulsification, TES, CO_2 entrapment	Multifunctional system
Overall Novelty	Application specific materials	Single bio-surfactant for three domain	Integrated performance

In addition to conventional aqueous extraction, green techniques such as ultrasound-assisted extraction [235] and microwave-assisted extraction [396] are considered promising. These methods enhance mass transfer, reduce extraction time, and lower solvent consumption while improving recovery of saponin-rich fractions. Enzyme-assisted extraction [397] is another eco-friendly option, where cellulase or protease can break plant cell walls and release more surface-active compounds without harsh chemicals. Supercritical CO_2 extraction [398], although requiring specialized equipment, offers high purity extracts without residual solvents and is suitable for scale-up. Use of ethanol-water mixtures as green solvents is also discussed to enhance selectivity and improve surfactant purity. These alternative approaches support sustainable processing, reduce environmental impact, and offer potential for large-scale production of fenugreek-based natural surfactant for industrial applications.

Chapter 9

Conclusion and Future Directions

9.1 Conclusion

This research focused on the development of a sustainable, plant-derived natural surfactant from fenugreek seeds and its multifunctional applications in energy and environmental systems. The work began with successful synthesis of surfactant using a soxhlet extraction method, followed by an in-depth physicochemical and structural characterization. Techniques such as FTIR, UV–Vis, XPS, FESEM-EDX and rheological measurements confirmed the surfactant's functional groups, surface activity, thermal stability, and morphological features. This study successfully developed a plant-derived natural surfactant from fenugreek seeds using a Soxhlet extraction method, achieving a yield of 12.76 ± 11 g per 100 g of raw material, demonstrating the feasibility of scalable extraction. The synthesized surfactant exhibited CMC of 0.2 wt%, which is significantly lower than most reported plant-based surfactants, indicating higher efficiency at reduced dosage. Surface activity measurements showed a surface tension reduction to 22 mN/m and an oil-water interfacial tension of ~10 mN/m, confirming its strong interfacial performance. Surfactant showed potential in formation of stable oil-water emulsions at low concentration (0.2 wt%) and maintained emulsion stability under salinity up to 3 wt%, with minimal droplet coalescence and favorable zeta potential values, indicating resistance to flocculation and phase separation. Wettability studies revealed a significant contact angle reduction (74º to 48º), confirming the transition from oil-wet to water-wet conditions, which improved multiphase fluid

mobilization in porous media. This behavior highlights its applicability in subsurface fluid recovery and wastewater treatment systems. The synergistic interaction between the natural surfactant and silica nanoparticles enhanced colloidal stability and rheological behavior, reducing nanoparticle agglomeration under saline conditions. In thermal energy storage applications, the surfactant-enabled PCM emulsion exhibited a latent heat of 1205.17 J/g during melting and 1284.83 J/g during freezing, substantially higher than values reported for pure PCM systems, confirming improved thermal reliability and energy storage capacity. Additionally, the surfactant-fly ash hybrid system demonstrated promising CO_2 entrapment potential (370.38 g-CO_2/kg-fly ash), providing a sustainable route for industrial waste utilization and carbon sequestration. Overall, this work establishes a single, biodegradable and cost-competitive bio-surfactant capable of delivering multifunctional performance across energy, environmental and carbon management applications.

In summary, this research provides a comprehensive foundation for the development and application of natural surfactants derived from renewable sources. The fenugreek-based surfactant demonstrated excellent interfacial activity, environmental compatibility, thermal stability, and adaptability across a range of engineering systems. Its successful performance in emulsification, fluid mobilization, nanofluid stabilization, energy storage, and CO_2 entrapment demonstrates its versatility and industrial relevance. This work contributes significantly to the ongoing global effort to replace synthetic, petrochemical-based surfactants with biodegradable and eco-friendly alternatives. It also opens new avenues for integrating natural surfactants in advanced material systems and sustainable process engineering.

9.2 Future Research Priorities

A key direction for future research is the scale-up of natural surfactant production, with a focus on cost-effective and energy-efficient extraction techniques. The transition from laboratory-scale synthesis to commercial viability demands the development of scalable methods that minimize both energy input and raw material costs. Following this, pilot-scale validation in real-world systems such as oil reservoirs, carbon sequestration sites, and TES units will be critical. These demonstrations will help bridge the gap between controlled lab conditions and the complex dynamics of field environments.

9.2.1 Role of Life Cycle Assessment and Techno-Economic Analysis

To ensure real-world adoption and sustainable integration into industrial applications, future work must incorporate comprehensive Life Cycle Assessments (LCA) and Techno-Economic Analyses (TEA). While lab-scale production may show cost parity between natural and synthetic surfactants, these comparisons often ignore the broader environmental and economic implications.

- LCA provides a holistic view of the environmental footprint, accounting for each stage of the product's life cycle—from raw material extraction and synthesis to use and eventual disposal. It helps pinpoint resource-intensive stages and suggests optimizations to reduce carbon emissions, water consumption, and energy demand.
- TEA, on the other hand, evaluates financial viability by analyzing capital and operational expenditures, scalability, and potential return on investment. It identifies opportunities for cost savings, for example through simplified processing steps, lower toxicity management costs, and better alignment with green supply chains.

Together, LCA and TEA offer a realistic and comprehensive projection of the surfactant's feasibility, guiding not only researchers but also industry stakeholders and policymakers in making informed decisions.

9.2.2 Broader Sustainability and Policy Impact

For instance, although renewable feedstock-based surfactants might appear economically comparable to synthetic ones at the lab scale, LCA may reveal they generate significantly lower greenhouse gas emissions, are biodegradable, and pose minimal ecological risks. TEA may further reveal advantages such as reduced need for hazardous waste handling and better compatibility with circular supply chains. Thus, embedding LCA and TEA frameworks into future research is vital not just for validation, but for shaping policy directives and commercial strategies that align with global sustainability goals.

9.2.3 Scientific and Technological Extensions

Several avenues exist to further enhance the performance and application scope of natural surfactants:

- Hybrid formulations incorporating natural surfactant–polymer (NSP) systems should be investigated for improved emulsification, thermal stability, and interfacial activity—particularly in TES and enhanced oil recovery contexts.
- Reactive transport modeling that integrates biosurfactant parameters can enable better predictions of wettability alteration, CO_2 entrapment behavior, and long-term performance under reservoir-like conditions.

- Expanding the feedstock base to include underutilized resources such as agricultural residues, algal biomass, and industrial waste could significantly improve both sustainability metrics and economic feasibility.

9.2.4 Integration into Energy and Environmental Systems

In the domain of thermal energy storage, there is a compelling opportunity to integrate natural surfactants into components such as solar thermal collectors, building-integrated storage modules, and industrial waste heat recovery units. Key performance indicators for such applications would include long-term thermal cycling behavior, phase change material (PCM) stability, and resilience to variable climatic conditions.

9.2.5 Environmental and Safety Considerations

Environmental safety remains a cornerstone of sustainable surfactant deployment. Future studies should therefore explore:

- Degradation kinetics, to understand breakdown pathways under different environmental conditions.
- By-product analysis, to identify any potentially hazardous transformation products.
- Ecotoxicological profiling, to evaluate impacts on aquatic and terrestrial ecosystems.

These assessments will ensure that the use and disposal of these materials are safe, responsible, and compliant with environmental standards.

9.2.6 Advancing Fundamental Understanding

In-depth investigations into multiphase flow dynamics and interfacial behavior at the pore and core scales are essential. Techniques such as micro-computed tomography (micro-CT) and

micromodel visualization can offer unprecedented insight into how these surfactants behave in heterogeneous porous media, which is crucial for optimizing performance in subsurface applications.

9.2.7 Pathways to Commercialization and Policy Integration

Lastly, for the widespread adoption of green surfactants, there is a pressing need to establish:

Standardized testing protocols to ensure reliability and comparability.

- Regulatory frameworks that support market entry and safe use.
- Commercialization pathways, developed in close collaboration with industry partners and supported by public-private innovation platforms.

These measures will facilitate a smoother transition from innovation to market, ensuring that bio-derived surfactants become an integral part of sustainable industrial practices.

To conclude, this thesis not only underscores the potential of natural surfactants in enabling cleaner, safer, and more sustainable processes but also provides a clear roadmap for their future development and integration. By combining rigorous scientific inquiry with robust environmental and economic assessments, the next generation of bio-based surfactants can meaningfully contribute to global goals for green chemistry, climate action, and the circular economy.

References

[1] K. Tsujii, Surface activity : principles, phenomena, and applications, Academic Press, San Diego, CA, 1998.

[2] C.N. Mulligan, Rhamnolipid biosurfactants: Solubility and environmental issues, in: Thermodyn. Solubility Environ. Issues, (2007) 279–298.

[3] S. Kumar, A. Mandal, Studies on interfacial behavior and wettability change phenomena by ionic and nonionic surfactants in presence of alkalis and salt for enhanced oil recovery, Appl. Surf. Sci. 372 (2016) 42–51.

[4] P.S. Piispanen, M. Persson, P. Claesson, T. Norin, Surface properties of surfactants derived from natural products. Part 2: Structure/property relationships - Foaming, dispersion, and wetting, J. Surfactants Deterg. 7 (2004) 161–167.

[5] N. Liu, T.J. Zhan, Y.W. Zhang, X.M. Yin, L.X. Zhang, Experimental investigation of comprehensive effects of surfactant and inclined mode on spray cooling heat transfer, Int. J. Therm. Sci. 136 (2019) 457–466.

[6] B.S. Sekhon, Surfactants: Pharmaceutical and Medicinal Aspects, J. Pharm. Technol. Res. Manag. 1 (2013) 43–68.

[7] A.A. Siyal, M.R. Shamsuddin, A. Low, N.E. Rabat, A review on recent developments in the adsorption of surfactants from wastewater, J. Environ. Manage. 254 (2020) 109797.

[8] N. Pal, N. Saxena, K. V. Divya Laxmi, A. Mandal, Interfacial behaviour, wettability alteration and emulsification characteristics of a novel surfactant: Implications for enhanced oil recovery, Chem. Eng. Sci. 187 (2018) 200–212.

[9] M.C. Prieto-Blanco, M. Fernández-Amado, P. López-Mahía, S. Muniategui-Lorenzo, D. Prada-Rodríguez, Surfactants in Cosmetics: Regulatory Aspects and Analytical Methods, in: Anal. Cosmet. Prod. Second Edition. (2018) 249–287.

[10] A. Eivazihollagh, I. Svanedal, H. Edlund, M. Norgren, On chelating surfactants: Molecular perspectives and application prospects, J. Mol. Liq. 278 (2019) 688–705.

[11] E. Golabi, F.S. Azad, S.S. Ayatollahi, S.N. Hosseini, N. Akhlaghi, Experimental study of wettability alteration of limestone rock from oil-wet to water-wet using various surfactants, SPE Heavy Oil Conf. 1 (2012) 746–761.

[12] D.Y. Atta, B.M. Negash, N. Yekeen, A.D. Habte, A state-of-the-art review on the application of natural surfactants in enhanced oil recovery, J. Mol. Liq. (2021) 114888.

[13] F. Vassenden, T. Holt, A. Ghaderi, A. Solheim, Foam propagation on semi-reservoir scale, SPE Reserv. Eval. Eng. 2 (1999) 436–441.

[14] H.A. Yousefvand, A. Jafari, Stability and flooding analysis of nanosilica/ NaCl /HPAM/SDS solution for enhanced heavy oil recovery, J. Pet. Sci. Eng. 162 (2018) 283–291.

[15] S.I. Karakashev, M. V. Grozdanova, Foams and antifoams, Adv. Colloid Interface Sci. 176–177 (2012) 1–17.

[16] C. Costa, B. Medronho, A. Filipe, I. Mira, B. Lindman, H. Edlund, M. Norgren, Emulsion formation and stabilization by biomolecules: The leading role of cellulose, Polymers 11 (2019) 1570.

[17] E. Günther, T. Schmid, H. Mehling, S. Hiebler, L. Huang, Subcooling in hexadecane

emulsions, Int. J. Refrig. 33 (2010) 1605–1611.

[18] E. Gayathiri, P. Prakash, N. Karmegam, S. Varjani, M.K. Awasthi, B. Ravindran, Biosurfactants: Potential and Eco-Friendly Material for Sustainable Agriculture and Environmental Safety—A Review, Agronomy 12 (2022) 1–35.

[19] A. Pradhan, A. Bhattacharyya, Quest for an eco-friendly alternative surfactant: Surface and foam characteristics of natural surfactants, J. Clean. Prod. 150 (2017) 127–134.

[20] S. Chitikela, S.K. Dentel, H.E. Allen, Modified method for the analysis of anionic surfactants as methylene blue active substances, Analyst 120 (1995) 2001–2004.

[21] M.T. Muhammad, M.N. Khan, Eco-friendly, biodegradable natural surfactant (Acacia Concinna): An alternative to the synthetic surfactants, J. Clean. Prod. 188 (2018) 678–685.

[22] V. Vrbanović Mijatović, L. Šerman, O. Gamulin, Analysis of pulmonary surfactant by Fourier transform infrared spectroscopy after exposure to sevoflurane and isoflurane, Bosn. J. Basic Med. Sci. 17 (2017) 38–46.

[23] M. Norouzpour, M. Nabipour, A. Azdarpour, H. Akhondzadeh, R.M. Santos, A. Keshavarz, Experimental investigation of the effect of a quinoa-derived saponin-based green natural surfactant on enhanced oil recovery, Fuel 318 (2022) 123652.

[24] D.J. McClements, C.E. Gumus, Natural emulsifiers — Biosurfactants, phospholipids, biopolymers, and colloidal particles: Molecular and physicochemical basis of functional performance, Adv. Colloid Interface Sci. 234 (2016) 3–26.

[25] S.S. Shadizadeh, R. Kharrat, Experimental investigation of matricaria chamomilla extract effect on oil-water interfacial tension: Usable for chemical enhanced oil recovery, Pet. Sci.

Technol. 33 (2015) 901–907.

[26] M. Rahmati, M. Mashayekhi, R. Songolzadeh, A. Daryasafar, Effect of natural leaf-derived surfactants on wettability alteration and interfacial tension reduction in water-oil system: EOR application, J. Japan Pet. Inst. 58 (2015) 245–251.

[27] F. Md, Biosurfactant: Production and Application, J. Pet. Environ. Biotechnol. 03 (2012).

[28] S. Mukherjee, P. Das, R. Sen, Towards commercial production of microbial surfactants, Trends Biotechnol. 24 (2006) 509–515.

[29] L. Quintero, An overview of surfactant applications in drilling fluids for the petroleum industry, J. Dispers. Sci. Technol. 23 (2002) 393–404.

[30] A. Singh, K.R. Chaturvedi, T. Sharma, Natural surfactant for sustainable carbon utilization in cleaner production of fossil fuels: Extraction, characterization and application studies, J. Environ. Chem. Eng. 9 (2021) 106231.

[31] L. Rigano, N. Lionetti, Quillaja triterpenic saponins can act as a natural emulsifier and dispersing agent to offer a real alternative to synthetic surfactants, J. SPC 82 (2009) 1–4.

[32] A.B. Chhetri, K.C. Watts, M.S. Rahman, M.R. Islam, Soapnut extract as a natural surfactant for enhanced oil recovery, Energy Sources, Part A Recover. Util. Environ. Eff. 31 (2009) 1893–1903.

[33] M.A. Ahmadi, S. Zendehboudi, A. Shafiei, L. James, Nonionic surfactant for enhanced oil recovery from carbonates: Adsorption kinetics and equilibrium, Ind. Eng. Chem. Res. 51 (2012) 9894–9905.

[34] M. Pordel Shahri, S.R. Shadizadeh, M. Jamialahmadi, Applicability test of new surfactant

produced from Zizyphus Spina-Christi leaves for enhanced oil recovery in carbonate reservoirs, J. Japan Pet. Inst. 55 (2012) 27–32.

[35] A. Khorram Ghahfarokhi, A. Dadashi, A. Daryasafar, J. Moghadasi, Feasibility study of new natural leaf-derived surfactants on the IFT in an oil–aqueous system: experimental investigation, J. Pet. Explor. Prod. Technol. 5 (2015) 375–382.

[36] Q.Q. Zhang, B.X. Cai, W.J. Xu, H.Z. Gang, J.F. Liu, S.Z. Yang, B.Z. Mu, Novel zwitterionic surfactant derived from castor oil and its performance evaluation for oil recovery, Colloids Surfaces A Physicochem. Eng. Asp. 483 (2015) 87–95.

[37] M. Rahmati, M. Mashayekhi, R. Songolzadeh, A. Daryasafar, Effect of natural leaf-derived surfactants on wettability alteration and interfacial tension reduction in water-oil system: EOR application, J. Japan Pet. Inst. 58 (2015) 245–251.

[38] N. Saxena, N. Pal, S. Dey, A. Mandal, Characterizations of surfactant synthesized from palm oil and its application in enhanced oil recovery, J. Taiwan Inst. Chem. Eng. 81 (2017) 343–355.

[39] A.A. Isari, M. Eslahati, S. Moradi, A. Eslahati, Feasibility Investigation of A Novel Natural Surfactant Extracted from Eucalyptus Leaves for Enhanced Oil Recovery of Carbonates: Experimental Study, Pet. Chem. Ind. Int. 1 (2018) 1–5.

[40] N. Saxena, A. Saxena, A. Mandal, Synthesis, characterization and enhanced oil recovery potential analysis through simulation of a natural anionic surfactant, J. Mol. Liq. 282 (2019) 545–556.

[41] J. Machale, D. Al-Bayati, M. Almobarak, M. Ghasemi, A. Saeedi, T.K. Sen, S.K.

Majumder, P. Ghosh, Interfacial, Emulsifying, and Rheological Properties of an Additive of a Natural Surfactant and Polymer and Its Performance Assessment for Application in Enhanced Oil Recovery, Energy Fuels 35 (2021) 4823–4834.

[42] S.K. Magham, J.A. Ali, A. Khaksar Manshad, P.T. Jaf, B.S. Hisqel, Investigation of the Passiflora Plant as a Promising Natural Surfactant for Enhanced Oil Recovery: Insights into Crude Oil-Water-Rock Interaction, Energy Fuels 37 (2023) 11881–11892.

[43] R.J. Pugh, Foaming, foam films, antifoaming and defoaming, Adv. Colloid Interface Sci. 64 (1996) 67–142.

[44] D. Yin, D. Zhao, Main Controlling Factor of Polymer-Surfactant Flooding to Improve Recovery in Heterogeneous Reservoir, Adv. Mater. Sci. Eng. 2017 (2017).

[45] S. Llamas, E. Santini, L. Liggieri, F. Salerni, D. Orsi, L. Cristofolini, F. Ravera, Adsorption of Sodium Dodecyl Sulfate at Water-Dodecane Interface in Relation to the Oil in Water Emulsion Properties, Langmuir 34 (2018) 5978–5989.

[46] B. Kichatov, A. Korshunov, V. Gubernov, A. Kiverin, I. Yakovenko, Combustion of heptane-in-water emulsion foamed with hydrogen-oxygen mixture, Fuel Process. Technol. 198 (2020) 106230.

[47] M.K. Baloch, G. Hameed, Emulsification of oil in water as affected by different parameters, J. Colloid Interface Sci. 285 (2005) 804–813.

[48] Z. Fu, M. Liu, J. Xu, Q. Wang, Z. Fan, Stabilization of water-in-octane nano-emulsion. Part I: Stabilized by mixed surfactant systems, Fuel 89 (2010) 2838–2843.

[49] M.R.N. El-Din, A.M. Al-Sabagh, Preparation of Water-in-Hexane Nanoemulsions Using

Low Energy Emulsification Method, J. Dispers. Sci. Technol. 33 (2012) 68–74.

[50] K. Golemanov, S. Tcholakova, N.D. Denkov, T. Gurkov, Selection of surfactants for stable paraffin-in-water dispersions, undergoing solid-liquid transition of the dispersed particles, Langmuir 22 (2006) 3560–3569.

[51] B. Bera, R. Khazal, K. Schroën, Coalescence dynamics in oil-in-water emulsions at elevated temperatures, Sci. Rep. 11 (2021) 1–10.

[52] S. Kumar, V. Mahto, Emulsification of Indian heavy crude oil using a novel surfactant for pipeline transportation, Pet. Sci. 14 (2017) 372–382.

[53] A. Nafisifar, A. Khaksar Manshad, S. Reza Shadizadeh, Evaluation of a new green synthesized surfactant from linseeds - chemical EOR implications from sandstone petroleum reservoirs, J. Mol. Liq. 342 (2021) 117263.

[54] Y. Yang, M.E. Leser, A.A. Sher, D.J. McClements, Formation and stability of emulsions using a natural small molecule surfactant: Quillaja saponin (Q-Naturale®), Food Hydrocoll. 30 (2013) 589–596.

[55] N. Pal, N. Saxena, A. Mandal, Studies on the physicochemical properties of synthesized tailor-made gemini surfactants for application in enhanced oil recovery, J. Mol. Liq. 258 (2018) 211–224.

[56] R.S. Kumar, K.R. Chaturvedi, S. Iglauer, J. Trivedi, T. Sharma, Impact of anionic surfactant on stability, viscoelastic moduli, and oil recovery of silica nanofluid in saline environment, J. Pet. Sci. Eng. 195 (2020) 107634.

[57] R. Goswami, K.R. Chaturvedi, R.S. Kumar, B.H. Chon, T. Sharma, Effect of ionic strength

on crude emulsification and EOR potential of micellar flood for oil recovery applications in high saline environment, J. Pet. Sci. Eng. 170 (2018) 49–61.

[58] M. Puerto, G.J. Hirasaki, C.A. Miller, J.R. Barnes, Surfactant systems for EOR in high-temperature, high-salinity environments, Proc. - SPE Symp. Improv. Oil Recover. 1 (2010) 356–375.

[59] K. Babu, N. Pal, V.K. Saxena, A. Mandal, Synthesis and characterization of a new polymeric surfactant for chemical enhanced oil recovery, Korean J. Chem. Eng. 33 (2016) 711–719.

[60] S. Mukherjee, Preparation and Stability of Nanofluids-A Review, IOSR J. Mech. Civ. Eng. 9 (2013) 63–69.

[61] Y. He, Y. Jin, H. Chen, Y. Ding, D. Cang, H. Lu, Heat transfer and flow behaviour of aqueous suspensions of TiO_2 nanoparticles (nanofluids) flowing upward through a vertical pipe, Int. J. Heat Mass Transf. 50 (2007) 2272–2281.

[62] S. Chakraborty, P.K. Panigrahi, Stability of nanofluid: A review, Appl. Therm. Eng. 174 (2020) 115259.

[63] N. Kumar, A. Mandal, Wettability alteration of sandstone rock by surfactant stabilized nanoemulsion for enhanced oil recovery—A mechanistic study, Colloids Surfaces A Physicochem. Eng. Asp. 601 (2020) 125043.

[64] H. Rezvani, B.P. Binks, D. Nguyen, Surfactant-Nanoparticle Formulations for Enhanced Oil Recovery in Calcite-Rich Rocks, Langmuir 40 (2024) 24989–25002.

[65] H. Farhadi, S. Riahi, S. Ayatollahi, H. Ahmadi, Experimental study of nanoparticle-

surfactant-stabilized CO_2 foam: Stability and mobility control, Chem. Eng. Res. Des. 111 (2016) 449–460.

[66] S. Al-Anssari, L.N. Nwidee, M. Arif, S. Wang, A. Barifcani, M. Lebedev, S. Iglauer, Wettability alteration of carbonate rocks via nanoparticle-anionic surfactant flooding at reservoirs conditions, SPE Symp. Prod. Enhanc. Cost Optim. 2017 (2017) 189203-ms.

[67] A. Daghbandan, A. Shahrabadi, M. Arabiyoun, Adsorption of Glycyrrhiza glabra natural nonionic surfactant onto the carbonate reservoir rock in the presence of SiO_2 nanoparticles surface: Towards enhanced oil recovery, J. Environ. Chem. Eng. 10 (2022) 107109.

[68] R. Saha, R.V.S. Uppaluri, P. Tiwari, Impact of Natural Surfactant (Reetha), Polymer (Xanthan Gum), and Silica Nanoparticles to Enhance Heavy Crude Oil Recovery, Energy Fuels 33 (2019) 4225–4236.

[69] A. Nourinia, A.K. Manshad, S.R. Shadizadeh, J.A. Ali, S. Iglauer, A. Keshavarz, A.H. Mohammadi, M. Ali, Synergistic Efficiency of Zinc Oxide/Montmorillonite Nanocomposites and a New Derived Saponin in Liquid/Liquid/Solid Interface-Included Systems: Application in Nanotechnology-Assisted Enhanced Oil Recovery, ACS Omega 7 (2022) 24951–24972.

[70] F. Agyenim, N. Hewitt, P. Eames, M. Smyth, A review of materials, heat transfer and phase change problem formulation for latent heat thermal energy storage systems (LHTESS), Renew. Sustain. Energy Rev. 14 (2010) 615–628.

[71] X. Yimin, L. Qiang, Science In China (Series E) Convective heat transfer and flow characteristics of Cu-water nanofluid, Convect. Heat Transf. 45 (2002).

[72] B. Chen, X. Wang, Y. Zhang, H. Xu, R. Yang, Experimental research on laminar flow performance of phase change emulsion, Appl. Therm. Eng. 26 (2006) 1238–1245.

[73] X. Zhang, J.Y. Wu, J. Niu, PCM-in-water emulsion for solar thermal applications: The effects of emulsifiers and emulsification conditions on thermal performance, stability and rheology characteristics, Sol. Energy Mater. Sol. Cells 147 (2016) 211–224.

[74] M. Mazzotti, J. Carlos, R. Allam, K.S. Lackner, F. Meunier, E.M. Rubin, J.C. Sanchez, K. Yogo, R. Zevenhoven, Mineral carbonation and industrial uses of carbon dioxide, in: IPCC Spec. Rep. Carbon Dioxide Capture Storage, (2005) 319–338.

[75] W.J.J. Huijgen, G.J. Ruijg, R.N.J. Comans, G.J. Witkamp, Energy consumption and net CO_2 sequestration of aqueous mineral carbonation, Ind. Eng. Chem. Res. 45 (2006) 9184–9194.

[76] W.J.J. Huijgen, G.J. Witkamp, R.N.J. Comans, Mineral CO_2 sequestration by steel slag carbonation, Environ. Sci. Technol. 39 (2005) 9676–9682.

[77] Q. Liu, W. Liu, J. Hu, L. Wang, J. Gao, B. Liang, H. Yue, G. Zhang, D. Luo, C. Li, Energy-efficient mineral carbonation of blast furnace slag with high value-added products, J. Clean. Prod. 197 (2018) 242–252.

[78] I. Galan, C. Andrade, P. Mora, M.A. Sanjuan, Sequestration of CO_2 by concrete carbonation, Environ. Sci. Technol. 44 (2010) 3181–3186.

[79] Y. Wei, X. Du, S. Liu, Y. Wen, Q. Liao, G. Jiao, T. Shimaoka, S. Tang, Promotion of chloride removal from MSWI fly ash by an accelerated wet-carbonation process to enhance ash recycling in cement manufacture, J. Environ. Chem. Eng. 12 (2024) 112591.

[80] H. Sukkathanyawat, A. Bampenrat, T. Jarunglumlert, C. Prommuak, Modification of waste sugarcane bagasse fly ash for CO_2 capture application, Mater. Renew. Sustain. Energy 11 (2022) 267–276.

[81] K.J. Reddy, W.L. Lindsay, F.W. Boyle, E.F. Redente, Solubility Relationships and Mineral Transformations Associated with Recarbonation of Retorted Shales, J. Environ. Qual. 15 (1986) 129–133.

[82] Y. Sun, V. Parikh, L. Zhang, Sequestration of carbon dioxide by indirect mineralization using Victorian brown coal fly ash, J. Hazard. Mater. 209–210 (2012) 458–466.

[83] G. Qian, H. Zhang, X. Zhang, P.C. Chui, Modification of MSW fly ash by anionic chelating surfactant, J. Hazard. Mater. 121 (2005) 251–258.

[84] H.O. Howsaway, R. El-Sayed, Synthesis of Potential Pharmaceutical Heterocycles as Surface Active Agents, J. Surfactants Deterg. 20 (2017) 681–694.

[85] D. Jain, I. Pancha, S.K. Mishra, A. Shrivastav, S. Mishra, Purification and characterization of haloalkaline thermoactive, solvent stable and SDS-induced protease from Bacillus sp.: A potential additive for laundry detergents, Bioresour. Technol. 115 (2012) 228–236.

[86] X. Long, N. He, Y. He, J. Jiang, T. Wu, Biosurfactant surfactin with pH-regulated emulsification activity for efficient oil separation when used as emulsifier, Bioresour. Technol. 241 (2017) 200–206.

[87] S.M. Sohail, I. Ahmad, H. Khan, W. Ahmad, Influence of surfactants on dispersity of Pakistani crude oils for resource recovery and residue reduction during distillation, J. Environ. Chem. Eng. 7 (2019) 102952.

[88] J. Gao, M. Hao, T. Wu, Y. Li, Efficient treatment of crude oil-contaminated hydrodesulphurization catalyst by using surfactant/solvent mixture, J. Environ. Chem. Eng. 9 (2021) 105890.

[89] S.K. Nandwani, M. Chakraborty, S. Gupta, Adsorption of Surface Active Ionic Liquids on Different Rock Types under High Salinity Conditions, Sci. Rep. 9 (2019) 1–16.

[90] S. Song, L. Zhu, W. Zhou, Simultaneous removal of phenanthrene and cadmium from contaminated soils by saponin, a plant-derived biosurfactant, Environ. Pollut. 156 (2008) 1368–1370.

[91] W. Tang, X. Wu, C. Huang, Z. Ling, C. Lai, Q. Yong, Natural surfactant-aided dilute sulfuric acid pretreatment of waste wheat straw to enhance enzymatic hydrolysis efficiency, Bioresour. Technol. 324 (2021) 124651.

[92] C. Negin, S. Ali, Q. Xie, Most common surfactants employed in chemical enhanced oil recovery, Petroleum 3 (2017) 197–211.

[93] W.B. Jensen, The origin of the Soxhlet extractor, J. Chem. Educ. 84 (2007) 1913–1914.

[94] K. Holmberg, B. Jönsson, B. Kronberg, B. Lindman, Surfactants and Polymers in Aqueous Solution, John Wiley & Sons, Ltd, Chichester, UK, 2002.

[95] B. Boruah, M. Gogoi, Plant based natural surfactants, Asian J. Home Sci. 8 (2013) 759–762.

[96] S. Chen, H. Liu, H. Sun, X. Yan, G. Wang, Y. Zhou, J. Zhang, Synthesis and physiochemical performance evaluation of novel sulphobetaine zwitterionic surfactants from lignin for enhanced oil recovery, J. Mol. Liq. 249 (2018) 73–82.

[97] M.A. Ahmadi, S.R. Shadizadeh, Adsorption of novel nonionic surfactant and particles mixture in carbonates: Enhanced oil recovery implication, Energy Fuels (2012) 4655–4663.

[98] S.T. Muntaha, M.N. Khan, Natural surfactant extracted from Sapindus mukurossi as an eco-friendly alternate to synthetic surfactant - A dye surfactant interaction study, J. Clean. Prod. 93 (2015) 145–150.

[99] K.R. Chaturvedi, J. Trivedi, T. Sharma, Single-step silica nanofluid for improved carbon dioxide flow and reduced formation damage in porous media for carbon utilization, Energy 197 (2020) 117276.

[100] K.R. Chaturvedi, A.K. Singh, T. Sharma, Impact of shale on properties and oil recovery potential of sandstone formation for low-salinity waterflooding applications, Asia-Pacific J. Chem. Eng. 14 (2019) e2352.

[101] K. Raghav Chaturvedi, R. Kumar, J. Trivedi, J.J. Sheng, T. Sharma, Stable Silica Nanofluids of an Oilfield Polymer for Enhanced CO_2 Absorption for Oilfield Applications, Energy Fuels 32 (2018) 12730–12741.

[102] K.R. Chaturvedi, R. Narukulla, M. Amani, T. Sharma, Experimental investigations to evaluate surfactant role on absorption capacity of nanofluid for CO_2 utilization in sustainable crude mobilization, Energy 225 (2021) 120321.

[103] K.R. Chaturvedi, T. Sharma, Rheological analysis and EOR potential of surfactant treated single-step silica nanofluid at high temperature and salinity, J. Pet. Sci. Eng. 196 (2021) 107704.

[104] K.R. Chaturvedi, J. Trivedi, T. Sharma, Evaluation of Polymer-Assisted Carbonated Water

Injection in Sandstone Reservoir: Absorption Kinetics, Rheology, and Oil Recovery Results, Energy Fuels 33 (2019) 5438–5451.

[105] K.R. Chaturvedi, T. Sharma, Carbonated polymeric nanofluids for enhanced oil recovery from sandstone reservoir, J. Pet. Sci. Eng. 194 (2020) 107499.

[106] M.B. Haider, D. Jha, B. Marriyappan Sivagnanam, R. Kumar, Thermodynamic and Kinetic Studies of CO_2 Capture by Glycol and Amine-Based Deep Eutectic Solvents, J. Chem. Eng. Data 63 (2018) 2671–2680.

[107] K.R. Chaturvedi, D. Ravilla, W. Kaleem, P. Jadhawar, T. Sharma, Impact of Low Salinity Water Injection on CO_2 Storage and Oil Recovery for Improved CO_2 Utilization, Chem. Eng. Sci. 229 (2021) 116127.

[108] M. Sagir, M. Mushtaq, M.S. Tahir, M.B. Tahir, A.R. Shaik, Surfactants for enhanced oil recovery applications, Surfactants Enhanc. Oil Recover. Appl. (2020) 1–129.

[109] S. Kumar, P. Panigrahi, R.K. Saw, A. Mandal, Interfacial Interaction of Cationic Surfactants and Its Effect on Wettability Alteration of Oil-Wet Carbonate Rock, Energy Fuels 30 (2016) 2846–2857.

[110] A. Bera, T. Kumar, K. Ojha, A. Mandal, Adsorption of surfactants on sand surface in enhanced oil recovery: Isotherms, kinetics and thermodynamic studies, Appl. Surf. Sci. 284 (2013) 87–99.

[111] M.S. Almutairi, M. Ali, Direct detection of saponins in crude extracts of soapnuts by FTIR, Nat. Prod. Res. 29 (2015) 1271–1275.

[112] M.S. Ahn, E.Y. Jie, S.Y. Song, H.S. Kim, I.J. Kim, S.W. Kim, Simultaneous estimation of

saponin contents from soybean seed using Fourier transform infrared spectroscopy and high-performance liquid chromatography analysis, Plant Biotechnol. Rep. 10 (2016) 403–414.

[113] K. Samal, C. Das, K. Mohanty, Eco-friendly biosurfactant saponin for the solubilization of cationic and anionic dyes in aqueous system, Dye. Pigment. 140 (2017) 100–108.

[114] K. Ma, L. Cui, Y. Dong, T. Wang, C. Da, G.J. Hirasaki, S.L. Biswal, Adsorption of cationic and anionic surfactants on natural and synthetic carbonate materials, J. Colloid Interface Sci. 408 (2013) 164–172.

[115] X. Kong, Y. Zhu, H. Lei, C. Wang, Y. Zhao, E. Huo, X. Lin, Q. Zhang, M. Qian, W. Mateo, R. Zou, Z. Fang, R. Ruan, Synthesis of graphene-like carbon from biomass pyrolysis and its applications, Chem. Eng. J. 399 (2020) 125808.

[116] R.R. de Sousa Junior, C.A.S. dos Santos, N.M. Ito, A.N. Suqueira, M. Lackner, D.J. dos Santos, PHB Processability and Property Improvement with Linear-Chain Polyester Oligomers Used as Plasticizers, Polymers 14 (2022) 1–17.

[117] H. Liu, D. Xie, L. Qian, X. Deng, Y.X. Leng, N. Huang, The mechanical properties of the ultrahigh molecular weight polyethylene (UHMWPE) modified by oxygen plasma, Surf. Coatings Technol. 205 (2011) 2697–2701.

[118] A. Selmani, I. Coha, K. Magdić, B. Čolović, V. Jokanović, S. Šegota, S. Gajović, A. Gajović, D. Jurašin, M. Dutour Sikirić, Multiscale study of the influence of cationic surfactants on amorphous calcium phosphate precipitation, CrystEngComm 17 (2015) 8529–8548.

[119] H. Wei, J. Chen, N. Fu, H. Chen, H. Lin, S. Han, Biomass-derived nitrogen-doped porous carbon with superior capacitive performance and high CO_2 capture capacity, Electrochim. Acta 266 (2018) 161–169.

[120] A. Tofoni, F. Tavani, I. Persson, P. D'Angelo, P K-Edge XANES Calculations of Mineral Standards: Exploring the Potential of Theoretical Methods in the Analysis of Phosphorus Speciation, Inorg. Chem. 62 (2023) 11188–11198.

[121] Y. Foucaud, M. Badawi, L.O. Filippov, O. Barres, I. V. Filippova, S. Lebègue, Synergistic adsorptions of Na_2CO_3 and Na_2SiO_3 on calcium minerals revealed by spectroscopic and: Ab initio molecular dynamics studies, Chem. Sci. 10 (2019) 9928–9940.

[122] C. Yuan, Y. Li, Q. Li, R. Jin, L. Ren, Purification of tea saponins and evaluation of its effect on alcohol dehydrogenase activity, Open Life Sci. 13 (2018) 56–63.

[123] A. Muniyan, K. Ravi, U. Mohan, R. Panchamoorthy, Characterization and in vitro antibacterial activity of saponin-conjugated silver nanoparticles against bacteria that cause burn wound infection, World J. Microbiol. Biotechnol. 33 (2017) 1–12.

[124] N. Saxena, N. Pal, K. Ojha, S. Dey, A. Mandal, Synthesis, characterization, physical and thermodynamic properties of a novel anionic surfactant derived from: Sapindus laurifolius, RSC Adv. 8 (2018) 24485–24499.

[125] A.L. George, G.F. White, Optimization of the methylene blue assay for anionic surfactants added to estuarine and marine water, Environ. Toxicol. Chem. 18 (1999) 2232–2236.

[126] L. Cui, M. Puerto, J.L. López-Salinas, S.L. Biswal, G.J. Hirasaki, Improved methylene blue two-phase titration method for determining cationic surfactant concentration in high-

salinity brine, Anal. Chem. 86 (2014) 11055–11061.

[127] M. Mohebbifar, M.H. Ghazanfari, M. Vossoughi, Experimental Investigation of Nano-Biomaterial Applications for Heavy Oil Recovery in Shaly Porous Models: A Pore-Level Study, J. Energy Resour. Technol. 137 (2015) 1–9.

[128] N. Pal, N. Saxena, A. Mandal, Equilibrium and dynamic adsorption of gemini surfactants with different spacer lengths at oil/aqueous interfaces, Colloids Surfaces A Physicochem. Eng. Asp. 533 (2017) 20–32.

[129] M.B. Haider, D. Jha, B. Marriyappan Sivagnanam, R. Kumar, Modelling and simulation of CO_2 removal from shale gas using deep eutectic solvents, J. Environ. Chem. Eng. 7 (2019) 102747.

[130] A. Haghtalab, M. Mohammadi, Z. Fakhroueian, Absorption and solubility measurement of CO_2 in water-based ZnO and SiO_2 nanofluids, Fluid Phase Equilib. 392 (2015) 33–42.

[131] M. Arshadi, H. Taghvaei, M.K. Abdolmaleki, M. Lee, H. Eskandarloo, A. Abbaspourrad, Carbon dioxide absorption in water/nanofluid by a symmetric amine-based nanodendritic adsorbent, Appl. Energy 242 (2019) 1562–1572.

[132] S. Li, Z. Li, P. Wang, Experimental Study of the Stabilization of CO_2 Foam by Sodium Dodecyl Sulfate and Hydrophobic Nanoparticles, Ind. Eng. Chem. Res. 55 (2016) 1243–1253.

[133] S. Kalliadasis, H.C. Chang, Apparent dynamic contact angle of an advancing gas-liquid meniscus, Phys. Fluids 6 (1994) 12–23.

[134] R. Murakami, S. Kobayashi, M. Okazaki, A. Bismarck, M. Yamamoto, Effects of contact

angle and flocculation of particles of oligomer of tetrafluoroethylene on oil foaming, Front. Chem. 6 (2018) 435.

[135] N. Denkov, S. Tcholakova, N. Politova-Brinkova, Physicochemical control of foam properties, Curr. Opin. Colloid Interface Sci. 50 (2020) 101376.

[136] A. Telmadarreie, J. Trivedi, Static and Dynamic Performance of Wet Foam and Polymer-Enhanced Foam in the Presence of Heavy Oil, Colloids and Interfaces 2 (2018) 38.

[137] M.A. Muherei, R. Junin, A.B. Bin Merdhah, Adsorption of sodium dodecyl sulfate, Triton X100 and their mixtures to shale and sandstone: A comparative study, J. Pet. Sci. Eng. 67 (2009) 149–154.

[138] M. Mourabet, H. El Boujaady, A. El Rhilassi, H. Ramdane, M. Bennani-Ziatni, R. El Hamri, A. Taitai, Defluoridation of water using Brushite: Equilibrium, kinetic and thermodynamic studies, Desalination 278 (2011) 1–9.

[139] M.A. Wahab, S. Jellali, N. Jedidi, Ammonium biosorption onto sawdust: FTIR analysis, kinetics and adsorption isotherms modeling, Bioresour. Technol. 101 (2010) 5070–5075.

[140] M.M. Ayad, A.A. El-Nasr, Adsorption of cationic dye (methylene blue) from water using polyaniline nanotubes base, J. Phys. Chem. C 114 (2010) 14377–14383.

[141] T.S. Khayyun, A.H. Mseer, Comparison of the experimental results with the Langmuir and Freundlich models for copper removal on limestone adsorbent, Appl. Water Sci. 9 (2019) 170.

[142] B. Samiey, M.R. Dargahi, Kinetics and thermodynamics of adsorption of congo red on cellulose, Cent. Eur. J. Chem. 8 (2010) 906–912.

[143] I. Lakatos, L.S. Julianna, Global oil demand and role of chemical EOR methods in the 21st century, Int. J. Oil, Gas Coal Technol. 1 (2008) 46–64.

[144] A. Davies, M.D. Simmons, Demand for 'advantaged' hydrocarbons during the 21st century energy transition, Energy Reports 7 (2021) 4483–4497.

[145] A.O. Gbadamosi, R. Junin, M.A. Manan, A. Agi, A.S. Yusuff, An overview of chemical enhanced oil recovery: recent advances and prospects, Int. Nano Lett. 9 (2019) 171–202.

[146] A.I.C.G. and E.L.B.N. F. D. S. Curbelo, Petroleum Science and Technology Enhanced Oil Recovery and Adsorption of Ionic Surfactant, Pet. Sci. Technol. 7 (2013) 663–671.

[147] J.J. Sheng, Introduction to MEOR and Its Field Applications in China, First Edit, Elsevier Inc., (2013) 543-559.

[148] F.O. Asl, G. Zargar, A.K. Manshad, M. Arif, S. Iglauer, A. Keshavarz, Impact of PAM-ZnO nanocomposite on oil recovery, Fuel 332 (2023) 125941.

[149] P. Druetta, F. Picchioni, Surfactant-polymer interactions in a combined enhanced oil recovery flooding, Energies 13 (2020) 6520.

[150] S. Park, E.S. Lee, W.R.W. Sulaiman, Adsorption behaviors of surfactants for chemical flooding in enhanced oil recovery, J. Ind. Eng. Chem. 21 (2015) 1239–1245.

[151] R.E. Terry, Enhanced oil recovery., in: Encycl. Phys. Sci. Technol. (1980) 503–518.

[152] B. Govreau, B. Marcotte, A. Sheehy, K. Town, B. Zahner, S. Tapper, F. Akintunji, Field Applications of Organic Oil Recovery-A New MEOR Method, First Edit, Elsevier Inc. (2013) 581-614.

[153] L. Fu, G. Zhang, J. Ge, K. Liao, H. Pei, P. Jiang, X. Li, Study on organic alkali-surfactant-

polymer flooding for enhanced ordinary heavy oil recovery, Colloids Surfaces A Physicochem. Eng. Asp. 508 (2016) 230–239.

[154] W. Pu, C. Shen, B. Wei, Y. Yang, Y. Li, A comprehensive review of polysaccharide biopolymers for enhanced oil recovery (EOR) from flask to field, J. Ind. Eng. Chem. 61 (2018) 1–11.

[155] T.T. Nguyen, C. Morgan, L. Poindexter, J. Fernandez, Application of the Hydrophilic–Lipophilic Deviation Concept to Surfactant Characterization and Surfactant Selection for Enhanced Oil Recovery, J. Surfactants Deterg. 22 (2019) 983–999.

[156] M. Arif, S.A. Abu-Khamsin, S. Iglauer, Wettability of rock/CO_2 /brine and rock/oil/CO_2 -enriched-brine systems:Critical parametric analysis and future outlook, Adv. Colloid Interface Sci. 268 (2019) 91–113.

[157] S. Das, Q. Nguyen, P.D. Patil, W. Yu, R.T. Bonnecaze, Wettability Alteration of Calcite by Nonionic Surfactants, Langmuir 34 (2018) 10650–10658.

[158] N. Pal, N. Kumar, A. Verma, K. Ojha, A. Mandal, Performance Evaluation of Novel Sunflower Oil-Based Gemini Surfactant(s) with Different Spacer Lengths: Application in Enhanced Oil Recovery, Energy Fuels 32 (2018) 11344–11361.

[159] H. Khayati, A. Moslemizadeh, K. Shahbazi, M.K. Moraveji, S.H. Riazi, An experimental investigation on the use of saponin as a non-ionic surfactant for chemical enhanced oil recovery (EOR) in sandstone and carbonate oil reservoirs: IFT, wettability alteration, and oil recovery, Chem. Eng. Res. Des. 160 (2020) 417–425.

[160] A.M. Alsabagh, A.A. Aboulrous, M.M. Abdelhamid, T. Mahmoud, A.S. Haddad, R. Rafati,

Improvement of Heavy Oil Recovery by Nonionic Surfactant/Alcohol Flooding in Light of the Alkane Carbon Number and Interfacial Tension Properties, ACS Omega 6 (2021) 18668–18683.

[161] S. Kumar, A. Mandal, Investigation on stabilization of CO_2 foam by ionic and nonionic surfactants in presence of different additives for application in enhanced oil recovery, Appl. Surf. Sci. 420 (2017) 9–20.

[162] K.R. Chaturvedi, T. Sharma, Carbonated polymeric nanofluids for enhanced oil recovery from sandstone reservoir, J. Pet. Sci. Eng. 194 (2020) 107499.

[163] R.S. Kumar, T. Sharma, Stable SiO_2–TiO_2 composite-based nanofluid of improved rheological behaviour for high-temperature oilfield applications, Geosystem Eng. 23 (2020) 51–61.

[164] K.R. Chaturvedi, R. Kumar, J. Trivedi, J.J. Sheng, T. Sharma, Stable Silica Nanofluids of an Oilfield Polymer for Enhanced CO_2 Absorption for Oilfield Applications, Energy Fuels 32 (2018) 12730–12741.

[165] R.S. Kumar, T. Al-Arbi Ganat, T. Sharma, Performance evaluation of silica nanofluid for sand column transport with simultaneous wettability alteration: An approach to environmental issue, J. Clean. Prod. 303 (2021) 127047.

[166] A. Samanta, K. Ojha, A. Sarkar, A. Mandal, Surfactant and Surfactant-Polymer Flooding for Enhanced Oil Recovery, Adv. Pet. Explor. Dev. 2 (2011) 13–18.

[167] A. Singh, K.R. Chaturvedi, T. Sharma, Green materials for carbon storage in depleted oilfields: An experimental study, Mater. Today Proc. (2022) 168–174.

[168] E. Carey, C. Stubenrauch, Properties of aqueous foams stabilized by dodecyltrimethylammonium bromide, J. Colloid Interface Sci. 333 (2009) 619–627.

[169] R.A. Nasralla, H.A. Nasr-El-Din, Double-layer expansion: Is it a primary mechanism of improved oil recovery by low-salinity waterflooding?, SPE Reserv. Eval. Eng. 17 (2014) 49–59.

[170] M. Arabloo, M.H. Ghazanfari, D. Rashtchian, Spotlight on kinetic and equilibrium adsorption of a new surfactant onto sandstone minerals: A comparative study, J. Taiwan Inst. Chem. Eng. 50 (2015) 12–23.

[171] K. Babu, N. Pal, A. Bera, V.K. Saxena, A. Mandal, Studies on interfacial tension and contact angle of synthesized surfactant and polymeric from castor oil for enhanced oil recovery, Appl. Surf. Sci. 353 (2015) 1126–1136.

[172] S.K. Mofrad, A.H. Saeedi Dehaghani, An experimental investigation into enhancing oil recovery using smart water combined with anionic and cationic surfactants in carbonate reservoir, Energy Reports 6 (2020) 543–549.

[173] F. Han, Y.Y. Deng, P.L. Wang, J. Song, Y.W. Zhou, B.C. Xu, Synthesis and characterization of glucosamide surfactant, J. Surfactants Deterg. 16 (2013) 155–159.

[174] M. Hasanzadeh, V. Mottaghitalab, M. Rezaei, Rheological and viscoelastic behavior of concentrated colloidal suspensions of silica nanoparticles: A response surface methodology approach, Adv. Powder Technol. 26 (2015) 1570–1577.

[175] R.S. Kumar, T. Sharma, Stability and rheological properties of nanofluids stabilized by SiO_2 nanoparticles and SiO_2-TiO_2 nanocomposites for oilfield applications, Colloids Surfaces A

Physicochem. Eng. Asp. 539 (2018) 171–183.

[176] M. Arif, A.Z. Al-Yaseri, A. Barifcani, M. Lebedev, S. Iglauer, Impact of pressure and temperature on CO_2-brine-mica contact angles and CO_2-brine interfacial tension: Implications for carbon geo-sequestration, J. Colloid Interface Sci. 462 (2016) 208–215.

[177] T. Huhtamäki, X. Tian, J.T. Korhonen, R.H.A. Ras, Surface-wetting characterization using contact-angle measurements, Nat. Protoc. 13 (2018) 1521–1538.

[178] J. Chinnam, D. Das, R. Vajjha, J. Satti, Measurements of the contact angle of nanofluids and development of a new correlation, Int. Commun. Heat Mass Transf. 62 (2015) 1–12.

[179] P. Estellé, D. Cabaleiro, G. Żyła, L. Lugo, S.M.S. Murshed, Current trends in surface tension and wetting behavior of nanofluids, Renew. Sustain. Energy Rev. 94 (2018) 931–944.

[180] H. Zhong, T. Yang, H. Yin, J. Lu, K. Zhang, C. Fu, Role of Alkali type in chemical loss and ASP-flooding enhanced oil recovery in Sandstone formations, SPE Reserv. Eval. Eng. 23 (2020) 431–445.

[181] G.S. Kusumah, O. Vazquez, Evolution of pH and retention of different alkali species for ASP flooding field applications, SPE Bergen One Day Semin. 2017 (2017)185886-ms.

[182] R. Saha, R.V.S. Uppaluri, P. Tiwari, Influence of emulsification, interfacial tension, wettability alteration and saponification on residual oil recovery by alkali flooding, J. Ind. Eng. Chem. 59 (2018) 286–296.

[183] M. Nedjhioui, N. Moulai-Mostefa, A. Morsli, A. Bensmaili, Combined effects of polymer/surfactant/oil/alkali on physical chemical properties, Desalination 185 (2005) 543–

550.

[184] T. Tichelkamp, H. Hosseinzade Khanamiri, M. Nourani, J. Åge Stensen, O. Torsæter, G. Øye, EOR Potential of Mixed Alkylbenzenesulfonate Surfactant at Low Salinity and the Effect of Calcium on “optimal Ionic Strength,” Energy Fuels 30 (2016) 2919–2924.

[185] K. Panthi, K.K. Mohanty, E ff ect of Alkaline Pre fl ush in an Alkaline-Surfactant-Polymer Flood, Energy Fuels 27 (2013) 764–771.

[186] N. Husein, M.H. Yunan, I. Ismail, W.R.W. Sulaiman, N. V. Boyou, Enhanced oil recovery by alkaline-surfactant-polymer alternating with waterflooding, Chem. Eng. Trans. 63 (2018) 823–828.

[187] H.S. Al-Hashim, V. Obiora, H.Y. Al-Yousef, F. Fernandez, W. Nofal, Alkaline surfactant polymer formulation for carbonate reservoirs, Pet. Sci. Technol. 23 (2005) 723–746.

[188] E. Carrero, N. V. Queipo, S. Pintos, L.E. Zerpa, Global sensitivity analysis of Alkali-Surfactant-Polymer enhanced oil recovery processes, J. Pet. Sci. Eng. 58 (2007) 30–42.

[189] N.T. Su, D. Fornasiero, R. Sedev, J. Ralston, The role of surfactant structure on foam behaviour, Colloids Surfaces A Physicochem. Eng. Asp. 263 (2005) 233–238.

[190] Q. Wu, L. Ding, L. Zhang, J. Ge, M.A. Rahman, I.G. Economou, D. Guérillot, Polymer enhanced foam for improving oil recovery in oil-wet carbonate reservoirs: A proof of concept and insights into the polymer-surfactant interactions, Energy 264 (2023) 126256.

[191] K.D. Wantke, H. Fruhner, Determination of Surface Dilational Viscosity Using the Oscillating Bubble Method, J. Colloid Interface Sci. 237 (2001) 185–199.

[192] K. Małysa, Wet foams: Formation, properties and mechanism of stability, Adv. Colloid

Interface Sci. 40 (1992) 37–83.

[193] T. Majeed, T.I. Sølling, M.S. Kamal, Foamstability: The interplay between salt-, surfactant- and critical micelle concentration, J. Pet. Sci. Eng. 187 (2020) 106871.

[194] D.C.H. Cheng, E. Gulari, Micellization and intermicellar interactions in aqueous sodium dodecyl benzene sulfonate solutions, J. Colloid Interface Sci. 90 (1982) 410–423.

[195] G. Bournival, Z. Du, S. Ata, G.J. Jameson, Foaming and gas dispersion properties of non-ionic surfactants in the presence of an inorganic electrolyte, Chem. Eng. Sci. 116 (2014) 536–546.

[196] P. Amani, S.I. Karakashev, N.A. Grozev, S.S. Simeonova, R. Miller, V. Rudolph, M. Firouzi, Effect of selected monovalent salts on surfactant stabilized foams, Adv. Colloid Interface Sci. 295 (2021) 102490.

[197] S.I. Karakashev, E.D. Manev, Frothing behavior of nonionic surfactant solutions in the presence of organic and inorganic electrolytes, J. Colloid Interface Sci. 235 (2001) 194–196.

[198] I.B. Ivanov, R.I. Slavchov, E.S. Basheva, D. Sidzhakova, S.I. Karakashev, Hofmeister effect on micellization, thin films and emulsion stability, Adv. Colloid Interface Sci. 168 (2011) 93–104.

[199] S. Sett, S.I. Karakashev, S.K. Smoukov, A.L. Yarin, Ion-specific effects in foams, Adv. Colloid Interface Sci. 225 (2015) 98–113.

[200] J. Wang, The effect of inorganic salts on the viscosity behavior of sodium dodecyl benzenesulfonate solution with high concentration, Colloids Surfaces A Physicochem. Eng.

Asp. 70 (1993) 15–21.

[201] L. Zhang, L. Tian, H. Du, S. Rouzière, N. Wang, A. Salonen, Foams Stabilized by Surfactant Precipitates: Criteria for Ultrastability, Langmuir 33 (2017) 7305–7311.

[202] Q. Xu, M. Nakajima, S. Ichikawa, N. Nakamura, P. Roy, H. Okadome, T. Shiina, Effects of surfactant and electrolyte concentrations on bubble formation and stabilization, J. Colloid Interface Sci. 332 (2009) 208–214.

[203] K. Hazarika, S.B. Gogoi, Effect of alkali on alkali–surfactant flooding in an Upper Assam oil field, J. Pet. Explor. Prod. Technol. 10 (2020) 1591–1601.

[204] J.J. Sheng, Alkaline-Surfactant-Polymer Flooding, 2011.

[205] Y. Ma, J. Hou, F. Zhao, Z. Song, Linearly descending viscosity for alkaline-surfactant-polymer flooding mobility modification in multilayer heterogeneous reservoirs, RSC Adv. 8 (2018) 8269–8284.

[206] M.Y. Khan, A. Samanta, K. Ojha, A. Mandal, Design of alkaline/surfactant/polymer (ASP) slug and its use in enhanced oil recovery, Pet. Sci. Technol. 27 (2009) 1926–1942.

[207] A.A. Olajire, Review of ASP EOR (alkaline surfactant polymer enhanced oil recovery) technology in the petroleum industry: Prospects and challenges, Energy 77 (2014) 963–982.

[208] M.E.S. Abdel-Raouf, Factors Affecting the Stability of Crude Oil Emulsions, in: Crude Oil Emuls. Compos. Stab. Charact. (2012) 183–204.

[209] H.J. Oschmann, U. Prahl, D. Severin, Separation of paraffin from crude oil by supercritical fluid extraction, Pet. Sci. Technol. 16 (1998) 133–143.

[210] S. Allenson, A. Johnston, Comparison Of Different Experimental Techniques Used For

Wax Deposition Testing, Rio Oil Gas Expo Conf. Proc. (2008) 1–10.

[211] J. Huang, J. Xu, K. Chen, T. Wang, C. Cui, X. Wei, R. Zhang, L. Li, X. Guo, Synthesis of triblock copolymers via RAFT polymerization and their application as surfactants for crude oil-in-water emulsion, Ind. Eng. Chem. Res. 54 (2015) 1564–1575.

[212] N. Sakthipriya, M. Doble, J.S. Sangwai, Action of biosurfactant producing thermophilic Bacillus subtilis on waxy crude oil and long chain paraffins, Int. Biodeterior. Biodegrad. 105 (2015) 168–177.

[213] V. Hoshyargar, S.N. Ashrafizadeh, Optimization of flow parameters of heavy crude oil-in-water emulsions through pipelines, Ind. Eng. Chem. Res. 52 (2013) 1600–1611.

[214] M.A. Ahmadi, Z. Ahmad, L.T.K. Phung, T. Kashiwao, A. Bahadori, Evaluation of the ability of the hydrophobic nanoparticles of SiO_2 in the EOR process through carbonate rock samples, Pet. Sci. Technol. 34 (2016) 1048–1054.

[215] Desnelli, D. Mujahidin, Y. Permana, C.L. Radiman, Copolymerization of Acrylamide with 9- and 10-Acrylamidodecanoic Acids, Macromol. Symp. 353 (2015) 198–204.

[216] M. V. Kok, Progress and recent utilization trends in petroleum recovery: Steam injection and in-situ combustion, Energy Sources, Part A Recover. Util. Environ. Eff. 34 (2012) 2253–2259.

[217] N.K. Maurya, P. Kushwaha, A. Mandal, Studies on interfacial and rheological properties of water soluble polymer grafted nanoparticle for application in enhanced oil recovery, J. Taiwan Inst. Chem. Eng. 70 (2017) 319–330.

[218] A.F. Belhaj, K.A. Elraies, S.M. Mahmood, N.N. Zulkifli, S. Akbari, O.S.E. Hussien, The

effect of surfactant concentration, salinity, temperature, and pH on surfactant adsorption for chemical enhanced oil recovery: a review, J. Pet. Explor. Prod. Technol. 10 (2020) 125–137.

[219] P.J. Liyanage, S. Solairaj, G.W. Pinnawala Arachchilage, H.C. Linnemeyer, D.H. Kim, U. Weerasooriya, G.A. Pope, Alkaline surfactant polymer flooding using a novel class of large hydrophobe surfactants, SPE - DOE Improv. Oil Recover. Symp. Proc. 2 (2012) 1415–1431.

[220] F. Ameli, S. Moghadam, S. Shahmarvand, Polymer flooding, in: Chem. Methods, (2021) 33–94.

[221] N.N. Zulkifli, S.M. Mahmood, S. Akbari, A.A.A. Manap, N.I. Kechut, K.A. Elrais, Evaluation of new surfactants for enhanced oil recovery applications in high-temperature reservoirs, J. Pet. Explor. Prod. Technol. 10 (2020) 283–296.

[222] T. Al-Sahhaf, A.S. Ahmed, A. Elkamel, Producing ultralow interfacial tension at the oil/water interface, Pet. Sci. Technol. 20 (2002) 773–788.

[223] K.C. Taylor, H.A. Nasr-El-Din, The effect of synthetic surfactants on the interfacial behaviour of crude oil/alkali/polymer systems, Colloids Surfaces A Physicochem. Eng. Asp. 108 (1996) 49–72.

[224] A. Bhardwaj, S. Hartland, Dynamics of Emulsification and Demulsification of Water in Crude Oil Emulsions, Ind. Eng. Chem. Res. 33 (1994) 1271–1279.

[225] S. Drexler, J. Faria, M.P. Ruiz, J.H. Harwell, D.E. Resasco, Amphiphilic nanohybrid catalysts for reactions at the water/oil interface in subsurface reservoirs, Energy Fuels 26

(2012) 2231–2241.

[226] J.L. Salager, L. Marquez, A.A. Peña, M. Rondón, F. Silva, E. Tyrode, Current phenomenological know-how and modeling of emulsion inversion, Ind. Eng. Chem. Res. 39 (2000) 2665–2676.

[227] H. Deymeh, S.R. Shadizadeh, R. Motafakkerfard, Experimental investigation of Seidlitzia rosmarinus effect on oil-water interfacial tension: Usable for chemical enhanced oil recovery, Sci. Iran. 19 (2012) 1661–1664.

[228] K. Ogino, M. Onishi, Interfacial action of natural surfactants in oil/water systems, J. Colloid Interface Sci. 83 (1981) 18–25.

[229] A. Singh, T. Sharma, R.S. Kumar, M. Arif, Biosurfactant Derived from Fenugreek Seeds and Its Impact on Wettability Alteration, Oil Recovery, and Effluent Treatment of a Rock System of Mixed Composition, Energy Fuels 37 (2023) 6683–6696.

[230] J. Zhang, D. Ge, X. Wang, W. Wang, D. Cui, G. Yuan, K. Wang, W. Zhang, Influence of Surfactant and Weak-Alkali Concentrations on the Stability of O/W Emulsion in an Alkali-Surfactant-Polymer Compound System, ACS Omega 6 (2021) 5001–5008.

[231] X. Zhang, F. Li, X. Zhao, Treatment of surfactants with concentrations below critical micelle concentration by ultrafiltration: A mini-review, Water Cycle 3 (2022) 50–55.

[232] K.S. Lee, J.H. Lee, Hybrid Chemical EOR Using Low-Salinity and Smart Waterflood, in: Hybrid Enhanc. Oil Recover. Using Smart Waterflooding, Gulf Professional Publishing, (2019) 65–110.

[233] O.M. Haghighi, G. Zargar, A.K. Manshad, M. Ali, M.A. Takassi, J.A. Ali, A. Keshavarz,

Effect of environment-friendly non-ionic surfactant on interfacial tension reduction and wettability alteration; Implications for enhanced oil recovery, Energies 13 (2020) 3988.

[234] S.R.M. Dashtaki, J.A. Ali, B. Majeed, A.K. Manshad, I. Nowrouzi, S. Iglauer, A. Keshavarz, Evaluation the role of natural surfactants from Tanacetum and Tarragon plants in EOR applications, J. Mol. Liq. 361 (2022) 119576.

[235] I. Nowrouzi, A.H. Mohammadi, A.K. Manshad, Characterization and evaluation of a natural surfactant extracted from Soapwort plant for alkali-surfactant-polymer (ASP) slug injection into sandstone oil reservoirs, J. Mol. Liq. 318 (2020) 114369.

[236] R. Narukulla, U. Ojha, T. Sharma, Stable & re-dispersible polyacryloyl hydrazide-Ag nanocomposite Pickering emulsions, Soft Matter 13 (2017) 6118-6128.

[237] B. Sami, A. Azdarpour, B. Honarvar, M. Nabipour, A. Keshavarz, Application of a novel natural surfactant extracted from Avena Sativa for enhanced oil recovery during low salinity water flooding: Synergism of natural surfactant with different salts, J. Mol. Liq. 362 (2022) 119693.

[238] T.S.T. Ariffin, E. Yahya, H. Husin, The rheology of light crude oil and water-in-oil-emulsion, Procedia Eng. 148 (2016) 1149–1155.

[239] J.K.M. William, S. Ponmani, R. Samuel, R. Nagarajan, J.S. Sangwai, Effect of CuO and ZnO nanofluids in xanthan gum on thermal, electrical and high pressure rheology of water-based drilling fluids, J. Pet. Sci. Eng. 117 (2014) 15–27.

[240] C. Liu, H. Du, L. Dong, X. Wang, Y. Zhang, G. Yu, B. Li, X. Mu, H. Peng, H. Liu, Properties of Nanocelluloses and Their Application as Rheology Modifier in Paper Coating,

Ind. Eng. Chem. Res. 56 (2017) 8264–8273.

[241] T. Sharma, J.S. Sangwai, Silica nanofluids in polyacrylamide with and without surfactant: Viscosity, surface tension, and interfacial tension with liquid paraffin, J. Pet. Sci. Eng. 152 (2017) 575–585.

[242] O. Massarweh, A.S. Abushaikha, The use of surfactants in enhanced oil recovery: A review of recent advances, Energy Reports 6 (2020) 3150–3178.

[243] A. Kakati, N.K. Jha, G. Kumar, J.S. Sangwai, Application of low salinity water flooding for light paraffinic crude oil reservoir, SPE Symp. Prod. Enhanc. Cost Optim. (2017) 189249-ms.

[244] B.F. Hou, Y.F. Wang, Y. Huang, Mechanistic study of wettability alteration of oil-wet sandstone surface using different surfactants, Appl. Surf. Sci. 330 (2015) 56–64.

[245] H.M.B. Al-Hashemi, O.S.B. Al-Amoudi, A review on the angle of repose of granular materials, Powder Technol. 330 (2018) 397–417.

[246] P.A. Rakhmanto, L. Satiawati, R. Setiati, A. Nugrahanti, S. Irawan, Effect of Sand Grain Size on Spontaneous Imbibition of Surfactant Solution, J. Earth Energy Sci. Eng. Technol. 4 (2021) 2–6.

[247] Y. Saulick, S. Lourenço, B. Baudet, Effect of particle size on the measurement of the apparent contact angle in sand of varying wettability under air-dried conditions, in: E3S Web Conf. 9 (2016) 09003.

[248] Z. Bachari, A.A. Isari, H. Mahmoudi, S. Moradi, E.H. Mahvelati, Application of Natural Surfactants for Enhanced Oil Recovery-Critical Review, IOP Conf. Ser. Earth Environ. Sci.

221 (2019) 012039.

[249] N. Saxena, A. Saxena, A. Mandal, Synthesis, characterization and enhanced oil recovery potential analysis through simulation of a natural anionic surfactant, J. Mol. Liq. 282 (2019) 545–556.

[250] J. Bryan, A. Kantzas, Enhanced heavy-oil recovery by alkali-surfactant flooding, in: SPE Annu. Tech. Conf. Proc. (2007) 3642–3654.

[251] H. Pei, G. Zhang, J. Ge, P. Jiang, J. Zhang, Y. Zhong, Study of polymer-enhanced emulsion flooding to improve viscous oil recovery in waterflooded heavy oil reservoirs, Colloids Surfaces A Physicochem. Eng. Asp. 529 (2017) 409–416.

[252] X. Shang, Y. Bai, J. Sun, C. Dong, Performance and displacement mechanism of a surfactant/compound alkaline flooding system for enhanced oil recovery, Colloids Surfaces A Physicochem. Eng. Asp. 580 (2019) 123679.

[253] F. Yu, H. Jiang, Z. Fan, F. Xu, H. Su, J. Li, Formation and Flow Behaviors of in Situ Emulsions in Heavy Oil Reservoirs, Energy Fuels 33 (2019) 5961–5970.

[254] A. Singh, T. Sharma, Design and performance evaluation of Alkaline-Surfactant-Polymer slug of a natural surfactant of fenugreek in saline media for Foaming/Emulsification applications, J. Mol. Liq. 395 (2023) 123912.

[255] A. Omidi, A.K. Manshad, S. Moradi, J.A. Ali, S.M. Sajadi, A. Keshavarz, Smart- and nano-hybrid chemical EOR flooding using Fe_3O_4/eggshell nanocomposites, J. Mol. Liq. 316 (2020) 113880.

[256] A.H. Abbas, R.A. Abd Alsaheb, J.K. Abdullah, Comparative study of natural chemical for

enhanced oil recovery: Focus on extraction and adsorption at quartz sand surface, Petroleum 9 (2022) 83–93.

[257] F.D. Martin, J.C. Oxley, H. Lim, Enhanced recovery of a “J” Sand crude oil with a combination of surfactant and alkaline chemicals, in: Proc. - SPE Annu. Tech. Conf. Exhib. (1985) 14293-ms.

[258] A. Ruiz, A. Pinazo, L. Pérez, A. Manresa, A.M. Marqués, Green Catanionic Gemini Surfactant-Lichenysin Mixture: Improved Surface, Antimicrobial, and Physiological Properties, ACS Appl. Mater. Interfaces 9 (2017) 22121–22131.

[259] A. Samanta, K. Ojha, A. Mandal, A. Sarkar, Extraction and Characterization of an Eco-Friendly Surfactant for Its Use in Enhanced Oil Recovery, J. Pet. Eng. Technol. 3 (2013) 20-29.

[260] H. Esfandyari, S.R. Shadizadeh, F. Esmaeilzadeh, A. Davarpanah, Implications of anionic and natural surfactants to measure wettability alteration in EOR processes, Fuel 278 (2020) 118392.

[261] K.R. Chaturvedi, A. Pandey, R. Kumar, T. Sharma, Role of hydrogen to promote hydrate formation of flue gas mixture of CO_2 and N_2 in silica nanofluid of single-step origin, J. Environ. Chem. Eng. 9 (2021) 106591.

[262] N. Lashari, T. Ganat, S. Kalam, T.A. Chandio, T. Sharma, S. Qureshi, Impact of a novel HPAM/GO-SiO_2 nanocomposite on interfacial tension: Application for enhanced oil recovery, Pet. Sci. Technol. 40 (2022) 290–309.

[263] R. Raman Ujjwal, T. Sharma, J.S. Sangwai, U. Ojha, Rheological investigation of a random

copolymer of polyacrylamide and polyacryloyl hydrazide (PAM-ran-PAH) for oil recovery applications, J. Appl. Polym. Sci. 134 (2017) 44648.

[264] R. Narukulla, U. Ojha, T. Sharma, Effect of NaCl concentration on stability of a polymer-Ag nanocomposite based Pickering emulsion: Validationviarheological analysis with varying temperature, RSC Adv. 10 (2020) 21545–21560.

[265] K.R. Chaturvedi, M. Fogat, T. Sharma, Low Temperature rheological characterization of single-step silica nanofluids: An additive in refrigeration and gas hydrate drilling applications, J. Pet. Sci. Eng. 204 (2021) 108742.

[266] N.N. Zaki, Surfactant stabilized crude oil-in-water emulsions for pipeline transportation of viscous crude oils, Colloids Surfaces A Physicochem. Eng. Asp. 125 (1997) 19–25.

[267] S. Xie, S. Chen, S. Chen, Q. Zhu, Q. Zhu, X. Li, X. Li, D. Wang, D. Wang, S. Shen, M. Jin, M. Jin, G. Zhou, G. Zhou, Y. Zhu, L. Shui, L. Shui, L. Shui, Janus Nanoparticles with Tunable Amphiphilicity for Stabilizing Pickering-Emulsion Droplets via Assembly Behavior at Oil-Water Interfaces, ACS Appl. Mater. Interfaces 12 (2020) 26374–26383.

[268] A. Debnath, A. Pandey, T. Chaturvedi, Krishna Raghav Sharma, Evaluation of performance spectra of mono and divalent low saline brine injection in sandy-carbonates for mobilization of crude oil, Colloids Surfaces A Physicochem. Eng. Asp. 640 (2022) 128506.

[269] N.R. Biswal, J.K. Singh, Interfacial behavior of nonionic Tween 20 surfactant at oil-water interfaces in the presence of different types of nanoparticles, RSC Adv. 6 (2016) 113307–113314.

[270] P. Hosseininoosheri, H.R. Lashgari, K. Sepehrnoori, A novel method to model and

characterize in-situ bio-surfactant production in microbial enhanced oil recovery, Fuel 183 (2016) 501–511.

[271] K.L. Mittal, Contact Angle, Wettability and Adhesion,Volume 4, CRC Press, (2006) 7823–7830.

[272] A. Singh, A.R. Kashyap, M.M. Abdullah, S. Vajpayee, T. Sharma, Investigation on Rheological Characterization and Salt Tolerance Potential of Paraffinic O/W Emulsions of Natural Surfactant for Crude Emulsification and Mobilization, Ind. Eng. Chem. Res. 63 (2024) 10825–41.

[273] T. Sharma, J.S. Sangwai, Effects of electrolytes on the stability and dynamic rheological properties of an oil-in-water pickering emulsion stabilized by a nanoparticle-surfactant-polymer system, Ind. Eng. Chem. Res. 54 (2015) 5842–5852.

[274] K.R. Chaturvedi, R. Narukulla, T. Sharma, CO_2 capturing evaluation of single-step silica nanofluid through rheological investigation for nanofluid use in carbon utilization applications, J. Mol. Liq. 304 (2020) 112765.

[275] S.M. Shams, Y. Kazemzadeh, M. Riazi, F.B. Cortés, Effect of pressure on the optimal salinity point of the aqueous phase in emulsion formation, J. Mol. Liq. 362 (2022) 119783.

[276] T. Frising, C. Noïk, C. Dalmazzone, The liquid/liquid sedimentation process: From droplet coalescence to technologically enhanced water/oil emulsion gravity separators: A review, J. Dispers. Sci. Technol. 27 (2006) 1035–1057.

[277] M. Rondón, P. Bouriat, J. Lachaise, J.L. Salager, Breaking of water-in-crude oil emulsions. 1. Physicochemical phenomenology of demulsifier action, Energy Fuels 20 (2006) 1600–

1604.

[278] X. Wang, V. Alvarado, Effects of Aqueous-Phase Salinity on Water-in-Crude Oil Emulsion Stability, J. Dispers. Sci. Technol. 33 (2012) 165–170.

[279] Y. Kazemzadeh, I. Ismail, H. Rezvani, M. Sharifi, M. Riazi, Experimental investigation of stability of water in oil emulsions at reservoir conditions: Effect of ion type, ion concentration, and system pressure, Fuel 243 (2019) 15–27.

[280] S. Maaref, A. Kantzas, S.L. Bryant, The effect of silanization assisted nanoparticle hydrophobicity on emulsion stability through droplet size distribution analysis, Chem. Eng. Sci. 201 (2019) 175–190.

[281] A.L. Márquez, A. Medrano, L.A. Panizzolo, J.R. Wagner, Effect of calcium salts and surfactant concentration on the stability of water-in-oil (w/o) emulsions prepared with polyglycerol polyricinoleate, J. Colloid Interface Sci. 341 (2010) 101–108.

[282] K.R. Chaturvedi, T. Sharma, Enhanced carbon capture and storage in depleted sandstone reservoirs using silica nanofluids, in: Mater. Today Proc. 46 (2021) 5298–5303.

[283] K.R. Chaturvedi, A.K. Singh, T. Sharma, Impact of shale on properties and oil recovery potential of sandstone formation for low-salinity waterflooding applications, Asia-Pacific J. Chem. Eng. 14 (2019) 1–14.

[284] K. Hazarika, S.B. Gogoi, A. Kumar, Polymer flooding and its effects on enhanced oil recovery special reference to Upper Assam Basin, Pet. Res. 8 (2023) 54–62.

[285] A. Novriansyah, W. Bae, C. Park, A.K. Permadi, S.S. Riswati, Optimal design of alkaline-surfactant-polymer flooding under low salinity environment, Polymers 12 (2020) 1–11.

[286] S. Hocine, A. Cuenca, A. Magnan, A. Tay, P. Moreau, An Extensive Study of the Thermal Stability of Anionic Chemical EOR Surfactants - Part 1 Stability in Aqueous Solutions, IPTC-18974-MS, (2016) 1–22.

[287] J. Lu, C. Britton, S. Solairaj, P.J. Liyanage, D.H. Kim, S. Adkins, G.W.P. Arachchilage, U. Weerasooriya, G.A. Pope, Novel large-hydrophobe alkoxy carboxylate surfactants for enhanced oil recovery, SPE J. 19 (2014) 1024–1034.

[288] J.C. Baret, F. Kleinschmidt, A. El Harrak, A.D. Griffiths, Kinetic aspects of emulsion stabilization by surfactants: A microfluidic analysis, Langmuir 25 (2009) 6088–6093.

[289] N.A.C. Sidik, M.N.A.W.M. Yazid, R. Mamat, A review on the application of nanofluids in vehicle engine cooling system, Int. Commun. Heat Mass Transf. 68 (2015) 85–90.

[290] F.D.S. Curbelo, V.C. Santanna, E.L.B. Neto, T.V. Dutra, T.N.C. Dantas, A.A.D. Neto, A.I.C. Garnica, Adsorption of nonionic surfactants in sandstones, Colloids Surfaces A Physicochem. Eng. Asp. 293 (2007) 1–4.

[291] A.O. Mmbuji, R. Cao, Y. Li, X. Xu, E.X. Ricky, Nanoparticle-Assisted Surfactant / Polymer Formulations for Enhanced Oil Recovery in Sandstone Reservoirs : From Molecular Interaction to Field Application, Energy Fuels 37 (2023) 17094–17112.

[292] R.J.K.U. Ranatunga, C.T. Nguyen, B.A. Wilson, W. Shinoda, S.O. Nielsen, Molecular dynamics study of nanoparticles and non-ionic surfactant at an oil-water interface, Soft Matter 7 (2011) 6942–6952.

[293] D.E. Tambe, M.M. Sharma, The effect of colloidal particles on fluid-fluid interfacial properties and emulsion stability, Adv. Colloid Interface Sci. 52 (1994) 1–63.

[294] T. Sharma, G.S. Kumar, B.H. Chon, J.S. Sangwai, Thermal stability of oil-in-water Pickering emulsion in the presence of nanoparticle, surfactant, and polymer, J. Ind. Eng. Chem. 22 (2015) 324–334.

[295] T. Sharma, N. Velmurugan, P. Patel, B.H. Chon, J.S. Sangwai, Use of Oil-in-water Pickering Emulsion Stabilized by Nanoparticles in Combination with Polymer Flood for Enhanced Oil Recovery, Pet. Sci. Technol. 33 (2015) 1595–1604.

[296] Y. Zhou, X. Wu, X. Zhong, W. Sun, H. Pu, J.X. Zhao, Surfactant-Augmented Functional Silica Nanoparticle Based Nanofluid for Enhanced Oil Recovery at High Temperature and Salinity, ACS Appl. Mater. Interfaces 11 (2019) 45763–45775.

[297] S. Ko, C. Huh, Use of nanoparticles for oil production applications, J. Pet. Sci. Eng. 172 (2019) 97–114.

[298] K.R. Chaturvedi, J. Trivedi, T. Sharma, Single-step silica nanofluid for improved carbon dioxide flow and reduced formation damage in porous media for carbon utilization, Energy 197 (2020) 117276.

[299] T. Sharma, S. Iglauer, J.S. Sangwai, Silica Nanofluids in an Oilfield Polymer Polyacrylamide: Interfacial Properties, Wettability Alteration, and Applications for Chemical Enhanced Oil Recovery, Ind. Eng. Chem. Res. 55 (2016) 12387–12397.

[300] Z. Briceño-Ahumada, J.F.A. Soltero-Martínez, R. Castillo, Aqueous foams and emulsions stabilized by mixtures of silica nanoparticles and surfactants: A state-of-the-art review, Chem. Eng. J. Adv. 7 (2021) 100116.

[301] K.R. Chaturvedi, J. Trivedi, T. Sharma, Evaluation of Polymer-Assisted Carbonated Water

Injection in Sandstone Reservoir: Absorption Kinetics, Rheology, and Oil Recovery Results, Energy Fuels 33 (2019) 5438–5451.

[302] H. Tan, K.C. Tam, R.D. Jenkins, Rheological properties of semidilute hydrophobically modified alkali-soluble emulsion polymers in sodium dodecyl sulfate and salt solutions, Langmuir 16 (2000) 5600–5606.

[303] R. Pal, Rheological behaviour of surfactant-flocculated water-in-oil emulsions, Colloids Surfaces A Physicochem. Eng. Asp. 71 (1993) 173–185.

[304] J.H.J. Thijssen, A.B. Schofield, P.S. Clegg, How do (fluorescent) surfactants affect particle-stabilized emulsions?, Soft Matter 7 (2011) 7965–7968.

[305] L. Hendraningrat, S. Li, O. Torsæter, A coreflood investigation of nanofluid enhanced oil recovery, J. Pet. Sci. Eng. 111 (2013) 128–138.

[306] G.M. El-sayed, M.M. Kamel, N.S. Morsy, F.A. Taher, Encapsulation of Nano Disperse Red 60 via Modified Miniemulsion Polymerization. I. Preparation and Characterization, J. Appl. Polym. Sci. 125 (2012) 1318–1329.

[307] H. Setia, R. Gupta, R.K. Wanchoo, Stability of nanofluids, Mater. Sci. Forum 757 (2013) 139–149.

[308] L.N. Nwidee, M. Lebedev, A. Barifcani, M. Sarmadivaleh, S. Iglauer, Wettability alteration of oil-wet limestone using surfactant-nanoparticle formulation, J. Colloid Interface Sci. 504 (2017) 334–345.

[309] M. Mohajeri, M. Hemmati, A.S. Shekarabi, An experimental study on using a nanosurfactant in an EOR process of heavy oil in a fractured micromodel, J. Pet. Sci. Eng.

126 (2015) 162–173.

[310] M.A. Ahmadi, S.R. Shadizadeh, Induced effect of adding nano silica on adsorption of a natural surfactant onto sandstone rock: Experimental and theoretical study, J. Pet. Sci. Eng. 112 (2013) 239–247.

[311] G. Cheraghian, L. Hendraningrat, A review on applications of nanotechnology in the enhanced oil recovery part B: effects of nanoparticles on flooding, Int. Nano Lett. 6 (2016) 1–10.

[312] D.C. Standnes, T. Austad, Wettability alteration in carbonates: Interaction between cationic surfactant and carboxylates as a key factor in wettability alteration from oil-wet to water-wet conditions, Colloids Surfaces A Physicochem. Eng. Asp. 216 (2003) 243–259.

[313] A. Sharma, V. V. Tyagi, C.R. Chen, D. Buddhi, Review on thermal energy storage with phase change materials and applications, Renew. Sustain. Energy Rev. 13 (2009) 318–345.

[314] N. Şahan, H. Paksoy, Novel shapeable phase change material (PCM) composites for thermal energy storage (TES) applications, Sol. Energy Mater. Sol. Cells 174 (2018) 380–387.

[315] G. Alva, Y. Lin, G. Fang, An overview of thermal energy storage systems, Energy 144 (2018) 341–378.

[316] N.H.S. Tay, M. Liu, M. Belusko, F. Bruno, Review on transportable phase change material in thermal energy storage systems, Renew. Sustain. Energy Rev. 75 (2017) 264–277.

[317] D. Zhou, C.Y. Zhao, Y. Tian, Review on thermal energy storage with phase change materials (PCMs) in building applications, Appl. Energy 92 (2012) 593–605.

[318] A. Fallahi, G. Guldentops, M. Tao, S. Granados-Focil, S. Van Dessel, Review on solid-solid

phase change materials for thermal energy storage: Molecular structure and thermal properties, Appl. Therm. Eng. 127 (2017) 1427–1441.

[319] L.F. Cabeza, A. Castell, C. Barreneche, A. De Gracia, A.I. Fernández, Materials used as PCM in thermal energy storage in buildings: A review, Renew. Sustain. Energy Rev. 15 (2011) 1675–1695.

[320] S. Shoeibi, F. Jamil, S.M. Parsa, S. Mehdi, H. Kargarsharifabad, S.A.A. Mirjalily, W. Guo, H.H. Ngo, B.-J. Ni, M. Khiadani, Recent advancements in applications of encapsulated phase change materials for solar energy systems: A state of the art review, J. Energy Storage 94 (2024) 112401.

[321] N.I. Ibrahim, A. Yahiaoui, J.A. Garkuwa, R. Ben Mansour, S. Rehman, Solar cooling with absorption chillers, thermal energy storage, and control strategies: A review, J. Energy Storage 97 (2024) 112762.

[322] A. Islam, A.K. Pandey, R. Saidur, B. Aljafari, V.V. Tyagi, Advancements in foam-based phase change materials: Unveiling leakage control, enhanced thermal conductivity, and promising applications, J. Energy Storage 74 (2023) 109380.

[323] G. Zhang, Y. Guo, B. Zhang, X. Yan, W. Lu, G. Cui, Y. Du, Preparation and control mechanism of nano-phase change emulsion with high thermal conductivity and low supercooling for thermal energy storage, Energy Reports 8 (2022) 8301–8311.

[324] L. Liu, J. Niu, J.Y. Wu, Formulation of highly stable PCM nano-emulsions with reduced supercooling for thermal energy storage using surfactant mixtures, Sol. Energy Mater. Sol. Cells 223 (2021) 110983.

[325] Z. Said, A.K. Pandey, A.K. Tiwari, B. Kalidasan, F. Jamil, A.K. Thakur, V.V. Tyagi, A. Sarı, H.M. Ali, Nano-enhanced phase change materials: Fundamentals and applications, Prog. Energy Combust. Sci. 104 (2024) 101162.

[326] P. Johnson, A. Trybala, V. Starov, V.J. Pinfield, Effect of synthetic surfactants on the environment and the potential for substitution by biosurfactants, Adv. Colloid Interface Sci. 288 (2021) 102340.

[327] S.O. Badmus, H.K. Amusa, T.A. Oyehan, T.A. Saleh, Environmental risks and toxicity of surfactants: overview of analysis, assessment, and remediation techniques, Environ. Sci. Pollut. Res. 28 (2021) 62085–62104.

[328] T. Cserháti, E. Forgács, G. Oros, Biological activity and environmental impact of anionic surfactants, Environ. Int. 28 (2002) 337–348.

[329] J. Zembrzuska, I. Budnik, Z. Lukaszewski, Monitoring of selected non-ionic surfactants in river water by liquid chromatography-tandem mass spectrometry, J. Environ. Manage. 169 (2016) 247–252.

[330] A. Singh, T. Sharma, M.M.S. Abdullah, J.J. Trivedi, Effect of a Natural Surfactant (Fenugreek Seeds) on Emulsification and Mobilization of Paraffins via Pore-Scale Micromodel Experiments, Langmuir 40 (2024) 18098–18111.

[331] N. Pal, K. Samanta, A. Mandal, A novel family of non-ionic gemini surfactants derived from sunflower oil: Synthesis, characterization and physicochemical evaluation, J. Mol. Liq. 275 (2019) 638–653.

[332] A. Singh, T. Sharma, K. Raghav, J. Trivedi, Effect of silica nanoparticles on crude oil

emulsions stabilized by a natural surfactant from Fenugreek Seeds and polyacrylamide for subsurface oil mobilization applications, Colloids Surfaces A Physicochem. Eng. Asp. 702 (2024) 135084.

[333] A. Singh, K. Raghav Chaturvedi, T. Sharma, An experimental evaluation of green surfactants to stabilize silica nanofluids in saline conditions and its application in CO_2 absorption, Int. J. Chem. React. Eng. 22 (2024) 1–9.

[334] U. Nithiyanantham, A. Zaki, Y. Grosu, L. González-Fernández, A. Anagnostopoulos, M.E. Navarro, Y. Ding, J.M. Igartua, A. Faik, Effect of silica nanoparticle size on the stability and thermophysical properties of molten salts based nanofluids for thermal energy storage applications at concentrated solar power plants, J. Energy Storage 51 (2022) 104276.

[335] X. Chen, Z. Tang, Y. Chang, H. Gao, P. Cheng, Z. Tao, J. Lv, Toward Tailoring Chemistry of Silica-Based Phase Change Materials for Thermal Energy Storage, IScience 23 (2020) 101606.

[336] D. Chen, Y. Chen, X. Guo, W. Tao, J. Wang, S. Gao, J. Gao, Mesoporous silica nanoparticles with wrinkled structure as the matrix of myristic acid for the preparation of a promising new shape-stabilized phase change material via simple method, RSC Adv. 8 (2018) 34224–34231.

[337] A. Reza, M. Hassan, Effect of SiO_2 Nanoparticles on Thermal Properties of Polyaniline/ Palmitic Acid Composite as an Energy Storage System, Iran. J. Chem. Chem. Eng. 41 (2022) 3304–3313.

[338] P. Manoj Kumar, K. Mylsamy, P.T. Saravanakumar, Experimental investigations on thermal properties of nano-SiO_2/paraffin phase change material (PCM) for solar thermal

energy storage applications, Energy Sources, Part A Recover. Util. Environ. Eff. 42 (2020) 2420–2433.

[339] S.U. Ilyas, R. Pendyala, N. Marneni, Preparation, sedimentation, and agglomeration of nanofluids, Chem. Eng. Technol. 37 (2014) 2011–2021.

[340] E.J.W. Verwey, Theory of the Stability of Lyophobic Colloids, J. Phys. Colloid Chem. 51 (1947) 631–636.

[341] M. Abdullah, S.R. Malik, M.H. Iqbal, M.M. Sajid, N.A. Shad, S.Z. Hussain, W. Razzaq, Y. Javed, Sedimentation and stabilization of nano-fluids with dispersant, Colloids Surfaces A Physicochem. Eng. Asp. 554 (2018) 86–92.

[342] E.R. Bobicki, Q. Liu, Z. Xu, H. Zeng, Carbon capture and storage using alkaline industrial wastes, Prog. Energy Combust. Sci. 38 (2012) 302–320.

[343] B.K. Hembram, M.K. Yadav, T. Sharma, V.C. Nair, Single-Step Silica Nanofluid for the Improved Thermodynamics and Kinetics of Methane Hydrate Stabilized by a Conventional Promoter, Energy Fuels 38 (2024) 12741–12753.

[344] R.S. Kumar, R. Narukulla, T. Sharma, Comparative Effectiveness of Thermal Stability and Rheological Properties of Nanofluid of SiO_2-TiO_2 Nanocomposites for Oil Field Applications, Ind. Eng. Chem. Res. 59 (2020) 15768–15783.

[345] N. Aslfattahi, R. Saidur, A. Arifutzzaman, R. Sadri, N. Bimbo, M.F.M. Sabri, P.A. Maughan, L. Bouscarrat, R.J. Dawson, S.M. Said, B.T. Goh, N.A.C. Sidik, Experimental investigation of energy storage properties and thermal conductivity of a novel organic phase change material/MXene as A new class of nanocomposites, J. Energy Storage 27 (2020)

101115.

[346] D. Cabaleiro, F. Agresti, L. Fedele, S. Barison, C. Hermida-Merino, S. Losada-Barreiro, S. Bobbo, M.M. Piñeiro, Review on phase change material emulsions for advanced thermal management: Design, characterization and thermal performance, Renew. Sustain. Energy Rev. 159 (2022) 112238.

[347] X. Fu, W. Yu, Y. Lin, D. Wang, H. Shi, F. Yan, Preparation of concentrated stable fluids containing silver nanoparticles in nonpolar organic solvent, J. Dispers. Sci. Technol. 26 (2005) 575–580.

[348] H. Waqas, M.J. Hasan, S.M.R.S. Naqvi, D. Liu, T. Muhammad, S.M. Eldin, C. Kang, Enhancing the performance of thermal energy storage by adding nano-particles with paraffin phase change materials, Nanotechnol. Rev. 13 (2024) 20230180.

[349] R. Ranjbarzadeh, A. Moradikazerouni, R. Bakhtiari, A. Asadi, M. Afrand, An experimental study on stability and thermal conductivity of water/silica nanofluid: Eco-friendly production of nanoparticles, J. Clean. Prod. 206 (2019) 1089–1100.

[350] K. Apmann, R. Fulmer, A. Soto, S. Vafaei, Thermal conductivity and viscosity: Review and optimization of effects of nanoparticles, Materials 14 (2021) 1–75.

[351] C.O. Metin, K.M. Rankin, Q.P. Nguyen, Phase behavior and rheological characterization of silica nanoparticle gel, Appl. Nanosci. 4 (2014) 93–101.

[352] D. Zhou, S.W. Bennett, A.A. Keller, Increased mobility of metal oxide nanoparticles due to photo and thermal induced disagglomeration, PLoS One 7 (2012) 1–8.

[353] A.R. Alian, S.A. Meguid, Molecular dynamics simulations of the effect of waviness and

agglomeration of CNTs on interface strength of thermoset nanocomposites, Phys. Chem. Chem. Phys. 19 (2017) 4426–4434.

[354] H. Kourki, M. Mortezaei, M.H. Navid Famili, Prediction of the viscoelastic response of filler network in highly nanofilled polymer composites, J. Compos. Mater. 49 (2015) 3799–3807.

[355] J. Wang, E. Kang, U. Sultan, B. Merle, A. Inayat, B. Graczykowski, G. Fytas, N. Vogel, Influence of Surfactant-Mediated Interparticle Contacts on the Mechanical Stability of Supraparticles, J. Phys. Chem. C 125 (2021) 23445–23456.

[356] N. Kumar, A. Mandal, Surfactant Stabilized Oil-in-Water Nanoemulsion: Stability, Interfacial Tension, and Rheology Study for Enhanced Oil Recovery Application, Energy Fuels 32 (2018) 6452–6466.

[357] M. Zembyla, B.S. Murray, A. Sarkar, Water-in-oil emulsions stabilized by surfactants, biopolymers and/or particles: a review, Trends Food Sci. Technol. 104 (2020) 49–59.

[358] J. Vialetto, S.N. Ramakrishna, L. Isa, M. Laurati, Effect of particle stiffness and surface properties on the non-linear viscoelasticity of dense microgel suspensions, J. Colloid Interface Sci. 672 (2024) 814–823.

[359] M. Yuan, C. Xu, T. Wang, T. Zhang, X. Pan, F. Ye, Supercooling suppression and crystallization behaviour of erythritol/expanded graphite as form-stable phase change material, Chem. Eng. J. 413 (2021) 127394.

[360] N. Beaupere, U. Soupremanien, L. Zalewski, Nucleation triggering methods in supercooled phase change materials (PCM), a review, Thermochim. Acta 670 (2018) 184–201.

[361] P. Murugan, P. Ganesh Kumar, V. Kumaresan, M. Meikandan, K. Malar Mohan, R. Velraj, Thermal energy storage behaviour of nanoparticle enhanced PCM during freezing and melting, Phase Transitions 91 (2018) 254–270.

[362] S.A. Vanapalli, J. Palanuwech, J.N. Coupland, Stability of emulsions to dispersed phase crystallization: Effect of oil type, dispersed phase volume fraction, and cooling rate, Colloids Surfaces A Physicochem. Eng. Asp. 204 (2002) 227–237.

[363] D. Cabaleiro, C. Hermida−Merino, S. Losada−Barreiro, F. Agresti, L. Lugo, D. Hermida−Merino, M.M. Piñeiro, Preparation and characterization of stable methyl myristate−in−water nanoemulsions as advanced working fluids for cooling systems, J. Mol. Liq. 395 (2024) 123933.

[364] V. Chinnasamy, S. Appukuttan, Preparation and thermal properties of lauric acid/myristyl alcohol as a novel binary eutectic phase change material for indoor thermal comfort, Energy Storage 1 (2019) e80.

[365] M. Lavanya, A.A. Machado, Surfactants as biodegradable sustainable inhibitors for corrosion control in diverse media and conditions: A comprehensive review, Sci. Total Environ. 908 (2024) 168407.

[366] Y. Wan, X. Wang, H. Sun, Y. Li, K. Zhang, Y. Wu, Corrosion behavior of copper at elevated temperature, Int. J. Electrochem. Sci. 7 (2012) 7902–7914.

[367] J. Korzekwa, Modification of the structure and properties of oxide layers on aluminium alloys: A review, Rev. Adv. Mater. Sci. 62 (2023) 1–26.

[368] IPCC, IPCC Special Report; Chapter 1 — Global Warming of 1.5°C, (2018) 1-630.

[369] J. Chateau, A Framework for Climate Change Mitigation in India, IMF Work. Pap. (2023) 1-49.

[370] INCCA, India : Greenhouse Gas Emissions 2007-Executive Summary, Indian Netw. Clim. Chang. Assessment, (2010).

[371] S.Y. Pan, Y.H. Chen, L.S. Fan, H. Kim, X. Gao, T.C. Ling, P.C. Chiang, S.L. Pei, G. Gu, CO_2 mineralization and utilization by alkaline solid wastes for potential carbon reduction, Nat. Sustain. 3 (2020) 399–405.

[372] A. Uliasz-Bocheńczyk, E. Mokrzycki, Mineralna sekwestracja, CO_2, granulowane żużle wielkopiecowe, metoda bezpośrednia gaz−ciało stałe, Gospod. Surowcami Miner. / Miner. Resour. Manag. 33 (2017) 111–124.

[373] Y. Zhang, L. Yu, K. Cui, H. Wang, T. Fu, Carbon capture and storage technology by steel-making slags: Recent progress and future challenges, Chem. Eng. J. 455 (2023) 140552.

[374] K.S. You, S.H. Lee, S.H. Hwang, H.S. Kim, J.W. Ahn, CO_2 sequestration via a surface-modified ground granulated blast furnace slag using NaOH solution, Mater. Trans. 52 (2011) 1972–1976.

[375] L. Ji, H. Yu, X. Wang, M. Grigore, D. French, Y.M. Gözükara, J. Yu, M. Zeng, CO_2 sequestration by direct mineralisation using fly ash from Chinese Shenfu coal, Fuel Process. Technol. 156 (2017) 429–437.

[376] H.Y. Jo, J.H. Kim, Y.J. Lee, M. Lee, S.J. Choh, Evaluation of factors affecting mineral carbonation of CO_2 using coal fly ash in aqueous solutions under ambient conditions, Chem. Eng. J. 183 (2012) 77–87.

[377] Y. Soong, D.L. Fauth, B.H. Howard, J.R. Jones, D.K. Harrison, A.L. Goodman, M.L. Gray, E.A. Frommell, CO_2 sequestration with brine solution and fly ashes, Energy Convers. Manag. 47 (2006) 1676–1685.

[378] M. Back, M. Kuehn, H. Stanjek, S. Peiffer, Reactivity of alkaline lignite fly ashes towards CO_2 in water, Environ. Sci. Technol. 42 (2008) 4520–4526.

[379] G. Montes-Hernandez, R. Pérez-López, F. Renard, J.M. Nieto, L. Charlet, Mineral sequestration of CO_2 by aqueous carbonation of coal combustion fly-ash, J. Hazard. Mater. 161 (2009) 1347–1354.

[380] A. Uliasz-Bocheńczyk, E. Mokrzycki, Z. Piotrowski, R. Pomykała, Estimation of CO_2 sequestration potential via mineral carbonation in fly ash from lignite combustion in Poland, Energy Procedia 1 (2009) 4873–4879.

[381] M.G. Nyambura, G.W. Mugera, P.L. Felicia, N.P. Gathura, Carbonation of brine impacted fractionated coal fly ash: Implications for CO_2 sequestration, J. Environ. Manage. 92 (2011) 655–664.

[382] A.L. Yaumi, I.A. Hussien, R.A. Shawabkeh, Surface modification of oil fly ash and its application in selective capturing of carbon dioxide, Appl. Surf. Sci. 266 (2013) 118–125.

[383] D. Lee, H. Cho, J. Lee, C. Huh, K. Mohanty, Fly ash nanoparticles as a CO_2 foam stabilizer, Powder Technol. 283 (2015) 77–84.

[384] N.D. Hegde, A. Venkateswara Rao, Organic modification of TEOS based silica aerogels using hexadecyltrimethoxysilane as a hydrophobic reagent, Appl. Surf. Sci. 253 (2006) 1566–1572.

[385] M. Criado, A. Palomo, A. Fernández-Jiménez, Alkali activation of fly ashes. Part 1: Effect of curing conditions on the carbonation of the reaction products, Fuel 84 (2005) 2048–2054.

[386] B. Xu, K.M. Poduska, Linking crystal structure with temperature-sensitive vibrational modes in calcium carbonate minerals, Phys. Chem. Chem. Phys. 16 (2014) 17634–17639.

[387] S.I. Kuriyavar, R. Vetrivel, S.G. Hegde, A. V. Ramaswamy, D. Chakrabarty, S. Mahapatra, Insights into the formation of hydroxyl ions in calcium carbonate: Temperature dependent FTIR and molecular modelling studies, J. Mater. Chem. 10 (2000) 1835–1840.

[388] K.N. Islam, M.Z.B.A. Bakar, M.E. Ali, M.Z. Bin Hussein, M.M. Noordin, M.Y. Loqman, G. Miah, H. Wahid, U. Hashim, A novel method for the synthesis of calcium carbonate (aragonite) nanoparticles from cockle shells, Powder Technol. 235 (2013) 70–75.

[389] J.H. Bang, Y. Yoo, S.W. Lee, K. Song, S. Chae, CO_2 mineralization using brine discharged from a seawater desalination plant, Minerals 7 (2017) 207.

[390] M.A. Ahmadi, S.R. Shadizadeh, Experimental investigation of adsorption of a new nonionic surfactant on carbonate minerals, Fuel 104 (2013) 462–467.

[391] A.K. Sood, M. Aggarwal, Evaluation of micellar properties of sodium dodecylbenzene sulphonate in the presence of some salts, J. Chem. Sci. 130 (2018) 1–7.

[392] Z. Zhu, Y. Wen, J. Yi, Y. Cao, F. Liu, D.J. McClements, Comparison of natural and synthetic surfactants at forming and stabilizing nanoemulsions: Tea saponin, Quillaja saponin, and Tween 80, J. Colloid Interface Sci. 536 (2019) 80–87.

[393] K. Bilen, F. Takgil, K. Kaygusuz, Thermal energy storage behavior of $CaCl_2.6H_2O$ during melting and solidification, Energy Sources, Part A Recover. Util. Environ. Eff. 30 (2008)

775–787.

[394] M. Liu, M. Belusko, N.H. Steven Tay, F. Bruno, Impact of the heat transfer fluid in a flat plate phase change thermal storage unit for concentrated solar tower plants, Sol. Energy 101 (2014) 220–231.

[395] M. Yusuf, M.H. Wathon, V. Thanasaksukthawee, A. Saul, S. Tangparitkul, Adsorption of Saponin Natural Surfactant on Carbonate Rock and Comparison to Synthetic Surfactants: An Enhanced Oil Recovery Prospective, Energy Fuels 35 (2021) 11193–11202.

[396] S. Akbari, A.H. Nour, R.M. Yunus, Determination of phenolics and saponins in fenugreek seed extracted via microwave-assisted extraction method at the optimal condition, IOP Conf. Ser. Mater. Sci. Eng. 736 (2020) 022024.

[397] S.S. Nadar, P. Rao, V.K. Rathod, Enzyme assisted extraction of biomolecules as an approach to novel extraction technology: A review, Food Res. Int. 108 (2018) 309–330.

[398] B. Díaz-Reinoso, A. Moure, H. Domínguez, J.C. Parajó, Supercritical CO_2 Extraction and Purification of Compounds with Antioxidant Activity, J. Agric. Food Chem. 54 (2006) 2441–2469.

RESEARCH PERFORMANCE EVALUATION COMMITTEE (RPEC)

1. Dr. Satish Kumar Sinha

   Head of Department

   Department of Petroleum Engineering & Geoengineering

2. Dr. Tushar Sharma (Supervisor)

   Associate Professor

   Department of Petroleum Engineering & Geoengineering

3. Dr. Arshad Aijaz

   Assistant Professor

   Department of Energy and Human Science

4. Dr. Amit Kumar

   Assistant Professor

   Department of Petroleum Engineering & Geoengineering

PUBLICATIONS

Research Articles (in thesis)

1. **Singh A,** Chaturvedi KR, Sharma, T. Natural Surfactant for Sustainable Carbon Utilization in Cleaner Production of Fossil Fuels: Extraction, Characterization and Application Studies. Journal Environmental Chemical Engineering, 2021, 9, 106231. (IF = 7.4)

2. **Singh A**, Sharma T, Kumar RS, Arif M. Biosurfactant Derived from Fenugreek Seeds and Its Impact on Wettability Alteration, Oil Recovery, and Effluent Treatment of a Rock System of Mixed Composition. Energy and Fuels, 2023, *37*, 6683–6696. (IF = 5.2)

3. **Singh A**, Sharma T. Design and Performance Evaluation of Alkaline-Surfactant-Polymer Slug of a Natural Surfactant of Fenugreek in Saline Media for Foaming/Emulsification Applications. Journal of Molecular Liquids, 2023, *395*, 123912. (IF = 5.3)

4. **Singh A**, Kashyap AR, Abdullah MM, Vajpayee S, Sharma T. Investigation on Rheological Characterization and Salt Tolerance Potential of Paraffinic O/W Emulsions of Natural Surfactant for Crude Emulsification and Mobilization. Industrial & Engineering Chemistry Research, 2024, 63, 10825–10841. (IF = 3.8)

5. **Singh A**, Sharma T, Abdullah MMS, Trivedi JJ. Effect of a Natural Surfactant (Fenugreek Seeds) on Emulsification and Mobilization of Paraffins via Pore-Scale Micromodel Experiments. Langmuir, 2024, 40, 18098–18111. (IF = 3.7)

6. **Singh A**, Sharma T, Chaturvedi KR, Trivedi J. Effect of silica nanoparticles on crude oil emulsions stabilized by a natural surfactant from Fenugreek Seeds and polyacrylamide for

subsurface oil mobilization applications. Colloids and Surfaces A: Physicochemical and Engineering Aspects, 2024, 702, 135084. (IF = 4.9)

7. **Singh A**, Abdullah MMS, Iglauer S, Keshavarz A, Sharma, T. Sustainable biomass derived natural surfactant of soybean seeds in fly ash industrial waste utilization for carbon storage: Evaluation of environmental impact. Journal Environmental Chemical Engineering, 2024, 12, 114530. (IF = 7.4)

8. **Singh A**, Sharma T, Abdullah MMS, Vishal V. Stable nano-enhanced phase change material emulsions of natural surfactant and silica nanoparticles for thermal energy storage applications. Applied Thermal Engineering, 2025, 720, 126236. (IF = 6.1)

Book Chapter

1. Narukulla R, **Singh A**, Chaturvedi KR, Sharma T. Surfactants in EOR in "Advancements in Chemical Enhanced Oil Recovery" edited by Sharma, Chaturvedi, Ganat and Ali (CRC Press)

International Conferences

1. **Singh A,** Chaturvedi KR, Sharma, T. Green materials for carbon storage in depleted oilfields: An experimental study MMETFP2021: International Symposium on Materials of the Millennium: Emerging Trends and Future Prospects, Pandit Deendayal Energy University, Gujarat, India, November 19-21, 2021.

2. **Singh A,** Chaturvedi KR, Sharma, T. An experimental evaluation of green surfactants to stabilize silica nanofluids in saline conditions and its application in CO_2 absorption.

International Conference on Energy Sustainability and Advanced Materials – 2022 (ICESAM-2022)" part of the Energy Summit-2022, UPES, Dehradun, India.

3. **Singh A,** Sharma, T. Performance Evaluation of Natural Surfactant Extracted from Fenugreek Seeds for Subsurface Resource Mobilization: Synthesis, Characterization and Stability Studies, International Conference of Computational Modelling and Sustainable Energy (ICCMSE 2023), Pandit Deendayal Energy University, Gujarat, India, December 15-17, 2023. (*Best Poster Award*)

4. **Singh A,** Chaturvedi KR, Sharma, T. Use of Green Nano Emulsions for Effective Carbon Capture and Geo-storage. ACS Fall 2023, San Francisco August 13–17, 2023.

CURRICULUM VITAE

Email (O): 20pe0002@rgipt.ac.in

Mob: +917619872302

ALPANA SINGH

OBJECTIVE

To evolve into a competent professional by building upon my technical acumen, scientific temperament and organizational capabilities in a professional atmosphere and develop as a capable professional who is able to play an important role in improving the academic output and social development of my host institute.

ACADEMICS

Examination	**Discipline**	**School/College**	**Board/ University**	**Year**	**C.P.I/%**
Ph.D.		Rajiv Gandhi Institute of Petroleum Technology		Thesis submitted	7.77/10
Masters in Technology **(Hons)**	Energy Technology and Management	Madan Mohan Malviya University of Technology, Gorakhpur		2015	80.3%
Bachelors in Technology	Mechanical Engineering	Skyline Institute of Engineering & Technology	GBTU, Lucknow	2012	72.42%
12^{th}	PCM	RLB, Vikas Nagar	Central Board of Secondary Education	2008	67.8%
10^{th}		RLB, Vikas Nagar	Central Board of Secondary Education	2006	74%

HIGHLIGHTS OF PHD THESIS

Title: "Synthesis, Characterization and Performance Evaluation of Bio-derived Surfactant in Emulsification, Carbon Entrapment and Thermal Energy Storage."

In this work, novel Bio-derived surfactant extracted from fenugreek seeds was explored for multifunctional applications. The work involved synthesis and characterization of a bio-derived surfactant, with demonstrated applications in emulsion stabilization, nanofluid formulation, thermal energy storage and CO_2 entrapment through industrial waste utilization. Emphasis was placed on performance under saline conditions and integration with nanoparticles for enhanced functionality.

AREAS OF RESEARCH

Biomass, Green materials, Microfluidics, Carbon capture & storage, Green Synthesis, Emulsions, Foams, Thermal Energy Storage, Phase change materials, Waste valorization.

RESEARCH OUTPUT

Book (as editor)

1. Sharma T, Hirani H, Singh A. **Smart Fluids for Clean Energy Technologies**, CRC Taylor & Francis- Apple Academic Press (Author agreement signed: Manuscript under preparation)

Journal publications

1. **Singh A**, Sharma T, Abdullah MMS, Vishal V. Stable nano-enhanced phase change material emulsions of natural surfactant and silica nanoparticles for thermal energy storage applications. **Applied Thermal Engineering**, 2025. **(IF = 6.1)**
2. **Singh A,** Hembram BK, Iglauer S, Keshavarz A, Sharma T. Pore-scale micromodel experiments for performance evaluation of polymeric nanofluids in CO_2 flow through porous media for carbon utilization and storage, **Journal of Molecular Liquids**, 2025. **(IF = 5.2)**
3. **Singh A,** Chaturvedi KR, Abdullah, MS, Iglauer S, Singh AK, Sharma T. Polymeric nanofluids of oilfield polymers for subsurface flow applications: Synthesis, interfacial and rheological analysis, **Colloid and Surfaces A**, 2025. **(IF: 5.4)**
4. Dinesh NSV, **Singh A,** Sharma T, Sivasankar. Dynamics of In Situ CO_2 Foam Using Natural and Synthetic Surfactants under Different Injection Modes in Sandstones: Implications on Enhancing Oil Recovery and CO_2 Sequestration, **Energy and Fuels**, 2025. **(IF = 5.3)**

5. **Singh A**, Abdullah, MS, Iglauer S, Keshavarz A, Sharma T. Sustainable Biomass derived Natural Surfactant of Soybean Seeds in Fly Ash Industrial Waste Utilization for Carbon Storage: Evaluation of Environmental Impact, **Journal of Environmental Chemical Engineering**, 2024. **(IF = 7.4)**
6. **Singh A**, Sharma T, Chaturvedi KR, Trivedi, J. Effect of silica nanoparticles on crude oil emulsions stabilized by a natural surfactant from Fenugreek Seeds and polyacrylamide for subsurface oil mobilization applications, **Colloid and Surfaces A**, 2024 **(IF: 5.2)**
7. **Singh A**, Sharma T, Abdullah, MS, Trivedi, J. Effect of Natural Surfactant (fenugreek seeds) on Emulsification and Mobilization Applications of Paraffins via Pore-scale Micromodel Experiments, **Langmuir,** 2024. **(IF: 3.7)**
8. **Singh A**, Kashyap AR, Abdullah, MS, Vajpayee, S, Sharma T. Investigation on Rheological Characterization and Salt Tolerance Potential of Paraffinic O/W Emulsions of Natural Surfactant for Crude Emulsification and Mobilization, **Industrial and Engineering Chemistry Research**, 2024. **(IF: 4.2)**
9. **Singh A**, Sharma T. Design and Performance Evaluation of Alkaline-Surfactant-Polymer Slug of a Natural Surfactant of Fenugreek in Saline Media for Foaming/Emulsification Applications, **Journal of Molecular Liquids,** 2023. **(IF = 6.633**)
10. **Singh A**, Sharma T. Bio-surfactant derived from fenugreek seeds and its impact on wettability alteration, oil recovery, and effluent treatment of a rock system of mixed composition, **Energy and Fuels**, 2023. **(IF = 5.3)**
11. **Singh A**, Sharma T. Implications of Sand Mobilization on Stability and Rheological Properties of Carbon Dioxide Foam and Its Transport Mechanism in Unconsolidated Sandstone, **Energy**, 2023. **(IF = 9)**
12. **Singh A**, Chaturvedi KR, Sharma T. Natural surfactant for sustainable carbon utilization in cleaner production of fossil fuels: Extraction, characterization and application studies, **Journal of Environmental Chemical Engineering**, 2021. **(IF = 5.909)**
13. Gangwar A, Gupta DK, **Singh A**. Theoretical Analysis of Heat Absorption and rejection in Building with PCM and provide cooling effect, **International Journal of Mechanical Engineering and Information Technology**, December,2017
14. Tiwari R, Ashraf MA, Tripathi S, **Singh A**. Super Bike: With Wheel Optionality, **International Journal of Current Research,** December 2017.

15. Srivastava PK, **Singh A**, Srivastava NK, Gigoo SK. Thermal Analysis of Tube-Fin Cross Flow Heat Exchanger, **International Journal of Mechanical Engineering and Technology** (IJMET) 7 (5), 2016.

Book Chapters

1. Narukulla R, **Singh A**, Chaturvedi KR, Sharma T. Surfactants in EOR in "Advancements in Chemical Enhanced Oil Recovery" edited by Sharma, Chaturvedi, Ganat and Ali (CRC Press) 2024.

Articles under consideration

1. **Singh A,** Hirani H, Sharma T, Trivedi J. Synergistic Interaction of Biomass-derived Surfactant and Nano-composite and its impact on Thermal Energy Storage Potential of Conventional PCM. Fuel. (Under Review)
2. **Singh A,** Hirani H, Sharma T. Biomass-derived Surfactant to Improve Salt Tolerance Potential of ZnO Nanofluid for Wettability Alteration and Surface Adsorption in Porous Media. Journal of Molecular Liquids. (Under Review)

Conference presentations

1. **Singh A**, Sharma, T. Biomass derived sustainable solvents: Application in emulsification and thermal energy storage, Flash Talk at **ACS Meetings Global Virtual Symposia Spring 2025 on Sustainable Solvents***,* March 23-27, 2025.
2. **Singh A**, Sharma, T. Performance Evaluation of Natural Surfactant Extracted from Fenugreek Seeds for Subsurface Resource Mobilization: Synthesis, Characterization and Stability Studies, **International Conference of Computational Modelling and Sustainable Energy (ICCMSE 2023)**, Pandit Deendayal Energy University, Gujarat, India, December 15-17, 2023. (*Best Poster Award*)
3. **Singh A**, Chaturvedi KR, Sharma, T. Use of Green Nano Emulsions for Effective Carbon Capture and Geo-storage. **ACS Fall 2023**, San Francisco August 13–17, 2023.
4. **Singh A**, Chaturvedi KR, Sharma, T. An experimental evaluation of green surfactants to stabilize silica nanofluids in saline conditions and its application in CO_2 absorption. **International Conference on Energy Sustainability and Advanced Materials – 2022 (ICESAM-2022) part of the Energy Summit-2022**, UPES, Dehradun, India.

5. **Singh A**, Chaturvedi KR, Sharma, T. Green materials for carbon storage in depleted oilfields: An experimental study **MMETFP2021: International Symposium on Materials of the Millennium: Emerging Trends and Future Prospects**, Pandit Deendayal Energy University, Gujarat, India, November 19-21, 2021.
6. **Singh A**, Srivastava NK, Yadav V, Kumar D. Thermodynamics Study and improving efficiency of Biomass Gasifier, **Advance Research in Electrical and Electronic Engineering** (AREEE), July 27-28, 2015.
7. Yadav V, **Singh A**, Enhancing effectiveness of heat exchanger by using nanofluid. **ICMMSA-2014** Proceedings organized by MNNIT Allahabad December 22-24, 2014.

FDP/ Webinar/ Workshop/ Conference Participation

1. **Best Poster Award** for presenting poster entitled "Performance Evaluation of Natural Surfactant Extracted from Fenugreek Seeds for Subsurface Resource Mobilization: Synthesis, Characterization and Stability studies" at **International Conference on Computational Modelling and Sustainable Energy,** PDEU Gandhinagar, 15-17 December 2023.
2. International Conference on **Recent Trends in Energy Science and Engineering**, organized by Department of Science and Humanities, RGIPT Jais, October 2021.
3. IIPE SPE Webinar Series on **Geothermal Anywhere: Opportunities & Challenges** on 06.11.2021
4. IIPE SPE Webinar Series on **Petroleum Products & Pipelines: Project Execution & Operations** on 09.10.2021.
5. IIPE SPE Webinar Series on **Get Inspired Hired Admired** on 28.08.2021
6. IIPE SPE Webinar Series on **Graduate Research Opportunities: The Good, The Bad & The Ugly** on 18.08.2021
7. Workshop on **Research Related Solution for Faculty and Research Scholars** organized by RGIPT Jais in collaboration with IEEE UP Section, January 2022.
8. Two-week workshop on **Innovation in Technology Leading to Entrepreneurship** organized by Institution's Innovation Council, IQAC & Innovation cell of GKCEM, Kolkata from 14.02.2022 to 25.02.2022.
9. **AWSAR** Webinar on **Popular Science Writing** organized by DST, Government of India And Vigyan Prasar (VP) on 10.09.2021

10. Workshop on **Train the Trainer on Exam Reforms** organized by TEQIP-3, BVB College of Engineering & Technology, Hubballi and NPIU, December 2020
11. Webinar on **Career Opportunities for Students post Covid-19** organized by Himalayan Group of Institutions June 2020.
12. ATAL FDP on **Energy Engineering** organized by Velammal Engineering College, September 2020.
13. Faculty Development Program on **MATLAB & its Application in Electrical Engineering** organized by RRSIMT, Amethi, February 2019.

NATIONAL EXAMS QUALIFIED

- Qualified **Graduate Aptitude Test in Engineering 2013** in Mechanical Engineering.

POSITIONS OF RESPONSIBILITY

- Question Paper Setter, Dr. A.P.J. Abdul Kalam Technical University, formerly Uttar Pradesh Technical University, State Government run affiliating university in Lucknow, Uttar Pradesh, 2018-2020.
- Head, Maintenance and Housekeeping Committee, RRSIMT 2020.
- Member, Proctorial Committee, Department of Mechanical Engineering, RRSIMT 2015-2017.
- Member, Cultural Committee, RRSIMT 2017-2020.
- Faculty Mentor (Student Projects), Department of Mechanical Engineering, RRSIMT 2016-2020.
- Faculty Representative (Conducting Seminars), Department of Mechanical Engineering, RRSIMT 2016-2020.

EQUIPMENT SKILLS

HPHT Rheometer, Pore scale micromodels, Viscometers, Dynamic Foam Analyzer, Surface Tensiometer, UV-Visible spectrophotometry, Measurement & Metrology tools, Zeta Potential, Dynamic Light Scattering.

WORK EXPERIENCE

- July, 2015- August 2020, Assistant Professor, Department of Mechanical Engineering, Rajarshi Rananjay Sinh Institute of Management and Technology (RRSIMT), Amethi, Uttar Pradesh.

PERSONAL DETAILS

- Date of Birth (DD-MM-YYYY): 10-05-1991
- Father's Name: Mr. Ajay Kumar Singh

- Mother’s Name: Mrs. Aneeta Singh
- Husband’s Name: Mr. Jitender Kumar
- Marital status: Married
- Nationality: Indian
- Permanent address: C-100, HAL Korwa, Amethi, U.P.

References/contact details

1. **Dr. Tushar Sharma** (PhD Thesis Supervisor),
   Assistant Professor, Dept. of Petroleum Engineering & Geoengineering,
   Rajiv Gandhi Institute of Petroleum Technology, Jais, Amethi-229304, India.
   Ph. No. - +91 7080044156
   Email Id- tsharma@rgipt.ac.in
2. **Prof. Japan Trivedi**,
   Professor, Petroleum Engineering, Faculty of Engineering - Civil and Environmental Engineering, University of Alberta, Edmonton, Canada.
   Ph. No. - +1 (780) 492-1247
   Email Id- jtrivedi@ualberta.ca
3. **Prof. Stefan Iglauer**,
   Professor & Director, Centre for Sustainable Energy and Resources,
   School of Engineering, Edith Cowan University, Joondalup, Australia.
   Ph. No. -+61 8 6304 5832
   Email Id- s.iglauer@ecu.edu.au
4. **Prof. Vikram Vishal**,
   Professor, Department of Earth Sciences,
   Indian Institute of Technology, Bombay-400076, India
   Ph. No. +91-22-2576 7254
   Email Id- v.vishal@iitb.ac.in
5. **Prof. Alireza Keshavarz,**
   Associate Professor, School of Engineering,
   Edith Cowan University, Joondalup, Australia.
   Ph. No. +61 8 6304 2855
   Email Id- a.keshavarz@ecu.edu.au

End